UNIVERSIDADE FEDERAL DE CIÊNCIAS DA SAÚDE DE PORTO ALEGRE – UFCSPA
CURSO DE PÓS-GRADUAÇÃO EM BIOCIÊNCIAS

Dominique Santos Rubenich

THE ROLE OF TUMOR-ASSOCIATED NEUTROPHILS IN CANCER PROGRESSION

Porto Alegre
2024

Dominique Santos Rubenich

THE ROLE OF TUMOR-ASSOCIATED NEUTROPHILS IN CANCER PROGRESSION

Thesis submitted to the Graduate Program in Biosciences at the Federal University of Health Sciences of Porto Alegre as a requirement for obtaining the degree of **Doctor**.

Principal Investigator: Prof. Dr. Elizandra Braganhol

Porto Alegre
2024

Catalogação na Publicação

Santos Rubenich, Dominique
The role of tumor-associated neutrophils in cancer progression / Dominique Santos Rubenich. -- 2024.
444 f. : 30 cm.

Tese (doutorado) -- Universidade Federal de Ciências da Saúde de Porto Alegre, Programa de Pós-Graduação em BioCiências, 2024.

Orientador(a): Elizandra Braganhol.

1. neutrófilos. 2. glioblastoma. 3. carcinoma de cabeça e pescoço. 4. microambiente tumoral. I. Título.

Sistema de Geração de Ficha Catalográfica da UFCSPA com os dados fornecidos pelo(a) autor(a).

INSTITUTIONS:

Universidade Federal de Ciências da Saúde de Porto Alegre (UFCSPA), Brazil

Braganhol Lab – Immuno-oncology Lab

Bioanalytical Unit

Cellular Biology Lab

Molecular Biology Lab

Pathology Lab

Universidade Federal do Rio Grande do Sul (UFRGS), Brazil

Department of Morphology Sciences, Faculty of Dentistry

Irmandade Santa Casa de Misericórdia de Porto Alegre (ISCMPA), Brazil

Center of Neurosurgery, São José Hospital

Hospital de Clínicas de Porto Alegre (HCPA), Brazil

Instituto de Cardiologia, Brazil

Fundação Universitária do Instituto de Cardiologia (IC-FUC)

Universidade de São Paulo (USP), Brazil

Department of Immunology, Transplant immunology Lab

Université Laval, Canada

Centre de Recherche du Centre hospitalier universitaire de Québec

Département de Microbiologie-Infectiologie et d'Immunologie, Faculté de Médecine

Regensburg Universität, Germany

Clinic and Polyclinic for Internal Medicine III, University Hospital Regensburg

Department of Oral and Maxillofacial Surgery, University Hospital Regensburg

Leibniz Institute for Immunotherapy (LIT)

FINANTIAL SUPPORT:

The authors would like to thank the Conselho Nacional de Desenvolvimento Científico e Tecnológico (CNPq - 142520/2020-9), Coordenação de Aperfeiçoamento de Pessoal de Nível Superior (CAPES; code 001), Fundação de Amparo à Pesquisa do Estado do Rio Grande do Sul (FAPERGS - 19/2551-0000663-2, PPSUS - 21/ 2551-0000078-3, FIPE 2019–0446, German Academic Exchange Service (DAAD - #57588369, #57705675), Walter Schulz Foundation, Helga-Reifert-Foundation and Verein zur Förderung der wissenschaftlichen Zahnheilkunde in Bayern e. V. (VFwZ) and Universidade Federal de Ciências da Saúde de Porto Alegre. We would like to express our gratitude for the Brazilian Ministry of Health and the Department of Science and Technology of the Secretariat of Science, Technology and Strategic Inputs - Decit/SCTIE which, through the PPSUS program, promotes research towards the population's main health problems.

ACKNOWLEDGMENTS:

Despite these four years dedicated to the doctorate, I must say that this thesis began to be built many years earlier. We are all a sequence of choices, and each choice is based on the moment we are in, but mainly on the people around us.

From a young age, I have always had the privilege of having a very supportive family. They supported me as a gymnast, attending competitions and strictly following training schedules (including vacations). They helped me with my studies and training to become the Oktoberfest princess. They insisted on exchange programs and learning foreign languages. They always emphasized the importance of education for my future. They always accepted and pursued all my dreams and desires with me. I had a foundation that certainly influences me to this day and has contributed to reaching the places I have reached. Therefore, I am immensely grateful to my parents, Eldon Rubenich (*in memoriam*) and Marlova Santos, for all their unconditional support in my development. I also want to extend this gratitude to my uncles, Suzi and Valmor, and my grandmother, Cleyde, for also being present, supporting, and listening to me incessantly about my work.

I reserve a special space to thank my sister, Aline. She has never spared any effort to assist in each step. Whether at home or in the lab. Yes, in the lab. She was my improvised research assistant on days I needed extra hands. She counted cell markers, learned to use software to help with manual analyses, and was my escape vehicle on days we needed to measure ELISA absorbance, when we were in a lab with broken equipment and had to rush to another location. I must say that some of these data would not have been completed without her help.

Speaking of research assistants interns, I had the challenge of mentoring eight undergraduate students in biomedicine and biomedical informatics. To this day, I cannot believe how, in such a short time, these students embraced my experimental plans and dedicated themselves (sweat and blood) to help me achieve my goals. I decided to thank them in chronological order: Natalia, my first intern during my master's and who stayed until the completion of her underg thesis;

Veronica, who joined during the pandemic and started her undergrad thesis right after the lockdown ended. With her, I entered a new world, colorectal cancer, and together we had to overcome many stages and processes since it was a new topic for both of us. Maico, one of the most challenging because it was completely outside my area of expertise. Maico, now a biomedical informatician, started his research internship at the beginning of the pandemic with the goal of developing software, a proposal of mine that obviously seemed simple. Because of him, I took bioinformatics courses to at least understand and assist in the production. Mariana, who worked closely with me on research with nude mice. Kerolainy, who joined the group with a very specific request. She wanted to overcome her trauma from the lab bench and complete her undergrad thesis with RNAseq analysis, another area beyond my knowledge. Gabriela G, who agreed to standardize an entire study in the area of NETs while I was on a sandwich doctorate. With entirely remote guidance, and now as a master's student, she never left my side and participated in key experiments. Alana, who asked to do her thesis entirely in molecular biology and agreed to analyze the expression of 10 genes, also entirely remotely. Jordana, my last research intern and underg thesis mentee, our work is still ongoing, but since she joined the group, she has always been essential. I look at these eight individuals with great pride. Their work was very well evaluated, with many techniques delivered and a lot of expertise in their presentations. Nevertheless, I must emphasize that even though I was part of their mentorship, they were essential to my personal development. With them, I learned to lead a team, to delegate, to teach. A team where I supported and was supported, the true "no one is left behind".

Speaking of the group, the Braganhol Lab has been a place of support these last few years. I want to highlight Dr. Priscila's role, who, as a postdoc, welcomed me to the lab and taught me many cell culture techniques. Dr. Fernanda, who managed the lab during the pandemic and organized activities so we could continue our work. Beyond the lab, she was also a great friend. Dr. Gabriela D, who has been with me since the master's. We were a duo for collecting data for COVID-19 epidemiological research, we built the scientific communication Instagram (@cienciatraduzida), wrote projects and paper together. We saw each other embark

abroad and experience highs and lows, never abandoning one another. To the other members and associates of the group, I thank you for the laughs, the advice, and the hugs.

Regarding the sandwich doctorate, I need to highlight the essential role of Dr. Daniela in welcoming me, being my German family, and offering not just a home but also her friendship. To Prof. Dr. Richard Bauer for adopting me when I found myself alone and supporting my experiments. To Sophia, Sara, Panis, for the support and all the life experiences we had together. My stay in Germany was wonderful because of all of you.

To my academic friends, Desirée and Paula, and non-academic friends, Álvaro and Eduardo, who were and remain by my side, donated blood for my research, and brainstormed when I needed, my heartfelt thanks.

Finally, to my advisor Prof. Dr. Elizandra Braganhol. Without her support, I would not have done what I did, gone where I went, or reached where I have reached.

To all of you, my heartfelt thanks.

LIST OF ABREVIATIONS, SYMBOLS AND UNITS:

3D	Three dimensional
A1	Adenosine receptor A1
A2A	Adenosine receptor A2a
A2B	Adenosine receptor A2b
A3	Adenosine receptor A3
ADO	Adenosine
AI	Artificial Intelligence
ALDH1	Aldehyde Dehydrogenase 1
ALIX	ALG-2-interacting protein X
Ang	Angiopoietin
ATP	Adenosine triphosphate
ATRX	alpha-thalassemia mental retardation X-linked
BV8	Prokineticin
CAF	Cancer-associated fibroblast
cAMP	Cyclic adenosine monophosphate
CD133	Prominin-1
CD170	Siglec-5
CD73	ecto-5'-nucleotidase
circRNA	Circular RNA
DNA	Deoxyribonucleic Acid
EGFR	Epidermal growth factor receptor
EMT	Epithelial-Mesenchymal Transition
ESCRT	Endosomal Sorting Complex Required for Transport
EV	Extracellular vesicles
FGF2	Fibroblast Growth Factor 2
G6PD	Glucose-6-Phosphate Dehydrogenase
GB	Glioblastoma
G-CSF	Granulocyte-colony stimulating factor
h	hour
HMGB1	High Mobility Group Box 1

HNSCC	Head and Neck Squamous Cell Carcinoma
HPV	Human Papillomavirus
HSP	Heat Shock Protein
IDH	Isocitrate dehydrogenase
IFN-γ	Interferon-γ
IL	Interleukin
ILV	Intraluminal Vesicles
kDa	kilo Dalton
lncRNA	Long Non-Coding RNA
MDSC	Myeloid-derived suppressor cell
miRNA	MicroRNA
ML	Machine-Learning
MMP-9	Metalloproteinase-9
MPO	Myeloperoxidase
mRNA	Messenger RNA
MVB	Multivesicular Bodies
NE	Neutrophil Elastase
NETs	Neutrophil extracellular traps
NEX	Neutrophil-derived exosome
NFP	Neurofilament protein
NLR	Neutrophil-to-Lymphocyte Ratio
nm	nanometer
NØ	Neutrophil
NO	nitric oxide
NSE	Neuron-specific enolase
P1/P1R	Purinergic receptors 1
P2/P2R	Purinergic receptors 2
P2X	Purinergic receptors 2X
P2Y	Purinergic receptors 2Y
P53	Tumor Protein P53
PD-1	Programmed Death-1
PD-L1	Programmed Death-Ligand 1

Pi	inorganic phosphate
PI3K	Phosphoinositide 3-kinases
pre-RNA	Precursor RNA
pri-miRNA	Primary MicroRNA
PTEN	Phosphatase and tensin homolog
PTX3	Pentraxin 3
Rab	Ras-related Protein in Brain
RNA	Ribonucleic acid
RNS	Reactive nitrogen species
ROS	Reactive oxygen species
RTK	Receptor Tyrosine Kinase
scRNA-seq	Single Cell RNA sequencing
SNARE	Soluble NSF Attachment Protein Receptor
Sp11	Synaptophysin
SSC47	UM-SCC-47/University of Michigan-Squamous Cell Carcinoma-47
TAM	Tumor-associated macrophage
TAN	Tumor-associated neutrophil
TEX	Tumor-derived exosome
TGFβ	Transforming growth factor-beta
TGN	Trans-Golgi Network
TIMP-1	Tissue inhibitor of metalloproteinases-1
TLR9	Toll-Like Receptor 9
TME	Tumor Microenvironment
TNF-α	Tumor Necrosis Factor alpha
TRAIL	TNF-related apoptosis-inducing ligand
Treg	Regulatory T Cell
TSG101	Tumor Susceptibility Gene 101
TSP-1	Thrombospondin-1
VEGF-A	Vascular endothelial growth factor A

LIST OF FIGURES AND TABLES:

RESUMO

A comunicação eficaz entre as células tumorais e seu ambiente circundante é crucial para a função do tecido, crescimento tumoral, progressão da doença e prognóstico do paciente. Esta tese investiga os diversos papéis dos neutrófilos (NØ) no câncer, com foco particular na sua reprogramação e modulação fenotípica dentro do microambiente tumoral (TME). Para abordar o impacto da modulação bidirecional dos neutrófilos associados ao tumor na progressão tumoral, o estudo é dividido em duas seções principais: uma focada no carcinoma de células escamosas de cabeça e pescoço (HNSCC) e a outra no glioblastoma (GB). Em ambos HNSCC e GB, a modulação dos NØ em direção a um fenótipo pró-tumoral impulsiona significativamente a progressão tumoral. Isso é evidenciado pela angiogênese tumorigênica aumentada, metástase, evasão tumoral, promoção do crescimento e imunossupressão. Os achados experimentais demonstram que tanto as células tumorais quanto os exossomos derivados do tumor (TEX) prolongam a vida útil dos NØ e induzem a NETose, contribuindo para um ambiente imunossupressor. Além disso, o secretoma de NØ modulados por exossomos promove a angiogênese anormal através da desregulação dos sinais de VEGF-A e Ang-2, avançando ainda mais a progressão tumoral. Um alvo terapêutico potencial foi identificado na interferência do sinal de adenosina (ADO) nos NØ, o que poderia melhorar a resposta tumoral às terapias combinadas. Além disso, a correlação entre a morfologia dos NØ e piores desfechos clínicos destaca o potencial das características dos neutrófilos como novos biomarcadores prognósticos. Compreender a reprogramação dos NØ pelas células tumorais e os efeitos mediados pelos TEX pode levar a intervenções inovadoras visando melhorar os resultados do tratamento do câncer, particularmente em HNSCC e GB, onde a infiltração de NØ influencia significativamente a progressão tumoral.

ABSTRACT

Effective communication between tumor cells and their surrounding environment is crucial for tissue function, tumor growth, disease progression, and patient prognosis. This thesis investigates the diverse roles of neutrophils (NØ) in cancer, with a particular focus on their reprogramming and phenotypic modulation within the tumor microenvironment (TME). To address the impact of bidirectional modulation of tumor-associated neutrophils on tumor progression, the study is divided into two main sections: one focusing on head and neck squamous cell carcinoma (HNSCC) and the other on glioblastoma (GB). In both HNSCC and GB, NØ modulation towards a pro-tumor phenotype significantly drives tumor progression. This is evidenced by enhanced tumorigenic angiogenesis, metastasis, tumor evasion, growth promotion, and immunosuppression. Experimental findings demonstrate that both tumor cells and tumor-derived exosomes (TEX) extend NØ lifespan and induce NETosis, contributing to an immunosuppressive environment. Additionally, the secretome of exosome-modulated NØ promotes abnormal angiogenesis through VEGF-A and Ang-2 signaling dysregulation, further advancing tumor progression. A potential therapeutic target was identified in the impairment of adenosine (ADO) signaling in NØ, which could enhance tumor response to combined therapies. Furthermore, the correlation between NØ morphology and poorer clinical outcomes highlights the potential of NØ characteristics as novel prognostic biomarkers. Understanding NØ reprogramming by tumor cells and TEX-mediated effects can lead to innovative interventions aimed at improving cancer treatment outcomes, particularly in HNSCC and GB, where NØ infiltration significantly influences tumor progression.

INTRODUCTION:

Comparing Tumor Microenvironments

In the quest to enhance cancer treatment success and improve patient outcome, there is a growing recognition of the need to explore alternative therapeutic targets. Although healthy tissues are robust against perturbations (BASANTA; ANDERSON, 2017), tumors are capable of interfering with tissue homeostasis to the point that the system is unable to recover the internal balance (FRANCIS; BORNIGER, 2021), providing support for the growth of mutated cells and microenvironment changes. This complex microenvironment consists of blood and lymphatic vessels, fibroblasts, endothelial and immune cells, cytokines, extracellular matrix and vesicles (HANAHAN; WEINBERG, 2011; WU, Shiman *et al.*, 2019).

With this regard, Siddhartha Mukherjee in "The Emperor of All Maladies" provides key insights in evolving understanding of cancer as a dynamic and heterogeneous group of diseases rather than a singular entity. Mukherjee highlights the complex nature of cancer and the lyrical insights into cellular biology to emphasize the need to adopt a more comprehensive approach. The narrative emphasizes the importance of personalized medicine, recognizing the uniqueness of each cancer and the necessity of tailoring treatments accordingly. It becomes evident that targeting a singular aspect of a disease often falls short. A paradigm shift towards a multi-target therapy emerges as a promising avenue to address the dynamic nature of tumors.

Concerning tumor heterogeneity and the imperative for innovative approaches, this thesis reveals the intricate panorama of two distinct yet profoundly lethal tumors, highlighting the critical need for novel strategies in addressing their unique characteristics. Head and Neck Squamous Cell Carcinoma (HNSCC) and Glioblastoma (GB) are distinct types of cancers, each originated in different anatomical locations and presenting unique challenges in terms of diagnosis, treatment, and prognosis (GONG *et al.*, 2023; MAJD; DE GROOT, 2019).

HNSCC is a prevalent form of cancer, with approximately 600,000 new cases reported annually worldwide. It is more common in older individuals and is strongly associated with risk factors such as tobacco and alcohol use, as well as human papillomavirus (HPV) infection in specific cases (LEEMANS; SNIJDERS; BRAKENHOFF, 2018). HPV_{neg} cases tend to display a higher degree of genomic instability, increased aggressiveness, and resistance to therapy, while HPV_{pos} tumors often exhibit a more favorable prognosis due to the unique etiological and molecular profile (KÜRTEN *et al.*, 2021). HNSCC primarily affects the mucosal linings of the oral cavity, pharynx, and larynx, comprising a heterogeneous group of cancers. HNSCC demonstrates a higher propensity for metastasis to regional lymph nodes and distant organs (LEEMANS; SNIJDERS; BRAKENHOFF, 2018). Due to the therapy resistance, the thesis focused on HNSCC-HPV_{neg} type.

On the other hand, GB is a type of brain tumor that exhibit phenotypic and genetic characteristics related to glial cells and is the most aggressive form of primary brain cancer. It represents over 80% of malignant gliomas and has a higher incidence in older adults. There is no clearly established link to specific environmental or lifestyle factors, and the exact cause remains elusive (OMURO; DEANGELIS, 2013).

However, both cancers follow a similar triad protocol that involves a combination of resection surgery, radiotherapy and chemotherapy (LEEMANS; SNIJDERS; BRAKENHOFF, 2018; LI *et al.*, 2019; STUPP; VAN DEN BENT; HEGI, 2005). The use of immunotherapy, particularly immune checkpoint inhibitors like durvalumab (anti-programmed death-ligand 1 (PD-L1)), has shown promise in treating recurrent or metastatic HNSCC, nonetheless, with less than 10% response rate (HERBST *et al.*, 2022; SCHULZ, Daniela *et al.*, 2019). While GB is notorious for its resistance to conventional and innovative therapies as well. Novel treatments, including immunotherapies and targeted therapies, are actively being investigated but not yet with successful results (LI *et al.*, 2019). Early trials in patients with recurrent or metastatic HNSCC, who historically responded poorly to chemotherapy, initially showed improvement of clinical outcomes with the use of anti-PD-1 antibodies like nivolumab or pembrolizumab (MORELLO *et al.*, 2017). Many types

of cancer exploit the overexpression of co-inhibitory ligands to evade attack by cytotoxic T lymphocytes, a mechanism observed in numerous solid tumors. Despite some promising results, antibody-based PD-1/PD-L1 immunotherapy in HNSCC often leads to limited improvement or even its hyperprogression (SCHULZ, D. *et al.*, 2021; SCHULZ, Daniela *et al.*, 2019). Previous research focused on the immune role of the PD-1/PD-L1 interaction, but evidence shows PD-L1 also promotes tumor growth through cell-intrinsic mechanisms (EICHBERGER *et al.*, 2020). Recent study suggest PD-L1's regulation is complex, with multiple tumor cell-intrinsic functions unrelated to immune control (SCHULZ, Daniela *et al.*, 2023). This topic is discussed in more details in **appendix 1**.

Despite their disparate origins, both GB and HNSCC cancers share common features in terms of permissive tumor microenvironment (TME). They share a characteristic invasive and infiltrative growth pattern, allowing them to extend into adjacent tissues. This invasive nature poses challenges for surgeons attempting complete resection of the tumors. Moreover, the ability to sustain the formation of new vessels supports the rapid proliferation of tumor cells by ensuring an adequate blood supply to the growing tumor (IDA MICAILY, 2020; SUT, 2020). Moreover, both create a TME characterized by an abundance of immunosuppressive factors, influencing the antitumor immune response (CHEN, Zhihong; HAMBARDZUMYAN, 2018; WEI *et al.*, 2020). Lastly, HNSCC and GB present significant therapeutic challenges. Their resistance to conventional treatments, necessitates the exploration of innovative therapeutic approaches for more effective disease management (MORTEZAEE, 2020). The Table 1 summarizes the main characteristics exhibited by GB and HNSCC.

	GB	HNSCC	Reference
Location	Brain	Oral cavity, hypopharynx, oropharynx, and larynx	(LI *et al.*, 2019)(LEEMANS; SNIJDERS; BRAKENHOFF, 2018)
Incidence	308.102,00	890.000,00	
Risk factors	?	Cigarette smoking, alcohol consumption, inadequate nutrition, poor oral hygiene, HPV and Epstein–Barr virus, and *Candida albicans* infections	
Age peak	55 to 60	50 to 70	
5-year overall survival	9.8%	50%	
Treatment protocol	Combination of surgery, chemotherapy, and radiation.	Combination of surgery, chemotherapy, and radiation.	
Tumor microenvironment	low immunogenicity, cold tumor	HPV_{neg} cold tumor HPV_{pos} hot tumor	(CHEN, Zhihong; HAMBARDZUMYAN, 2018)(KÜRTEN *et al.*, 2021)
Prognostic factor	IDH1 and IDH2 gene mutation	HPV status	(KORSHUNOV *et al.*, 2019; LEEMANS; SNIJDERS; BRAKENHOFF, 2018)
Histopathological	IDH, EGFR, ATRX, P53, NFP, NSE, Sp11, Ki67	P53, CD44, CD133, ALDH1	(GONÇALVES *et al.*, 2020; GONG *et al.*, 2023)
Molecular markers	deletion mutation of PTEN, G6PD, PI3K	EGFR, PI3K, PD-L1, EMT markers	

Table 1: Comparative table of GB and HNSCC characteristics. Abbreviations: ALDH1: Aldehyde Dehydrogenase 1; ATRX: Alpha Thalassemia/Mental Retardation Syndrome X-linked; CD133: Prominin-1; EGFR: Epidermal Growth Factor Receptor; EMT markers: Epithelial-Mesenchymal Transition markers; G6PD: Glucose-6-Phosphate Dehydrogenase; HPV: Human Papillomavirus; IDH: Isocitrate Dehydrogenase; Ki67: A marker for cell proliferation; NFP: Neurofilament Protein; NSE: Neuron-Specific Enolase; P53: Tumor Protein P53; PD-L1: Programmed Death-Ligand 1; PI3K: Phosphoinositide 3-Kinase; PTEN: Phosphatase and Tensin Homolog

Therefore, extensive research has pointed out the crucial role of the TME in cancer progression and infiltration (MAJD; DE GROOT, 2019). Interactions between immune and tumor cells in diverse TMEs significantly shape cancer progression and treatment response. The body's immune response, comprising innate (e.g., macrophages, neutrophils) and adaptive defense mechanisms (T- and B-lymphocytes), converges within the TME, influencing tumor cells through cellular contact, or soluble mediators like cytokines or extracellular vesicles (HAAS; OBENAUF, 2019; SHARMA; ALLISON, 2015). Immune responses in tumors are

dynamic, influenced by the site characteristics. In inflamed (*hot-tumor*) TMEs, active immune cells signal a better prognosis, initiating immune-mediated tumor control. Conversely, immunosuppressive (*cold-tumor* – **Figure 1**) TMEs, featuring regulatory T cells (Tregs) and myeloid-derived suppressor cells (MDSCs), hinder effective immune responses, presenting a challenge for immunotherapy (CHEN, Daniel S; MELLMAN, 2017; KATHER *et al.*, 2018; RAD *et al.*, 2022). Thus, as tumors evolve, they modulate the TME, altering immune cells' behavior from pro-inflammatory to supporting cancer progression. To the same extent, "An Elegant Defense" by Matt Richtel delves into the sophisticated immune system. Richtel emphasizes the delicate balance required for optimal immune function, exploring instances where this intricate system can turn against the body. Strategies targeting immune responses, disrupting immunosuppression, and promoting inflammation in the TME offer promise across diverse cancer types (CERVANTES-VILLAGRANA *et al.*, 2020; DE LEVE; WIRSDÖRFER; JENDROSSEK, 2019).

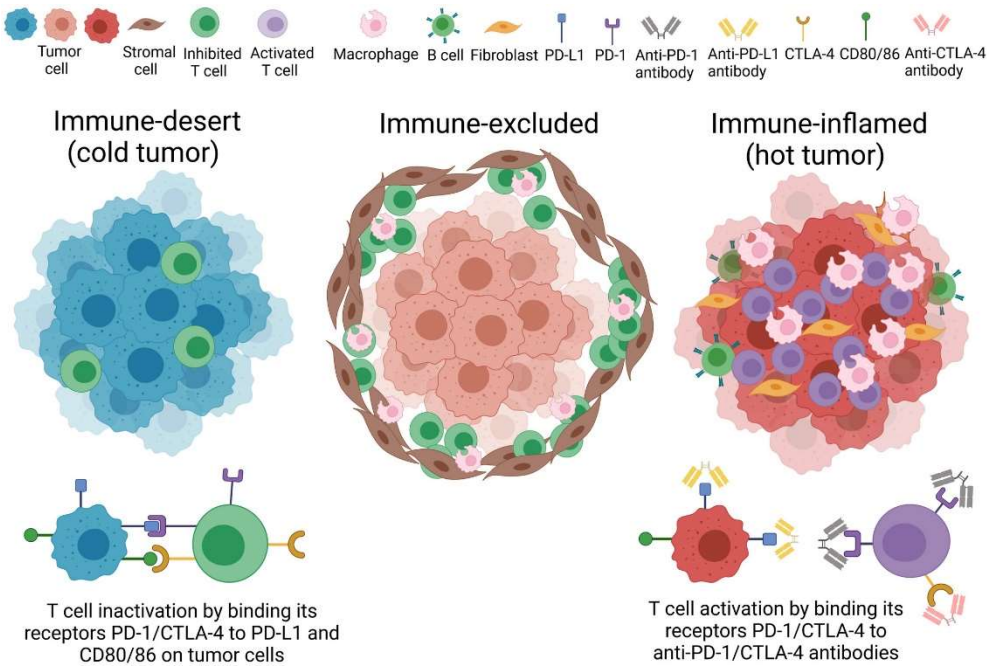

Figure 2: The characteristics of different types of tumor microenvironments. Adapted from (RAD *et al.*, 2022).

Recent studies discuss the significant role of neutrophils (NØ) in tumor progression (GIESE; HIND; HUTTENLOCHER, 2019; JAILLON *et al.*, 2020). Patients with elevated levels of circulating NØ demonstrate increased infiltration in the tumor tissue, such as HNSCC (MASCARELLA *et al.*, 2018) and GB (GOMES

DOS SANTOS *et al.*, 2021), correlating with poor prognosis (LECOT *et al.*, 2019a). Constituting a substantial portion of circulating leukocytes, NØ exhibit phenotypic and functional plasticity, acting either as pro-tumor or anti-tumor entities (GRANOT; JABLONSKA, 2015). The controversy surrounding their contribution to tumor progression highlights the need for further investigations into their role within the TME.

In recent years, the simplistic view of NØ function has been challenged, and interest in their biology is growing. It is now understood that NØ participate in the immune response by regulating and recruiting other immune cells, such as monocytes/macrophages and dendritic cells, and by interacting with B and T cells (SCAPINI; CASSATELLA, 2014). It is crucial to recognize that communication is bidirectional. To that extent, similar to the classification of macrophages into M1 and M2 types, the activation spectrum of NØ can be grouped according to a similar logic: pro-inflammatory/anti-tumor polarization and anti-inflammatory/pro-tumor polarization (GIESE; HIND; HUTTENLOCHER, 2019).

Tumor-associated Neutrophils

Neutrophils are the most abundant immune cells in circulation, accounting for about 50-70% of all leukocytes and serving as the first line of defense against infections (SADIK; KIM; LUSTER, 2011). NØ primary defense mechanisms include phagocytosis, degranulation, and the release of neutrophil extracellular traps (NETs) (WANG, Jing, 2018). Armed with cytotoxic granules, they release antimicrobial compounds, proteases, and contribute to oxidative responses. Besides their antimicrobial role, recent research indicates their involvement in antigen presentation, influencing T cell responses, and antibody-dependent killing (MAYADAS; CULLERE; LOWELL, 2014; NATHAN, 2006). Neutrophils undergo maturation and differentiation in the bone marrow and are released into the bloodstream upon reaching full maturity (MACKEY; COFFELT; CARLIN, 2019; MONTALDO *et al.*, 2022). On this matter, tumor cells take advantage of this process and can excessively activate granulopoiesis, leading to neutrophilia in patients,

increasing the previous discussed NLR (ROSALES, 2018; URIBE-QUEROL; ROSALES, 2015).

Tumor-associated neutrophils (TANs) have a dual role within the TME. On one side, they can initiate pro-inflammatory responses, contributing to the overall inflammation within the tumor (CARNEVALE *et al.*, 2020).

To one hand, they can destroy tumor cells through direct cytotoxic actions involving the production of reactive oxygen species (ROS), TNF-related apoptosis-inducing ligand (TRAIL), and nitric oxide (NO) (EL-BENNA *et al.*, 2016; JAILLON *et al.*, 2020; KOGA *et al.*, 2004). Additionally, either NØ can function as antigen-presenting cells, aiding the antitumor immune response, or support Th1 polarization and the antitumor activity of unconventional T cells (GOVERNA *et al.*, 2017; PONZETTA *et al.*, 2019). Moreover, in the early stages of lung cancer, NØ play a supportive role by enhancing T cell function (ERUSLANOV *et al.*, 2014). NØ are essential for cancer cell elimination through antibody-dependent cellular cytotoxicity and antibody-dependent cellular phagocytosis (BEHRENS; VAN EGMOND; VAN DEN BERG, 2023). With this regard, the engagement of Fc receptors triggers NØ activation and their effector functions. Besides, another study demonstrated NØ-mediated tumor cytotoxicity lead to tumor necrosis (BAKEMA *et al.*, 2011).

Despite possessing potential antitumor functions, NØ exhibit versatility, adopting distinct activation response and phenotypes influenced by the microenvironment, which in turn sustain tumor progression (BALLESTEROS *et al.*, 2020; LECOT *et al.*, 2019b; MÓCSAI, 2013).

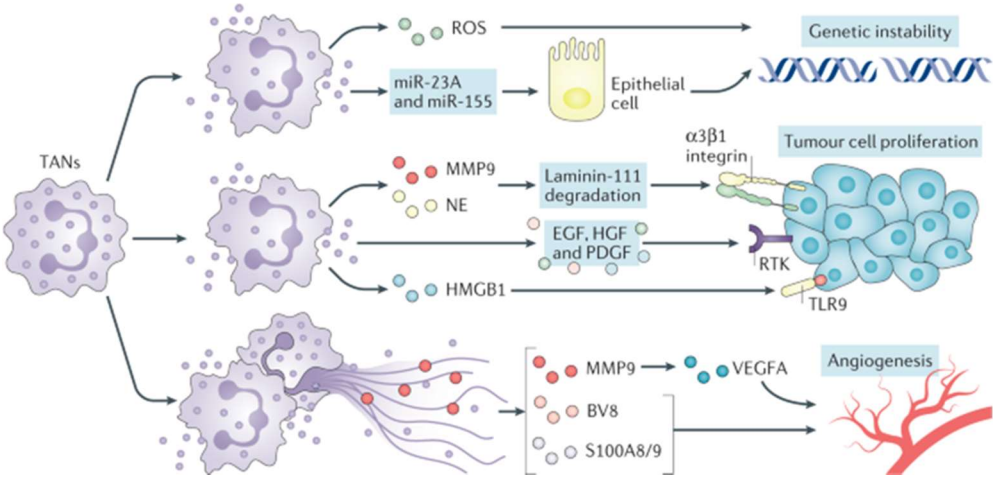

Figure 3: Neutrophils in tumor promotion. Adapted from (JAILLON *et al.*, 2020). Abbreviations: BV8: Prokineticin; HMGB1: High Mobility Group Box 1; MMP9: Matrix Metallopeptidase 9; miR-23A: MicroRNA 23A; miR-155: MicroRNA 155; NE: Neutrophil Elastase; ROS: Reactive Oxygen Species; RTK: Receptor Tyrosine Kinase; S100A8/9: S100 Calcium Binding Protein A8/A9 (also known as calprotectin); TLR9: Toll-Like Receptor 9; VEGF-A: Vascular Endothelial Growth Factor A

Therefore, on the other hand, pro-tumor TANs have been shown to stimulate angiogenesis, a process crucial for the development of new blood vessels. NØ play a key role in producing vascular endothelial growth factor A (VEGF-A) and releasing metalloproteinase-9 (MMP-9), promoting angiogenesis and tissue invasion (GALDIERO *et al.*, 2018). This, in turn, facilitates the increased blood supply necessary for sustained tumor growth (TAZZYMAN; LEWIS; MURDOCH, 2009). Additionally, TANs contribute to immunosuppression by attracting tumor-associated macrophages (TAM) and Tregs, besides inhibiting T lymphocytes response (PILLAY *et al.*, 2013; ZHANG *et al.*, 2020). In addition, NØ infiltration can contribute to genetic instability through the production of ROS and nitrogen (RNS) species (MICHAELI *et al.*, 2017). The same extend, neutrophil extracellular traps (NETs) release, a characteristic function of NØ, to build a DNA-web by briefly comprising granular proteins like elastase (NE) and myeloperoxidase (MPO), form a nuclear network with distinct cell death mechanisms, diverging from apoptosis and necrosis. This process involves nuclear envelope disintegration, exposing content to the cytosol and causing intercellular membrane damage, leading to organelle loss and compromised plasma membrane integrity (**Figure 2**) (AMULIC;; SOLLBERGER, 2018; HANN *et al.*, 2020; LOFFREDO *et al.*, 2017). In tumor conditions, these NETs are implicated in poor prognosis, tumor-associated thrombosis and metastasis formation by potentially capturing circulating tumor cells, aiding their disposition in

other tissues (CHEN, Naifei; HE; CUI, 2022; COOLS-LARTIGUE *et al.*, 2014; DEMERS; WAGNER, 2014; ZHA *et al.*, 2020).

Further details about this topic were addressed in the **Chapter 1**.

Tumor-immune cell communication through exosomes

Tumor cells employ sophisticated strategies to communicate with immune cells, shaping the TME and influencing immune responses (RUBENICH *et al.*, 2021). Exosomes, small extracellular vesicles (sEV) released by various cell types, including tumor cells, play a pivotal role in this intercellular communication. These vesicles, sized between 30–150 nm, originate from multivesicular bodies (MVBs) and exhibit a membrane topography resembling their parent cells (MINCIACCHI; FREEMAN; DI VIZIO, 2015).

Briefly, the biogenesis of exosomes starts with the formation of early endosomes, which internalize extracellular material through membrane budding. These early endosomes mature into late endosomes, incorporating membrane proteins and cargoes from the plasma membrane. Late endosomes then transform into MVBs, forming intraluminal vesicles (ILVs) by invaginating the endosomal membrane, capturing cytoplasmic components. MVBs face two potential fates: fusion with lysosomes for degradation or fusion with the cell membrane, releasing exosomes into the extracellular space (**Figure 3**). The decision between these pathways is tightly regulated by cellular conditions and signaling (BEBELMAN *et al.*, 2018; MATHIEU *et al.*, 2019; YUE *et al.*, 2020). Exosomes carry a complex cargo reflective of their parent cells, including proteins, nucleic acids, lipids, and glycans forming glycoconjugates or lipid rafts on the vesicle surface. Noteworthy, proteins in exosomes include membrane trafficking molecules, integrins, transmembrane proteins, and tetraspanins (e.g., CD9, CD63, CD81), often used as surface markers of exosomes (JEPPESEN *et al.*, 2019; KALLURI; LEBLEU, 2020; RAEVEN; ZIPPERLE; DRECHSLER, 2018).

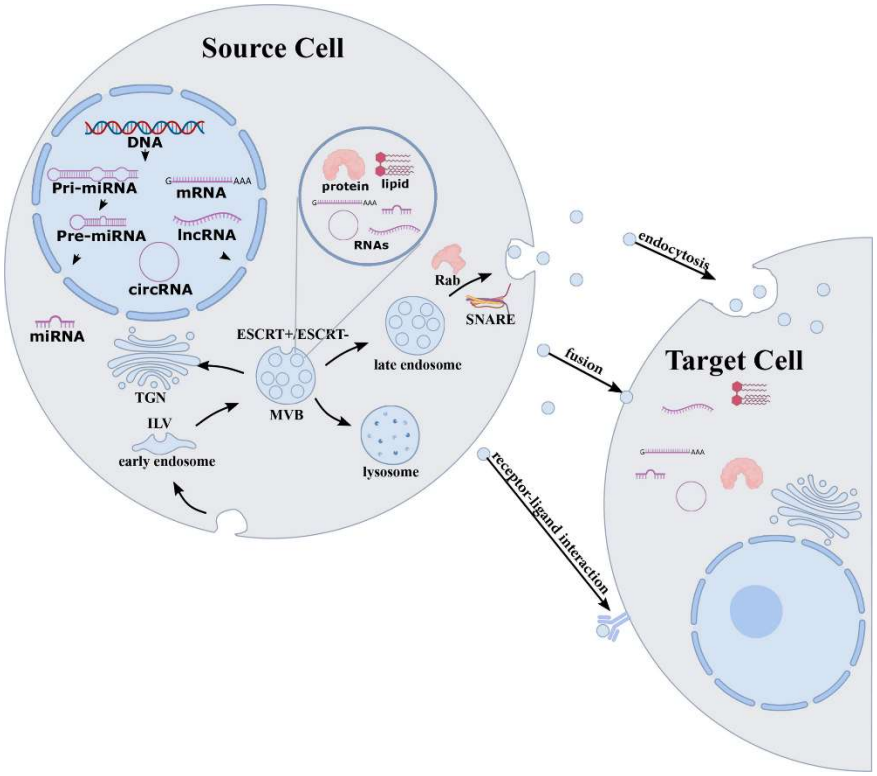

Figure 4: **Schematic representation of the biogenesis, cargo and secretion of exosomes**. Adapted from (YUE *et al.*, 2020). Abbreviations: circRNA: Circular RNA; DNA: Deoxyribonucleic Acid; ESCRT: Endosomal Sorting Complex Required for Transport; ILV: Intraluminal Vesicle; lncRNA: Long Non-Coding RNA; miRNA: MicroRNA; mRNA: Messenger RNA; MVB: Multivesicular Body; pre-RNA: Precursor RNA; pri-miRNA: Primary MicroRNA; Rab: Ras-related Protein in Brain; SNARE: Soluble NSF Attachment Protein Receptor; TGN: Trans-Golgi Network

The content of sEVs can be influenced by the local microenvironment and various stimuli like tissue hypoxia, oxidative stress, or chemotherapeutics. Despite the early stage of understanding sEV biology, their ability to induce reprogramming in recipient cells has been observed, with effects varying based on molecular composition and functional heterogeneity in recipient cells (ALMEIDA *et al.*, 2019; BUI; MASCARENHAS; SUMAGIN, 2018). Laden with diverse cargo, exosomes act as messengers facilitating the transfer of crucial information between cells. In the context of tumor-immune communication, tumor-derived exosomes (TEX) harbor specific molecules that can either enhance or suppress immune responses (LUDWIG, Nils *et al.*, 2020; YANG *et al.*, 2017). TEX may carry immunosuppressive molecules like PD-L1 or transforming growth factor-beta (TGFβ), inhibiting immune cell activity, particularly T cells (LUDWIG, Sonja *et al.*, 2018). Conversely, they can also transfer tumor cell-derived antigens, activating immune responses. TEX can alter the activation state of macrophages, directing them toward a pro-tumor, anti-

inflammatory phenotype (FIANI *et al.*, 2020). Recent findings highlight the role of exosomes in modulating NØ functions, adding a new dimension to cancer perspectives (RUBENICH *et al.*, 2021). Importantly, exosome-mediated communication extends beyond local effects, exerting systemic influences. TEX released into circulation disseminate information to distant sites, preparing pre-metastatic niches and modulating immune responses in distant organs (**Figure 4**) (FENG *et al.*, 2019). This topic is discussed in more details in the **Chapter 1** of this thesis.

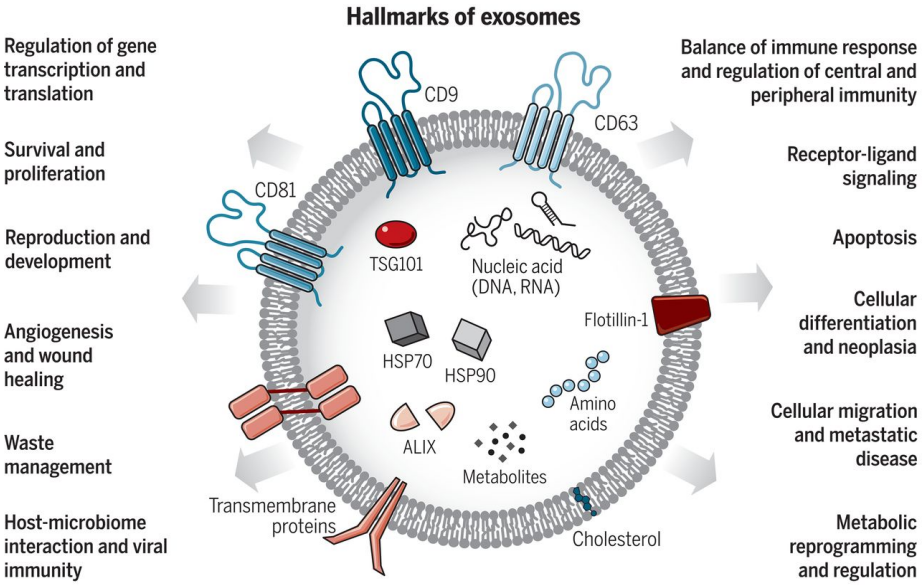

Figure 5: Hallmarks of exosomes. Adapted from (KALLURI; LEBLEU, 2020)**.** Abbreviations: ALIX: ALG-2-interacting protein X; HSP: Heat Shock Protein; TSG101: Tumor Susceptibility Gene 101

Purinergic signaling

Considering that tumor cells are always developing methods of tumor escape, inhibition of the immune response by excess adenosine triphosphate (ATP) and adenosine (ADO) is a very effective mechanism (ALLARD, Bertrand *et al.*, 2017). The direct relationship of purinergic signaling in the progression of cancer, such as GB [83] and HNSCC [84], correlates with various malignant processes such as migration, epithelial to mesenchymal transition (EMT), invasion, proliferation, chemoresistance, differentiation, tumor growth, angiogenesis, and invasiveness (GELSLEICHTER *et al.*, 2023).

The heightened inflammation and stress in the TME lead to the release of purines, such as ATP, from damaged cells (DOSCH *et al.*, 2018). Ectonucleotidases facilitate the conversion of extracellular ATP to adenosine (ADO). This process involves enzymes like NTPDase1/CD39 hydrolyzing ATP to AMP, which is then converted to ADO by CD73 (GELSLEICHTER *et al.*, 2023) (**Figure 5**). In addition to the direct influence in the activation and functional properties of NØ (CHEN, Yu *et al.*, 2010; GIULIANI; SARTI; DI VIRGILIO, 2020; GRASSI, 2010), instigates the hypothesis that phenotype modulation could be linked by this pathway.

ADO mediates its effects through P1 purinoceptors, including A1, A2A, A2B, and A3, which are G protein-coupled receptors (CORRIDEN *et al.*, 2008; WANG, Sheng *et al.*, 2021). A1 and A3 receptors are inhibitory, reducing intracellular cAMP levels, while A2A and A2B receptors are generally excitatory, increasing cAMP levels. The sensitivity of P1 receptors to ADO varies depending on its extracellular concentration, with A1 receptors preferred at lower levels and A2A and A3 receptors favored at higher levels (CAMPOS-CONTRERAS; DÍAZ-MUÑOZ; VÁZQUEZ-CUEVAS, 2020; DI VIRGILIO; VUERICH, 2015; LINDEN, 2011).

P1 receptors are widely expressed, with roles in various systems, including immune function. Briefly, A1 receptors promote NØ chemotaxis, A2A receptors induce immunosuppressive responses, A2B receptors drive inflammatory responses, and A3 receptors modulate NØ chemotaxis and mast cell degranulation (GRASSI, 2010). ADO tends to exert immunosuppressive effects, hindering TAN-mediated immune responses and inhibiting pro-inflammatory cytokine release (ALLARD, Bertrand *et al.*, 2017; ARAB; HADJATI, 2019). To that extend, activation of $A2_A$ receptors on TANs can compromise their cytotoxic capabilities, potentially promoting tumor growth and immune evasion (TANG *et al.*, 2010).

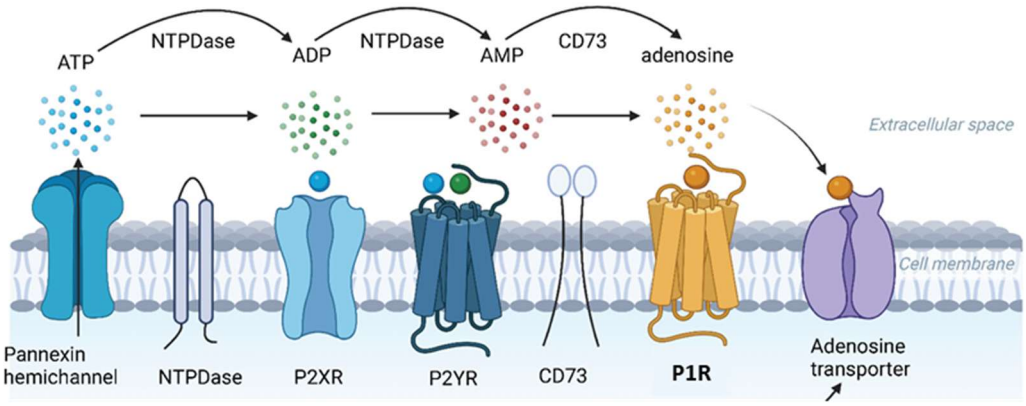

Figure 6: The elements of the purinergic signaling system. Adapted from (VLAJKOVIC; THORNE, 2022).

Manipulating purinergic pathway emerges as a promising therapeutic approach to modulate TAN activity. Such interventions could tip the balance toward antitumor immune responses, paving the way for the development of novel immunotherapies (ALLARD, David *et al.*, 2019; ARAB; HADJATI, 2019).

The hypothesis: neutrophils as a convergent target:

The numerous new cancer cases, especially those showing resistance to existing treatments leading to reduced survival rates, highlight the need for a deeper understanding of the disease. Theories targeting new therapeutic avenues, encompassing both chemotherapy and immunotherapy, often encounter practical challenges observed in clinical settings and patient responses. For those exhibiting resistance, few treatment options remain. Consequently, new areas of research seek insights into why and how tumor cells successfully evade our treatment strategies through adjacent cells.

One recent focus is understanding the communication between tumor cells and the immune system, particularly innate immune cells. This shift in perspective shows great promise, especially as the immune infiltrate composition in non-responsive tumors is limited to myeloid and regulatory cells. Emphasizing this perspective has led to discoveries proving that our immune cells are much more than classically activated as taught and described in textbooks. The spectrum of

activation, well-documented in T lymphocytes, is now being observed in macrophages and, more recently, in NØ. The hypothesis that tumors can manipulate cells within their niche and systemically has led us into the universe of TAN.

This thesis is based on studying the cellular behavior and activation of NØ in two tumor types with high mortality rates and minimal response to conventional therapies considered gold standard. Two distinct tumor types were selected to observe whether the behavior of TAN follows a pattern of response.

Both GB and HNSCC are recognized as aggressive tumor types. Different cancer types exhibit unique characteristics that profoundly affect their behavior, responses to treatments, and overall prognosis. Research explores the presence of cells with an inflammatory profile in the TME, with NØ identified as key player. While evidence indicates the existence of NØ with anti- and pro-tumor phenotypes, the mechanisms influencing their functional behavior and role in cancer perpetuation remain unclear. The emerging evidence poses new questions, delving into the spectrum of NØ activation, the molecular basis of their plasticity, and their significance in activation, expression, and regulation. The importance of purinergic signaling in NØ response emerges as a potential strategy to inhibit the pro-tumor phenotype. This knowledge aims to advance cancer research, with the potential to enhance patient outcomes and broaden the spectrum of treatment options for these tumors.

Thus, this thesis unfolds across ten chapters focusing on NØ functionality and response both in head and neck squamous cell carcinoma (HNSCC) and glioblastoma (GB).

OBJECTIVES:

Main objective:

Investigate the bidirectional modulation of tumor-associated neutrophils in tumor progression.

Specific Objectives:

1. Summarize existing literature on how exosomes facilitate communication between the tumor microenvironment (TME) and neutrophils, exploring their impact on cellular behavior and function.

2. Apply bioinformatics methods to elucidate how extracellular vesicles (EVs) contribute to shaping the cellular makeup of the TME, focusing on their influence on different cell types.

3. Investigate how exosomes derived from HNSCC cells attract and interact with neutrophils, leading to the induction of an immunosuppressive phenotype that supports cancer progression through CD73/PD-L1 axis, with a focus on neutrophil ADO signaling.

4. Explore how HNSCC-derived exosomes regulate neutrophil apoptosis, particularly examining the role of ADO signaling in modulating survival.

5. Assess the ability of HNSCC-derived exosomes to induce the release of neutrophil extracellular traps (NETs) via ADO-dependent signaling.

6. Investigate how TEX influence neutrophil phenotype towards a pro-tumor angiogenic state, impacting the development of aberrant tumor vasculature in HNSCC.

7. Explore the communication and reprogramming between neutrophils and glioblastoma (GB), assessing how neutrophils promote GB progression following interaction and influence by the TME.

8. Analyze the participation of ADO signaling in tumor-associated neutrophil in sustaining immunosuppression in GB.

9. Establish the clinical significance of neutrophil morphology in the context of GB, examining its implications for disease progression.

10. Develop an artificial intelligence (AI) model utilizing computer vision techniques to classify and detect the polarization state of peripheral neutrophils in patients with GB.

PREFACE

In order to address the impact of bidirectional modulation of tumor-associated neutrophils in tumor progression, the specific objectives proposed were organized in 2 main sections, as follow:

The first section begins with a Review article (**Chapter 1**) produced during the COVID19 pandemic, which explored the existing literature about how exosomes participate of the neutrophil-tumor cell crosstalk (RUBENICH *et al.*, 2021).

The effects of TEX derived from HNSCC on the TME are well-documented in various studies. However, the specific mechanisms through which these EVs influence TME composition are still not well understood. Therefore, the **Chapter 2** (KALLINGER *et al.*, 2023) employed a bioinformatics approach to elucidate the role of HNSCC-derived EVs in shaping the cellular makeup of the TME. We focused on two recently identified gene signatures associated with increased TEX release.

The following chapter were produced during the period abroad in the 1 year-doctorate program.

The impact of NØ modulation by TEX on immune response and tumor outcomes is explored through various approaches. Their significance in immunosuppression within the TME, by increasing the expression of the CD73/PD-L1 axis (**Chapter 3**, Rubenich et al 2024 – under review *Journal of Extracellular Vesicles*), as well as modulating survival-promoting biochemical pathways leading to increased NØ viability via NFκB activation (**Chapter 4**, Rubenich et al 2024 – under review *Frontiers in Immunology*), indicates that the strong presence of NØ in the tumor niche supports disease progression. Similarly, **Chapter 5** (Rubenich et al, 2024 - under review at *Biochem Biophys Res Communication*) delves into the characteristic action mechanism of NØ, namely NØ Extracellular Traps (NETs), demonstrating that NETs induction increases malignancy markers, suppression, and metastasis. Based on these findings, we investigate the importance of pro-tumor NØ in forming new blood vessels and their capacity to promote defective tumor angiogenesis (**Chapter 6** - under preparation). This dataset reveals that the

pro-tumor NØ phenotype drives tumor progression both through direct action on the tumor and by modulating the microenvironment.

In the second section, the chapters focus on studies in glioblastoma performed at UFCSPA. The overarching objective remains understanding the bidirectional communication between NØ and tumors, revealing tumor adaptation to NØ presence and direct modulation of NØ by tumor cells (**Chapter 7**, (RUBENICH *et al.*, 2023)). Next, we characterize tumor biopsy samples to quantify and correlate them with the ADO pathway of TAN. This led to the identification of a nuclear PD-L1 in patient samples that significantly correlated with NØ gene modulation and immunosuppression (**Chapter 8** – under preparation). In addition, after slide observations we propose that the tumor outcome and phenotypic alteration of NØ in glioma patients can be visualized under microscope. Therefore, we proposed NØ as prognostic biomarkers through NØ morphological evaluation (**Chapter 9** – under preparation). This section ends with the attempt to develop a prognostic software using artificial intelligence for image recognition to predict immune response to tumors (**Chapter 10** – under preparation).

As you delve into the following chapters, you will find detailed explorations of the fundamental role of NØ in cancer progression, each contributing to a deeper understanding of the phenomena discussed here.

Enjoy reading!

SUMÁRIO:

Chapter 1: Small extracellular vesicle-mediated bidirectional crosstalk between neutrophils and tumor cells

Cytokine and Growth Factor Reviews

(https://www.sciencedirect.com/journal/cytokine-and-growth-factor-reviews)

Impact Factor: 13

DOI: https://doi.org/10.1016/j.cytogfr.2021.08.002

PMID: 34479816

PMCID: PMC9235060

Accepted 24 August 2021

Cytokine and Growth Factor Reviews xxx (xxxx) xxx

Contents lists available at ScienceDirect

Cytokine and Growth Factor Reviews

journal homepage: www.elsevier.com/locate/cytogfr

Small extracellular vesicle-mediated bidirectional crosstalk between neutrophils and tumor cells

Dominique S. Rubenich [a,b], Natália Omizzollo [a,b], Mirosław J. Szczepański [c], Torsten E. Reichert [d], Theresa L. Whiteside [e,f], Nils Ludwig [d,1,*], Elizandra Braganhol [a,b,**,1]

[a] Programa de Pós-Graduação em Biociências, Universidade Federal de Ciências da Saúde de Porto Alegre (UFCSPA), Porto Alegre, RS, Brazil
[b] Instituto de Cardiologia do Rio Grande do Sul/Fundação Universitária do Instituto de Cardiologia (IC-FUC), Porto Alegre, RS, Brazil
[c] Department of Biochemistry, Medical University of Warsaw, 02-097, Warsaw, Poland
[d] Department of Oral and Maxillofacial Surgery, University Hospital Regensburg, 93053, Regensburg, Germany
[e] Departments of Pathology, Immunology and Otolaryngology, University of Pittsburgh School of Medicine, Pittsburgh, PA, 15213, USA
[f] UPMC Hillman Cancer Center, Pittsburgh, PA, 15213, USA

ARTICLE INFO

Keywords:
Neutrophils
Small extracellular vesicles
Tumor-derived exosomes (TEX)
Tumor-associated neutrophils (TAN)
Tumor microenvironment (TME)

ABSTRACT

Neutrophils are the first line of defense against tissue injury and play an important role in tumor progression. Tumor-associated neutrophils (TANs) mediate pro-tumor immunosuppressive activity and their infiltration into tumors is associated with poor outcome in a variety of malignant diseases. The tumor cell-neutrophil crosstalk is mediated by small extracellular vesicles (sEVs) also referred to as exosomes which represent a major mechanism for intercellular communication. This review will address the role of neutrophil-derived sEVs (NEX) in reprogramming the TME and on mechanisms that regulate the dual potential of NEX to promote tumor progression on one hand and suppress tumor growth on the other. Emerging data suggest that both, NEX and tumor-derived sEVs (TEX) carry complex molecular cargos which upon delivery to recipient cells in the tumor microenvironment (TME) modulate their behavior and reprogram them to mediate pro-inflammatory or immunosuppressive responses. Although it remains unknown how the balance between the often conflicting signaling of TEX and NEX is regulated, this review is an attempt to provide insights into mechanisms that underpin this complex bidirectional crosstalk. A better understanding of the signals NEX process or deliver in the TME might lead to the development of novel approaches to the control of tumor progression in the future.

1. Introduction

The tumor microenvironment (TME) is a structurally complex, tumor-driven milieu of various cells, all programmed to promote tumor growth. In addition to tumor cells, blood vessels, extracellular matrix (ECM) components and other non-malignant cells, including fibroblasts, epithelial cells, and immune cells are components of the TME (Fig. 1**A**). Neutrophils are also identified in the TME of most human tumors, although for many years, their presence in human tumors was a subject of considerable controversy [1]. More recent studies confirm that neutrophils are a component of the TME in most, if not all, human tumors and suggest that infiltration of neutrophils into the tumor is linked to poor prognosis [2].

Neutrophils are a component of the innate immune system, representing 50–70 % of circulating leukocytes in humans under normal physiological conditions [3]. They are the first cell type recruited to the site of tissue injury. After neutrophil granulopoiesis and mobilization, their recruitment is mainly mediated by CXCR1/CXCR2 in response to pathogen-associated or damage-associated molecular patterns (PAMPs and DAMPs, respectively) [4]. Neutrophils effectively participate in immune/inflammatory responses, utilizing various mechanisms such as phagocytosis, degranulation and/or extracellular trap (NET) formation (Fig. 1**B**) [5]. They also secrete a variety of chemokines, which promote the recruitment of other immune cells, including macrophages [6].

* Corresponding author at: University Hospital Regensburg, Franz-Josef-Strauss-Allee 11, D-93053, Regensburg, Germany.
** Corresponding author at: Universidade Federal de Ciências da Saúde (UFCSPA), Sarmento Leite, 245 – Main Building – Room 304, 90.050-170, Porto Alegre, RS, Brazil.
E-mail addresses: nils.ludwig@ukr.de (N. Ludwig), ebraganhol@ufcspa.edu.br (E. Braganhol).
[1] These authors contributed equally.

https://doi.org/10.1016/j.cytogfr.2021.08.002
Received 3 August 2021; Accepted 24 August 2021
Available online 28 August 2021

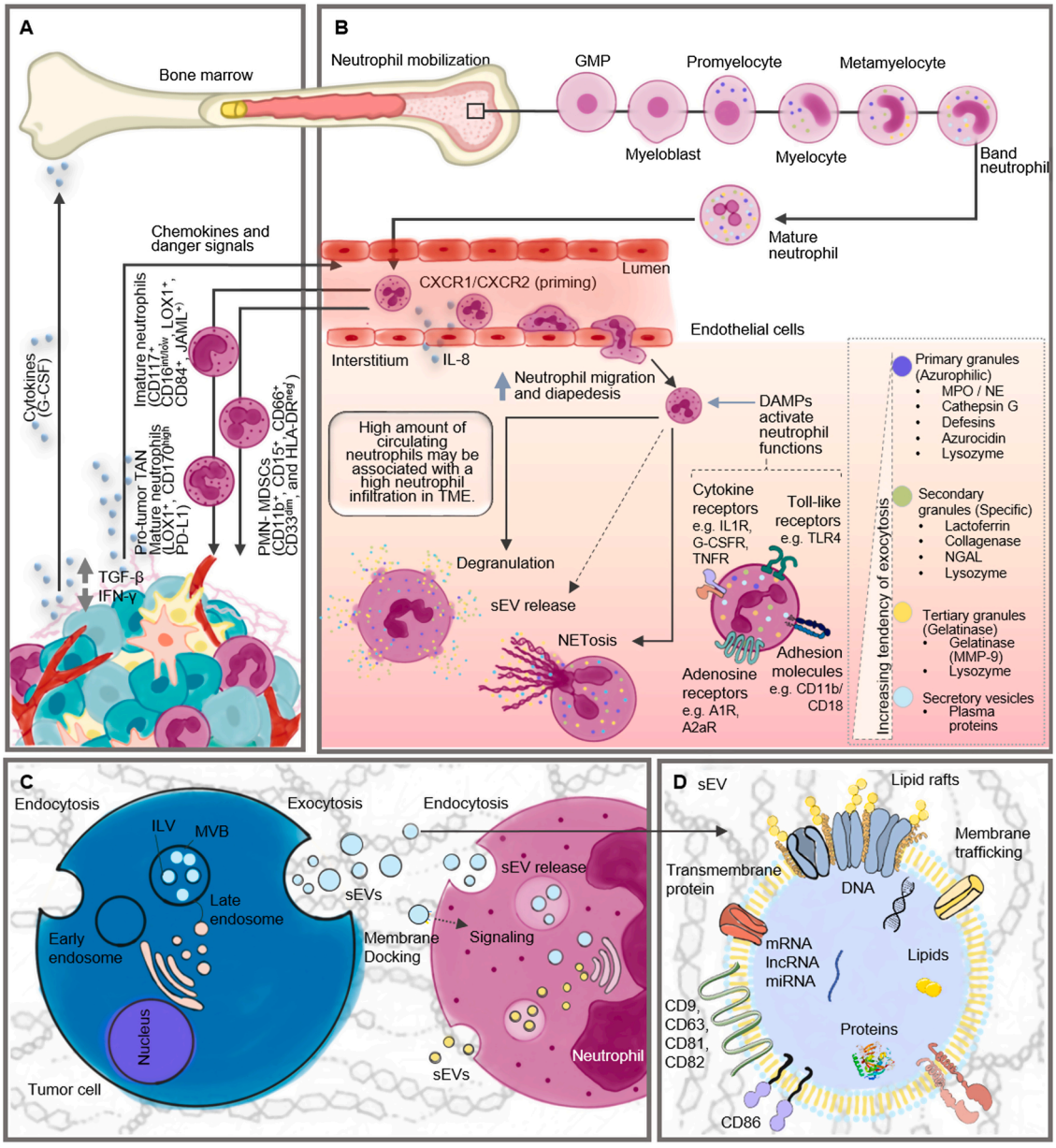

Fig. 1. Neutrophil mobilization and functions in cancer. **(A)** Cells in the TME release cytokines, such as G-CSF, which induces granulopoiesis in the bone marrow, and chemokines which stimulate the migration of different neutrophil subpopulations. Some factors, such as TGF-β, are involved in promoting a pro-tumor phenotype in neutrophils. **(B)** Granulopoiesis is the formation and maturation of neutrophils, which is also important for granule production. Neutrophils are attracted to the bloodstream through cytokines and chemokines, especially by the release of IL-8 and their activation *via* CXCR2. Neutrophil primes with the first stimuli and enhanced expression of adhesion molecules, which allows diapedesis. When neutrophils reach the tumor site, they are exposed to second stimuli, such as DAMPs, and accomplish their major functions: NETosis, degranulation and extracellular vesicle release. Neutrophils express a variety of cell surface proteins: chemokine receptors, for responding to chemokines; toll-like receptors, which recognize tumor molecules, such as HMGB1; adhesion molecules for migration and diapedesis; activation markers; adenosine receptors, which bind ADO and enhance immunosuppressive functions. **(C)** Tumor cells are capable of producing sEVs as a mean of cell communication. The biogenesis of these sEVs occurs *via* initial endocytosis, which forms early endosomes and later MVBs with ILVs, followed by exocytosis and sEV release. sEVs can be internalized by recipient cells and reprogram its phenotype and functions. Neutrophils can internalize sEVs *via* endocytosis. Also, neutrophils are capable of producing their own sEVs (NEX), which are released to the extracellular space and interact with a variety of different cells types. **(D)** General cargo composition of sEVs: the cargo changes according to the metabolism of the parent cell and each sEV can carry different molecules even if derived from the same cell. Abbreviations: G-CSF - granulocyte colony-stimulating factor, IFNγ – interferon gamma, TGF-β - transforming growth factor beta, IL-8 - interleukin-8, CXCR2 - CXC chemokine receptor 2, DAMPs - damage-associated molecular patterns, PMN - polymorphonuclear, MPO - myeloperoxidase, NE – neutrophil elastase, MMP-9 – metalloproteinase 9, NGAL – neutrophil gelatinase-associated lipocalin, sEVs – small extracellular vesicles, MVB – multivesicular, ILV - intraluminal vesicles, HMGB1 - high mobility group box 1, ADO – adenosine.

Neutrophils are characterized by phenotypic and functional plasticity, that enables them to play multiple roles in immune/inflammatory responses. It is in this context that the concept of neutrophil heterogeneity has been introduced [7]. Indeed, the existence of the neutrophil polarization spectrum characterized by N1 and N2 phenotypes, similar to those described for macrophages, has been proposed [8]. N1 neutrophils are inflammatory and N2 neutrophils are involved in tissue reconstitution/regeneration and angiogenesis, which are especially important for the support of tumor growth. This functional polarization does not exclude the likely possibility that the same neutrophil is capable of

performing a spectrum of functions depending on the conditions in the microenvironment.

The participation of neutrophils in tumor progression has been controversial and the neutrophil plasticity has been used to explain their dual role in the TME [9]. The ability of neutrophils to communicate with other immune cells, such as macrophages, lymphocytes or natural killer (NK) cells has been recognized as a key feature of their biology. The ability of both tumors and neutrophils to produce and release small extracellular vesicles (sEVs) to the extracellular environment is an important mechanism for communication with other cells [10]. It is likely that sEVs may be responsible for neutrophil capabilities to "sense" and respond to external signals in the TME as well as tumor cells to modulate and promote a convenient environment through the release of tumor-derived small extracellular vesicles (TEX). sEVs have been in the limelight as a major intercellular communication system in health and disease [11]. Therefore, this review will address the role of neutrophil-derived small extracellular vesicles (NEX) and TEX in reprogramming the TME and on mechanisms that regulate the potential of sEVs to promote tumor progression.

2. The role of neutrophils in cancer

Neutrophil infiltration in solid tumors has been associated with worse prognosis [12]. The number and phenotypic as well as functional attributes of tumor-infiltrating neutrophils can serve as biomarkers of response to chemotherapy or immunotherapy and survival in patients with cancer [2]. Although interactions of neutrophils with tumor or non-malignant cells in the TME are not yet fully understood, their engagement in sophisticated bidirectional interactions with these cells has been reported [13]. Emerging evidence associates increase in the number of circulating neutrophils with poor prognosis in different types of malignancies, including glioblastoma [14]. Prognostic relevance of neutrophils is usually based on calculations of the neutrophil to lymphocyte ratio (NLR). The NLR has been used as a prognostic factor of overall survival (OS) in many types of solid tumors, including gastric [15] and head and neck [16] cancers and high NLR values associate with worse prognosis for cancer patients [17]. Moreover, it has been shown to correlate with the abundance of neutrophils infiltrating the TME [18]. Importantly, not only the number but also the location of neutrophils within the TME appears to impact their activation and functions and can, therefore, have prognostic relevance. Also, OS varies, depending on whether neutrophils are localized in the tumor nests (intratumoral), around the tumor nests (peritumoral), or in the tumor-associated stroma [2,19,20].

Tumor-associated neutrophils (TANs) are predominantly classified based on their phenotypes, as discussed below. Recent studies report the existence of different subpopulations of neutrophils in the TME, which are characterized by distinct functions during tumor progression [21]. One hallmark of neutrophils is their phenotypic plasticity which can be modulated by environmental conditions. Thus, activation of neutrophils largely depends on the surrounding microenvironment [22]. TANs are known to act either as tumor promotors or as tumor suppressors, depending on the microenvironmental context, which clearly changes as the tumor develops and progresses. The dual role of TANs reflects the constantly changing complexity of the TME and of TAN interactions with different cell types, such as tumor-associated macrophages [23]. Today, the nomenclature of TANs still needs to be established and the definition of phenotypes for different TAN subsets in the TME awaits further studies [9].

Current evidence indicates that TANs promote tumor growth, invasion, angiogenesis, and metastasis in various types of cancer [24]. TANs are exposed to a variety of stimuli in the TME, such as granulocyte colony-stimulating factor (G-CSF), interleukin (IL)-8, and transforming growth factor β (TGF-β), which alter their maturation and polarization states [25]. Neutrophils mediating anti-tumor activities are known for their cytolytic activity directed at tumor cells and, at the same time, for displaying an immunostimulatory profile (*i.e.*, TNF-α^{high}, $CCL3^{high}$, ICAM-1^{high}, $Arginase^{low}$). These TANs produce higher levels of superoxide and hydrogen peroxide, in contrast to pro-tumor TANs, which mediate immunosuppressive functions and upregulate expression of chemokines CCL2, 3, 4, 8, 12, and 17 as well as CXCL1, 2, 8 and 16 [26]. According to Jaillon et al. human pro-tumor TANs are characterized by expression of LOX-1^+, $CD170^{high}$ and PD-$L1^+$, while anti-tumor TANs express $CD54^+$, $HLA\text{-}DR^+$, $CD86^+$, and $CD15^{high}$. Immature TANs express $CD117^+$, $CD16^{int/low}$, LOX-1^+, $CD84^+$, and $JAML^+$ (Fig. 1**A**). Besides, mouse pro-tumor TANs express $Ly6G^+$, $CD11b^+$, PD-$L1^+$, $CD170^{high}$ and mouse anti-tumor neutrophils express $Ly6G^+$, $CD170^{low}$, $CD177^+$, $CD54^+$, and $CD16^+$. Immature mouse TANs are known for expressing $Ly6G^+$, $CD11b^+$, $CD117^+$, $CD170^{low}$, $CD101^-$, $CD84^+$, and $JAML^+$ [27].

Another immune cell subset accumulating in tumors are the myeloid-derived suppressor cells (MDSCs). Their major function is the suppression of anti-tumor T cell functions and promotion of tumor progression. In cancer and in other pathological conditions, G-CSF is overproduced and favors MDSC generation, as extensively reviewed [28,29]. MDSC activity in the TME is closely related to the neutrophil (G-MDSC) or monocyte (M-MDSC) differentiation [28,30]. It is currently under debate whether the origin of the MDSC population is the same as that of neutrophils. However, just recently, G-MDSCs, also known as polymorphonuclear MDSCs (PMN-MDSCs), were described as "neutrophils with proven immunosuppressive activity" [27,31]. Numbers of PMN-MDSCs are elevated in the blood of cancer patients and they are thought to exert tumor-promoting functions, including suppression of the adaptive immune responses, stimulation of angiogenesis, and shaping of pre-metastatic niches [32]. It has also been described that the protein expression profile of pro-tumor G-MDSCs includes $CD11b^+$, $CD15^+$, $CD66^+$, $CD33^{dim}$, and $HLA\text{-}DR^{neg}$ [33]. To discriminate neutrophils from PMN-MDSCs, a panel of several markers, including expression of the lectin-type oxidized LDL receptor 1 (LOX-1) are currently used. LOX-1^+ neutrophils are potent suppressors of T cell proliferation and genomically resemble MDSCs, while LOX-1^- neutrophils do not mediate immunosuppressive effects [34].

Cell interactions involved in the neutrophil-tumor crosstalk that takes place in the TME are illustrated in Fig. 1. First, the figure presents cytokine-mediated effects on granulopoiesis in the bone marrow, maturation of neutrophils, and their diapedesis and entry into the TME. Next, the capability of TANs to produce and release sEVs is presented. TANs have recently emerged as a major producer of sEVs that are engaged in promoting tumor growth and impacting disease outcome. Therefore, TANs have acquired clinical relevance, and understanding of the mechanisms that are responsible for TAN-mediated tumor-promoting activities are of great importance.

3. Small extracellular vesicles (sEVs) and their role in cancer

Small extracellular vesicles (sEVs) or also referred to as exosomes are currently in the limelight as potential mediators of intercellular crosstalk [35]. sEVs are a subset of EVs deriving from multivesicular bodies (MVBs) and sized at 30–150 nm in diameter. They are of particular interest, due to their unique biogenesis and the surface membrane topography that mimics that of parental cells [36]. This EV subset is distinct from larger (~500 nm) microvesicles and even larger (~1000 nm) apoptotic bodies (Fig. 1**C**) [37]. The biogenesis of sEVs has been extensively investigated and has been recently reviewed [35]. The cargo of sEVs released by parent cells is complex, reflects the content of parent cells and consists of proteins, nucleic acids, lipids and glycans, forming glycoconjugates or lipid rafts on the sEV surface. The protein content of sEVs is enriched in membrane trafficking molecules, integrins, transmembrane proteins and tetraspanins (CD9, CD63, CD81). The latter are often used as sEV surface markers (Fig. 1**D**) [38]. The overall cargo of sEVs can shift depending on the local microenvironment of the parent cells, and various environmental stimuli such as tissue hypoxia,

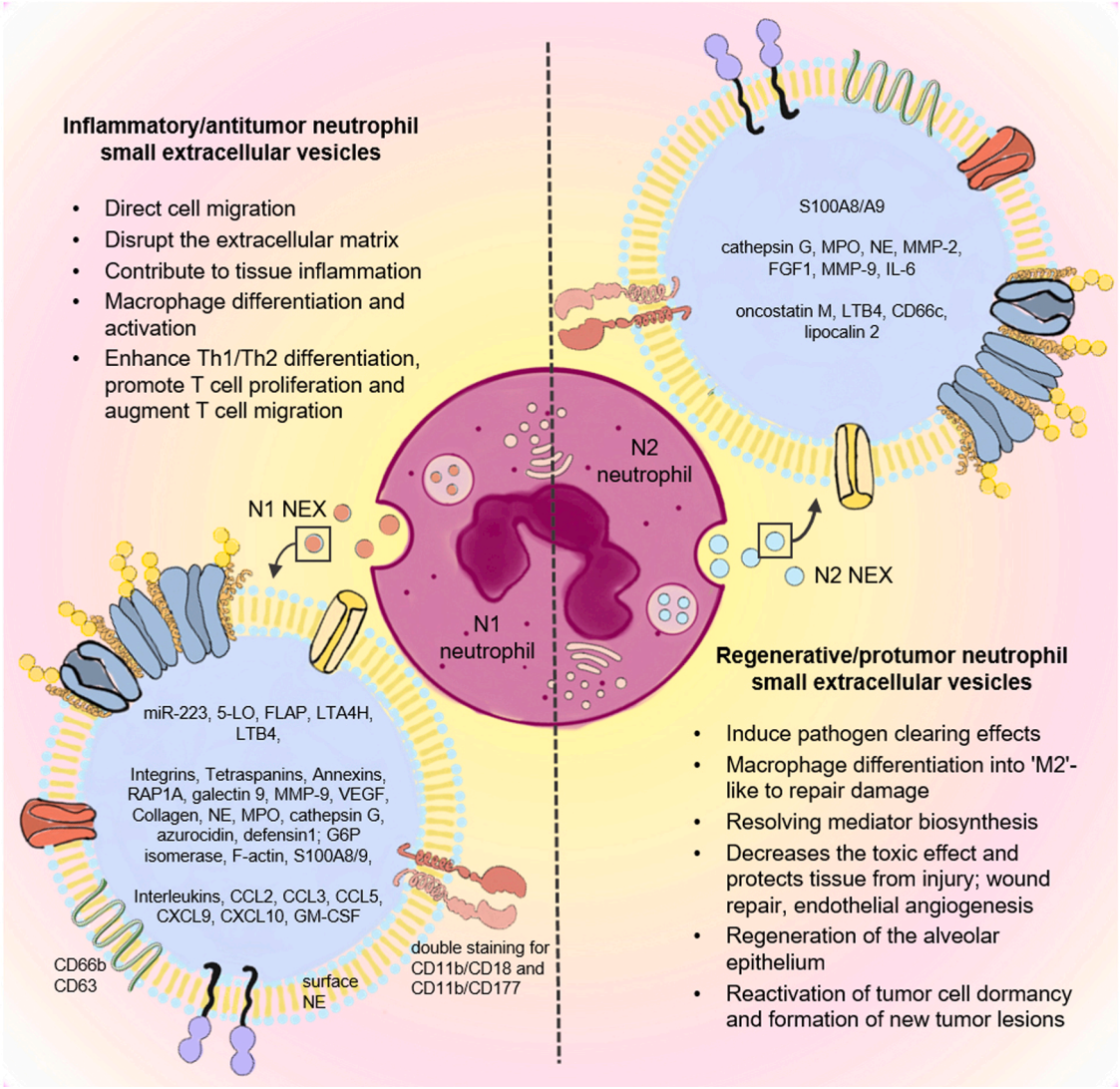

Fig. 2. Differential neutrophil polarization as source of N1 and N2 NEX. The phenotypes and biological functions of neutrophils are heterogenous and it is most likely that this heterogeneity is reflected in NEX. The molecular content of NEX was found to be varying depending on the microenvironmental conditions of the parent cells, thus N1 and N2 neutrophils might produce N1 NEX and N2 NEX, respectively. N1 NEX have the potential to promote anti-tumor effects and might enhance the anti-tumor immune response with special regards to lymphocytes. N2 NEX carry tumor-promoting cargo components, which are potentially involved in promoting tumor growth, survival, angiogenesis and escape of immune surveillance.
Abbreviations: NEX – neutrophil-derived small extracellular vesicles, A2MG – alpha-2-macroglobulin, MPO - myeloperoxidase, NE – neutrophil elastase, MMP-2 – mettaloproteinase-2, FGF1 - fibroblast growth factor 1, MMP-9 – mettaloproteinase-9, HSPs - heat shock proteins, IL-6 – interleukin-6, LTB4 - leukotriene B4, 5-LO - 5-lipoxygenase, FLAP - 5-lipoxygenase-activating protein, LTA4H - leukotriene A4 Hydrolase, VEGF - vascular endothelial growth factor.

oxidative stress or chemotherapeutics are known to alter the content of sEVs [37].

Today, understanding of the sEV biology is in its infancy, but their capability to induce reprogramming of recipient cells has been noted and followed. The effects sEVs induce in recipient cells vary depending on their molecular cargo and probably also on the molecular make up of recipient cells, resulting in functional heterogeneity [37]. Interactions between sEVs and recipient cells usually involve delivery of the sEV cargo to recipient cells, but it can also occur without any cargo delivery. This happens when sEVs interact directly with receptors on the surface of recipient cells. The mechanism(s) underpinning membrane docking of sEVs is still unclear; however, commonly described surface proteins, such as integrins appear to be involved [39]. Cells internalize sEVs using various endocytic pathways, including clathrin-dependent endocytosis, and clathrin-independent pathways such as caveolin-mediated uptake, macropinocytosis, phagocytosis, and lipid raft-mediated internalization (Fig. 1**C**) [40].

sEVs entering the recipient cell, such as an immune cell, exert various effects that are biologically relevant and include alterations in functional competence. Specifically, tumor cell-derived small extracellular vesicles (TEX) impair anti-tumor functions of immune cells [41]. Cancer patients have elevated levels of circulating sEVs decorated with immunosuppressive proteins on the surface membrane and able to suppress immune cell functions [42,43]. The presence of the immunosuppressive sEVs in patients' plasma was associated with poor prognosis in colorectal cancer and recently also in non-small cell lung cancer (NSCLC) [41,44]. Breast cancer-derived sEVs were reported to carry proteins and miRNA that correlated with tumor recurrence and metastasis [45]. These preliminary findings indicate that sEVs have a potential to serve as a component of non-invasive liquid tumor biopsy along with circulating tumor cells (CTC) and cell free DNA (cfDNA) [46].

Table 1
Cargo components of NEX and their functional role according to neutrophil activation state.

NEX type	Function	Cargo	Description	Ref.
N1 inflammatory	N0 mobilization	miR-223	crucial functions in myeloid lineage development	[60]
		5-LO	5-LO catalyzes two steps in biosynthesis of leukotrienes contributing to innate immunity	[62]
		FLAP	FLAP is necessary for the activation of 5-LO and synthesis of leukotriene, both lipid mediators of inflammation	[55]
		LTA4H	converts leukotriene A4 to leukotriene B4	[55]
		LTB4	induce the adhesion and activation of leukocytes on the endothelium; potent neutrophil chemoattractant	[55]
	Cell migration	F-Actin	cell motility	[95]
		S100A8/9	stimulates leukocyte recruitment and induces cytokine secretion	[91]
		Integrins	facilitate cell-cell and cell-extracellular matrix adhesion; mediate cellular signals such as regulation of the cell cycle, organization of the intracellular cytoskeleton, and movement of new receptors to the cell membrane	[39, 63]
		RAP1A	regulates signaling pathways that affect cell proliferation and adhesion; Rap1 activation has been implicated in preventing solid tumor metastasis	[63]
	Cell metabolism	G6P Isomerase	involved in glycolysis and gluconeogenesis, as well as the pentose phosphate pathway	[95]
		Galectin 9	may affect recipient cell metabolism through its cytoplasmic action in control of AMPK	[63]
	Cell modulation	Proinflammatory cytokines	recruitment and activation of immune cells	[65]
	Tissue lesion	NE	play a role in degenerative and inflammatory diseases by its proteolysis of collagen-IV and elastin of the extracellular matrix	[69]
		MPO	produces HOCl during the neutrophil's respiratory burst; causes tissue lesions	[91]
		Cathepsin G	important role in breaking down tissues at inflammatory sites	[66]
		Azurocidin	important multifunctional inflammatory mediator	[95]
		Defensin 1	recruitment of T lymphocytes	[95]
		MMP-9	involved in the degradation of the extracellular matrix	[71]
		Tetraspanins	may interact with and regulate other platelet receptors	[38]
		Annexins	inhibits leukocyte (specifically neutrophils) extravasation and downregulates the magnitude of the inflammatory response	[63]
		Collagen	structural	[63]
	Tumor growth / progression	LTB4	acts on non-immune cells *via* BLT1 to initiate and/or amplify pathological inflammation; LTB4-BLT1 axis in cancer, either tumor inhibitory or tumor-promoting, depending on the different target cells	[55]
		MPO	excessive generation of MPO-derived oxidants has been linked to tissue damage and in the initiation and progression of cancer	[68]
		NE	can directly stimulate proliferative pathways by extracellular transactivation of membrane receptors by MAPK signaling	[66]
		FGF1	regulation of cell survival, cell division, angiogenesis, cell differentiation, and cell migration	[70]
		MMP-2	contributes to cell migration by interacting with collagen	[70]
N2 regenerative	Evasion / Metastasis	CD66c	adhesion protein on cell surface	[66]
		Lipocalin 2	abnormal expression serves critical roles in the epithelial-to-mesenchymal transition process, angiogenesis, and cell migration and invasion	[72]
		MMP-9	angiogenesis	[71]
	TME regulation	Oncostatin M	induces collagen production and proliferation	[96]
		IL6	promotes tumorigenesis by regulating signaling pathways, which includes apoptosis, cell survival, proliferation and metabolism, angiogenesis, invasiveness and metastasis	[97]
		Cathepsin G	anti-inflammatory response	[66]
		S100A8/9	recruitment of MDSCs and stimulation of their immunosuppressive functions	[91]

Abbreviations: NEX: neutrophil-derived small extracellular vesicles; N1: anti tumor neutrophil; N0: inactivated neutrophil; miR-223: microRNA-223; 5-LO: arachidonate 5-lipoxygenase; FLAP: 5-lipoxygenase-activating protein; LTA4H: leukotriene-A4 hydrolase; LTB4: leukotrine B4; F-actin: actin filaments; S100A8/A9: calcium-binding protein A8/A9; RAP1A: ras-related protein; AMPK: 5′ adenosine monophosphate-activated protein kinase; NE: neutrophil elastase; MPO: myeloperoxidase; HOCl: hypochlorous acid; MMP-9: matrix metallopeptidase 9; N2: pro-tumor neutrophil; FGF1: fibroblast growth factor 1; MMP-2: matrix metallopeptidase 2; CD66c: cell adhesion molecule 6; IL-6: interleukin 6.

4. Neutrophil-derived small extracellular vesicles (NEX)

Neutrophils, like all other cells, produce and release sEVs that we have identified as "NEX". Initially, NEX were considered to be neutrophil granules, but more careful scrutiny indicated that NEX have features that distinguish them from granules and other secretory vesicles. Neutrophil granules are formed during neutrophil maturation in the bone marrow and are fully formed, pre-packed and ready for release in response to stimuli encountered during a neutrophil life span [47]. In contrast, the biogenesis of NEX is initiated in mature neutrophils in response to intracellular metabolic changes and/or extracellular, environmental stress. NEX are formed and released on the "as needed" basis and their molecular/genetic composition, reflecting that of the parent cell, is tailored to meet the existing physiological or pathological situation. NEX may be especially useful in pathological conditions, where they are "first responders", effectively signaling the presence of danger and/or summoning help. In line with this, NEX activities mirror those of the parent cell. As indicated above, neutrophils might be functionally polarized into inflammatory N1 and regenerative N2 subtypes. If so, then it would be expected that N1 neutrophils produce N1 NEX, while N2 neutrophils release N2 NEX, each NEX subtype functionally recapitulating the parent cell [48]. Fig. 2 illustrates the potential of the individual neutrophil to produce and release NEX subtypes packaged in the mother cell to carry inflammatory or regenerative cargos. This scenario fits well with the above-described plasticity of neutrophils and their capacity for swift activation and responsiveness to incoming signals. Fig. 2 also presents phenotypic profiles of N1 and N2 NEX as well as their cargo profiles and functions associated with each NEX subtype.

NEX can be isolated from supernatants of neutrophil cultures using the same methods employed for sEV isolation [49]. Despite the same methodology for isolation and characterization, there are few studies focusing on NEX and even fewer experiments relating to the role of NEX in cancer. Neutrophils have recently emerged as a key player in the TME and little is known about their tumor-promotion mechanisms. Studies have proven the complexity of neutrophil interactions among malignant and non-malignant cells [1,50–52], therefore, further studies are needed to fully comprehend the tumor-neutrophil crosstalk mediated by NEX.

5. The role of NEX in cancer

It is well established that neutrophils secrete NEX under different physiologic and pathologic conditions and that secreted NEX are functionally capable of mediating a variety of biological effects. Studies of the NEX involvement in inflammation, tissue repair, and autoimmune diseases [53,54] indicate that neutrophils promote a positive feedback in order to enhance their migration and activation in different disease settings by releasing NEX [55]. Therefore, NEX appear to have a heterogeneous role, by mediating both inflammatory and anti-inflammatory states, which reflects their plasticity: They can act as inflammatory or regulatory vesicles, as shown in Table 1 [56,57]. It is unclear whether NEX also play a functional role in malignant diseases. The finding that TANs have an immunosuppressive profile and thus might promote tumor progression suggests that NEX also contribute to changes that occur in the TME during tumorigenesis.

Chronic inflammatory processes often preceed malignancy, and the involvement of neutrophils in inflammation suggests that NEX with the N1-like phenotype (Fig. 2) may be involved as well. The N1 NEX carrying factors that increase the recruitment of neutrophils along with other immune cells to inflamed tissues are the first to arrive at the TME. The N1 NEX carry miR-223 which plays a crucial role in the development of the myeloid lineage cells [58–60]. It acts directly at granulopoiesis and mobilizes neutrophils to transition from the bone marrow to blood stream [60]. Delivered in N1 NEX to the TME, it promotes immune cell recruitment (Fig. 2). It has been observed that down-regulation of miR-223 in the TME is associated with tumor aggressiveness and worse prognosis [61]. Several other factors known to be involved in cell migration were also detected in N1 NEX, including 5-lipoxygenase-activating protein (FLAP), 5-lipoxygenase (5-LO), and leukotriene B4 (LTB_4) [55,62]. Moreover, it was shown that N1 NEX carry factors such as RAP1A and integrins [63] that modulate adhesion of rolling neutrophils to endothelial cells. Interestingly, RAP1A has also been reported to prevent metastasis [64]. N1 NEX can also carry pro-inflammatory cytokines, such as IL-1β, IL-2 and IL-4 [65]. Overall, N1 NEX have the potential to mediate anti-tumor effects and might enhance anti-tumor immune responses in the TME.

Once malignancy is established and inflammatory milieu is replaced by the ECM supporting tumor growth, infiltrating neutrophils assume a different role [25]. It is possible that the developing tumor induces recruitment of different neutrophil populations into the TME and that NEX participate in this recruitment. Elevated numbers of circulating and infiltrating TANs with the N2 phenotype might also be associated with the initiation of the production of regenerative N2 NEX. N2 NEX carry factors responsible for tumor progression and mediate immunosuppression (Fig. 2). For instance, excessive MPO levels in the TME delivered by N2 NEX have been related to tumor progression [66,67]. MPO promotes metabolism of carcinogenic chemicals that compromise DNA repair and contributes to the appearance of new mutations [68]. Also, NE, another cargo component of N2 NEX [66], stimulates oncogenic signaling and activates proliferation pathways driven by MAPK [69]. N2 NEX also carry numerous components which are involved in accelerating angiogenesis, tumor invasion, and metastasis, such as fibroblast growth factor-1 (FGF-1), matrix metalloproteinase 2 and 9 (MMP-2, MMP-9) [70,71], CD66c, and lipocalin 2 [66,72]. Finally, the cargo of N2 NEX contributes to the immunosuppressive profile of the TME. N2 NEX can carry anti-inflammatory cytokines and antiproteases that maintain an immunosuppressive environment [73]. To conclude, N2 NEX carry tumor-promoting cargo components, which appear to regulate all aspects of tumor growth and metastasis, including angiogenesis and immune suppression.

Despite some similar content in both N1 and N2 NEX, they express a dual response regarding the environmental stimuli. For instance, MPO and NE are described as cargo of both N1 and N2 NEX, since the same molecular pathway that supports inflammation is also operating in support of tumor growth. This dual activity enhances immunity [67], but simultaneously facilitates tumor progression and metastasis through upregulating MMP activity and imposes tumor cell mutation by MPO enzymatic activity [74]. Moreover, the controversial role of reactive oxygen species (ROS) is widely discussed in cancer. Cancer cells increase their rate of ROS production by adapting to the TME. However, excessive levels of ROS can increase oxidative stress and induce cancer cell death [75]. Tumor cells boost their antioxidant capacity in order to avoid ROS escalation and maintain redox balance. Thus, it is suggested that – in comparison to non-neoplastic cells - tumor cells have an altered redox environment, therefore, an increased sensitivity to alterations in ROS levels in the TME [76]. This dual role supports that cargo components of NEX can either contribute to or inhibit tumor progression depending on the microenvironmental milieu.

6. NEX can carry different messages in early *vs* late stages of tumor growth

Observations indicating that TANs found in the TME are no longer inflammatory cells but have assumed different phenotypic and functional characteristics implies that NEX produced in the TME are also different. The shift from N1 to N2 NEX is more conspicuous in advanced tumors and it has been proposed that the developing tumors acquire capabilities to educate, alter and reprogram functions of immune and non-immune cells in the TME [77]. The implication of these experiments is that tumors communicate with surrounding and distant cells *via* sEVs. The intercellular communication of neutrophils with malignant and non-malignant cells is not exclusive for tumor cells in the TME as it also involves various non-malignant cells. Therefore, cell communication *via*

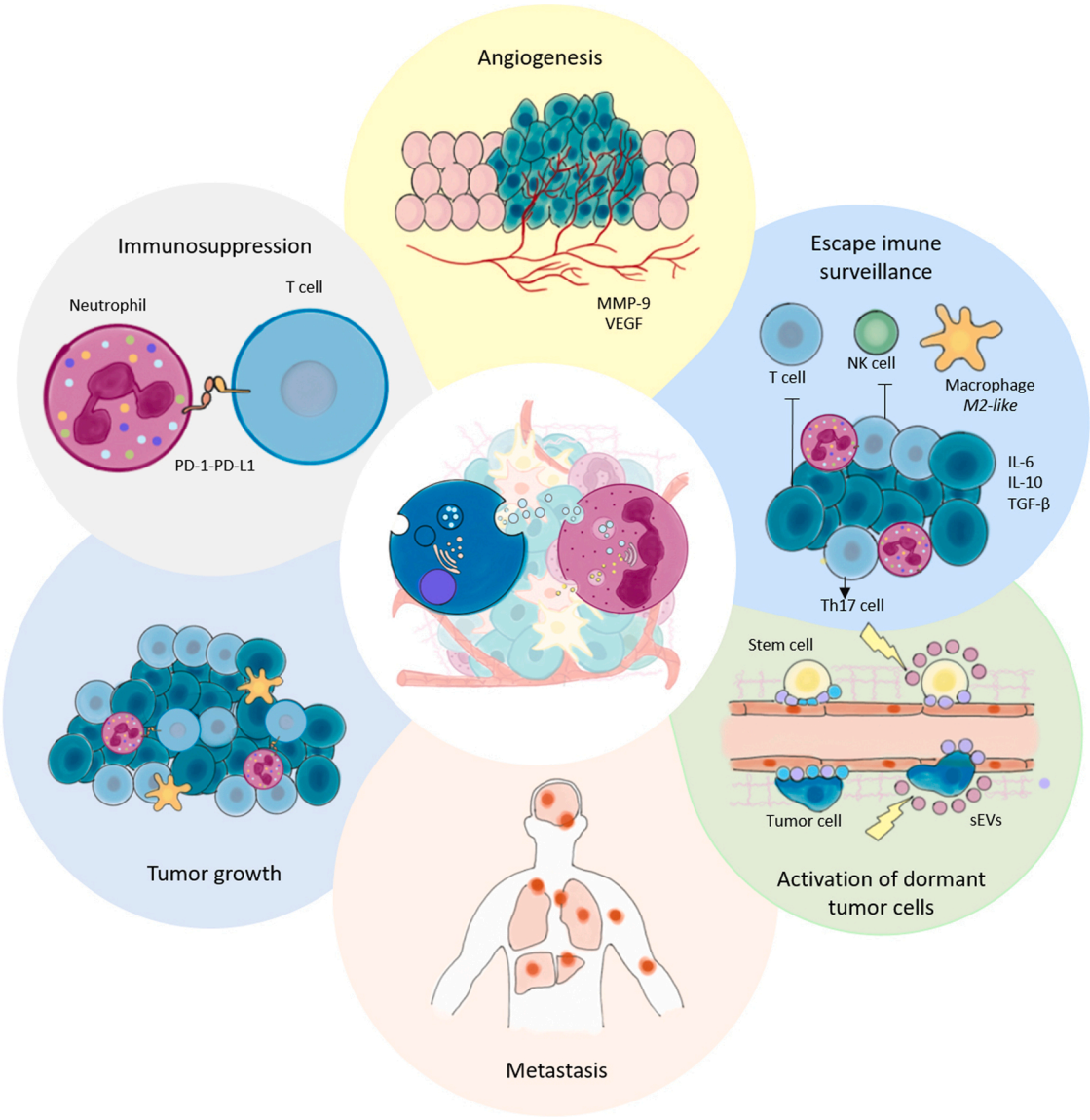

Fig. 3. Tumor cells release TEX which interact with a variety of cell types, including TANs in the TME and neutrophils at distant sites. TEX were shown to alter the phenotype and functional behavior of neutrophils. This figure summarizes the tumor-promoting effects of neutrophils reprogrammed by the tumor.
Abbreviations: TEX – tumor-derived small extracellular vesicles, TANs – tumor-associated neutrophils, TME – tumor microenvironment, MMP-9 – mettaproteinase-9, VEGF - vascular endothelial growth factor, PD1 - programmed cell death protein 1, PDL1 - programmed cell death ligand 1, IL – interleukin.

sEVs appears to be an important modulator of neutrophil responses [13].

It was demonstrated that TEX from glioblastoma cells reprogram macrophage subsets. In this regard, TEX reprogram naïve macrophages or shift M1- into M2-like macrophages, but also educate M2 macrophages into strong immunosuppressive TAMs [78]. Accordingly, TANs are different from neutrophils in normal healthy or even inflamed tissues because of the influence of the TME. Similar to macrophages, TANs may acquire either an anti-tumor (N1) or a pro-tumor (N2) activity [9]. N1 TANs exhibit higher production of ROS and, thus are cytotoxic to tumor cells [79]. On the other hand, N2 TANs endorse tumor growth and dissemination by inducing ECM remodeling and angiogenesis [80]. As good inflammatory cells, neutrophils send signals *via* NEX to the emerging tumor. The first events probably release N1 NEX with anti-tumor signals. However, if tumor prevails and grows, it assumes control and reprograms every cell around. At this point, neutrophils might become N2, release N2 NEX, and help promote tumor growth. This shift is well documented for macrophages [78] and only limited experimental data is available for TANs. However, a recent publication from Kolonics et al. is proposing a similar mechanism for neutrophils and NEX. The authors showed, that neutrophils produce a wide range of EVs, mostly depending on the environmental conditions [48].

7. Tumor-derived small extracellular vesicles (TEX) as drivers of pro-tumor neutrophil responses

It is well recognized that non-tumor cells in the TME contribute to tumor progression and that the TME is organized to promote tumor growth. The TME is characterized by the presence of a variety of factors, including VEGF, colony stimulating factor 1 (CSF1), and platelet-derived growth factor (PDGF) that induce angiogenesis, recruitment of macrophages and neutrophils, and promote tumor cell proliferation, respectively [81]. Moreover, the presence of immunomodulatory molecules in the TME has been described as a key factor for tumor progression and is one of the major mechanism of the tumor cell escape from immune surveillance. For instance, tumor-associated endothelial cells secrete CXCL1/2 which promotes the recruitment of neutrophils into the TME [82]. However, the factors which are released by tumor cells do not only exist in their soluble forms, they can also be associated

Table 2
TEX as modulators of neutrophil response in cancer.

Disease	Experimental model	Source of sEVs	Cargo components	Induced biological effects	Ref.
Lung/ovarian cancer	*in vivo* and clinical	neutrophils	S100A8/A9	reactivation of dormant tumor cells and formation of new tumor lesions	[91]
Breast cancer	*in vivo*	4T1 cell line	unknown	NETs release, cancer-related thrombosis	[83]
Colorectal cancer	*in vivo*	CT26 cell line	unknown	stimulation of neutrophils	[98]
Colorectal cancer	*in vitro, in vivo*	HCT15, HT29, and CT26 cell lines	miRNA-146a	increase of tumor-infiltrating neutrophils and decrease of tumor-infiltrating T cells	[87]
Colorectal cancer	*in vitro, in vivo*	DKs-8, DKO-1 cell lines/APC-WT and APC-KRAS^{G12D} mice	KRAS	IL-8 upregulation, neutrophil migration and infiltration, NETs, tumor progression	[84]
Colon cancer	*in vivo*	CT26 cell line	HSP72	immunosuppressive activity of MDSCs	[89]
Renal cell carcinoma	*in vitro, in vivo*	Renca cell	HSP70	immunosuppressive activity of MDSCs	[99]
Oral squamous cell carcinoma	*in vivo*	Cal-27 and SCCVII cell lines	miR-21	immunosuppressive activity of MDSCs	[88]
Breast, lung, and ovarian cancer	*ex vivo, in vivo*	breast, lung, and ovarian cancer	HSP70	immunosuppressive activity of MDSCs	[100]
Gastric cancer	*in vitro*	cell line BGC-823, HGC-27, MGC-803, and SGC-7901	HMGB1, HSP70, fibronectin	angiogenesis, metastasis	[13]
Gastric cancer	*in vitro*	gastric cancer cell lines	HMGB1	induction of PD-L1 expression on neutrophils	[86]
Pancreatic ductal adenocarcinoma	*in vivo*	pancreatic ductal adenocarcinomas	migration inhibitory factor (MIF)	migration of bone marrow-derived macrophages and neutrophils, metastatic niche formation	[90]

Abbreviations: sEVs: small extracellular vesicles; S100A8/A9: calcium-binding protein A8/A9; 4T1: breast cancer cell line; NETs: neutrophil extracellular traps; CT26: colon carcinoma cell line; HCT15: colon carcinoma cell line; HT29: colon carcinoma cell line; miRNA-146a: micro-RNA 146-a; HSP72: heat shock protein 72; MDSC: myeloid derived suppressor cell; HSP70: heat shock protein 70; Cal-27: oral squamous carcinoma cell line; SCC VII: oral squamous carcinoma cell line; miR-21: microRNA-21; BGC-823: gastric cancer cell line; HGC-27: gastric cancer cell line; MGC-803: gastric cancer cell line; SGC-7901: gastric cancer cell line; HMGB1: high mobility group box 1; PD-L1: programmed death-ligand 1.

with sEVs. TEX deriving from breast cancer cells induced NETs release and accelerated cancer-associated thrombosis [83]. Indeed, it has been recently demonstrated that colorectal derived sEVs transfer mutant KRAS to recipient neutrophils and other tumor cells, upregulating IL-8 production, increasing neutrophil migration and activating netosis [84]. Beyond that, HMGB1 appears to be an important cargo component of TEX. HMGB1, a sterile inflammatory molecule and DAMP released from various cells during stress has been implicated in inflammation and it is considered as a neutrophil recruiter [85]. TEX isolated from gastric cancer cells carried HMGB1 and prolonged neutrophil survival. HMGB1-positive TEX also activated the Toll-like receptor 4/NF-κB cascade, inducing a pro-tumor phenotype in neutrophils [13]. Besides, HMGB1 modulated neutrophils *in vitro* to suppress T cell proliferation, activation, and function by inducing PD-L1 expression [86]. Indeed, CD66$^+$ neutrophil infiltration correlated with decreased CD8$^+$ T cell infiltration, leading to tumor progression [87]. In oral squamous cell carcinoma, TEX isolated from cells cultured in hypoxic conditions carried miR-21 and enhanced the suppressive effect of CD11b$^+$Gr-1$^+$ MDSCs in a PTEN/PD-L1-axis-dependent manner, which, in turn, suppressed anti-tumor functions of γδ T cells. γδ T cells are a diverse subgroup of T cells involved in both innate and adaptive responses and they have been demonstrated to be involved in immune regulatory and tumor surveillance activities [88]. In several malignant entities it was shown that TEX carry heat shock protein (Hsp)-70 and Hsp72 which suppressed the activity of CD11b$^+$Gr-1$^+$ MDSCs *via* TLR2/STAT3 and, thus, stimulated tumor progression [89].

Neutrophils have been directly associated with tumor metastasis in several *in vivo* and clinical analyses [9]. In this regard, HMGB1-positive TEX induced the expression of inflammatory factors in neutrophils, which promoted gastric cancer cell migration [13]. Indeed, TEX modulate the ECM, and TEX-induced fibronectin deposition was shown to initiate a pre-metastatic niche formation [90]. Interestingly, stress-associated adrenergic hormones were described to induce a fast S100A8/9 release from neutrophils unrelated to either degranulation or NETs formation. These proteins result in an accumulation of oxidized lipids in dormant tumor cells through MPO activity and seem to engage their reactivation and initiation of new cancer lesions [91]. Moreover, a recent study has demonstrated that TEX from melanoma were able to recruit pro-tumor neutrophils to a pre-metastatic niche [92]. This data indicates the importance of the role of neutrophils throughout the carcinogenic process, as demonstrated by Tyagi et al. in breast cancer with a premetastatic pulmonary site [93].

Neutrophils play a relevant role in both innate immunity and triggering adaptive immunity. Especially, pro-tumor neutrophils or TANs promote tumor progression by accelerating angiogenesis, metastasis formation, CD8$^+$ T cell exclusion, a loss of immune surveillance, and reactivation of dormant cells (Fig. 3). There is evidence in the literature that the recruitment and activation of neutrophils and especially the reprogramming towards TANs might be mediated by TEX (Table 2). Understanding the sEV-mediated crosstalk between tumor cells and neutrophils shows the potential to increase the overall understanding of neutrophil biology.

8. Concluding remarks

The understanding of the multifaceted role of neutrophils in cancer is of current interest and bears the potential to uncover important biological aspects, which may become important for the development of future therapeutic targets. Neutrophils are equipped and ready to shift from one mode of surveillance to completely different mode of tumor-promoting activity when tumor appears. sEVs are a crucial mechanism for intercellular communication and the investigation of their cargo components and ability to reprogram recipient cells are of great current interest. Recently, it was shown that the crosstalk between tumor cells and neutrophils is mediated by sEVs either released by tumor cells (TEX) or by neutrophils (NEX). There is a lot of uncertainty about these complex interactions and how they modulate the TME, ultimately creating a tumor-promoting microenvironment. However, the role of neutrophils in cancer proved to be extremely important and so far underestimated. Studies have shown their close relation to cancer metastasis, cancer-associated thrombosis through NETs release, and neutrophil uptake of oncogenic EVs.

Further *in vivo* investigations are necessary to evaluate whether the effects of NEX and TEX in the TME are as central as they are currently presented in the literature. Multiple studies attempted to deplete cancer cells, or mice of the effectors of the sEV biogenesis and in many instances cancer progression was not abrogated, or the changes were subtle [94]. An enhanced understanding of the sEV biogenesis and the cargo

components and functions of NEX and TEX in the TME are necessary to validate the concept that sEV-based intercellular communication is a driver of tumor progression. Most recent publications focus on sEVs as one subset of EVs, however, also other subsets such as exomeres, microvesicles, and apoptotic bodies were shown to play functional roles in the TME. It will be necessary to validate how central sEVs are to the EV-mediated intercellular communication in comparison to other EV subsets. Determination of the exact contributions of NEX and TEX to malignant entities will be the aim of future studies which are expected to: 1) provide more details about the complex biology of the TME; 2) give further insights into neutrophil biology; and 3) show the potential to discover new therapeutic strategies which will be based on targeting neutrophils with a tumor-promoting phenotype.

Declaration of Competing Interest

The authors report no declarations of interest.

Acknowledgments

The authors would like to thank the Fundação de Amparo à Pesquisa do Estado do Rio Grande do Sul (FAPERGS - 19/2551-0000663-2; 21/2551-0000078-3), Coordenação de Aperfeiçoamento de Pessoal de Nível Superior (CAPES; code 001), Conselho Nacional de Desenvolvimento Científico e Tecnológico (CNPq - 312187/2018-1; 400882/2019-1; 400882/2019-1), HCPA (FIPE - 2019–0446), and UFCSPA. D.S. Rubenich, N. Omizzollo, and E. Braganhol are recipients of CNPq fellowships. N. Ludwig was supported by the Walter Schulz Foundation (info@walter-schulz-stiftung.de). Partial support was provided by the NIH grant U01-DE029759 to T.L. Whiteside and from the National Science Centre, Poland (UMO-2017/26/M/NZ5/00877#) to M.J. Szczepański.

References

[1] Z.G. Fridlender, S.M. Albelda, Tumor-associated neutrophils: friend or foe? Carcinogenesis 33 (2012) 949–955, https://doi.org/10.1093/carcin/bgs123.
[2] M.E. Shaul, Z.G. Fridlender, Tumour-associated neutrophils in patients with cancer, Nat. Rev. Clin. Oncol. 16 (2019) 601–620, https://doi.org/10.1038/s41571-019-0222-4.
[3] S.M. Lawrence, R. Corriden, V. Nizet, The ontogeny of a neutrophil: mechanisms of granulopoiesis and homeostasis, Microbiol. Mol. Biol. Rev. 82 (2018) 1–22, https://doi.org/10.1128/mmbr.00057-17.
[4] M.D. Filippi, Neutrophil transendothelial migration: updates and new perspectives, Blood 133 (2019) 2149–2158, https://doi.org/10.1182/blood-2018-12-844605.
[5] C. Silvestre-Roig, Z.G. Fridlender, M. Glogauer, P. Scapini, Neutrophil diversity in health and disease, Trends Immunol. 40 (2019) 565–583, https://doi.org/10.1016/j.it.2019.04.012.
[6] C.D. Sadik, N.D. Kim, A.D. Luster, Neutrophils cascading their way to inflammation, Trends Immunol. 32 (2011) 452–460, https://doi.org/10.1016/j.it.2011.06.008.
[7] P. Hellebrekers, N. Vrisekoop, L. Koenderman, Neutrophil phenotypes in health and disease, Eur. J. Clin. Invest. 48 (2018), https://doi.org/10.1111/eci.12943.
[8] S.B. Coffelt, M.D. Wellenstein, K.E. De Visser, Neutrophils in cancer: neutral no more, Nat. Rev. Cancer 16 (2016) 431–446, https://doi.org/10.1038/nrc.2016.52.
[9] M.A. Giese, L.E. Hind, A. Huttenlocher, Neutrophil plasticity in the tumor microenvironment, Blood 133 (2019) 2159–2167, https://doi.org/10.1182/blood-2018-11-844548.
[10] O. Soehnlein, S. Steffens, A. Hidalgo, C. Weber, Neutrophils as protagonists and targets in chronic inflammation, Nat. Rev. Immunol. 17 (2017) 248–261, https://doi.org/10.1038/nri.2017.10.
[11] M.A. Cassatella, N.K. Östberg, N. Tamassia, O. Soehnlein, Biological roles of neutrophil-derived granule proteins and cytokines, Trends Immunol. 40 (2019) 648–664, https://doi.org/10.1016/j.it.2019.05.003.
[12] A.J. Gentles, A.M. Newman, C.L. Liu, S.V. Bratman, W. Feng, D. Kim, V.S. Nair, Y. Xu, A. Khuong, C.D. Hoang, M. Diehn, R.B. West, S.K. Plevritis, A.A. Alizadeh, The prognostic landscape of genes and infiltrating immune cells across human cancers, Nat. Med. 21 (2015) 938–945, https://doi.org/10.1038/nm.3909.
[13] X. Zhang, H. Shi, X. Yuan, P. Jiang, H. Qian, W. Xu, Tumor-derived exosomes induce N2 polarization of neutrophils to promote gastric cancer cell migration, Mol. Cancer 17 (2018) 1–16, https://doi.org/10.1186/s12943-018-0898-6.
[14] A. Rahbar, M. Cederarv, N. Wolmer-Solberg, C. Tammik, G. Stragliotto, I. Peredo, O. Fornara, X. Xu, M. Dzabic, C. Taher, P. Skarman, C. Söderberg-Nauclér, Enhanced neutrophil activity is associated with shorter time to tumor progression in glioblastoma patients, Oncoimmunology 5 (2016), https://doi.org/10.1080/2162402X.2015.1075693.
[15] T. Hirahara, T. Arigami, S. Yanagita, D. Matsushita, Y. Uchikado, Y. Uenosono, S. Ishigami, S. Natsugoe, Combined neutrophil-lymphocyte ratio and platelet-lymphocyte ratio predicts chemotherapy response and prognosis in patients with advanced gastric cancer, BMC Cancer 2014 (2019) 1–7, https://doi.org/10.1186/s12885-019-5903-y.
[16] J. Yoon, J. Roh, S. Kim, S. Choi, S. Yuhl, S. Yoon, Journal of Geriatric Oncology Prognostic value of neutrophil-to-lymphocyte ratio in older patients with head and neck cancer, J. Geriatr. Oncol. 11 (3) (2019) 417–422, https://doi.org/10.1016/j.jgo.2019.06.013.
[17] M. Gago-Dominguez, M. Matabuena, C.M. Redondo, S.P. Patel, A. Carracedo, S. M. Ponte, M.E. Martínez, J.E. Castelao, Neutrophil to lymphocyte ratio and breast cancer risk: analysis by subtype and potential interactions, Sci. Rep. 10 (2020) 1–11, https://doi.org/10.1038/s41598-020-70077-z.
[18] K. Takakura, Z. Ito, M. Suka, T. Kanai, Y. Matsumoto, S. Odahara, H. Matsudaira, K. Haruki, Y. Fujiwara, R. Saito, T. Gocho, K.I. Nakashiro, H. Hamakawa, M. Okamoto, M. Kajihara, T. Misawa, T. Ohkusa, S. Koido, Comprehensive assessment of the prognosis of pancreatic cancer: peripheral blood neutrophil-lymphocyte ratio and immunohistochemical analyses of the tumour site, Scand. J. Gastroenterol. 51 (2016) 610–617, https://doi.org/10.3109/00365521.2015.1121515.
[19] D.M. Kuang, Q. Zhao, Y. Wu, C. Peng, J. Wang, Z. Xu, X.Y. Yin, L. Zheng, Peritumoral neutrophils link inflammatory response to disease progression by fostering angiogenesis in hepatocellular carcinoma, J. Hepatol. 54 (2011) 948–955, https://doi.org/10.1016/j.jhep.2010.08.041.
[20] A. Carus, M. Ladekarl, H. Hager, H. Pilegaard, P.S. Nielsen, F. Donskov, Tumor-associated neutrophils and macrophages in non-small cell lung cancer: No immediate impact on patient outcome, Lung Cancer 81 (2013) 130–137, https://doi.org/10.1016/j.lungcan.2013.03.003.
[21] P.X. Liew, P. Kubes, The Neutrophil's role during health and disease, Physiol. Rev. 99 (2019) 1223–1248, https://doi.org/10.1152/physrev.00012.2018.
[22] L.G. Ng, R. Ostuni, A. Hidalgo, Heterogeneity of neutrophils, Nat. Rev. Immunol. 19 (2019) 255–265, https://doi.org/10.1038/s41577-019-0141-8.
[23] E. Uribe-Querol, C. Rosales, Neutrophils in cancer: two sides of the same coin, J. Immunol. Res. 2015 (2015), https://doi.org/10.1155/2015/983698.
[24] J. Cools-Lartigue, J. Spicer, B. McDonald, S. Gowing, S. Chow, B. Giannias, F. Bourdeau, P. Kubes, L. Ferri, Neutrophil extracellular traps sequester circulating tumor cells and promote metastasis, J. Clin. Invest. 123 (2013) 3446–3458, https://doi.org/10.1172/JCI67484.
[25] Z.G. Fridlender, J. Sun, S. Kim, V. Kapoor, G. Cheng, G.S. Worthen, S.M. Albelda, Polarization of TAN phenotype by TGFb: "N1" versus "N2" TAN, Cancer Cell 16 (2010) 183–194, https://doi.org/10.1016/j.ccr.2009.06.017.Polarization.
[26] Z.G. Fridlender, J. Sun, I. Mishalian, S. Singhal, G. Cheng, V. Kapoor, W. Horng, G. Fridlender, R. Bayuh, G.S. Worthen, S.M. Albelda, Transcriptomic analysis comparing tumor-associated neutrophils with granulocytic myeloid-derived suppressor cells and normal neutrophils, PLoS One 7 (2012), https://doi.org/10.1371/journal.pone.0031524.
[27] S. Jaillon, A. Ponzetta, D. Di Mitri, A. Santoni, R. Bonecchi, A. Mantovani, Neutrophil diversity and plasticity in tumour progression and therapy, Nat. Rev. Cancer 20 (2020) 485–503, https://doi.org/10.1038/s41568-020-0281-y.
[28] Filippo Veglia, Michela Perego, D. Gabrilovich, Myeloid-derived suppressor cells coming of age, Nat. Immunol. 176 (2018) 100–106, https://doi.org/10.1038/s41590-017-0022-x.Myeloid-derived.
[29] D.I. Gabrilovich, S. Ostrand-Rosenberg, V. Bronte, Coordinated regulation of myeloid cells by tumours, Nat. Rev. Immunol. 12 (2012) 253–268, https://doi.org/10.1038/nri3175.
[30] Lauren J. Bayne, Gregory L. Beatty, Nirag Jhala, Carolyn E. Clark, Andrew D. Rhim, Ben Z. Stanger, Robert H. Vonderheide, Tumor-derived granulocyte-macrophage colony stimulating factor regulates myeloid inflammation and T cell immunity in pancreatic cancer, Cancer Cell 21 (2012) 822–835, https://doi.org/10.1016/j.ccr.2012.04.025.Tumor-derived.
[31] V. Bronte, S. Brandau, S.H. Chen, M.P. Colombo, A.B. Frey, T.F. Greten, S. Mandruzzato, P.J. Murray, A. Ochoa, S. Ostrand-Rosenberg, P.C. Rodriguez, A. Sica, V. Umansky, R.H. Vonderheide, D.I. Gabrilovich, Recommendations for myeloid-derived suppressor cell nomenclature and characterization standards, Nat. Commun. 7 (2016) 1–10, https://doi.org/10.1038/ncomms12150.
[32] M.L. Sprouse, T. Welte, D. Boral, H.N. Liu, W. Yin, M. Vishnoi, D. Goswami-Sewell, L. Li, G. Pei, P. Jia, I.C. Glitza-Oliva, D. Marchetti, PMN-MDSCs enhance CTC metastatic properties through reciprocal interactions via ROS/notch/nodal signaling, Int. J. Mol. Sci. 20 (2019), https://doi.org/10.3390/ijms20081916.
[33] D.I. Gabrilovich, S. Nagaraj, Myeloid-derived suppressor cells as regulators of the immune system, Nat. Rev. Immunol. 9 (2009) 162–174, https://doi.org/10.1038/nri2506.
[34] V. Kumar, P. Cheng, T. Condamine, S. Mony, L.R. Languino, J.C. Mccaffrey, N. Hockstein, M. Guarino, G. Masters, F. Denstman, X. Xu, D.C. Altieri, H. Du, C. Yan, CD45 phosphatase inhibits STAT3 transcription factor activity in myeloid cells and promotes tumor-associated macrophage differentiation, Immunity 44 (2016) 303–315, https://doi.org/10.1016/j.immuni.2016.01.014.CD45.
[35] N. Ludwig, J.H. Azambuja, A. Rao, D.G. Gillespie, E.K. Jackson, T.L. Whiteside, Adenosine receptors regulate exosome production, Purinergic Signal. 16 (2) (2020) 231–240, https://doi.org/10.1007/s11302-020-09700-7.
[36] S. Gurunathan, M.-H. Kang, M. Jeyaraj, M. Qasim, J.-H. Kim, Review of the isolation, characterization, biological function, and multifarious therapeutic approaches of exosomes, Cells 8 (2019) 307, https://doi.org/10.3390/cells8040307.

[37] R. Kalluri, V.S. LeBleu, The biology, function, and biomedical applications of exosomes, Science (80-.) 367 (2020), https://doi.org/10.1126/science.aau6977.
[38] D.K. Jeppesen, A.M. Fenix, J.L. Franklin, J.N. Higginbotham, Q. Zhang, L. J. Zimmerman, D.C. Liebler, J. Ping, Q. Liu, R. Evans, W.H. Fissell, J.G. Patton, L. H. Rome, D.T. Burnette, R.J. Coffey, Reassessment of exosome composition, Cell 177 (2019) 428–445, https://doi.org/10.1016/j.cell.2019.02.029, e18.
[39] M. Mathieu, L. Martin-Jaular, G. Lavieu, C. Théry, Specificities of secretion and uptake of exosomes and other extracellular vesicles for cell-to-cell communication, Nat. Cell Biol. 21 (2019) 9–17, https://doi.org/10.1038/s41556-018-0250-9.
[40] L.A. Mulcahy, R.C. Pink, D.R.F. Carter, Routes and mechanisms of extracellular vesicle uptake, J. Extracell. Vesicles 3 (2014) 1–14.
[41] G. Chen, A.C. Huang, W. Zhang, G. Zhang, M. Wu, W. Xu, Z. Yu, J. Yang, B. Wang, H. Sun, H. Xia, Q. Man, W. Zhong, L.F. Antelo, B. Wu, X. Xiong, X. Liu, L. Guan, T. Li, S. Liu, R. Yang, Y. Lu, L. Dong, S. McGettigan, R. Somasundaram, R. Radhakrishnan, G. Mills, Y. Lu, J. Kim, Y.H. Chen, H. Dong, Y. Zhao, G. C. Karakousis, T.C. Mitchell, L.M. Schuchter, M. Herlyn, E.J. Wherry, X. Xu, W. Guo, Exosomal PD-L1 contributes to immunosuppression and is associated with anti-PD-1 response, Nature 560 (2018) 382–386, https://doi.org/10.1038/s41586-018-0392-8.
[42] T.L. Whiteside, Exosomes carrying immunoinhibitory proteins and their role in cancer, Clin. Exp. Immunol. 189 (2017) 259–267, https://doi.org/10.1111/cei.12974.
[43] S. Ludwig, T. Floros, M.N. Theodoraki, C.S. Hong, E.K. Jackson, S. Lang, T. L. Whiteside, Suppression of lymphocyte functions by plasma exosomes correlates with disease activity in patients with head and neck cancer, Clin. Cancer Res. 23 (2017) 4843–4854, https://doi.org/10.1158/1078-0432.CCR-16-2819.
[44] E. Vetsika, P. Sharma, I. Samaras, A. Markou, V. Georgoulias, T.L. Whiteside, A. Kotsakis, Small extracellular vesicles in pre-therapy plasma predict clinical outcome in non-small-cell lung cancer patients, Cancers (Basel) 13 (2021) 1–16, https://doi.org/10.3390/cancers13092041.
[45] M. Wang, S. Ji, G. Shao, J. Zhang, K. Zhao, Z. Wang, A. Wu, Effect of exosome biomarkers for diagnosis and prognosis of breast cancer patients, Clin. Transl. Oncol. 20 (2018) 906–911, https://doi.org/10.1007/s12094-017-1805-0.
[46] S.Y. Ko, W.J. Lee, H.A. Kenny, L.H. Dang, L.M. Ellis, E. Jonasch, E. Lengyel, H. Naora, Cancer-derived small extracellular vesicles promote angiogenesis by heparin-bound, bevacizumab-insensitive VEGF, independent of vesicle uptake, Commun. Biol. 2 (2019) 1–17.
[47] M. Ramadass, S.D. Catz, Molecular mechanisms regulating secretory organelles and endosomes in neutrophils and their implications for inflammation, Immunol. Rev. 273 (2016) 249–265, https://doi.org/10.1111/imr.12452.
[48] F. Kolonics, V. Szeifert, C.I. Timár, E. Ligeti, Á.M. Lőrincz, The functional heterogeneity of neutrophil-derived extracellular vesicles reflects the status of the parent cell, Cells 9 (2020), https://doi.org/10.3390/cells9122718.
[49] E.R. Allen, S.L. Lempke, M.M. Miller, D.M. Bush, B.G. Braswell, C.L. Estes, E. L. Benedict, A.R. Mahon, S.L. Sabo, M.C. Greenlee-Wacker, Effect of extracellular vesicles from S. aureus-challenged human neutrophils on macrophages, J. Leukoc. Biol. 108 (2020) 1841–1850, https://doi.org/10.1002/JLB.3AB0320-156R.
[50] J. Michaeli, M.E. Shaul, I. Mishalian, A.H. Hovav, L. Levy, L. Zolotriov, Z. Granot, Z.G. Fridlender, Tumor-associated neutrophils induce apoptosis of non-activated CD8 T-cells in a TNFα and NO-dependent mechanism, promoting a tumor-supportive environment, Oncoimmunology 6 (2017), https://doi.org/10.1080/2162402X.2017.1356965.
[51] B.M. Szczerba, F. Castro-Giner, M. Vetter, I. Krol, S. Gkountela, J. Landin, M. C. Scheidmann, C. Donato, R. Scherrer, J. Singer, C. Beisel, C. Kurzeder, V. Heinzelmann-Schwarz, C. Rochlitz, W.P. Weber, N. Beerenwinkel, N. Aceto, Neutrophils escort circulating tumour cells to enable cell cycle progression, Nature 566 (2019) 553–557, https://doi.org/10.1038/s41586-019-0915-y.
[52] T. Németh, M. Sperandio, A. Mócsai, Neutrophils as emerging therapeutic targets, Nat. Rev. Drug Discov. 19 (2020) 253–275, https://doi.org/10.1038/s41573-019-0054-z.
[53] K.R. Genschmer, D.W. Russell, C. Lal, T. Szul, P.E. Bratcher, B.D. Noerager, M. Abdul Roda, X. Xu, G. Rezonzew, L. Viera, B.S. Dobosh, C. Margaroli, T. H. Abdalla, R.W. King, C.M. McNicholas, J.M. Wells, M.T. Dransfield, R. Tirouvanziam, A. Gaggar, J.E. Blalock, Activated PMN exosomes: pathogenic entities causing matrix destruction and disease in the lung, Cell 176 (2019) 113–126, https://doi.org/10.1016/j.cell.2018.12.002, e15.
[54] M.A. Rahat, J. Shakya, Parallel aspects of the microenvironment in cancer and autoimmune disease, Mediators Inflamm. 2016 (2016) 1–17, https://doi.org/10.1155/2016/4375120.
[55] P.V. Afonso, M. Janka-Junttila, Y.J. Lee, C.P. McCann, C.M. Oliver, K.A. Aamer, W. Losert, M.T. Cicerone, C.A. Parent, LTB4 is a signal-relay molecule during neutrophil chemotaxis, Dev. Cell 22 (2012) 1079–1091, https://doi.org/10.1016/j.devcel.2012.02.003.
[56] L. Li, X. Zuo, Y. Xiao, D. Liu, H. Luo, H. Zhu, Neutrophil-derived exosome from systemic sclerosis inhibits the proliferation and migration of endothelial cells, Biochem. Biophys. Res. Commun. 526 (2020) 334–340, https://doi.org/10.1016/j.bbrc.2020.03.088.
[57] T.M. Bui, L.A. Mascarenhas, R. Sumagin, Extracellular vesicles regulate immune responses and cellular function in intestinal inflammation and repair, Tissue Barriers 6 (2018) 1–14, https://doi.org/10.1080/21688370.2018.1431038.
[58] V. Neudecker, K.S. Brodsky, E.T. Clambey, E.P. Schmidt, T.A. Packard, B. Davenport, T.J. Standiford, T. Weng, A.A. Fletcher, L. Barthel, J.C. Masterson, G.T. Furuta, C. Cai, M.R. Blackburn, A.A. Ginde, M.W. Graner, W.J. Janssen, R. L. Zemans, C.M. Evans, E.L. Burnham, D. Homann, M. Moss, S. Kreth, K. Zacharowski, P.M. Henson, H.K. Eltzschig, Neutrophil transfer of miR-223 to lung epithelial cells dampens acute lung injury in mice, Sci. Transl. Med. 9 (2017), https://doi.org/10.1126/scitranslmed.aah5360.
[59] A.C. Brook, R.H. Jenkins, A. Clayton, A. Kift-Morgan, A.C. Raby, A.P. Shephard, B. Mariotti, S.M. Cuff, F. Bazzoni, T. Bowen, D.J. Fraser, M. Eberl, Neutrophil-derived miR-223 as local biomarker of bacterial peritonitis, Sci. Rep. 9 (2019) 1–12, https://doi.org/10.1038/s41598-019-46585-y.
[60] F. Fazi, A. Rosa, A. Fatica, V. Gelmetti, M.L. De Marchis, C. Nervi, I. Bozzoni, A minicircuitry comprised of microRNA-223 and transcription factors NFI-A and C/EBPα regulates human granulopoiesis, Cell 123 (2005) 819–831, https://doi.org/10.1016/j.cell.2005.09.023.
[61] F. Citron, I. Segatto, G.L.R. Vinciguerra, L. Musco, F. Russo, G. Mungo, S. D'Andrea, M.C. Mattevi, T. Perin, M. Schiappacassi, S. Massarut, C. Marchini, A. Amici, A. Vecchione, G. Baldassarre, B. Belletti, Downregulation of miR-223 expression is an early event during mammary transformation and confers resistance to CDK4/6 inhibitors in luminal breast cancer, Cancer Res. 80 (2020) 1064–1077, https://doi.org/10.1158/0008-5472.CAN-19-1793.
[62] A.C. Szatmary, R. Nossal, C.A. Parent, R. Majumdar, Modeling neutrophil migration in dynamic chemoattractant gradients: assessing the role of exosomes during signal relay, Mol. Biol. Cell 28 (2017) 3457–3470, https://doi.org/10.1091/mbc.E17-05-0298.
[63] A. Vargas, F. Roux-Dalvai, A. Droit, J.P. Lavoie, Neutrophil-derived exosomes: a new mechanism contributing to airway smooth muscle remodeling, Am. J. Respir. Cell Mol. Biol. 55 (2016) 450–461, https://doi.org/10.1165/rcmb.2016-0033OC.
[64] D. Huang, Miller, Sudarshan Anand, Eric Murphy, Jay Desgrosellier, Dwayne Stupack, Sanford Shattil, David Schlaepfer, Cheresh, EGFR-dependent pancreatic carcinoma cell metastasis via Rap1 activation, Oncogene 176 (2012) 139–148, https://doi.org/10.1038/onc.2011.450.EGFR-dependent.
[65] K. Gao, J. Jin, C. Huang, J. Li, H. Luo, L. Li, Y. Huang, Y. Jiang, Exosomes derived from septic mouse serum modulate immune responses via exosome-associated cytokines, Front. Immunol. 10 (2019) 1–11, https://doi.org/10.3389/fimmu.2019.01560.
[66] S. Bekeschus, J.W. Lackmann, D. Gümbel, M. Napp, A. Schmidt, K. Wende, A neutrophil proteomic signature in surgical trauma wounds, Int. J. Mol. Sci. 19 (2018), https://doi.org/10.3390/ijms19030761.
[67] L.L. Reber, C.M. Gillis, P. Starkl, F. Jönsson, R. Sibilano, T. Marichal, N. Gaudenzio, M. Bérard, S. Rogalla, C.H. Contag, P. Bruhns, S.J. Galli, Neutrophil myeloperoxidase diminishes the toxic effects and mortality induced by lipopolysaccharide, J. Exp. Med. 214 (2017) 1249–1258, https://doi.org/10.1084/jem.20161238.
[68] Q. Meng, S. Wu, Y. Wang, J. Xu, H. Sun, R. Lu, N. Gao, H. Yang, X. Li, B. Tang, M. Aschner, R. Chen, Mpo promoter polymorphism rs2333227 enhances malignant phenotypes of colorectal cancer by altering the binding affinity of AP-2a, Cancer Res. 78 (2018) 2760–2769, https://doi.org/10.1158/0008-5472.CAN-17-2538.
[69] I. Lerman, M. De La Luz Garcia-Hernandez, J. Rangel-Moreno, L. Chiriboga, C. Pan, K.L. Nastiuk, J.J. Krolewski, A. Sen, S.R. Hammes, Infiltrating myeloid cells exert protumorigenic actions via neutrophil elastase, Mol. Cancer Res. 15 (2017) 1138–1152, https://doi.org/10.1158/1541-7786.MCR-17-0003.
[70] A.J. Paris, Y. Liu, J. Mei, N. Dai, L. Guo, L.A. Spruce, K.M. Hudock, J.S. Brenner, W.J. Zacharias, H.D. Mei, A.R. Slamowitz, K. Bhamidipati, M.F. Beers, S. H. Seeholzer, E.E. Morrisey, G.S. Worthen, Neutrophils promote alveolar epithelial regeneration by enhancing type ii pneumocyte proliferation in a model of acid-induced acute lung injury, Am. J. Physiol. - Lung Cell. Mol. Physiol. 311 (2016) L1062–L1075, https://doi.org/10.1152/ajplung.00327.2016.
[71] E.I. Deryugina, E. Zajac, A. Juncker-Jensen, T.A. Kupriyanova, L. Welter, J. P. Quigley, Tissue-infiltrating neutrophils constitute the major in vivo source of angiogenesis-inducing MMP-9 in the tumor microenvironment, Neoplasia (United States) 16 (2014) 771–788, https://doi.org/10.1016/j.neo.2014.08.013.
[72] S. Gomez-Chou, A. Swidnicka-Siergiejko, M. Chavez-Tomar, G. Lesinski, T. Bekaii-Saab, Z. Cruz-Monserrate, Lipocalin-2 promotes pancreatic ductal adenocarcinoma by regulating inflammation in the tumor microenvironment, Cancer Res. 77 (2017) 2647–2660.
[73] M. Horckmans, L. Ring, J. Duchene, D. Santovito, M.J. Schloss, M. Drechsler, C. Weber, O. Soehnlein, S. Steffens, Neutrophils orchestrate post-myocardial infarction healing by polarizing macrophages towards a reparative phenotype, Eur. Heart J. 38 (2017) 187–197, https://doi.org/10.1093/eurheartj/ehw002.
[74] N. Güngör, A.M. Knaapen, A. Munnia, M. Peluso, G.R. Haenen, R.K. Chiu, R.W. L. Godschalk, F.J. Van Schooten, Genotoxic effects of neutrophils and hypochlorous acid, Mutagenesis. 25 (2010) 149–154, https://doi.org/10.1093/mutage/gep053.
[75] V. Nogueira, Y. Park, C.C. Chen, P.Z. Xu, M.L. Chen, I. Tonic, T. Unterman, N. Hay, Akt determines replicative senescence and oxidative or oncogenic premature senescence and sensitizes cells to oxidative apoptosis, Cancer Cell 14 (2008) 458–470, https://doi.org/10.1016/j.ccr.2008.11.003.
[76] C. Gorrini, I.S. Harris, T.W. Mak, Modulation of oxidative stress as an anticancer strategy, Nat. Rev. Drug Discov. 12 (2013) 931–947, https://doi.org/10.1038/nrd4002.
[77] H. Peinado, M. Alečković, S. Lavotshkin, I. Matei, B. Costa-Silva, G. Moreno-Bueno, M. Hergueta-Redondo, C. Williams, G. García-Santos, C.M. Ghajar, A. Nitadori-Hoshino, C. Hoffman, K. Badal, B.A. Garcia, M.K. Callahan, J. Yuan, V.R. Martins, J. Skog, R.N. Kaplan, M.S. Brady, J.D. Wolchok, P.B. Chapman, Y. Kang, J. Bromberg, D. Lyden, Melanoma exosomes educate bone marrow progenitor cells toward a pro-metastatic phenotype through MET, Nat. Med. 18 (2012) 883–891, https://doi.org/10.1038/nm.2753.

[78] J.H. Azambuja, N. Ludwig, S.S. Yerneni, E. Braganhol, T.L. Whiteside, Arginase-1 + exosomes from reprogrammed macrophages promote glioblastoma progression, Int. J. Mol. Sci. 21 (2020) 3990, https://doi.org/10.3390/ijms21113990.

[79] Z. Granot, E. Henke, E.A. Comen, T.A. King, L. Norton, Tumor entrained neutrophils inhibit seeding in the premetastatic lung, Cancer Cell 20 (2011) 300–314, https://doi.org/10.1016/j.ccr.2011.08.012.

[80] M. Kowanetz, X. Wu, J. Lee, M. Tan, T. Hagenbeek, X. Qu, L. Yu, J. Ross, N. Korsisaari, T. Cao, H. Bou-Reslan, D. Kallop, R. Weimer, M.J.C. Ludlam, J. S. Kaminker, Z. Modrusan, N. Van Bruggen, F.V. Peale, R. Carano, Y.G. Meng, N. Ferrara, Granulocyte-colony stimulating factor promotes lung metastasis through mobilization of Ly6G+Ly6C+ granulocytes, Proc. Natl. Acad. Sci. U. S. A. 107 (2010) 21248–21255, https://doi.org/10.1073/pnas.1015855107.

[81] P. Igor, R. Franco, A. Perillo, L. Borges, D. Menezes, M. Pacheco, Pathology - Research and Practice Tumor microenvironment components: allies of cancer progression, Pathol. Res. Pract. 216 (1) (2019), 152729, https://doi.org/10.1016/j.prp.2019.152729.

[82] S. Acharyya, T. Oskarsson, S. Vanharanta, S. Malladi, J. Kim, P.G. Morris, K. Manova-todorova, M. Leversha, N. Hogg, V.E. Seshan, L. Norton, E. Brogi, A CXCL1 Paracrine Network Links Cancer Chemoresistance and Metastasis, 2012, pp. 165–178, https://doi.org/10.1016/j.cell.2012.04.042.

[83] A.C. Leal, D.M. Mizurini, T. Gomes, N.C. Rochael, E.M. Saraiva, M.S. Dias, C. C. Werneck, M.S. Sielski, C.P. Vicente, R.Q. Monteiro, Tumor-derived exosomes induce the formation of neutrophil extracellular traps: implications for the establishment of cancer-associated thrombosis, Sci. Rep. 7 (2017) 1–12, https://doi.org/10.1038/s41598-017-06893-7.

[84] A. Shang, C. Gu, W. Liu, X. Wang, B. Zeng, C. Chen, W. Chang, Y. Ping, J. Sun, P. Ji, J. Wu, W. Quan, Y. Yao, W. Hou, H. Zhou, W. Wang, Z. Sun, Y. Zhou, D. Li, Exosomal KRAS mutation promotes promotion of colorectal cancer by the formation of tumor-associated neutrophil extracellular traps, SSRN Electron. J. 1 (2020) 1–14, https://doi.org/10.2139/ssrn.3474494.

[85] V.V. Orlova, E.Y. Choi, C. Xie, E. Chavakis, A. Bierhaus, E. Ihanus, C. M. Ballantyne, C.G. Gahmberg, M.E. Bianchi, P.P. Nawroth, T. Chavakis, A novel pathway of HMGB1-mediated inflammatory cell recruitment that requires Mac-1-integrin, EMBO J. 26 (4) (2007) 1129–1139, https://doi.org/10.1038/sj.emboj.7601552.

[86] Y. Shi, J. Zhang, Z. Mao, H. Jiang, W. Liu, H. Shi, R. Ji, W. Xu, H. Qian, X. Zhang, Extracellular vesicles from gastric cancer cells induce PD-L1 expression on neutrophils to suppress T-cell immunity, Front. Oncol. 10 (2020) 1–9, https://doi.org/10.3389/fonc.2020.00629.

[87] W.C. Cheng, T.T. Liao, C.C. Lin, L.T.E. Yuan, H.Y. Lan, H.H. Lin, H.W. Teng, H. C. Chang, C.H. Lin, C.Y. Yang, S.C. Huang, J.K. Jiang, S.H. Yang, M.H. Yang, W. L. Hwang, RAB27B-activated secretion of stem-like tumor exosomes delivers the biomarker microRNA-146a-5p, which promotes tumorigenesis and associates with an immunosuppressive tumor microenvironment in colorectal cancer, Int. J. Cancer 145 (2019) 2209–2224, https://doi.org/10.1002/ijc.32338.

[88] L. Li, B. Cao, X. Liang, S. Lu, H. Luo, Z. Wang, S. Wang, J. Jiang, J. Lang, G. Zhu, Microenvironmental oxygen pressure orchestrates an anti- and pro-tumoral γδ T cell equilibrium via tumor-derived exosomes, Oncogene 38 (2019) 2830–2843, https://doi.org/10.1038/s41388-018-0627-z.

[89] F. Chalmin, S. Ladoire, G. Mignot, J. Vincent, M. Bruchard, J.P. Remy-Martin, W. Boireau, A. Rouleau, B. Simon, D. Lanneau, A. De Thonel, G. Multhoff, A. Hamman, F. Martin, B. Chauffert, E. Solary, L. Zitvogel, C. Garrido, B. Ryffel, C. Borg, L. Apetoh, C. Rébé, F. Ghiringhelli, Membrane-associated Hsp72 from tumor-derived exosomes mediates STAT3-dependent immunosuppressive function of mouse and human myeloid-derived suppressor cells, J. Clin. Invest. 120 (2010) 457–471, https://doi.org/10.1172/JCI40483.

[90] B. Costa-silva, N.M. Aiello, A.J. Ocean, S. Singh, B.K. Thakur, A. Becker, A. Hoshino, M.T. Mark, H. Molina, J. Xiang, T. Zhang, T. Theilen, G. García-santos, C. Williams, Y. Ararso, Y. Huang, G. Rodrigues, Pancreatic cancer exosomes initiate pre-metastatic niche formation in the liver, Nat. Cell Biol. 17 (2015) 816–826, https://doi.org/10.1038/ncb3169.

[91] M. Perego, V.A. Tyurin, Y.Y. Tyurina, J. Yellets, T. Nacarelli, C. Lin, Y. Nefedova, A. Kossenkov, Q. Liu, S. Sreedhar, H. Pass, J. Roth, T. Vogl, D. Feldser, R. Zhang, V.E. Kagan, D.I. Gabrilovich, Reactivation of dormant tumor cells by modified lipids derived from stress-activated neutrophils, Sci. Transl. Med. 12 (2020) 1–17, https://doi.org/10.1126/SCITRANSLMED.ABB5817.

[92] M. Schuldner, B. Dörsam, O. Shatnyeva, K.S. Reiners, A. Kubarenko, H.P. Hansen, F. Finkernagel, K. Roth, S. Theurich, A. Nist, T. Stiewe, A. Paschen, G. Knittel, H. C. Reinhardt, R. Müller, M. Hallek, E.P. von Strandmann, Exosome-dependent immune surveillance at the metastatic niche requires BAG6 and CBP/p300-dependent acetylation of p53, Theranostics 9 (2019) 6047–6062, https://doi.org/10.7150/thno.36378.

[93] A. Tyagi, S. Sharma, K. Wu, S.Y. Wu, F. Xing, Y. Liu, D. Zhao, R.P. Deshpande, R. B. D'Agostino, K. Watabe, Nicotine promotes breast cancer metastasis by stimulating N2 neutrophils and generating pre-metastatic niche in lung, Nat. Commun. 12 (2021) 1–18, https://doi.org/10.1038/s41467-020-20733-9.

[94] A. Bobrie, C. Thery, Exosomes and communication between tumours and the immune system: are all exosomes equal? Biochem. Soc. Trans. 41 (2013) 263–267, https://doi.org/10.1042/BST20120245.

[95] I.A. Shopova, I. Belyaev, P. Dasari, S. Jahreis, A.A. Brakhage, Human neutrophils produce antifungal extracellular vesicles against Aspergillus fumigatus, Host Microbe Biol. (2020) 1–19, https://doi.org/10.1128/mBio.00596-20.

[96] H. Lörchner, J. Pöling, P. Gajawada, Y. Hou, V. Polyakova, S. Kostin, J.M. Adrian-Segarra, T. Boettger, A. Wietelmann, H. Warnecke, M. Richter, T. Kubin, T. Braun, Myocardial healing requires Reg3β-dependent accumulation of macrophages in the ischemic heart, Nat. Med. 21 (2015) 353–362, https://doi.org/10.1038/nm.3816.

[97] C. Han, Y. Nie, H. Lian, R. Liu, F. He, H. Huang, S. Hu, Acute inflammation stimulates a regenerative response in the neonatal mouse heart, Cell Res. 25 (2015) 1137–1151, https://doi.org/10.1038/cr.2015.110.

[98] W.L. Hwang, H.Y. Lan, W.C. Cheng, S.C. Huang, M.H. Yang, Tumor stem-like cell-derived exosomal RNAs prime neutrophils for facilitating tumorigenesis of colon cancer, J. Hematol. Oncol. 12 (2019) 1–17, https://doi.org/10.1186/s13045-019-0699-4.

[99] J. Diao, X. Yang, X. Song, S. Chen, Y. He, Q. Wang, G. Chen, C. Luo, X. Wu, Y. Zhang, Exosomal Hsp70 mediates immunosuppressive activity of the myeloid-derived suppressor cells via phosphorylation of Stat3, Med. Oncol. 32 (2015), https://doi.org/10.1007/s12032-014-0453-2.

[100] J. Gobbo, G. Marcion, M. Cordonnier, A.M.M. Dias, N. Pernet, A. Hammann, S. Richaud, H. Mjahed, N. Isambert, V. Clausse, C. Rébé, A. Bertaut, V. Goussot, F. Lirussi, F. Ghiringhelli, A. De Thonel, P. Fumoleau, R. Seigneuric, C. Garrido, Restoring anticancer immune response by targeting tumor-derived exosomes with a HSP70 peptide aptamer, J. Natl. Cancer Inst. 108 (2016) 1–11, https://doi.org/10.1093/jnci/djv330.

Dominique S. Rubenich is a Ph.D. candidate in Biosciences from Federal University of Health Sciences of Porto Alegre, Brazil. Her main interest is characterizing and understanding the different components of the tumor microenvironment in malignancies of the central nervous system. Specifically, her work is dedicated to the role of tumor-associated neutrophils in glioblastoma and their contribution to tumor progression, immunosuppression, and drug resistance. Her aim is to improve the understanding of the complex interactions between tumor cells and neutrophils and to define how these interactions ultimately lead to promotion of tumor growth. The bidirectional intercellular communication between tumor cells and neutrophils *via* small extracellular vesicles might be one of the underlying mechanisms which may explain the tumor-promoting functions of neutrophils. Since only a limited amount of literature is available on this topic, Dominique decided to review what is currently known, emphasizing the importance of characterizing the cell-to-cell interactions and giving a future perspective, but also specifying current limitations which need to be addressed in future studies.

Chapter 2: Tumor gene signatures that correlate with release of extracellular vesicles shape the immune landscape in head and neck squamous cell carcinoma

Clinical & Experimental Immunology

(https://academic.oup.com/cei)

Impact Factor: 4.6

DOI: 10.1093/cei/uxad019

PMID: 36752300

PMCID: PMC10324554

Accepted 03 February 2023

Clinical and Experimental Immunology, 2023, **XX**, 1–12
https://doi.org/10.1093/cei/uxad019
Advance access publication 8 February 2023
Research Article

Research Article

Tumor gene signatures that correlate with release of extracellular vesicles shape the immune landscape in head and neck squamous cell carcinoma

Isabella Kallinger[1,‡], Dominique S. Rubenich[2,3,‡], Alicja Głuszko[4,‡], Aditi Kulkarni[5,6,7], Gerrit Spanier[1], Steffen Spoerl[1], Juergen Taxis[1], Hendrik Poeck[8], Mirosław J. Szczepański[4], Tobias Ettl[1], Torsten E. Reichert[1], Johannes K. Meier[1], Elizandra Braganhol[2,3], Robert L. Ferris[5,6,7,9], Theresa L. Whiteside[5,7,9,10] and Nils Ludwig[1,*]

[1]Department of Oral and Maxillofacial Surgery, University Hospital Regensburg, Regensburg, Germany
[2]Programa de Pós-Graduação em Biociências, Universidade Federal de Ciências da Saúde de Porto Alegre (UFCSPA), Porto Alegre, RS, Brazil
[3]Instituto de Cardiologia do Rio Grande do Sul/Fundação Universitária do Instituto de Cardiologia (IC-FUC), Porto Alegre, RS, Brazil
[4]Chair and Department of Biochemistry, Faculty of Medicine, Medical University of Warsaw, Warsaw, Poland
[5]UPMC Hillman Cancer Center, University of Pittsburgh, Pittsburgh, PA, USA
[6]Tumor Microenvironment Center, UPMC Hillman Cancer Center, Pittsburgh, PA, USA
[7]Department of Otolaryngology, University of Pittsburgh, Pittsburgh, PA, USA
[8]Clinic and Polyclinic for Internal Medicine III, University Hospital Regensburg and Leibniz Institute for Immunotherapy (LIT), Regensburg, Germany
[9]Department of Immunology, University of Pittsburgh, Pittsburgh, PA, USA
[10]Department of Pathology, University of Pittsburgh, Pittsburgh, PA, USA

[‡]Contributed equally.
[*]Correspondence: Nils Ludwig, Department of Oral and Maxillofacial Surgery, University Hospital Regensburg, Regensburg, Germany.
Email: nils.ludwig@ukr.de

Abstract

Head and neck squamous cell carcinomas (HNSCCs) evade immune responses through multiple resistance mechanisms. Extracellular vesicles (EVs) released by the tumor and interacting with immune cells induce immune dysfunction and contribute to tumor progression. This study evaluates the clinical relevance and impact on anti-tumor immune responses of gene signatures expressed in HNSCC and associated with EV production/release. Expression levels of two recently described gene sets were determined in The Cancer Genome Atlas Head and Neck Cancer cohort (n = 522) and validated in the GSE65858 dataset (n = 250) as well as a recently published single-cell RNA sequencing dataset (n = 18). Clustering into HPV(+) and HPV(−) patients was performed in all cohorts for further analysis. Potential associations between gene expression levels, immune cell infiltration, and patient overall survival were analyzed using GEPIA2, TISIDB, TIMER, and the UCSC Xena browser. Compared to normal control tissues, vesiculation-related genes were upregulated in HNSCC cells. Elevated gene expression levels positively correlated (P < 0.01) with increased abundance of CD4(+) T cells, macrophages, neutrophils, and dendritic cells infiltrating tumor tissues but were negatively associated (P < 0.01) with the presence of B cells and CD8(+) T cells in the tumor. Expression levels of immunosuppressive factors *NT5E* and *TGFB1* correlated with the vesiculation-related genes and might explain the alterations of the anti-tumor immune response. Enhanced expression levels of vesiculation-related genes in tumor tissues associates with the immunosuppressive tumor milieu and the reduced infiltration of B cells and CD8(+) T cells into the tumor.

Keywords: extracellular vesicles, exosomes, HNSCC, tumor-infiltrating immune cells, tumor microenvironment

Abbreviations: CAF: cancer-associated fibroblast; CD: cluster of differentiation; EVs: extracellular vesicles; EVsig: vesiculation-related genes; GEPIA2: gene expression profiling interactive analysis2; HNSCC: head and neck squamous cell carcinoma; HPV: human papilloma virus; MDSC: myeloid-derived suppressor cell; OS: overall survival; PBL: peripheral blood lymphocytes; PD-L1: programmed death-ligand 1; SEM: standard error of the mean; TCGA: the cancer genome atlas; TGFβ: transforming growth factor β; TIL: tumor-infiltrating lymphocytes; TIMER: tumor immune estimation resource; TISIDB: tumor–immune system interactions and drug bank database; TME: tumor microenvironment; Tregs: T regulatory cells; UCSC: University of California, Santa Cruz.

Introduction

Head and neck squamous cell carcinomas (HNSCCs) are a heterogeneous group of carcinomas that affect multiple anatomical sites including the oral cavity, pharynx, and larynx. They represent the largest proportion of all malignant tumors in the head and neck region and are considered the sixth most common malignancy worldwide [1]. The 5-year survival rate has improved only marginally in recent decades,

Received 3 September 2022; Revised 15 January 2023; Accepted for publication 3 February 2023

which emphasizes the need for advancements in the understanding of the tumor biology of HNSCC which will consequently translate into improvements of current treatment protocols [2].

Recently, release by tumor cells of extracellular vesicles (EVs) and their characterization has been one of the most intensively studied aspects of the tumor biology in various malignancies, including HNSCC [3]. These studies revealed that the release of different subsets of EVs by tumor cells is a major contributor to intercellular communication and induces functional alterations in the tumor microenvironment (TME) and at distant sites [4]. The EV subset of small EVs sized 30–150 nm that are derived from the endocytic pathway in tumor cells appears to play an important role in the TME [5]. They are actively produced by HNSCC cells, are released into extracellular space, and can be detected in all body fluids of HNSCC patients [6]. They carry a complex cargo of proteins, lipids, nucleic acids (microRNAs and other RNA-species), including soluble factors such as cytokines, chemokines, and numerous enzymes [5]. These cargo components are biologically active and induce functional changes in recipient cells [7], which can either be mediated by receptor/ligand interactions on the cell surface, fusion of EVs with the plasma membrane of the recipient cell, or by internalization of EVs via a variety of uptake mechanisms, including phagocytosis and endocytosis. Internalization of EVs has been shown to result in the transfer of factors which induce transcriptional changes in recipient cells. Recent studies emphasize that EVs released by HNSCC cells interact with different cell types leading to functional reprogramming of cells in the TME, including endothelial cells [7, 8], macrophages [9, 10], dendritic cells [11], CD4(+) and CD8(+) T cells [12, 13], B cells [14], T regulatory cells (Tregs) [14], and neurons [15]. Uniformly, these studies indicate that HNSCC-derived EVs reprogram recipient cells leading to promotion of tumor growth and ultimately to the establishment of a strongly immunosuppressive TME.

While the effects of HNSCC-derived EVs on individual cellular components of the TME are well described based on functional *in vitro*, *ex vivo*, or *in vivo* studies, the mechanisms underlying the effects of HNSCC-derived EVs on the TME composition remain unclear. In this study, we used a bioinformatics approach to better define the role EVs play in shaping the cellular composition of the TME. We have focused on two recently and independently published gene signatures whose expression has been linked to increased EV release from cancer cells [16, 17].

Table 1: Gene signatures associated with EV secretion[a]

Fathi *et al.* [16] "Fathi-EVsig"	Hurwitz *et al.* [17] "Hurwitz-EVsig"
ARF6	ANXA2
ATG3	ARF4
ATG12	BSG
BST2	CD59
CD9	CD81
CD63	HLA-A
CD82	HRAS
CHMP4C	HSPA1B
CIT	HSPB1
CTTN	ITGB1
DGKA	LGALS3BP
HGS	MYL3
PDCD6IP	MYL6
PKM2	NME2
PLD2	NRAS
RAB2B	RAB5C
RAB5A	RAB7A
RAB7A	RAC1
RAB9A	RALB
RAB11A	RAP1B
RAB27A	RHOA
RAB27B	SEC22B
RAB35	TAGLN2
RALA	UBE2D3
RALB	VAMP3
SDC1	
SDC2	
SDC3	
SDC4	
SDCBP	
SMPD3	
SNAP23	
STAM	
STX1A	
SYT7	
TSG101	
TSPAN8	
VAMP7	
VPS4A	
VTA1	
YKT6	

[a]Symbols of genes used in this study.

Materials and methods

Gene signatures

To test the correlation between clinical patient characteristics and the transcriptional signatures, we used two previously described sets of genes known to be involved in EV secretion (Table 1). The first signature (Fathi-EVsig) was published by Fathi *et al.* [16] and consists of 41 genes known to be involved in EV secretion based on previous findings in the literature. The second signature (Hurwitz-EVsig) was published by Hurwitz *et al.* [17] and it is based on the proteomic profiling of EVs isolated from 60 cell lines from the National Cancer Institute (NCI-60). The authors performed a subsequent network analysis of vesicle quantity and proteomes to identify EV components associated with vesicle secretion and created the gene signature shown in Table 1 based on their results. The signatures by Fathi *et al.* and Hurwitz *et al.* mostly consist of distinct genes, with *RAB7A* and *RALB* being the only genes which are included in both gene sets.

Additionally, gene signatures representing hypoxia, matrix metalloproteinases, cancer stem cells, and EMT were composed of following genes: *HIF1A*; *MMP2*, *MMP9*, and *MMP13*; *CD44*, *PROM1*, and *ALDH1A1*; *TWIST1*, *SNAI1*, and *SNAI2*, respectively. The gene set HALLMARK_ANGIOGENESIS (systematic name: M5944) was downloaded

from the open access molecular signature database (https://www.gsea-msigdb.org/gsea/msigdb/genesets.jsp) provided by UC San Diego Broad Institute. Dataset consisted of 36 genes known to be upregulated during formation of blood vessels and was used for correlation analysis.

RNA sequencing data acquisition

Gene expression levels based on RNA-seq data from HNSCC patients and clinical characteristics were obtained from the Cancer Genome Atlas (TCGA; https://gdc.nci.nih.gov) using the University of California, Santa Cruz (UCSC) Xena Browser [18]. Expression profiles of Fathi-EVsig and Hurwitz-EVsig were compared between a total of 522 cases of primary HNSCC and 44 normal control samples. Ninety-eight cases of HPV(+) HNSCC and 422 cases of HPV(−) HNSCC were used for further analysis. For data validation, the GSE65858 dataset was used with 250 cases of primary HNSCC which were further separated into 54 cases of HPV(+) HNSCC and 196 cases of HPV(−) HNSCC.

Single-cell RNA sequencing data acquisition

Transcriptomic profiles of peripheral blood lymphocytes (PBL) and tumor-infiltrating lymphocytes (TIL; n = 18 patients), as well as non-immune cells from patient tumors (n = 15 patients) were analyzed based on a previously published dataset [19, 20]. Using the scanpy.tl.score_genes() function, a gene signature score from both published EV signatures was calculated for each cell [21]. Cells were binned into appropriate groups, for calculating differences in the EV signature scores.

GEPIA2 analysis

To measure the expression levels of individual candidate genes as well as gene signatures in HNSCC and normal samples, the Gene Expression Profiling Interactive Analysis2 (GEPIA2; http://gepia2.cancer-pku.cn/) was used [22]. Moreover, the tool was used to generate overall survival and disease specific survival Kaplan–Meier plots, compare between subtypes, and perform correlation analysis.

TISIDB analysis

Tumor–immune system interactions and drug bank database (TISIDB; http://cis.hku.hk/TISIDB/) was used to determine the potential association between candidate genes and immunomodulators and chemokines in HNSCC patients [23]. Gene expression levels of immunomodulators and vesiculation-related genes were analyzed using Spearman correlation analysis. Data are presented as Fisher Z-transformation of correlation coefficient.

TIMER analysis

Tumor IMmune Estimation Resource (TIMER; https://cistrome.shinyapps.io/timer/), a web server for comprehensive analysis of tumor-infiltrating immune cells, was used to estimate the potential association between candidate genes, immune cell infiltration, and clinical parameters [24]. In this study, gene module was used to select genes of interest and visualize the correlation of its expression with immune infiltration levels in HNSCC patients. For further analysis, patients were separated into HPV(+) and HPV(−) HNSCC cases.

Statistical analysis

Statistical analysis was performed using GraphPad Prism version 9.4.0. Data are presented with P values determined in t tests or fold changes. For survival analyses, the Kaplan–Meier method was used to analyze the correlation between gene expression levels and survival, and the log-rank test to compare the survival curves. Correlations were assessed using Spearman's correlation analysis. Fisher Z-Transformation was used to transform the sampling distribution of correlation coefficients. A P value < 0.05 was defined as a statistically significant difference.

Results

Expression of vesiculation-related genes differs in HNSCC samples and normal tissues and has a negative impact on patient survival

Gene expression levels of vesiculation-related genes were increased in HNSCC tissues for both Fathi-EVsig (Fig. 1A) and Hurwitz-EVsig (Fig. 1B) compared to those in solid normal tissues, although not reaching statistically significant differences. Analysis of the individual gene expression levels of the vesiculation-related genes in tumors comparing to normal control tissues revealed that 19 of the 41 (Fathi-EVsig) and 12 of the 25 (Hurwitz-EVsig) vesiculation-related genes were upregulated in HNSCC, whereas the expression levels of 20 and 6 genes, respectively, were downregulated in HNSCCs compared to solid normal tissues (Fig. 1C and D). For both gene signatures no significant impact on overall survival was detectable (Fig. 1E and G); however, there was a trend that increased expression levels were associated with poor disease-free survival (Fig. 1F and H). For Hurwitz-EVsig, disease-free survival was significantly worse at high gene expression levels compared to patients with low expression levels (P = 0.031; Fig. 1H). Analysis of individual gene expression levels showed that nearly all genes of the Hurwitz-EVsig contributed to poor survival (Fig. 1J), while approximately half of the genes belonging to the Fathi-EVsig were associated with poor survival (Fig. 1I).

To validate these findings in an independent cohort and further investigate the expression patterns of the two EV signatures in HNSCC, a previously published single-cell sequencing dataset which included 18 HNSCC patients was analyzed. The expression levels of both gene signatures were significantly higher in non-immune cells, compared to expression levels in PBLs and TILs (Fig. 2A and D). Both EV signatures were equally expressed in pericytes, endothelial cells, fibroblasts, and epithelial cells; however, gene expression levels were significantly lower in immune cells. Dendritic cells, macrophages, and mast cells were the immune cell subsets with the highest expression levels of Fathi-EVsig and Hurwitz-EVsig (Fig. 2B, C, E, and F). Further, we compared the gene expression levels of the two EV signatures in PBLs and TILs and levels of Fathi-EVsig were significantly elevated in all studied immune cell subsets with the exception of monocytes and macrophages (Fig. 2G). CD8(+) T cells, dendritic cells, and Tregs were characterized by higher levels of Hurwitz-EVsig when comparing tumor-infiltrating and circulating cells (Fig. 2H). These results indicate that the EV release is accelerated in immune cells infiltrating the tumor tissue.

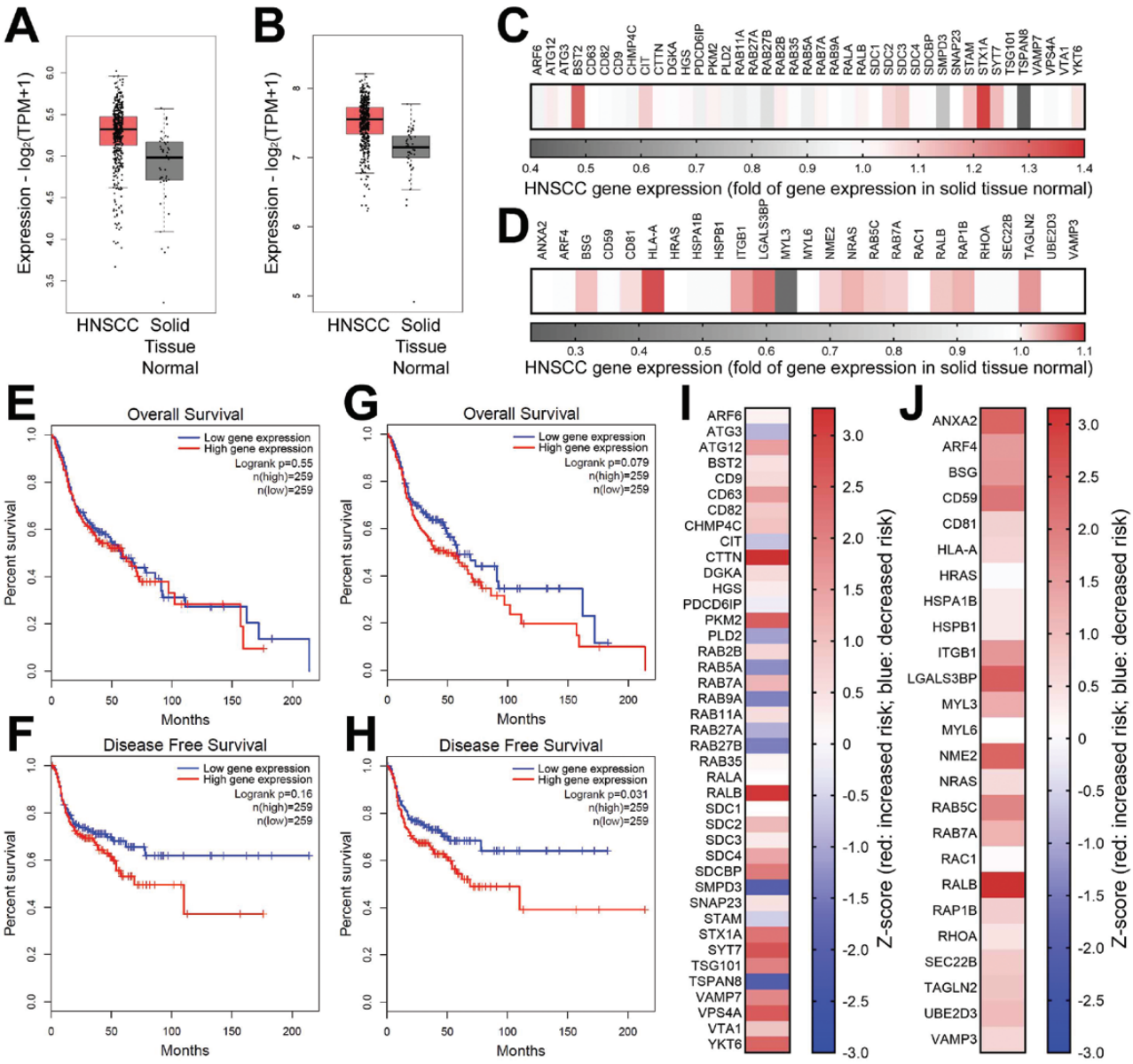

Figure 1: Analysis of gene expression levels of Fathi-EVsig and Hurwitz-EVsig in HNSCC and impact on patient survival. (A) Comparison of Fathi-EVsig gene expression in normal solid tissue (n = 44) and in primary HNSCC tumors (n = 519). (B) Comparison of Hurwitz-EVsig gene expression in normal solid tissue (n = 44) and in primary HNSCC tumors (n = 519). (C) Comparison of gene expression levels of the individual genes of the Fathi-EVsig in normal solid tissue (n = 44) and in primary HNSCC tumors (n = 519). (D) Comparison of gene expression levels of the individual genes of the Hurwitz-EVsig in normal solid tissue (n = 44) and in primary HNSCC tumors (n = 519). (E) Kaplan–Meier overall survival curves of Fathi-EVsig high expression *versus* low expression in patients diagnosed with HNSCC. (F) Kaplan–Meier disease free survival curves of Fathi-EVsig high expression *versus* low expression in patients diagnosed with HNSCC. (G) Kaplan–Meier overall survival curves of Hurwitz-EVsig high expression *versus* low expression in patients diagnosed with HNSCC. (H) Kaplan–Meier disease free survival curves of Hurwitz-EVsig high expression *versus* low expression in patients diagnosed with HNSCC. (I) Overall survival based on the expression of the individual genes of the Fathi-EVsig. Red: increased risk; Blue: decreased risk. (J) Overall survival based on the expression of the individual genes of the Hurwitz-EVsig. Red: increased risk; Blue: decreased risk (for colour figure refer to online version)

Associations of vesiculation-related genes with clinicopathologic data of HNSCC patients

To evaluate the clinical relevance of vesiculation-related genes, individual expression patterns were compared between patients with distinct clinical characteristics such as: tumor stage, tumor grade, perineural or lymphovascular invasion, remission/progression of disease, treatment approach (radiation or molecular targeted therapy), and habitual risk factors (alcohol or tobacco abuse). We were not able to detect significantly different values for these parameters; however, several trends were observable. Progressive disease stage was associated with decreased expression levels of vesiculation-related genes, especially for the Hurwitz-EVsig in stage III-IV patients and for the Fathi-EVsig in stage IVB and IVC patients (Fig. 3A). Levels of Fathi-EVsig were upregulated in patients with grade G4 tumors in comparison to G1, G2, and G3 tumors (Fig. 3B). For Hurwitz-EVsig, the gene expression levels decreased with higher grade of the

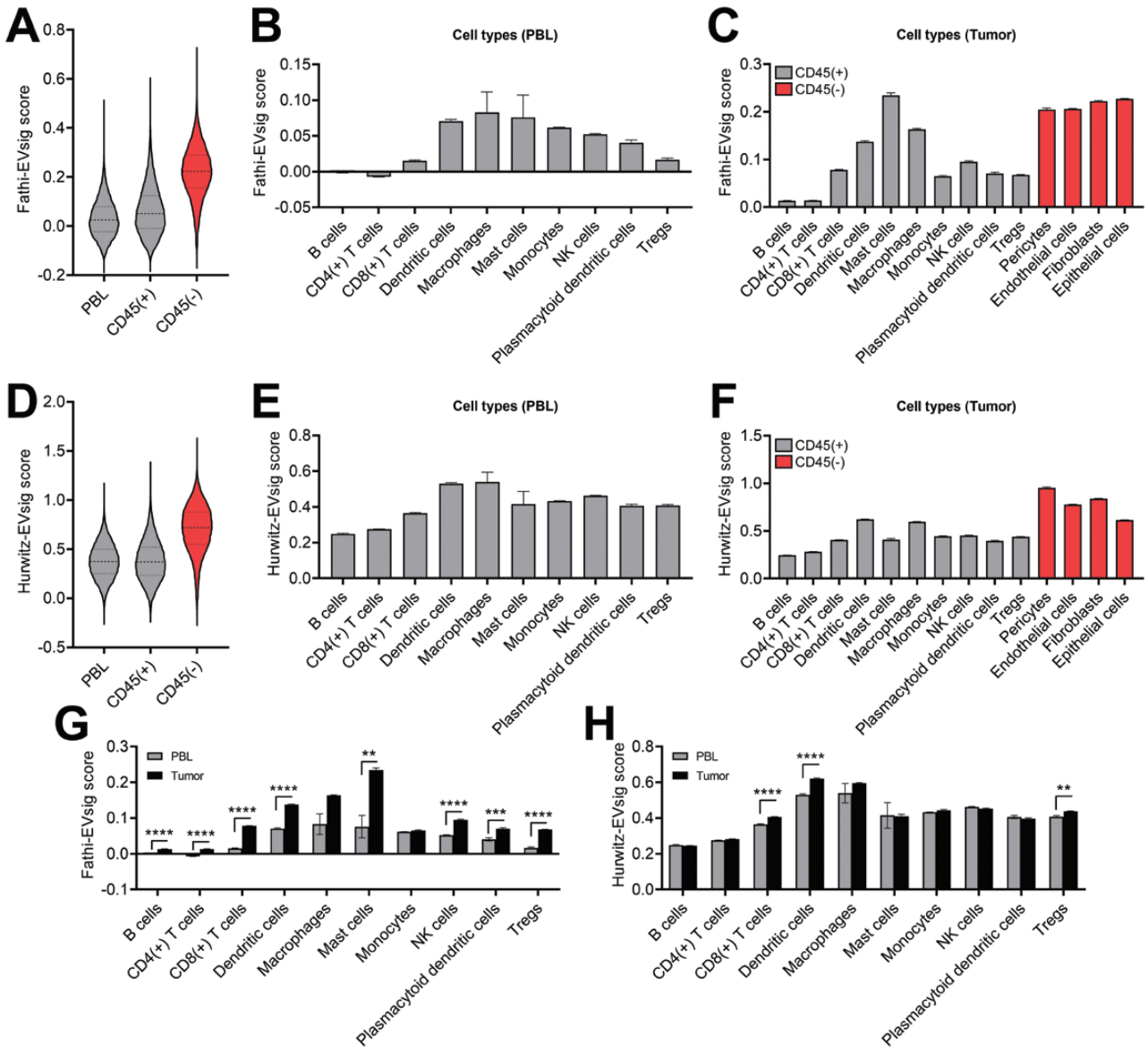

Figure 2: Analysis of gene expression levels of Fathi-EVsig and Hurwitz-EVsig in the HNSCC single-cell RNA sequencing cohort. (A) Expression of the Fathi-EVsig in PBL, CD45(+) tumor-infiltrating lymphocytes and CD45(−) cells. (B) Expression of the Fathi-EVsig by individual PBL subsets. (C) Expression of the Fathi-EVsig by individual immune and non-immune cell subsets. (D) Expression of the Hurwitz-EVsig in PBL, CD45(+) and CD45(−) cells. (E) Expression of the Hurwitz-EVsig by individual PBL subsets. (F) Expression of the Hurwitz-EVsig by individual immune and non-immune cell subsets. (G) Comparison of Fathi-EVsig gene expression levels in PBL and TILs. (H) Comparison of Hurwitz-EVsig gene expression levels in PBL and TILs. All values represent means ± SEM; $^{**}P < 0.01$ *versus* PBL; $^{***}P < 0.001$ *versus* PBL; $^{****}P < 0.0001$ *versus* PBL

tumors (Fig. 3B). The expression levels of Fathi-EVsig were similar in patients treated with or without radiation therapy or targeted molecular therapy (Fig. 3C and D). However, patients treated with radiation therapy or targeted molecular therapy showed downregulated gene expression levels of the Hurwitz-EVsig (Fig. 3C and D). Lymphovascular and perineural invasion were not associated with altered gene expression levels of Fathi-EVsig; however, expression levels of Hurwitz-EVsig were increased in patients with lymphovascular and perineural invasion (Fig. 3E and F). Alcohol or tobacco abuse, which are typical risk factors for HNSCC, was not associated with altered gene expression levels of both signatures (Fig. 3G and H). Gene expression levels of Fathi-EVsig were upregulated in patients showing partial remission/response and patients with persistent or stable disease (Fig. 3I). Gene expression levels of Hurwitz-EVsig were upregulated in patients showing partial remission/response, persistent disease, progressive disease, and stable disease in comparison to patients with complete remission/response (Fig. 3I).

mRNA levels of vesiculation-related genes positively correlate with malignant gene expression levels in HNSCC

To further characterize the molecular phenotype which is associated with the two EV gene signatures, correlations between gene expression levels of Fathi-EVsig and Hurwitz-EVsig with pro-malignant genes were analyzed. The analysis focused on hallmarks of HNSCC progression [1] and included

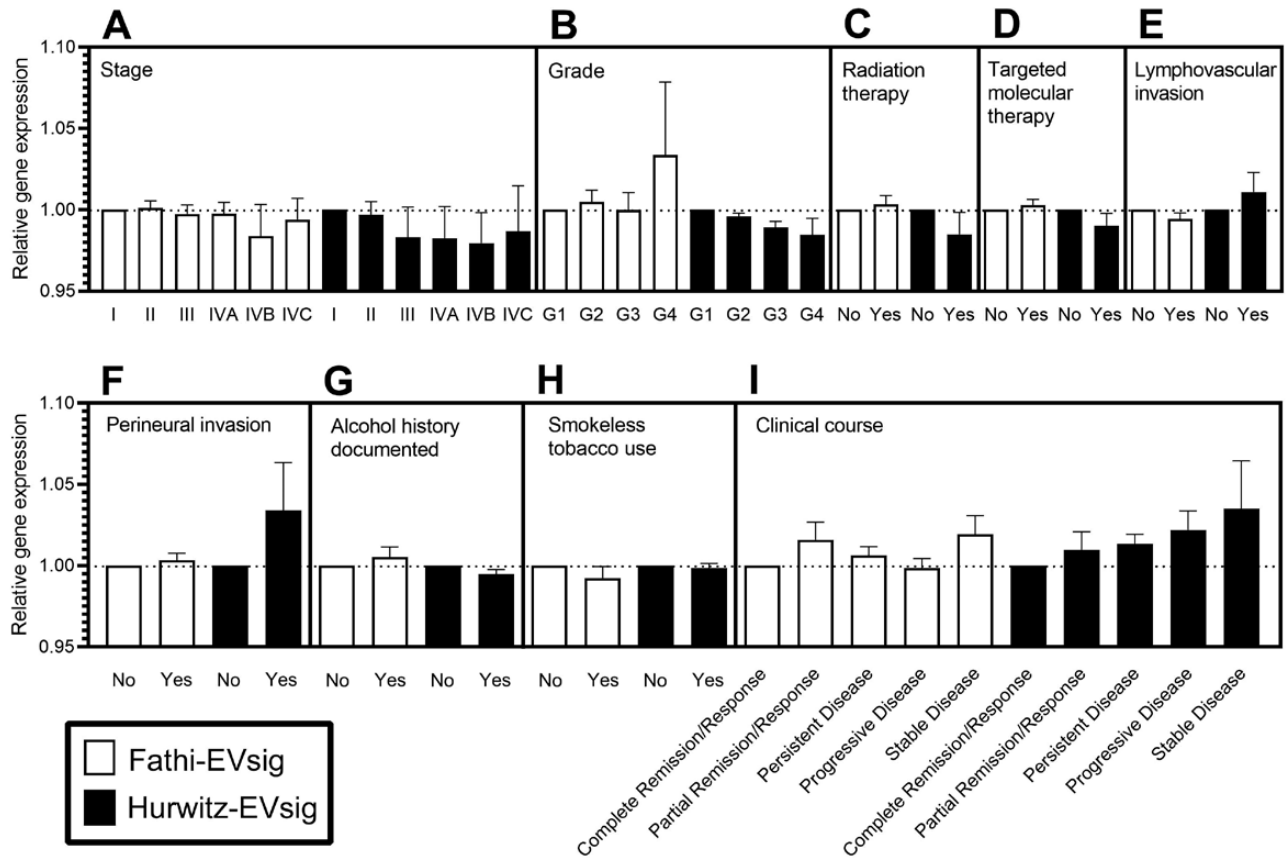

Figure 3: Correlation of Fathi-EVsig and Hurwitz-EVsig relative gene expression levels with clinical parameters of HNSCC patients. Clinical stage (A), neoplasm histologic grade (B), radiation therapy (C), targeted molecular therapy (D), lymphovascular invasion (E), perineural invasion (F), alcohol history (G), smokeless tobacco use (H), and clinical course (I). All values represent means ± SEM

HIF1A as a gene representing hypoxic conditions (Fig. 4A and F); the HALLMARK_ANGIOGENESIS gene set, representing tumor angiogenesis (Fig. 4B and G); *MMP2*, *MMP9*, and *MMP13* to represent matrix metalloproteinases (Fig. 4C and H); *CD44*, *PROM1*, and *ALDH1A1* to represent cancer stem cell properties (Fig. 4D and I); and *TWIST1*, *SNAI1*, and *SNAI2* to represent epithelial to mesenchymal transition (Fig. 4E and J). Fathi-EVsig and Hurwitz-EVsig both significantly correlated with all the above-mentioned malignant gene expression levels in HNSCC ($P < 0.001$; Fig. 4).

Correlation of vesiculation-related genes with immunomodulatory factors in HNSCC tissues

To evaluate the impact of vesiculation-related genes on the immune phenotype of HNSCC patients, gene expression levels of Fathi-EVsig and Hurwitz-EVsig were correlated with expression levels of genes known to play an immune-suppressive or immune-stimulatory role as well as with chemokines. While the Fathi-EVsig negatively correlated with most immunostimulatory factors (Fig. 5C), there was a highly significant positive correlation with *NT5E* (encoding for CD73) and *TGFB1* ($P < 0.0001$; Fig. 5A), suggesting that tumors with elevated expression levels of vesiculation-related genes have a potential impact on the immune landscape by adenosinergic and TGFβ signaling. There was also a significantly positive correlation with *CD274* (encoding for PD-L1) further indicating that vesiculation-related genes are associated with an immunosuppressive TME ($P < 0.001$; Fig. 5A). Interestingly, these results were identical when looking at the Hurwitz-EVsig, with mostly negative correlations with immunostimulatory factors (Fig. 5D) and highly significant correlations with *NT5E*, *TGFB1*, and *CD274* ($P < 0.0001$; Fig. 5B). These results indicate that the EV genetic profiles associate with a distinct immunosuppressive profile in HNSCC. Among chemokines, which exert a double-edged sword in cancer by their pro- or anti-tumor effects, both signatures correlated mostly with chemoattractant factors associated with tumor inflammation, reprogramming, EMT, and neovascularization. The most significant correlations were *CXCL8* in Fathi-EVsig, *CXCL11* in Hurwitz-EVsig, and *CCL27* in both ($P < 0.001$; Fig. 5E and F). *CXCL8* is known to be a neutrophil chemoattractant [25], *CXCL11* is considered as an inducer of PD-L1 expression [26], and *CCL27* is considered as a mediator of lymphatic endothelial cell migration during tumor-associated lymphangiogenesis [27]. *CXCL14*, also highly correlating with both EVsig datasets ($P < 0.001$; Fig. 5E and F), is known to be associated with reduced tumor growth and increased tumor infiltrating lymphocytes [28]. These results were validated in the non-TCGA bulk sequencing cohort and the overall correlation profiles of both EV signatures with immunosuppressive and immunostimulatory factors as well as with chemokines were found to be congruent. *TGFB1*, *NT5E*, and *CD274* were among the factors correlating best with both EV signatures (Fig. S1A and

B). The same was observed for the chemokines *CXCL14*, *CXCL11*, *CCL27*, and *CXCL8* (Fig. S1E and F).

mRNA levels of vesiculation-related genes were associated with a characteristic landscape of infiltrating immune cells

High gene expression levels of Fathi-EVsig correlated with elevated abundance of tumor-infiltrating CD4(+) T cells, macrophages, neutrophils, and dendritic cells into tumor tissues ($P < 0.01$; Fig. 6A). Elevated expression of Fathi-EVsig was also associated with an exclusion of B cells and CD8(+) T cells in HNSCC tissues ($P < 0.01$; Fig. 6A). Interestingly, the same correlations with immune cell abundance were also observed for the expression levels of Hurwitz-EVsig confirming our analysis of the Fathi-EVsig. Thus, elevated expression levels of Hurwitz-EVsig were associated with increased abundance of tumor-infiltrating CD4(+) T cells, macrophages, neutrophils, and dendritic cells ($P < 0.01$) and exclusion of B cells and CD8(+) T cells ($P < 0.01$; Fig. 6B). In the non-TCGA bulk sequencing validation cohort, we also observed an exclusion of B cells and CD8(+) T cells and increased infiltration abundance of neutrophils and dendritic cells. However, in contrast to the TCGA cohort the infiltration abundance of

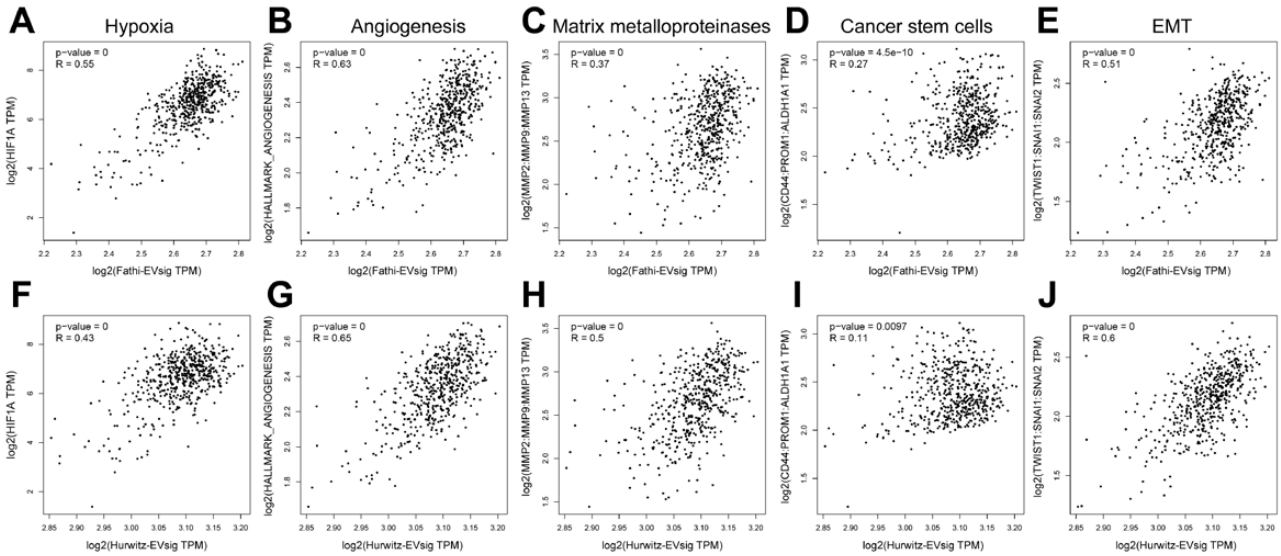

Figure 4: Correlation of Fathi-EVsig expression levels with *HIF1A* (A), HALLMARK_ANGIOGENESIS (GSEA, Molecular Signatures Database M5944) (B), *MMP2*, *MMP9*, and *MMP13* (C), *CD44*, *PROM1*, and *ALDH1A1* (D), *TWIST1*, *SNAI1*, and *SNAI2* (E). Correlation of Hurwitz-EVsig expression levels with *HIF1A* (F), HALLMARK_ANGIOGENESIS (GSEA, Molecular Signatures Database M5944) (G), *MMP2*, *MMP9*, and *MMP13* (H), *CD44*, *PROM1*, and *ALDH1A1* (I), *TWIST1*, *SNAI1*, and *SNAI2* (J). Correlation analysis (descriptive and inferential statistics) was performed using GEPIA2

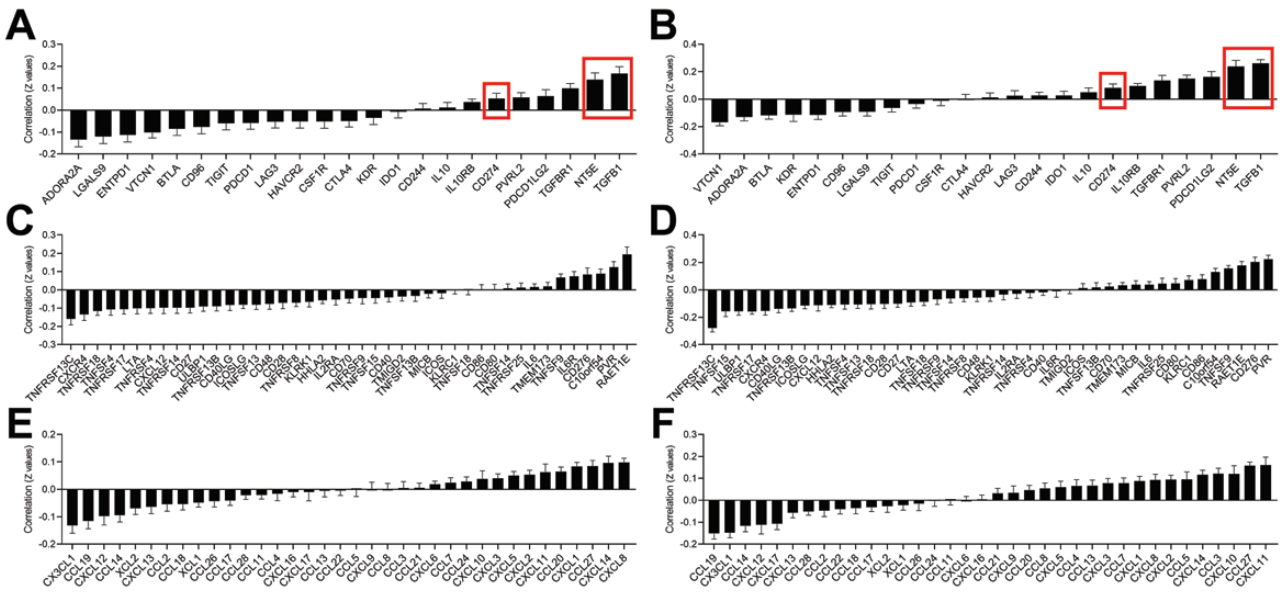

Figure 5: Correlation of vesiculation-related genes with immunomodulatory factors in HNSCC tissues. (A) Correlation between immunoinhibitory factors and the Fathi-EVsig. (B) Correlation between immunoinhibitory factors and the Hurwitz-EVsig. (C) Correlation between immunostimulatory factors and the Fathi-EVsig. (D) Correlation between immunostimulatory factors and the Hurwitz-EVsig. (E) Correlation between chemokines and the Fathi-EVsig. (F) Correlation between chemokines and the Hurwitz-EVsig. All values represent means ± SEM

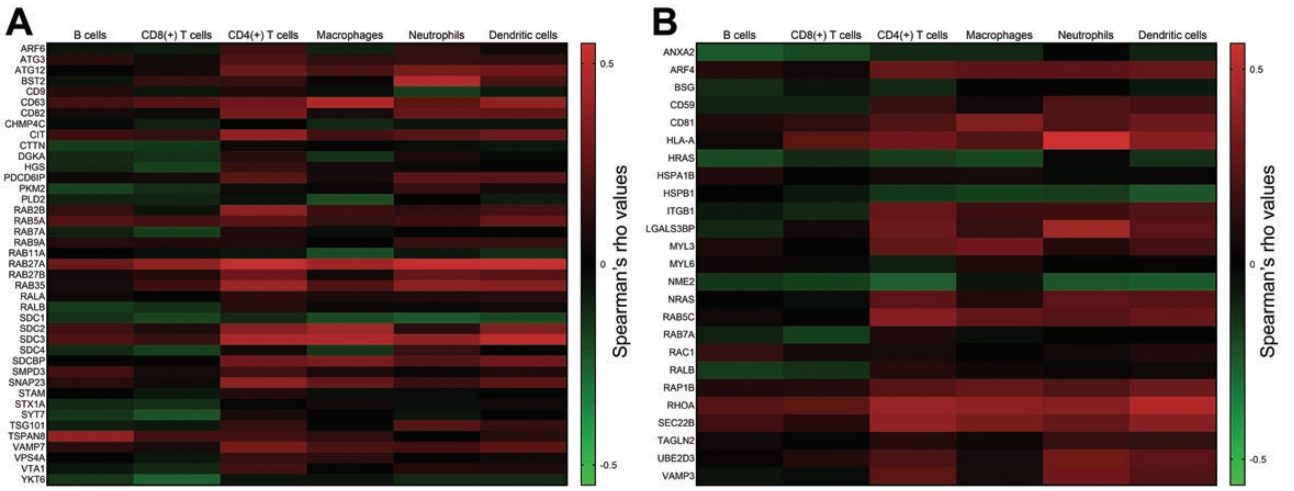

Figure 6: Correlation of vesiculation-related genes with immune cell infiltration. (A) Heat map visualizing the correlation of the expression levels of the Fathi-EVsig and the immune cell infiltration levels of B cells, CD8(+) T cells, CD4(+) T cells, macrophages, neutrophils, and dendritic cells. Each cell represents the Spearman's rho value of each gene of the Fathi-EVsig. (B) Heat map visualizing the correlation of the expression levels of the Hurwitz-EVsig and the immune cell infiltration levels of B cells, CD8(+) T cells, CD4(+) T cells, macrophages, neutrophils, and dendritic cells. Each cell represents the Spearman's rho value of each gene of the Hurwitz-EVsig

CD4(+) T cells and macrophages negatively correlated with expression levels of Fathi-EVsig and Hurwitz-EVsig (Fig. S2). In aggregate, these results indicate that the increased expression of vesiculation-related genes in the tumor is associated with a characteristic landscape of tumor-infiltrating immune cells, where immune effector cells are depleted.

Expression levels of vesiculation-related genes in HPV(+) and HPV(−) HNSCCs translate into distinct immunological profiles

HPV(+) and HPV(−) HNSCCs are characterized by the distinct composition of immune cells infiltrating in the tumor tissues [29]. HPV(+) tumors display much more strongly immune infiltration compared with HPV(−) tumors, with higher levels of T cell infiltration and CD8(+) T cell activation [30]. Therefore, the HNSCC cohorts were subdivided into HPV(+) and HPV(−) patients, and the gene expression levels of vesiculation-related genes and their impact on immune cell infiltration were analyzed separately. No differences were observed for the expression levels of Fathi-EVsig and Hurwitz-EVsig with regard to HPV status in the TCGA as well as in the validation bulk sequencing cohort (Figs. 7A; Supplementary S3A), and overall expression levels of vesiculation-related genes were associated with a similar immunological profile in HPV(+) and HPV(−) patients (Fig. 7B and C; Supplementary Fig. S3B and C). This profile was characterized by increased infiltration of CD4(+) T cells, macrophages, neutrophils, and dendritic cells and the exclusion of B cells and CD8(+) T cells (Fig. 7B and C). However, high gene expression levels of Fathi-EVsig in HPV(+) tumors correlated with an increased abundance of Tregs and a decreased abundance of CAFs and MDSCs when compared to HPV(−) tumors ($P < 0.05$; Fig. 7B). These significant differences were not detected in the non-TCGA bulk sequencing validation cohort, although we observed a similar trend for Tregs and CAFs (Fig. S3B). High gene expression levels of Hurwitz-EVsig in HPV(+) tumors correlated with a decreased abundance of CD4(+) T cells when compared to HPV(−) tumors ($P < 0.05$; Fig. 7C). The significant correlation of gene expression levels of the Hurwitz-EVsig with decreased abundance of CD4(+) T cells in HPV(+) tumors was also observed in the validation cohort ($P < 0.05$; Fig. S3C). Additionally, the levels of Hurwitz-EVsig expression in the validation cohort significantly correlated with decreased infiltration abundance of B cells and dendritic cells and increased abundance of CAFs ($P < 0.05$; Supplementary Fig. S3C). These results indicate that the landscape of infiltrating immune cells which is associated with vesiculation-related genes differs depending on the HPV status of the tumors.

To further define the expression patterns of the two EV signatures in HPV(+) and HPV(−) HNSCC, we separated the single-cell sequencing cohort based on the patients viral status into six HPV(+) and nine HPV(−) patients. While the gene expression levels appeared similar in the bulk sequencing cohorts (Figs. 7A; Supplementary S3A), clustering of the patients into EVsig^{low} and EVsig^{high} patients based on expression in only non-immune cells revealed that most HPV(+) patients had increased levels of Fathi-EVsig (Fig. 7D). Hurwitz-EVsig gene expression levels almost separated HPV(+) from HPV(−) patients and were elevated in HPV(−) patients (Fig. 7E). This also reflected in increased or decreased expression in HPV(+) epithelial cells of Fathi-EVsig and Hurwitz-EVsig, respectively ($P < 0.05$; Fig. 7F and G). Significantly higher levels of Hurwitz-EVsig were also found in HPV(−) fibroblasts compared to their HPV(+) counterparts ($P < 0.05$; Fig. 7G). Interestingly, the expression patterns in immune cells were distinct in HPV(+) and HPV(−) HNSCCs and both EV signatures were expressed significantly higher in HPV(−) B cells, CD4(+) T cells, plasmacytoid dendritic cells, and Tregs compared to their HPV(+) counterparts ($P < 0.05$; Fig. 7F and G). While the PBLs of HPV(+) and HPV(−) HNSCCs expressed similar levels of Fathi-EVsig (Fig. 7F), CD4(+) T cells, CD8(+) T cells, and monocytes expressed significantly higher levels of Hurwitz-EVsig in HPV(+) HNSCC ($P < 0.05$; Fig. 7G).

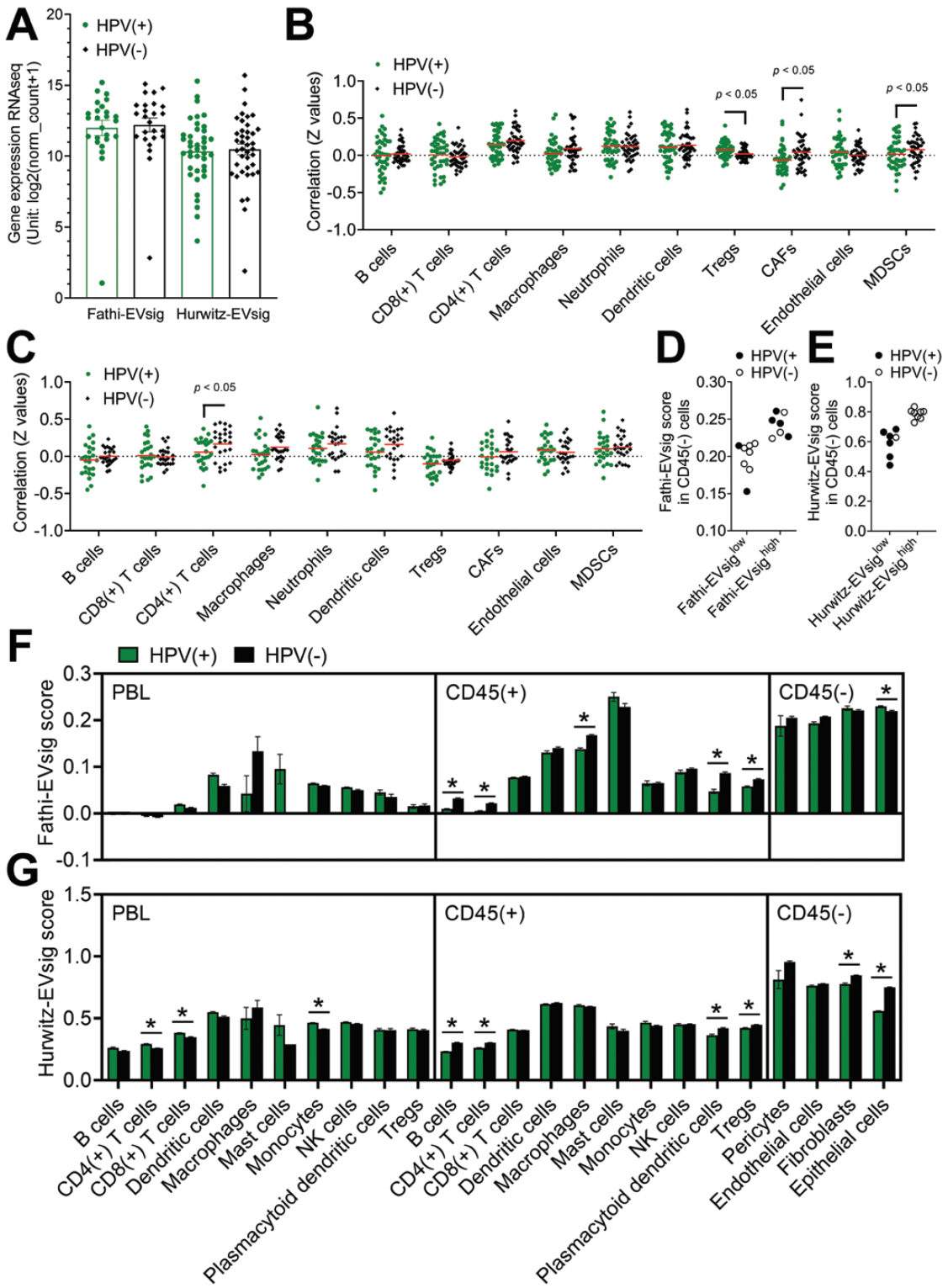

Figure 7: Comparison of vesiculation-related genes in HPV(+) and HPV(–) HNSCCs. (A) Comparison of Fathi-EVsig and Hurwitz-EVsig gene expression in HPV(+) and HPV(–) HNSCC patients. (B) Infiltration abundance of immune cells based on Fathi-EVsig expression in HPV(+) and HPV(–) patients. (C) Infiltration abundance of immune cells based on Hurwitz-EVsig expression in HPV(+) and HPV(–) patients. (D) Fathi-EVsig score in non-immune cells of individual HPV(+) and HPV(–) patients. (E) Hurwitz-EVsig score in non-immune cells of individual HPV(+) and HPV(–) patients. (F) Fathi-EVsig score in individual PBL, TIL, and non-immune cell subsets in HPV(+) and HPV(–) patients. (G) Hurwitz-EVsig score in individual PBL, TIL, and non-immune cell subsets in HPV(+) and HPV(–) patients. Values in F and G represent means ± SEM

Discussion

The progression of HNSCC is dependent on the formation of an immunosuppressive niche which favors tumor growth and metastasis. Understanding the mechanisms underlying the initiation and maintenance of this immunosuppressive microenvironment is of great current interest. Attention has been centered on communication between malignant and non-malignant cells in the TME, which leads to phenotypic and functional reprogramming of tumor resident and infiltrating cells and ultimately promotes disease progression. Tumor-derived EVs are reported to contribute to intercellular communication locally in the tumor and at distant sites [31]. We and others have demonstrated that HNSCC-derived EVs carry a cargo of biologically active components which promote tumor progression [7–10]. Although HNSCC-derived EVs are implicated in mediating cancer progression, their actual contribution to the formation of the tumor-promoting TME remains elusive. Here, we first searched for gene datasets related to EV production by tumor cells, and then used the available data for comparison of HNSCCs with high and low production rates of EVs.

Our bioinformatics analysis demonstrated that increased expression levels of vesiculation-related genes correlated with a profile of TGFβ and adenosinergic signaling in the tumor. Both signaling pathways are known to have major immunosuppressive effects in HNSCC and promote tumor progression [32–34]. The two main pathway components, TGFβ and CD73, were previously identified as functionally active cargo components in HNSCC-derived EVs [10, 35]. Recent literature emphasizes the role of EVs as carriers and producers of adenosine [36–38]. Our bioinformatics analysis based on gene expression levels of the adenosinergic pathway components has confirmed that this pathway is one of the major immunosuppressive mechanisms mediated by HNSCC-derived EVs. Our data demonstrated that—along with a TGFβ/CD73 profile—a collection of cytokine genes correlated with the expression of vesiculation-related genes in HNSCC patients. This observation supports the presence of a tumor-promoting environment in the TME. Expression levels of the vesiculation-related genes in the datasets we used, showed significant correlation with IL-8 ($P < 0.0001$), responsible for immune cell recruitment [39] and with IL-6 and IL-10 ($P < 0.01$), which mediate pro-tumor functions of neutrophils and macrophages [40, 41]. Concerning immunosuppressive function, IL-10 impairs CD8(+) T cells [42], which is consistent with our findings, since abundance of infiltrating CD8(+) T cells in tumor tissues was negatively associated with expression levels of the vesiculation-related genes in both EV signatures. Moreover, both EV signatures have positive correlation with immune checkpoints, such as CD274, CD276, PVR, and c10orf54 (Fig. 5A–D), which have become a hallmark of the immunosuppressive TME [43].

Tumor-derived EVs carry both immunosuppressive and immunostimulatory receptor/ligands and thus may be involved in various immunomodulatory pathways [44]. The cargo of tumor-derived EVs contains costimulatory molecules, major histocompatibility complex class I and class II molecules, tumor-associated antigens, and intraluminal growth-promoting cytokines in addition to a plethora of immunoinhibitory molecules [3, 45]. Analogous with these reports, we demonstrated that the EV signatures correlate with the expression levels of a variety of immunostimulatory factors as well as tumor-suppressive factors, such as *CXCL14*. Although this seems counterintuitive when looking at the immunosuppressive effects of tumor-derived EVs in the TME, it appears that stimulatory and inhibitory signals of tumor-derived EVs are delivered simultaneously. It remains unclear how this mode of delivery of multiple signals is able to stimulate or inhibit immune responses translates into specific functional alterations in recipient cells [3].

It is under current investigation, whether tumor-derived EVs play a distinct role in HPV(+) and HPV(−) HNSCC. Recent findings indicate that EVs from HPV(+) and HPV(−) tumors have differential protein contents that might translate to distinct functional effects and, thus, contribute to the disparity in immune responses that characterize HPV(+) and HPV(−) HNSCCs [46]. In direct comparison of EVs isolated from HPV(+) and HPV(−) HNSCCs, HPV(+) EVs were capable of sustaining dendritic cell functions and, therefore, may play a role in promoting anti-tumor immune responses in patients with HPV(+) HNSCC [11]. Our bioinformatics analysis validated these findings since we also observed distinct immune landscapes depending on the HPV status of the primary tumors. In HPV(+) tumors vesiculation-related genes correlated with an increased abundance of Tregs and a decreased abundance of CD4(+) T cells, CAFs, and MDSCs. These findings need further validation in clinical tumor samples as well as functional *in vitro* and *in vivo* studies and might accelerate the understanding of the differences in the immune landscape of viral- and carcinogen-driven HNSCC.

One of the current challenges in the field is the heterogeneity of EV subpopulations that tumors produce. Various subtypes of tumor-derived EVs may be released by the tumor, carrying different cargos and mediating different functions in recipient cells [47]. Capturing these subtypes selectively using protein markers or gene signatures remains a challenge. Therefore, the two gene signatures we used in this study may not reflect the complexity of EV biogenesis and their heterogeneity. Also, these gene signatures need to be validated *in vivo* by parallel analysis of tumor gene expression levels and quantification of local and circulating tumor-derived EVs. However, although the Fathi-EVsig and Hurwitz-EVsig share only two common genes and are, therefore, mostly independent signatures, they gave similar results, suggesting that the specific shaping of the immune landscape may be an overall mechanism which can be attributed to tumor-derived EVs.

Conclusions

The presented bioinformatic data indicate that tumor cell-derived EVs carrying a complex cargo of immunosuppressive proteins are likely to shape immune cell infiltration into the tumor by interaction with immune cells in the periphery or locally in the tumor. The biological effects of EVs—orchestrated by a variety of factors enriched in EVs—may shape and modulate the immune landscape in a very specific manner, with exclusion of effector lymphocytes and promotion of the abundant infiltration of CD4(+) T cells, macrophages, neutrophils, and dendritic cells. Also, gene signatures related to vesiculation are enriched in tumor cells and are potential immune biomarkers in HPV(+) and HPV(−) HNSCC. Our *in silico* results provide a baseline for future prospective studies to be conducted with a well-defined HNSCC patient cohort to

compare expression levels of vesiculation-related genes with plasma levels of EVs, immunopathology of the tumor, and clinical parameters. Overall, our analysis confirmed a large volume of data on tumor-derived EVs as key components of the reprogramming that characterizes the TME.

Supplementary Material

Supplementary data is available at *Clinical and Experimental Immunology* online.

Acknowledgements

N/A

Funding

I.K. was supported by the Verein zur Förderung der wissenschaftlichen Zahnheilkunde (VFwZ). D.S.R. was supported by the German Academic Exchange Service (DAAD) research grant #57588369. A.G. was supported by Medical University of Warsaw MB/M/48(79)#. M.J.S. was supported by National Science Centre, Poland UMO-2017/26/M/NZ5/00877#. T.L.W. was partially supported by grants U01-DE-029759 and R01-CA256068 from the National Institute of Health, USA. N.L. was supported by the Walter Schulz Foundation.

Conflict of interests

The authors declare that they have no conflict of interest.

Author contributions

Conceptualization: N.L.; Data curation: I.K., D.S.R., A.G., A.K., N.L.; Formal Analysis: I.K., D.S.R., A.G., A.K., N.L.; Funding acquisition: I.K., D.S.R., A.G., M.J.S., T.L.W., N.L., T.E., T.E.R.; Investigation: I.K., D.S.R., A.G., A.K., N.L.; Supervision: T.E.R., E.B., M.J.S., J.M., R.L.F., T.L.W., N.L.; Visualization: I.K., D.S.R., A.G., N.L.; Writing—original draft: I.K., D.S.R., A.G., N.L.; Writing—review and editing: G.S., S.S., J.T., H.P., M.J.S., T.E., T.E.R., J.M., E.B., R.L.F., T.L.W., N.L.

The animal research adheres to the ARRIVE guidelines (https://arriveguidelines.org/arrive-guidelines)

N/A

Permission to reproduce (for relevant content)

N/A

Clinical trial registration

N/A

Data Availability

The data presented in this study are available on request from the corresponding author.

References

1. Johnson DE, Burtness B, Leemans CR, Lui VWY, Bauman JE, Grandis JR. Head and neck squamous cell carcinoma. *Nat Rev Dis Prim* 2020, 6.
2. Coordes A, Lenz K, Qian X, Lenarz M, Kaufmann A, Albers A. Meta-analysis of survival in patients with HNSCC discriminates risk depending on combined HPV and p16 status. *Eur Arch Oto-Rhino-Laryngol* 2015.
3. Whiteside T. The effect of tumor-derived exosomes on immune regulation and cancer immunotherapy. *Futur Oncol* 2017, 13, 2583–92.
4. Ko SY, Lee WJ, Kenny HA, Dang LH, Ellis LM, Jonasch E, et al. Cancer-derived small extracellular vesicles promote angiogenesis by heparin-bound, bevacizumab-insensitive VEGF, independent of vesicle uptake. *Commun Biol* 2019, 2, 1–17.
5. Mashouri L, Yousefi H, Aref AR, Ahadi AM, Molaei F, Alahari SK. Exosomes: composition, biogenesis, and mechanisms in cancer metastasis and drug resistance. *Mol Cancer* 2019, 18, 1–14.
6. Ludwig N, Gillespie D, Reichert T, Jackson E, Whiteside TL. Purine metabolites in tumor-derived exosomes may facilitate immune escape of head and neck squamous cell carcinoma. *Cancers* 2020, 12, 1602.
7. Sato S, Vasaikar S, Eskaros A, Kim Y, Lewis JS, Zhang B, et al. EPHB2 carried on small extracellular vesicles induces tumor angiogenesis via activation of ephrin reverse signaling. *JCI Insight* 2019, 4, e132447. doi:10.1172/jci.insight.132447.
8. Ludwig N, Yerneni SS, Razzo BM, Whiteside TL. Exosomes from HNSCC promote angiogenesis through reprogramming of endothelial cells. *Mol Cancer Res* 2018, 16, 1798–1808. doi:10.1158/1541-7786.MCR-18-0358.
9. Ono K, Sogawa C, Kawai H, Tran MT, Taha EA, Lu Y, et al. Triple knockdown of CDC37, HSP90-alpha and HSP90-beta diminishes extracellular vesicles-driven malignancy events and macrophage M2 polarization in oral cancer. *J Extracell Vesicles* 2020, 9, 2–5.
10. Ludwig N, Yerneni S, Azambuja J, Gillespie D, Menshikova E, Jackson E, et al. Tumor-derived exosomes promote angiogenesis via adenosine A2B receptor signaling. *Angiogenesis* 2020, 23, 599–610.
11. Ludwig S, Sharma P, Theodoraki M-N, Pietrowska M, Yerneni SS, Lang S, et al. Molecular and functional profiles of exosomes from HPV(+) and HPV(–) head and neck cancer cell lines. *Front Oncol* 2018, 12, 445.
12. Razzo BM, Ludwig N, Hong C, Sharma P, Fabian KP, Fecek RJ, et al. Tumor-derived exosomes promote carcinogenesis of murine oral squamous cell carcinoma. *Carcinogenesis* 2019, 1, 9.
13. Ludwig S, Floros T, Theodoraki M-N, Hong C-S, Jackson EK, Lang S, et al. Suppression of lymphocyte functions by plasma exosomes correlates with disease activity in patients with head and neck cancer. *Clin Cancer Res* 2017, 23, 4843–54. doi:10.1158/1078-0432.CCR-16-2819.
14. Schuler PJ, Saze Z, Hong C-S, Muller L, Gillespie DG, Cheng D, et al. Human CD4+ CD39+ regulatory T cells produce adenosine upon co-expression of surface CD73 or contact with CD73+ exosomes or CD73+ cells. *Clin Exp Immunol* 2014, 177, 531–43. doi:10.1111/cei.12354.
15. Madeo M, Colbert PL, Vermeer DW, Lucido CT, Cain JT, Vichaya EG, et al. Cancer exosomes induce tumor innervation. *Nat Commun* 2018, 9, 4284.
16. Fathi M, Joseph R, Adolacion JRT, Martinez-Paniagua M, An X, Gabrusiewicz K, et al. Single-cell cloning of breast cancer cells secreting specific subsets of extracellular vesicles. *Cancers* 2021, 13.
17. Hurwitz SN, Rider MA, Bundy JL, Liu X, Singh RK, Meckes DG. Proteomic profiling of NCI-60 extracellular vesicles uncovers common protein cargo and cancer type-specific biomarkers. *Oncotarget* 2016, 7, 86999–7015. doi:10.18632/oncotarget.13569.
18. Goldman M, Craft B, Kamath A, Brooks A, Zhu J, Haussler D. The UCSC Xena platform for cancer genomics data visualization and interpretation. *bioRxiv* 2018, 326470.

19. Cillo AR, Kürten CHL, Tabib T, Qi Z, Onkar S, Wang T, et al. Immune landscape of viral- and carcinogen-driven head and neck cancer. *Immunity* 2020, 52, 183-99.e9. doi:10.1016/j.immuni.2019.11.014.
20. Kürten CHL, Kulkarni A, Cillo AR, Santos PM, Roble AK, Onkar S, et al. Investigating immune and non-immune cell interactions in head and neck tumors by single-cell RNA sequencing. *Nat Commun* 2021, 12, 1–16.
21. Wolf F, Angerer P, Scanpy TF. large-scale single-cell gene expression data analysis. *Genome Biol* 2018, 19.
22. Tang Z, Kang B, Li C, Chen T, Zhang Z. GEPIA2: an enhanced web server for large-scale expression profiling and interactive analysis. *Nucleic Acids Res* 2019, 47, W556–60. doi:10.1093/nar/gkz430.
23. Ru B, Wong CN, Tong Y, Zhong JY, Zhong SSW, Wu WC, et al. TISIDB: an integrated repository portal for tumor-immune system interactions. *Bioinformatics* 2019, 35, 4200-2. doi:10.1093/bioinformatics/btz210.
24. Li T, Fan J, Wang B, Traugh N, Chen Q, Liu JS, et al. TIMER: a web server for comprehensive analysis of tumor-infiltrating immune cells. *Cancer Res* 2017, 77, e108-10. doi:10.1158/0008-5472.CAN-17-0307.
25. Asokan S, Bandapalli OR. CXCL8 signaling in the tumor microenvironment. *Adv Exp Med Biol* 2021, 1302, 25–39. doi:10.1007/978-3-030-62658-7_3.
26. Puchert M, Obst J, Koch C, Zieger K, Engele J. CXCL11 promotes tumor progression by the biased use of the chemokine receptors CXCR3 and CXCR7. *Cytokine* 2020, 125, 154809. doi:10.1016/j.cyto.2019.154809.
27. Karnezis T, Farnsworth RH, Harris NC, Williams SP, Caesar C, Byrne DJ, et al. CCL27/CCL28-CCR10 chemokine signaling mediates migration of lymphatic endothelial cells. *Cancer Res* 2019, 79, 1558–72. doi:10.1158/0008-5472.CAN-18-1858.
28. Parikh A, Shin J, Faquin W, Lin DT, Tirosh I, Sunwoo JB, et al. Malignant cell-specific CXCL14 promotes tumor lymphocyte infiltration in oral cavity squamous cell carcinoma. *J ImmunoTher Cancer* 2020, 8, e001048. doi:10.1136/jitc-2020-001048.
29. Zhou D, Wang J, Wang J, Liu X. Profiles of immune cell infiltration and immune-related genes in the tumor microenvironment of HNSCC with or without HPV infection. *Am J Transl Res* 2021, 13, 2163–80.
30. Mandal R, Şenbabaoğlu Y, Desrichard A, Havel JJ, Dalin MG, Riaz N, et al. The head and neck cancer immune landscape and its immunotherapeutic implications. *JCI Insight* 2016, 1, 1–18.
31. Ludwig N, Rao A, Sandlesh P, Yerneni SS, Swain AD, Bullock KM, et al. Characterization of systemic immunosuppression by IDH mutant glioma small extracellular vesicles. *Neuro Oncol* 2021;24:197–209.
32. Deng WW, Li YC, Ma SR, Mao L, Yu G-T, Bu L-L, et al. Specific blockade CD73 alters the "exhausted" phenotype of T cells in head and neck squamous cell carcinoma. *Int J Cancer* 2018, 143, 1494–504. doi:10.1002/ijc.31534.
33. Ma SR, Deng WW, Liu JF, Mao L, Yu GT, Bu LL, et al. Blockade of adenosine A2A receptor enhances CD8+ T cells response and decreases regulatory T cells in head and neck squamous cell carcinoma. *Mol Cancer* 2017, 16, 1–15.
34. Ludwig N, Wieteska L, Hinck CS, Yerneni SS, Azambuja JH, Bauer RJ, et al. Novel TGFβ inhibitors ameliorate oral squamous cell carcinoma progression and improve the antitumor immune response of Anti–PD-L1 immunotherapy. *Mol Cancer Ther* 2021.
35. Jablonska J, Rist M, Spyra I, Tengler L, Domnich M, Kansy B, et al. Evaluation of immunoregulatory biomarkers on plasma small extracellular vesicles for disease progression and early therapeutic response in head and neck cancer. *Cells* 2022, 11, 902. doi:10.3390/cells11050902.
36. Ploeg EM, Ke X, Britsch I, Hendriks MAJM, Van der Zant FA, Kruijff S, et al. Bispecific antibody CD73xEpCAM selectively inhibits the adenosine-mediated immunosuppressive activity of carcinoma-derived extracellular vesicles. *Cancer Lett* 2021, 521, 109–18. doi:10.1016/j.canlet.2021.08.037.
37. Wang M, Jia J, Cui Y, Peng Y, Jiang Y. CD73-positive extracellular vesicles promote glioblastoma immunosuppression by inhibiting T-cell clonal expansion. *Cell Death Dis* 2021, 12, 1–11.
38. Turiello R, Capone M, Morretta E, Monti MC, Madonna G, Azzaro R, et al. Exosomal CD73 from serum of patients with melanoma suppresses lymphocyte functions and is associated with therapy resistance to anti-PD-1 agents. *J ImmunoTher Cancer* 2022, 10, e0040431–11. doi:10.1136/jitc-2021-004043.
39. Gauglitz GG, Finnerty CC, Herndon DN, Mlcak RP, Jeschke MG. Are serum cytokines early predictors for the outcome of burn patients with inhalation injuries who do not survive? *Crit Care* 2008, 12, 1–8.
40. Codony VL, Tavassoli M. Hypoxia-induced therapy resistance: available hypoxia-targeting strategies and current advances in head and neck cancer. *Transl Oncol* 2021, 14, 101017. doi:10.1016/j.tranon.2021.101017.
41. Zhang X, Zhang W, Yuan X, Fu M, Qian H, Xu W. Neutrophils in cancer development and progression: roles, mechanisms, and implications. *Int J Oncol* 2016, 49, 857–67. doi:10.3892/ijo.2016.3616.
42. Wang C, Li Y, Jia L, Kim JK, Li J, Deng P, et al. CD276 expression enables squamous cell carcinoma stem cells to evade immune surveillance. *Cell Stem Cell* 2021, 28, 1597–613.e7. doi:10.1016/j.stem.2021.04.011.
43. He X, Xu C. Immune checkpoint signaling and cancer immunotherapy. *Cell Res* 2020.
44. Wu J, Li S, Zhang P. Tumor-derived exosomes: immune properties and clinical application in lung cancer. *Cancer Drug Resist* 2022, 5, 102–13. doi:10.20517/cdr.2021.99.
45. Labani-Motlagh A, Naseri S, Wenthe J, Eriksson E, Loskog A. Systemic immunity upon local oncolytic virotherapy armed with immunostimulatory genes may be supported by tumor-derived exosomes. *Mol Ther Oncolytics* 2021, 20, 508–18.
46. Ludwig S, Marczak L, Sharma P, Abramowicz A, Gawin M, Widlak P, et al. Proteomes of exosomes from HPV(+) or HPV(-) head and neck cancer cells: differential enrichment in immunoregulatory proteins. *Oncoimmunology* 2019, 8, e15938081–11. doi:10.1080/2162402x.2019.1593808.
47. Couch Y, Buzàs EI, Vizio DD, Gho YS, Harrison P, Hill AF, et al. A brief history of nearly EV-erything—the rise and rise of extracellular vesicles. *J Extracell Vesicles* 2021, 10.

Supplementary Data

Tumor gene signatures that correlate with release of extracellular vesicles shape the immune landscape in head and neck squamous cell carcinoma

Isabella Kallinger, Dominique S. Rubenich, Alicja Głuszko, Aditi Kulkarni, Gerrit Spanier, Steffen Spoerl, Juergen Taxis, Hendrik Poeck, Mirosław J. Szczepański, Tobias Ettl, Torsten E. Reichert, Johannes Meier, Elizandra Braganhol, Robert L. Ferris, Theresa L. Whiteside, Nils Ludwig

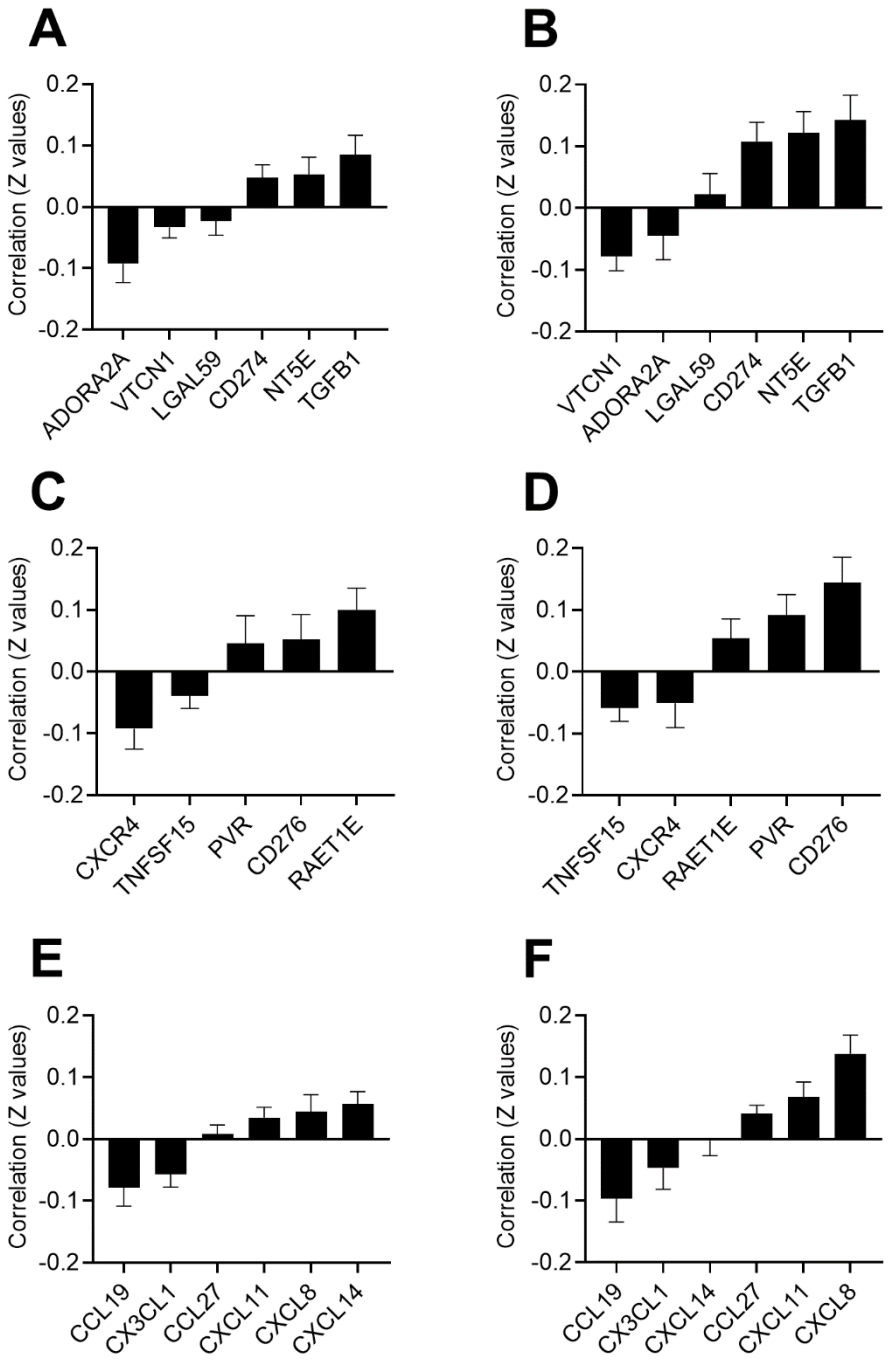

Figure S1. Correlation of vesiculation-related genes with immunomodulatory factors in HPV(-) HNSCC tissues of the GSE65858 validation cohort.. **(A)** Correlation between immunoinhibitory factors and the Fathi-EVsig. **(B)** Correlation between immunoinhibitory factors and the Hurwitz-EVsig. **(C)** Correlation between immunostimulatory factors and the Fathi-EVsig. **(D)** Correlation between immunostimulatory factors and the Hurwitz-EVsig. **(E)** Correlation between chemokines and the Fathi-EVsig. **(F)** Correlation between chemokines and the Hurwitz-EVsig.

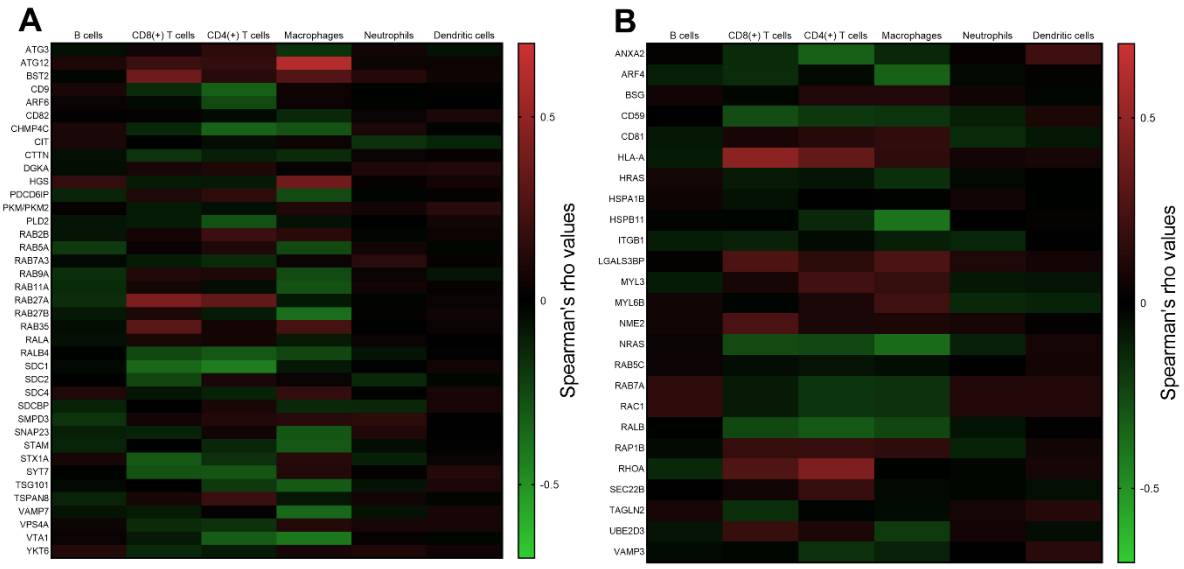

Figure S2. Correlation of vesiculation-related genes with immune cell infiltration in the GSE65858 validation cohort. **(A)** Heat map visualizing the correlation of the expression levels of the Fathi-EVsig and the immune cell infiltration levels of B cells, CD8(+) T cells, CD4(+) T cells, macrophages, neutrophils, and dendritic cells. Each cell represents the Z value of each gene of the Fathi-EVsig. **(B)** Heat map visualizing the correlation of the expression levels of the Hurwitz-EVsig and the immune cell infiltration levels of B cells, CD8(+) T cells, CD4(+) T cells, macrophages, neutrophils, and dendritic cells. Each cell represents the Z value of each gene of the Hurwitz-EVsig.

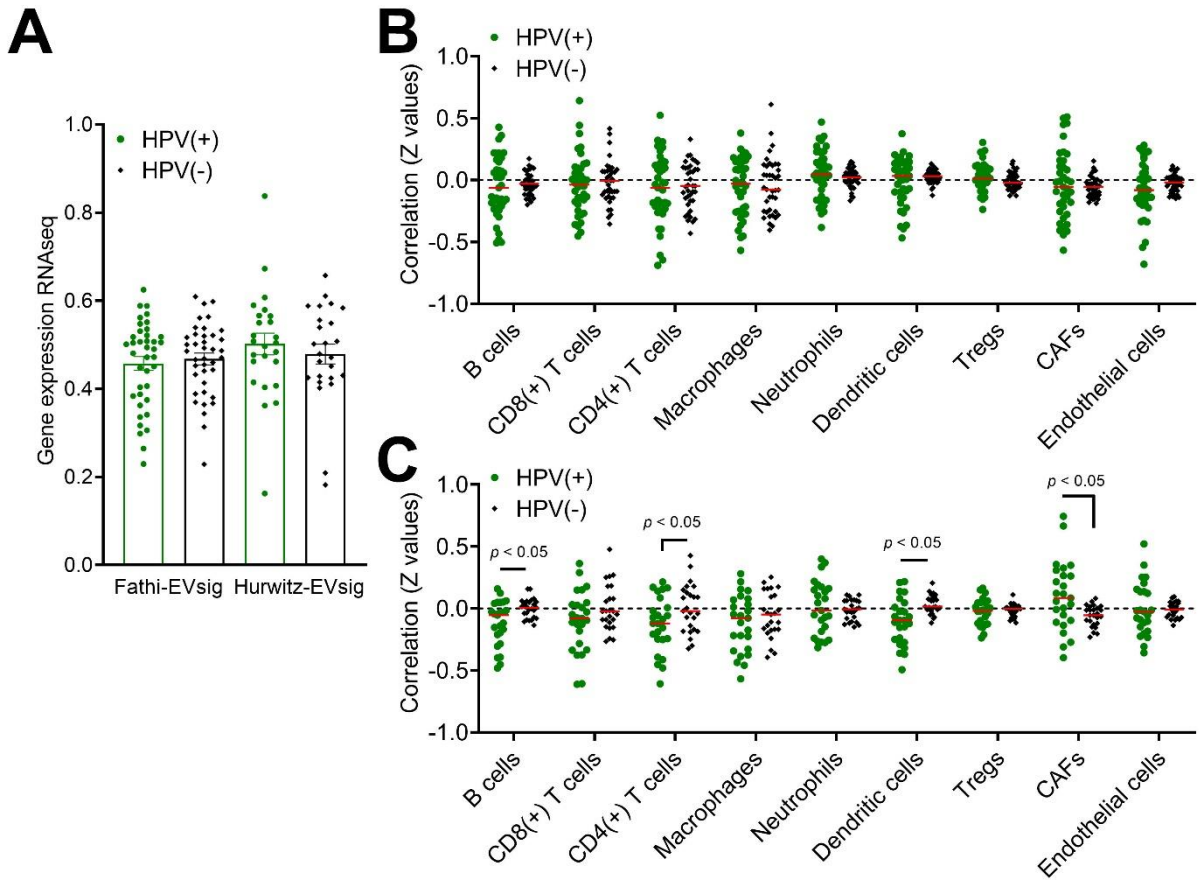

Figure S3. Comparison of vesiculation-related genes in HPV(+) and HPV(-) HNSCCs in the GSE65858 validation cohort. **(A)** Comparison of Fathi-EVsig and Hurwitz-EVsig gene expression in HPV(+) and HPV(−) HNSCC patients. **(B)** Infiltration abundance of immune cells based on Fathi-EVsig expression in HPV(+) and HPV(−) patients. **(C)** Infiltration abundance of immune cells based on Hurwitz-EVsig expression in HPV(+) and HPV(−) patients.

Chapter 3: The immunomodulatory ballet of tumor-derived extracellular vesicles and neutrophils orchestrating the dynamic CD73/PD-L1 axis in head and neck cancer

Journal of Extracellular Vesicles

(https://isevjournals.onlinelibrary.wiley.com/journal/20013078)

Impact Factor: 16

Submitted 06 February 2024

Manuscript Number JEXV-2024-02-0104

Under review

The immunomodulatory ballet of tumor-derived extracellular vesicles and neutrophils orchestrating the dynamic CD73/PD-L1 axis in head and neck cancer

Dominique S. Rubenich[1,2,3], Jordana L. Domagalski[3], Gabriela F.S. Gentil[3], Jonas Eichberger[1,2], Mathias Fiedler[1,2], Florian Weber[4], Marianne Federlin[5], Hendrik Poeck[6,7], Torsten E. Reichert[1], Tobias Ettl[1], Richard J. Bauer[1,2], Elizandra Braganhol[3], Daniela Schulz[1,2]*

[1]Department of Oral and Maxillofacial Surgery, University Hospital Regensburg, 93053 Regensburg, Germany
[2]Department of Oral and Maxillofacial Surgery, Experimental Oral and Maxillofacial Surgery, Center for Medical Biotechnology, University Hospital Regensburg, 93053 Regensburg, Germany
[3]Biosciences Graduate Program, Federal University of Health Science of Porto Alegre (UFCSPA), 90050-170 Porto Alegre, Brazil
[4]Institute of Pathology, University of Regensburg, 93053 Regensburg, Germany
[5]Department of Conservative Dentistry and Periodontology, University Medical Center Regensburg, 93053 Regensburg, Germany
[6]Clinic and Polyclinic for Internal Medicine III, University Hospital Regensburg, 93053 Regensburg, Germany
[7]Leibnitz Institute for Immunotherapy (LIT), 93053 Regensburg, Germany

***Correspondence:**

Dr. Daniela Schulz
University Hospital Regensburg
Dept. of Oral and Maxillofacial Surgery
Franz-Josef-Strauss Allee 11
93053 Regensburg
E-Mail: daniela.schulz@ukr.de

Abstract:

Head and neck squamous cell carcinoma (HNSCC) is a global cancer burden with a 5-year overall survival rate of around 50%, stagnant for decades. A tumor-induced immunosuppressive microenvironment contributes to HNSCC progression, with the adenosine (ADO) pathway and an upregulated expression of inhibitory immune checkpoint regulators playing a key role in this context. The correlation between high neutrophil-to-lymphocyte ratio (NLR) with advanced tumor staging suggests involvement of neutrophils (NØ) in cancer progression. Interestingly, we associated a high NLR with an increased intracellular PD-L1 localization in primary HNSCC samples, potentially mediating more aggressive tumor characteristics and therefore synergistically favoring tumor progression. Still, further research is needed to harness this knowledge for effective treatments and overcome resistance. Since it is hypothesized that the tumor microenvironment (TME) may be influenced by small extracellular vesicles (sEVs) secreted by tumors (TEX), this study aims to investigate the impact of HNSCC-derived TEX on NØ and blockade of ADO receptors as a potential strategy to reverse the pro-tumor phenotype of NØ. UMSCC47-TEX exhibited CD73 enzymatic activity involved in ADO signaling, as well as the immune checkpoint inhibitor PD-L1. Data revealed that TEX induce chemotaxis of NØ and the sustained interaction promotes a shift into a pro-tumor phenotype, dependent on ADO receptors (P1R), increasing $CD170^{high}$ subpopulation, $CD73^{+}$ and PD-L1 expression, followed by an immunosuppressive secretome. Blocking A3R reduced CD73 and PD-L1 expression. Co-culture experiments with HNSCC cells demonstrated that TEX-modulated NØ increase the CD73/PD-L1 axis, through Cyclin D-CDK4/6 signaling. To support these findings, the CAM model with primary tumor was treated with NØ supernatant. Moreover, these NØ promoted an increase in migration, invasion, and reduced cell death. Targeting P1R on NØ, particularly A3R, exhibited potential therapeutic strategy to counteract immunosuppression in HNSCC. Understanding the TEX-mediated crosstalk between tumors and NØ offers insights into immunomodulation for improving cancer therapies.

Running head: TEX-driven neutrophils shape CD73/PD-L1 axis

Key words: Exosome, tumor-associated neutrophils (TAN), adenosine signaling, Head and Neck Squamous Cell Carcinoma, cytoplasmatic PD-L1, biomarker, immune checkpoint resistance

Introduction:

Head and neck squamous cell carcinoma (HNSCCs) is a prevalent form of cancer, with approximately 600,000 new cases reported worldwide annually [1]. Despite extensive research and novel therapeutic approaches, the 5-year overall survival rate for HNSCC patients has stagnated at around 50% for decades [2].

Tumor cells use various mechanisms to induce and sustain a favorable chronic inflammatory environment, abundant in soluble factors that promote their own proliferation and survival [3]. The tumor microenvironment (TME) in HNSCC is characterized by significant immune alterations, often leading to an immunosuppressive niche, promoting tumor growth, invasion, and immune evasion and thereby challenging effective treatment [4]. Immune checkpoint molecules like PD-L1 are frequently overexpressed in a variety of tumor entities and provide a promising target for antibody-based PD-1/PD-L1 immunotherapy [5]. Despite some encouraging outcomes, immune checkpoint inhibition in HNSCC often yields limited improvement or even hyperprogression [6]. The heterogeneity of PD-L1 expression and the lack of reliable biomarkers still leads to unpredictable outcomes [7]. There is increasing evidence that PD-L1 expression as well as its subcellular localization is highly dynamic [8] and also mediates tumor cell-intrinsic functions that may trigger tumor-promoting effects [9–11].

Interestingly, there is emerging new research targeting CD73 and PD-L1 as a potential combination therapy, addressing two immunosuppressive tumor escape strategies at the same time [12–14]. The adenosine (ADO) pathway in HNSCC is acknowledged as a major contributor to tumor-mediated immunosuppression and tumor progression [15]. ADO is produced within the TME mostly through the enzymatic breakdown of ATP though the activity of the ectonucleotidases NTPD1 (CD39) and NT5E (CD73). Extracellular ADO contributes to immunosuppression. It serves as a potent signaling molecule that activates ADO receptors (P1R), A1, $A2_A$, $A2_B$ and A3, thereby modulating crucial cellular processes including differentiation, cell death and triggering an immunomodulatory response [16].

Also the presence of immunosuppressive immune cells such as regulatory T cells (Tregs) and myeloid-derived suppressor cells (MDSCs) can hinder the tumor immune response [4]. The myeloid infiltrate is a crucial component of the TME and significantly influences its progression [17]. Emerging evidence suggest a pivotal role of tumor-associated neutrophils (TANs) in the interplay between tumor and TME [18,19]. TANs are phenotypically modulated neutrophils (NØ) and, consequently, contribute to the perpetuation of the disease [20]. NØ modulation have been

shown to adapt according to tissue environment, and recently have been proposed the importance of tumor-derived extracellular vesicles (TEX) as main characters in tumor crosstalk.

Small extracellular vesicles (sEVs) have garnered significant attention for their potential role in facilitating intercellular communication. These sEVs, also known as exosomes, represent a distinct subset of extracellular vesicles originating from multivesicular bodies (MVBs) and typically measure between 30 and 150 nm in diameter. Particularly intriguing are their unique biogenesis process and surface membrane composition, which closely mirrors those of their parental cells [21]. Importantly, the cargo carried by sEVs can vary depending on the specific microenvironment. There is evidence to suggest that TEX, have the capacity to modulate the phenotype and functional behavior of NØ, influencing their immune responses [22].

In our present study, we show that tumor progression and the neutrophil-to-lymphocyte ratio (NLR) correlate with intracellular PD-L1 localization in tumor cells. Furthermore, we examined the ability of HNSCC-derived TEX to chemoattract and interact with NØ resulting in an induction of an immunosuppressive phenotype in NØ, thus promoting cancer progression. In addition, blocking ADO receptors can reverse the NØ pro-tumor phenotype. TEX-modulated pro-tumor NØ demonstrated different influence on tumor progression between four cell lines, however, an important similar pattern of increasing CD73/PD-L1 axis expression in tumor cells, may indicate their role in immunosuppressive TME.

Materials and Methods:

HNSCC patient cohort: Patient recruitment for primary HNSCC tissue samples, as well as the retrospective database analysis were conducted at the Department of Oral and Maxillofacial Surgery of the University Hospital Regensburg. 76 patients with HNSCC of various localizations were included in the study cohort. The patients were diagnosed and staged between 2016 and 2023 at the Department of Oral and Maxillofacial Surgery, University Hospital Regensburg. Clinical and histopathologic data as well as neutrophil and lymphocyte counts were collected from patients' medical records. All participants involved in this study were thoroughly informed about the nature and purpose of the study, as well as the procedures involved. Written informed consent was obtained from all individual participants involved in the study prior to sample collection. Ethical approval for this study was granted by the Ethics Committee at University Hospital Regensburg (AZ:16-299-101). All procedures performed in this study involving human participants were conducted in compliance with the ethical standards of the institutional research committee and with the 1964 Helsinki Declaration and its later amendments or comparable ethical standards.

Immunohistochemistry (IHC) of HNSCC patient samples: Formalin-fixed, paraffin-embedded tumor tissue was obtained from the archive of the Institute of Pathology at the University of Regensburg. From each block of samples, 3 micrometer (µm) thick sections were cut from the tumor center and tumor periphery. Sections were mounted on SuperFrost® Plus microscope slides (R. Langenbrinck Labor- u. Medizintechnik, Emmendingen, DE). IHC single-staining was performed for CD66b and PD-L1. IHC double-staining was performed for FoxP3 and CD3, following the standard protocol of the Institute of Pathology, University of Regensburg, using a BenchMark Ultra IHC/ISH system (Ventana Medical Systems, Inc, Tucson, AZ). Anti-CD66b (ab300122, Abcam, Cambridge, UK), anti-FOXP3 (14-4777-82, clone 236 A/E7, eBioscience, Thermo Fisher Scientific, San Diego, CA), anti-CD3 (A 0452; Dako GmbH, D), anti-PD-L1 (human PD-L1, clone 28-8, ab205921, Abcam), anti-PD-L1 (human PD-L1, clone E1L3N, #13684, Cell Signaling Technology, Danvers, MA, USA) and anti-PD-L1 (human PD-L1, clone 22C3, M3653, Dako GmbH) were used as primary antibodies. The Dako REAL Envision Detection System, Peroxidase/DAB+, Rabbit/Mouse (Dako, Glostrup, DK) was utilized for detection. Hematoxylin solution was used for counterstaining. Morphological staining with appropriate hematoxylin and eosin was performed as controls for all samples. PD-L1 membranous and cytoplasmic staining was observed on both immune and epithelial cells. Staining intensity was not considered in the scoring process, and evaluations of immune and tumor cells were conducted separately. The absolute number of intratumoral cells stained on the membrane in a

high-power field (HPF) at 400× magnification was counted for CD3, FoxP3 and CD66b. The relative number of tumor cells stained on membrane and cytoplasm were counted for PD-L1 and the absolute number of CD66b, CD3 and FoxP3. The HPF represents the area of the tumor where most of the cells of interest are located. The evaluation area at 400-fold magnification corresponded to a rectangle with a height of 256 µm and a width of 432 µm for the microscope used to achieve the highest possible reproducibility. Counting was performed manually by an experienced pathologist.

Primary human neutrophil isolation: Peripheral blood was obtained from healthy volunteers, using EDTA blood collection tubes (S-Monovette, Sarstedt AG & Co. KG, Nümbrecht, DE) and processed within 15 minutes following a protocol described in Chen et al. [23]. For all further assays, neutrophils cultivated in non-conditioned EDHI-FBS media were used as internal control. The institutional ethics review board of the University Hospital Regensburg (nº 20-1990-101) approved this study.

HNC cell lines: The human head and neck cancer cell line UMSCC47 (SCC47) was purchased from ATCC (Manassas, VA, USA). The human head and neck cancer cell lines FaDu (RRID: CVCL_1218) and SCC9 (RRID: CVCL_1685) were ordered from ATCC (Manassas, VA, USA) as part of the Head and Neck Panel TCP-1012. The human head and neck cancer cell line PCI52 (RRID: CVCL_RJ99) was kindly provided by Prof. Dr. Theresa. L. Whiteside (University of Pittsburgh Cancer Institute (PCI), Pittsburgh, PA, USA) in 2013 [24]. Authentication of PCI52 was performed by the Leibniz Institute German Collection of Microorganisms and Cell Cultures (DSMZ), Berlin, DE) via STR-DNA-typing using nonaplex PCR [A1806475-1].

Culture conditions for cell lines: Cells were cultured at 37°C under controlled conditions with 5% CO_2. The culture medium DMEM (PAN-Biotech, Aidenbach, DE) was supplemented with 1% L-glutamine (Sigma-Aldrich, St. Louis, MO, USA), 100 units/liter (U/L) penicillin/streptomycin 0.5 U/L (Sigma-Aldrich) and 10% fetal bovine serum (FBS) (Gibco, Carlsbad, CA, USA). The medium was changed every two to three days, and the cells were passaged prior to reaching confluence. Detachment of cells was achieved by incubation with Accutase™ solution (Sigma–Aldrich) for 5 to 10 minutes at 37°C.

Tumor spheroids: Spheroids were generated with the hanging drop technique. Per drop, $2x10^4$ cells were seeded in 30 µl cell culture medium, including 0.12% methylcellulose (Sigma–Aldrich), onto the inner part of the lid form a petri dish (Sigma-Aldrich). After seeding, the lid was carefully turned, and the petri dish closed. The cells formed 3-dimensional (3D) spheroids overnight at 37°C under controlled conditions with 5% CO_2. A volume of 10 milliliter (ml)

phosphate buffered saline (PBS) in the lower part of the petri dish prevented the drops from drying out.

TEX isolation: For TEX isolation the culture medium DMEM (PAN-Biotech) was supplemented with 1% L-glutamine (Sigma-Aldrich), 100 units per liter (U/L) penicillin/streptomycin 0.5 U/L (Sigma-Aldrich) and 10% sEV-depleted heat-inactivated fetal bovine serum (EDHI-FBS) (Gibco, Carlsbad, CA, USA). Depletion was achieved by ultracentrifugation at 100,000 relative centrifugal force (rcf) for 3 hours. A number of 2.5 x 10^6 cells were cultured in 150 cm^2 cell culture flasks (Greiner Bio-One, Kremsmünster, AT), containing a total volume of 25 ml culture medium. After 72 hours of incubation, the supernatants were carefully collected for further TEX isolation. 50 ml of SCC47 cell culture supernatant underwent a two-step centrifugation at room temperature (RT) for 10 minutes at 2,000 rcf, followed by 10,000 rcf at 4°C for 30 minutes. Subsequently, the supernatants were filtered through a 0.22 µm bacterial filter (Millex®-GP, Sigma Aldrich) attached to a 50 ml syringe (BD Plastipak™). Using Vivacell® 100 concentrators and a centrifugal force of 4,000 rcf, the filtered supernatants were concentrated down to 1 ml volume.

TEX characterization: TEX were isolated using the mini-size exclusion chromatography (mini-SEC) method, following the previously described protocol in [25]. A volume of 1 ml of fraction #4 was collected throughout the Sepharose™CL-2B (17014001, Cytiva, SE) column for further characterization. TEX protein concentration was determined by using a BCA protein assay (Pierce Biotechnology, Rockford, IL, USA). Tunable resistive pulse sensing (TRPS) was employed to assess the concentration and size distribution of particles in fraction #4. The assessment involved a NP100 nanopore at a 45.05 millimeter (mm) stretch, 0.64 Volt (V), and a 17 millibar (mbar). Samples were calibrated using 114 nanometer (nm) carboxylated polystyrene beads at a concentration of 2x10^{11} particles/ml. Data were recorded and analyzed with version 3.2 of the Izon software (http://www.izon.com). The results provided particle concentrations as the number of particles within fraction #4. Images were taken with scanning electron microscopy (SEM), low vacuum (LV) mode was utilized with energy-dispersive X-ray spectroscopy and proximity ligation assay techniques. The SEM was operated at a voltage of 4 kV with Spot 3, while maintaining a working distance of 10 mm and a pressure of 1.5 Torr. The aperture size was set to 6 for imaging purposes.

Neutrophil treatment with TEX and ADO signaling antagonists: For TEX-treated groups, a concentration of 10 µg of TEX / 10^6 NØ was added. The amount of TEX used in this setup was assessed via concentration curve. Lower tested amounts of TEX (1, 5, 7 µg) didn't show any

significant effect (data not shown). The following antagonists were used to block ADO signaling: AMPCP (CD73 inhibitor – 100 micromolar (μM), Tocris), CGS15943 (P1 antagonist – 0.1 μM, Tocris), PSB36 (A1R antagonist – 1 μM, Tocris), SCH442416 ($A2_AR$ antagonist – 1 μM, Tocris), MRS1754 ($A2_BR$ antagonist – 1 μM, Tocris) and PSB10 hydrochloride (A3R antagonist – 1 μM, Tocris, UK). The control group only included NØ. For further information about primary healthy NØ, see Supplementary Figure 1. NØ viability was assessed using the specified compound concentrations. No notable impact on NØ viability was observed.

Extracellular adenosine quantification: After 48 hours, the supernatant from 7 different biological experimental samples from each group: NØ CTRL, NØ with 10 μg TEX, and NØ treated with CD73 inhibition (AMPCP) and TEX, were evaluated through Human Adenosine ELISA kit (MBS2605344, MyBiosource, San Diego, CA, USA) according to manufacturer's instructions. Briefly, 100 μl of each sample was added in duplicates, absorbance was measured with 450 nm and the concentration values (ng/ml) were calculated with the standard curve equation.

Neutrophil transmigration assay: A 48-well plate was used containing NØ (10^6/ml) in the upper chamber with 3 μm micropore (662630, Greiner Bio-One), both with and without AMPCP and CGS15943 treatments. The lower chamber held PBS 1x and FBS as negative and positive controls respectively, while 10 μg TEX, diluted in DMEM ØFBS were used for the experimental groups. After incubation at 37°C with 5% CO_2 for 3 hours, migrated cells from the lower chamber were harvested. NØ counts were obtained using Neubauer's chamber, and results, normalized with the positive control to eliminate donor variability, are presented as percentage of NØ [26].

Neutrophil-TEX imaging: (1) *Scanning electron microscopy*: NØ w/ and w/o TEX were treated with 2.5% glutaraldehyde (Sigma-Aldrich) in Soerensen buffer for fixation. Post-fixation, the samples were rinsed with distilled water and dehydrated through an ascending alcohol series with 10%, 30%, 50%, 70%, and 90% ethanol (Sigma-Aldrich) for 10 minutes each, followed by three cycles in 100% alcohol, for 20 minutes each. The generated pellet was mixed with propylene oxide (Sigma-Aldrich), carefully dropped onto a stub with a coverslip, and air-dried for 30 minutes. Subsequently, the sample was sputter-coated with platinum for 40 seconds, using a working distance of 50 mm and a current of 30 mA. SEM settings were as follows: high voltage (HV), electron detector (EDT), 4 kV accelerating voltage, spot size 3 and a working distance of 10 mm. (2) *Immunofluorescence (IF)*: TEX were labeled with SYTO™ RNASelect™ (1:50, S32703, Invitrogen, Massachusetts, USA) prior to isolation. After 4 hours, samples were fixated with 4% paraformaldehyde (Merck), followed by Alexa Fluor™ 546 Phalloidin (A22283, Invitrogen) and VECTASHIELD® Antifade Mounting Medium with DAPI (A-1200, Vector

Laboratories, Inc., Newark, USA) staining. Photos were taken in magnification of 40x, to visualize TEX-NØ interactions. For NØ-TEX imaging, NØ were incubated with TEX for 4 hours. A deeper impact in the retention of TEX in the presence of the studied compounds was not further investigated.

Neutrophil phenotype characterization: After 48 hours incubation, NØ were evaluated using the BD LSRFortessa™ Cell Analyzer (BD, Franklin Lakes, NJ, USA). The $CD11b^{+}$ (1:50, 557754, BD) / $CD66b^{+}$ (1:100, 562254, BD) were used as NØ markers, following $CD170^{low}$ for anti-tumor phenotype and $CD170^{high}$ (1:20, 564371, BD) for pro-tumor phenotype, as described in Jaillon et al [27]. Next, the mean fluorescent intensity (MFI) of CD73 (1:20, 561258, BD) were tested in both phenotypes. Furthermore, the expression of PD-L1 was evaluated by western blotting (WB), using an anti-PD-L1 antibody (clone E1L3N, #13684, Cell Signaling Technology).

Secretome analysis: After 48 hours incubation, supernatants from non-treated (CTRL) and TEX-treated NØ were collected. We pooled five different biological experiments in each group. Using 10 µl containing 5 µg of protein each resulted in a cumulative protein amount of 25 µg per group. Each group was analyzed for the expression of 36 different cytokine-related proteins using the Human Cytokine Array Kit (ARY005B - Proteome Profiler, R&D Systems, Minneapolis, MN, USA), following the manufacturer's instructions.

Subcellular protein fractions: HNSSC tissue was fractionated with the Subcellular Protein Fractionation Kit for Tissues (Thermo Scientific, Waltham, MA, USA) according to the manufacturer's instructions. A tissue weight of 100 – 200 mg was used for each sample. Tissue was washed gently with ice-cold PBS. Excess liquid was removed. Tissue was cut into small pieces and placed in a pre-chilled tube for homogenization with a pestle (Kisker Biotech GmbH & Co. KG) in CEB-buffer. For removal of tissue debris, the homogenized tissue was transferred into the Pierce Tissue Strainer (Thermo Scientific) before performing the subcellular fractionation. Protease inhibitors (Halt™ Protease Inhibitor Cocktail 100x, Thermo Scientific) were added to each buffer to maintain integrity. All incubations were performed at 4°C unless otherwise noted. For long-term storage, fractions were stored at -80°C.

Western blot analysis: For SDS-PAGE, 10% agarose gels were loaded with 10 µg protein of fraction #4 or 20 µg of total protein lysate/fractionated proteins and transferred to a PVDF membrane. Membranes were incubated overnight at 4°C with primary antibodies. Primary antibodies for TEX characterization: anti-Calnexin (ab133615, Abcam), anti-HSP70 (ab181606), anti-CD9 (ab92726, Abcam), anti-TSG101 (ab125011, Abcam), anti-α-Tubulin (200-301-880, Rockland Immunochemicals, Philadelphia, USA). Primary antibodies for purinergic signaling:

anti-CD73 (ab133582, Abcam), anti-CD39 (223842, Abcam). Primary antibodies for primary tumor characterization: anti-PD-L1 (#13684, Cell Signaling Technology, Danvers, MA, USA (CST)), anti-PD-L1 (#51296, CST), anti-PD-L2 (#83723, CST), anti PD-1 (#86163, CST), anti-EGF Receptor (#4267, CST), anti-Vimentin (#5741, CST), anti-E-cadherin (610182, BD), anti-N-cadherin (610921, BD), anti-Twist (sc-81417, Santa Cruz Biotechnology, Dallas, TX, USA), anti-Snai1 (sc-393172, Santa Cruz Biotechnology), and anti-CD44 (#3570, CST), anti-VEGFR2 (#9698, CST), anti-VEGF (NB10023832, Novusbio, Uppsala, Sweden). Primary antibodies for analysis of the CD73/PD-L1 signaling cascade: anti-CDK6 (#3136, CST), anti-Cyclin D1 (#55506, CST). Anti-β-actin (ab8227, Abcam) was used as loading control. Secondary antibody Goat anti-rabbit (32460, Invitrogen, Waltham, MA, USA) or anti-mouse (32430, Invitrogen) when appropriate [28]. For signal detection SuperSignal™ West Femto substrate (34096, Thermo Scientific Waltham, MA, USA) was used. Colorimetric and chemiluminescent images were processed using the high-resolution, high-sensitivity ChemiDoc™ XRS+ Imaging System (Bio-Rad, Hercules, CA, USA). Equal loading of proteins was confirmed with Ponceau S (SERVA Electrophoresis GmbH, Heidelberg, DE) total protein staining. The analysis was carried out using Image Lab software 6.0.1 (Bio-Rad).

Chicken embryo chorioallantoic membrane (CAM) assay: Fertilized chicken eggs were acquired from an organic farmer (Herkner, Neutraubling, DE). They underwent a careful incubation process at 37.5°C and 63% humidity in a ProCon egg incubator (Grumbach, Aßlar, DE) for a period of 3 days, with regular rotation every 30 minutes. After that, a small window was cut in the eggshell and securely sealed using Durapore™ (1538-1, 3M, Saint Paul, MN, USA). On day 7, a piece of HNSCC primary tumor (PT) obtained from surgery of tumor resection (~30 µg was added to the top, followed by the addition of 60 µl of NØ supernatant from the following groups (n =5): PT, DMEM vehicle control; +NØ, secretome from healthy NØ; +TEX, secretome from TEX-modulated NØ; +CGS15943, secretome from pre-treated NØ with CGS15943, followed by TEX incubation. This treatment was repeated for three consecutive days. The experiment concluded on day 14 when the tumor was collected and lysed for WB evaluation of the proteins PD-L1, CD73 and CDK6 as previously described.

Co-cultivation of NØ, TEX and tumor cells: A number of $1x10^6$ NØ was pre-treated with 10 µg TEX for 24 hours, as described. Afterwards, the primed NØ were added to tumor cells for functional assays. The number of tumor cells was determined by the functional assay. For the proliferation and apoptosis assays 3,000 adherent tumor cells were seeded into a 96-well plate, for the spheroid spreading assay one tumor spheroid consisting of 20,000 tumor cells was seeded into a 96-well plate. After 48 hours of co-cultivation, the NØ were washed out from the

tumor cells to eliminate any NØ interference with subsequent enzymatic assays or the tumor cell protein lysate.

Proliferation assay: Cell proliferation was measured using CellTiter 96® AQueous One Solution Cell Proliferation Assay (MTS - Promega, Wisconsin, USA). Therefore, 3,000 tumor cells were seeded onto a 96-well plate (Greiner Bio-One) overnight. Proliferation was measured 48 hours after treatment according to the manufacturer's instructions.

Apoptosis assay: Apoptosis was measured using Apo-ONE® Homogeneous Caspase-3/7 Assay (Promega). Therefore, 3,000 tumor cells/well were seeded onto a 96-well plate (Greiner Bio-One) overnight. Apoptosis was measured 48 hours after treatment according to the manufacturer's instructions.

Live-cell imaging wound healing assay: To analyze cell migration, $1x10^5$ tumor cells were seeded onto a 96-well plate (Greiner Bio-One) overnight. After the scratch, cells were washed two times with PBS. After treatment, cell migration in serum-reduced culture medium (5% FBS) was observed for 48 hour using live-cell imaging (Axio Observer Microscope, Zeiss, Oberkochen, DE) with an imaging interval of 1 picture/hour at 40-fold magnification (ZENpro software, Zeiss). Afterwards, the wound healing progress was quantified at 0, 5, 10, 12, 15 and 18 hours after treatments by area measurement using Fiji ImageJ.

Spheroid spreading assay: To analyze cell spreading, one spheroid per 96-well (Greiner Bio-One) was seeded in 50 µl DMEM. Two hours after seeding, pictures of the attached spheroids were taken and defined as starting point of the experiment (0h). Images were taken with 2-fold magnification. Right after, cells were treated. The final volume was 100 µl of serum-reduced culture medium. Again, 48 hours after treatment pictures of spread spheroids were taken with same magnification (48h). For subsequent WB analysis, tumor cells were lyzed in radio-immunoprecipitation buffer (RIPA) buffer including protease inhibitors (Complete™ Mini Protease Inhibitor Cocktail) (Roche Diagnostics, Basel, CH). For quantification of the spread area, the diameter was measured with the ImageJ software and the change in the size of the area covered by cells was calculated. Therefore, the ratio of the area after 48 hours to the covered area after seeding (0h) was calculated and referred to as spreading ratio. Statistical analysis was performed using the GraphPad Prism 9 software (GraphPad Software, San Diego, CA, USA).

Statistical *analysis*: Data are presented as mean ± SD. Two-way analysis of variance (ANOVA) followed by Tukey–Kramer post-hoc test was performed or one-way ANOVA with Bonferroni's test, when appropriate. For correlation of NLR with intracellular PD-L1, Pearson test correlation matrix was performed to analyze the strength of association. Correlation was

interpreted as follow: weak 0.1-0.3 (positive); -0.1 to -0.3 (negative); medium 0.3 to 0.5 (positive); -0.3 to -0.5 (negative); strong (0.5 to 1.0 (positive); -0.5 to -1.0 negative). A P-value of < 0.05 was considered statistically significant with a confidence interval of 95%.

Design of illustrations: Figures showing experimental setup, cellular mechanistic and the graphical abstract were designed with Biorender.com.

Results

Proof of concept: Correlation of neutrophil-to-lymphocyte ratio with HNSCC progression

We started our investigation by examining the potential significance of neutrophils (NØ) in the progression of head and neck squamous cell carcinoma (HNSCC). To this end, we assessed the neutrophil-to-lymphocyte ratio (NLR) across different tumor stages in HNSCC patients, employing the staging criteria from the Union for International Cancer Control (UICC). We observed a distribution of NLR values across various disease stages. Our cohort consisted of 76 patients, with a gender distribution of 34.2% females and 65.8% males, with an average age of 67 ± 9.4 and 63.6 ± 7.9 years, respectively. The diverse tumor site includes 40.8% in the alveolar ridge, 26.3% in the oral cavity and/or tongue, and 19.7% at the floor of the mouth as most prevalent locations. The NLR was plotted against disease stages I through IVB, revealing a spread of values at each stage. Data demonstrate a significant increase in NLR in relation to UICC stage, reaching the highest value in the more aggressive type of tumor. The dot line represents the health threshold (NLR = 2.6 [29]) and it is possible to observe that patients data in the stage I and II in majority below the dot line, while the stage III shows a higher range between patients, including more samples over the threshold. Tumors classified as UICC stage IVA/B have an increased NLR before surgery, including all patients above the reference line. A shift in the NLR value along the UICC stages is visible. With this regard, the IVA ratio is almost double the stage I ($P < 0.001$) and stage II ($P < 0.01$). Moreover, the IVB stage follows the trend, white significant difference between stage I ($P < 0.01$) and II ($P < 0.05$). The median NLR appeared to increase with the advancement of the disease stage, suggesting a potential link between elevated NLR and disease progression (**Fig. 1**).

Characterization of pro-tumor markers in correlation with HNSCC progression

The following step was to randomly select five distinct primary tumors to further characterize their protein marker expression by western blotting (WB). The markers were divided into functional groups for better visualization (**Fig. 2A**). As HNSCC markers, we chose the epidermal growth factor receptor (EGFR) as a frequently overexpressed receptor targeted for HNC therapy and CD44, a cell adhesion molecule currently discussed as an HNSCC stem cell marker. High expression of vimentin and N-cadherin together with low expression of E-cadherin is associated with epithelial-to-mesenchymal transition (EMT). High expression of vimentin and PD-L1 is correlated with poor prognosis, as is high expression of the transcription factors TWIST, an oncogene, and Snai1, a tumor suppressor. The purinergic enzymes CD39 and CD73 are frequently associated with tumor malignancy,

and elevated levels of adenosine (ADO) in the TME functions as an immunosuppressive molecule. Likewise, overexpression of the inhibitory immune checkpoint molecules PD-L1 and PD-L2 is associated with immunosuppression. The secretion of VEGF and the expression of its receptor VEGFR2 is indicating the angiogenic potential of the tumor. The data suggest that each of the five selected tumors exhibits unique pathological features, as evidenced by the distinct expression profiles of tumor markers specific to HNSCC. These markers reflect the heterogeneity and the spectrum of oncogenic evolution within head and neck carcinogenesis. For instance, primary tumor (PT) #1 shows minimal or no expression of protein markers related to EMT, immune checkpoint regulation and angiogenesis, indicating a preliminary stage of epithelial cell dedifferentiation. Conversely, PT#3 exhibits high expression of these markers suggesting a more advanced stage of cancer progression. Additionally, this analysis highlights the purinergic enzymes expression CD39 and CD73. They are detectable in all PTs, similar to PD-L1, an important immune checkpoint target in immunotherapy.

Figure 2B presents the tumor, node, metastasis (TNM) status and patient treatment details for the five HNSCC primary tumor samples selected for this study. It indicates a great variability among the selected samples, which corroborates the characterization panel. The diversity of the five selected primary tumors is reflecting the clinical relevance of cancer pathogenesis and elucidating potential causal relationships for the following observations.

Further, we took a closer look at PD-L1 expression in the tumor samples. Here, we chose a novel approach and investigated the cellular localization of PD-L1 within the cells. Subcellular protein fractionation was performed to separate cells into distinct cellular compartments. Subsequently, the membrane and cytoplasmic protein fractions were analyzed for PD-L1 expression (**Fig. 2C**). The subcellular localization of PD-L1 may be indicative of its specific function and localization. Moreover, since EV cargos are prepared in the cytoplasm of the cell, cytoplasmic PD-L1 may also be packed in EVs for subsequent secretion. Interestingly, the ratio of membrane and cytoplasmic PD-L1 expression correlates with the expression pattern of tumor markers. Specifically, PT#1 is characterized by a high PD-L1 membrane expression (mPD-L1) and a lower cytoplasmic PD-L1 (cPD-L1) expression. This observation is in contrast to PT#3, which displays a pronounced cPD-L1 expression with a reduced mPD-L1 expression. The varying ratios of membrane-to-cytoplasmic PD-L1 (mPD-L1/cPD-L1) may indicate differential susceptibilities to immune checkpoint blockade therapies in HNSCC. It is also noteworthy that although PT#5 exhibited the highest overall PD-L1 expression in the characterization panel, the fractionation did not

reflect similar expression levels in the membrane and cytoplasmic compartments, indicating a potential nuclear localization that was not investigated in this study.

Considering the pivotal relevance of the subcellular localization of PD-L1 in tumor resistance and progression, we postulated that NLR correlates not only with more aggressive tumor characteristics but also with the intracellular distribution of PD-L1. A Spearman correlation analysis substantiated this hypothesis, revealing a positive correlation between NLR and cPD-L1 ($r = +0.60$) and a negative correlation with mPD-L1 expression ($r = -0.48$). Additionally, the analysis indicated a negative correlation between the mPD-L1/cPD-L1 ratio ($r = -0.54$), as demonstrated in **Fig. 2D** and **Supplementary Table 1**.

Currently, only the membrane expression of PD-L1 is relevant for the evaluation in the diagnostic process and the detection of intracellular PD-L1 is neglected. In **Fig. 2E**, we performed an IHC staining the tumor tissue sections with the human anti-PD-L1 antibody clone 28-8, which specifically detects cPD-L1 in addition to membrane-bound PD-L1. PT#1 and PT#3 were selected as representative tumors with lower (PT#1) and higher grade of dedifferentiation (PT#3). In the tissue section of PT#3 a higher percentage of PD-L1 positive cell was detected. Also, a strong cPD-L1 localization is visible in the IHC. Interestingly, PD-L1$^+$ tumor cells (here, mPD-L1 and cPD-L1 was counted as PD-L1$^+$) correlated with NØ infiltration, indicating a possible synergy of two immunosuppressive mechanisms involved in HNSCC progression. Moreover, we evaluated the central and periphery region of the tumor in relation to CD66b and PD-L1 markers. It is possible to observe a significant positive correlation between these two makers in the central region ($P = 0.0168$), while in the periphery follows the same pattern. The total mean of both areas for these markers also correlates ($P = 0.0051$).

These data underscore the integral role of NØ in the context of HNSCC, being potentially influenced by both the malignancy of the tumor and the subcellular localization patterns of PD-L1.

Immunosuppressive TEX carry PD-L1 and adenosine producing enzymes

HNSCC mediate immunosuppressive effects both locally within the TME and systemically. Investigating the potential of TEX to facilitate this immunosuppression we used the HNC cell line SCC47, known for its capacity of secreting high amounts of sEVs. Subcellular protein fractionation of these cells revealed a distribution of the CD73 enzyme, with a molecular weight of approximately 70 kDa across all fractions, with higher expression in the cytoskeletal fraction.

(**Fig. 3A**). Interestingly, the subcellular fractionation also revealed presence CD73 with a lower molecular weight of approximately 21 and 28 kDa. To the same extent, PD-L1 was predominantly detected at the cellular membrane, cytoskeleton, and nuclear soluble protein fraction, including PD-L1 variants around 70 and >150 kDa (**Fig. 3B**).

Subsequent TEX isolation using mini-SEC method yielded a population of particles isolated from fraction #4 with a size of 100 - 150 nm, confirmed by SEM to be vesicular aggregates (**Fig. 3C-D)**. WB analysis confirmed the presence of positive markers for CD9, TSG101, α-Tubulin, HSP70 in the absence of Calnexin (**Fig. 3E**). These results confirm that fraction #4 contained isolated SCC47 TEX.

Interestingly, **Fig. 3F** demonstrated that TEX carried the markers CD39 and CD73, indicating potential purinergic enzyme activity. They also exhibited PD-L1 expression (**Fig. 3G**).

Quantification of adenosine (ADO) in the supernatant of TEX-treated cultures indicated an increase in ADO production in the TEX-NØ mixed culture, which persisted albeit at a reduced level when the CD73 enzyme was pharmacologically inhibited with AMPCP, ($P < 0.05$, **Fig. 3H**), but still remained higher than in the control group without TEX treatment (NØ CTRL). The presented evidence suggests that TEX carry purinergic enzymes and can be a source of extracellular ADO. Altogether, data shows that both immunosuppressive proteins, PD-L1 and CD73, can be found in the intracellular compartment, which can indicate their presence as cargo in EVs. After isolating and characterizing SCC47-derived TEX, both purinergic and PD-L1 immunodetection was positive and a source of adenosine (ADO).

TEX–neutrophil crosstalk

To investigate the chemoattractive properties of TEX on NØ, we conducted a transwell migration assay (**Fig. 4A**). The number of NØ in the lower chamber was normalized using the positive control (CTRL) to exclude individual reactivity variables. In **Fig. 4B**, we observed a significant migration of NØ cells towards TEX ($P < 0.05$). This chemotactic response was attenuated by adenosine (ADO) signaling, as shown by reduced migration of NØ after blockade of the adenosine receptor P1R with CGS15943 and inhibition of CD73 with AMPCP ($P < 0.001$; $P < 0.0001$), suggesting that TEX-induced chemotaxis is modest but dependent on ADO signaling.

To further explore the interaction of TEX with NØ, we performed SEM imaging. Notably, SEM imaging revealed NØ surfaces bound with TEX, whereas CTRL NØ demonstrated a smooth surface (**Fig. 4C**). Immunofluorescence staining also revealed the retention of TEX (green) on the

NØ confirming the physical association between TEX and NØ. The ADO signaling impairment does not influence the TEX-NØ interaction, as shown in **Fig. 4D**.

Overall, the data suggest that TEX not only serve as chemoattractant to NØ but also maintain sustained interaction, highlighting a potential mechanism for TEX-mediated modulation of the NØ response. Blocking P1R and CD73 reduced NØ migration.

Characterization of TEX-modulated Neutrophils phenotype

Our analysis investigated how TEX influence the phenotype of NØ and whether they shift them to an anti- or pro-tumor state. Therefore, we selected $CD11b^{+}/CD66b^{+}$ cells that were classified into two distinct subsets, based on the expression levels of CD170. These subsets are referred to as "$CD170^{low}$" and "$CD170^{high}$" population. A representative gating strategy is shown in **Fig. 5A**. The combination of the analyzed marker expression $CD11b^{+}/CD66^{+}/CD170^{+}$ to define anti- and pro-tumor NØ subpopulations is supported by previous findings of Jaillon et al. [27].

In general, we observed that the interaction of NØ with TEX (+TEX) led to a significant increase in a $CD170^{high}$ pro-tumor population compared to the control group NØ w/o TEX (CTRL) ($P < 0.0001$ – **Fig. 5B**). Additionally, the ratio of $CD170^{high}$ to $CD170^{low}$ cells doubled following TEX treatment ($P < 0.001$). Regardless of the increase of the $CD170^{high}$ population, both subpopulations are present across all groups. Despite a predominant $CD170^{low}$ population in the CTRL group ($P < 0.05$), the addition of TEX consistently resulted in a higher proportion of $CD170^{high}$ cells. To determine the role of ADO signaling in NØ phenotypes, we blocked the adenosine receptor P1R and assessed CD170 positive subpopulations. Notably, blocking $A2_B$ receptor (MRS1754) led to a noticeable increase in the $CD170^{high}$ subpopulation in comparison to the control (NØ CTRL, $P < 0.05$), suggesting a potential link between ADO signaling and NØ phenotype polarization.

In **Fig. 5C**, the correlation between CD73 expression with regards to the activation of anti-/pro-tumor NØ was explored. TEX-modulated NØ showed a similar pattern in CD73 expression. The $CD170^{high}$ subpopulation exhibited higher CD73 expression, while the $CD170^{low}$ subpopulation demonstrated lower expression. Notably, when comparing to $CD170^{low}$ subpopulation in TEX group, there was more than a significant two-fold increase in CD73 MFI ($P < 0.005$). This increase also stood out in comparison to the CTRL group, where the $CD170^{high}$ subpopulation displayed double the CD73 intensity ($P < 0.005$). Treatment with the A3 receptor (A3R) antagonist PSB10 resulted in a decrease in CD73 expression, bringing the pro-tumor subgroup closer to control levels, indicating the role of ADO signaling in modulating the

phenotype. Interestingly, when blocking A3R, the subpopulation distribution in this group is similar to the CTRL, which indicates a possible reverse activation.

Furthermore, western blot analysis in **Fig. 5D** revealed that TEX treatment upregulates the immune checkpoint protein PD-L1 in NØ ($P < 0.05$). PD-L1 expression is, another marker associated with pro-tumor NØ. Interestingly, blocking $A2_BR$ exhibited a synergistic effect, further increasing PD-L1 protein expression compared to CTRL ($P < 0.005$) and TEX-modulated groups ($P < 0.05$). On the other hand, blocking A3R inhibited TEX modulation of PD-L1 expression ($P < 0.05$). Since the TEX incubation in each group is consistent, the variance of immunodetection in response to different treatments points out that PD-L1-TEX are not interfering in the PD-L1 NØ expression.

To investigate the impact of TEX on the secretome of NØ, we employed a Human Cytokine Array to detect multiple cytokines, chemokines, growth factors and other soluble proteins in cell culture supernatant of the NØ (**Supplementary Figure 4A**). Analysis indicated that TEX treatment led to a notable upregulation of two cytokines in the NØ secretome, as shown in **Fig. 5E**: CCL1/I-309 and Serpin E1/PAI-1 saw increases of 1.5-fold ($P < 0.05$) and >1.5-fold ($P < 0.0001$), respectively, compared to the control. However, this upregulation was attenuated when P1R was blocked in NØ by CGS15943, causing the levels of these cytokines to return to baseline. Conversely, TEX treatment induced a significant downregulation of 10 cytokines (**Fig. 5F**). Interestingly, blocking P1R (CGS15943) did not restore the secretion levels of these cytokines to normal, suggesting that the impact of TEX on their secretion was independent of P1R signaling.

The IHC analysis of the five above mention patients revealed that NØ infiltration in the tumor periphery can modulate the lymphocyte profile in both tumor periphery and tumor center (**Fig. 5G**). The correlation matrix indicates that in the tumor periphery, the presence of NØ ($CD66b^+$) positively correlates with Treg ($FoxP3^+$) and $CD3^+$ cell counts. Similarly, $CD3^+$ cells in the tumor periphery predominantly consist of Tregs. These findings highlight a significant influence of NØ on the infiltration of Tregs (**Fig. 5H**).

Interestingly, the immune profile in the tumor center is greatly influenced by peritumoral infiltration. The graph illustrates that increasing levels of peritumoral $CD66b^+$ and $FoxP3^+$ cells also increase the presence of both $CD3^+$ and $FoxP3^+$ cells in the central area. Furthermore, the FoxP3 marker negatively correlates with the NLR, indicating that higher levels of circulating NØ result in fewer lymphocytes infiltrating the tumor. This trend is also observed in the ratio of $FoxP3^+$ to $CD3^+$ cells, where a higher ratio suggests an increased presence of Tregs.

The data demonstrates that the FoxP3/CD3 ratio in the tumor center decreases with increased NØ infiltration in the periphery. Overall, this dataset illustrates a close relationship between NØ and lymphocyte profile infiltration, suggesting that NØ play a role in recruiting more Tregs.

These findings highlight the potential role of TEX in modulating the phenotype of NØ and suggest their involvement in the regulation of pro-tumor responses by selectively modulating the cytokine profile of NØ. Moreover, their effects on cytokine secretion may involve mechanisms beyond P1R activation.

The dynamic modulation of CD73/PD-L1 axis by pro-tumor neutrophils.

The previous observations raised the question of whether this acquired pro-tumor NØ phenotype could actually promote tumor progression. Therefore, SCC47-derived TEX were incubated with primary NØ, pre-treated with antagonist according to experimental group (+AMPCP+TEX; +MRS+TEX; +PSB10+TEX), for 24 hours. Next, the primed TEX-modulated NØ were cultured with four different HNC cell lines: SCC47, SCC9, PCI52 and FaDu, for 48 hours, as explained in the graphical experimental design (**Fig. 6A**). Since PD-L1 modulation in tumor cells is an interesting target of this study, we evaluated the PD-L1 expression in each cell line, along with the CD73 and CDK6 modulation. Representative WB results after co-cultivation of tumor spheroids from SCC47 with NØ are shown in **Fig. 6B** and **Supplementary Figure 5** for SCC47, SCC9, PCI52 and FaDu. The semiquantitative WB analysis of all cell lines in **Fig. 6C** shows significant influence of NØ incubation with the HNC cell lines. The expression of PD-L1 (0.17 ± 0.11; $P < 0.0001$) and CDK6 (0.35 ± 0.20; $P < 0.001$) is significantly downregulated in all cell lines, CD73 expression shows the same trend (0.35 ± 0.33 $P = 0.361$). Interestingly, co-cultivation with TEX-modulated NØ (+TEX) leads to an upregulation PD-L1 and CD73 expression across all cell lines, in comparison to the NØ control without TEX-modulation (+NØ). Moreover, inhibition of CD73 (+AMPCP+TEX) resulted in downregulation of PD-L1 in tumor cells, while blocking the adenosine receptor $A2_B$ with MRS1754 (+MRS+TEX) notably enhanced PD-L1 expression in compassion to +TEX. Blocking A3 receptor (+PSB10+TEX) showed no modulation on PD-L1 but a slight increase in CD73 expression, in comparison to the +TEX group. Altogether, quantitative analysis demonstrated a pattern of reduced PD-L1 and CD73 in tumor spheroids cultured with unmodified NØ (+NØ). Interesting to notice is a slight but significant increase of expression in these proteins when tumors were cultured with TEX-primed NØ (+TEX). As observed previously with NØ pro-tumor phenotype, blocking $A2_B$ in NØ synergized with TEX to promote tumor progression, by increasing both PD-L1 and CD73 proteins. Conversely, inhibiting CD73 activity (+AMPCP+TEX) or blocking A3R (+PSB10+TEX) attenuate the pro-tumor actions of NØ as

demonstrated by the decrease in the CD73/PD-L1 axis The figure also illustrates that the dynamic expression of the CD73/PD-L1 axis is linked to the inhibition of CDK4/6 signaling.

To validate the before mentioned data, an *in ovo/ex vivo* culture was performed with primary tumors (PT) from HNSCC patients (HPV^{neg}, low PD-L1 combined positive score (CPS = 25%) (**Fig. 6D,E)**. The tumors were treated with NØ-derived secretomes treated with SCC47-derived TEX. The results indicate an increase in PD-L1 and CD73, and a decrease in CDK6 and Cyclin D1 expression in tumors treated with TEX-modulated NØ secretome. Interestingly, healthy NØ secretome (PT+NØ) presented a slight decrease in PD-L1, and an increase in Cyclin D1, suggesting PD-L1 degradation via the Cyclin D-CDK4/6 pathway. Notably, the +TEX group and +CGS+TEX depict opposite responses. While +TEX treatment increased CD73 together with PD-L1 while Cyclin D1/CDK6 levels were decreased. The addition of CGS15943 (P1R antagonist) prior to TEX exposure reversed this effect, lowering the immunosuppressive axis and suggesting a more favorable tumor response. (**Fig. 6E**).

Endorsement of pro-tumor potential of TEX-modulated Neutrophils

The pro-tumor effects of the TEX-modulated NØ were also evaluated by functional assays with four different HNC cell lines: SCC47, SCC9, PCI52 and FaDu. **Fig. 7A** illustrates a representative result of the proliferation rate of cell line SCC47. The significances between the groups corroborates with the previous pattern described for CD73/PD-L1 axis expression. We observed a notable increase in the proliferation of SCC47 cells, when cultured with pro-tumor NØ, compared to healthy NØ. A similar result was observed in HNC cell line SCC9 ($P < 0.05$; **Supplementary Figure 7**). Interestingly, the group treated with the $A2_BR$ antagonist MRS1754 (+MRS+TEX) displayed even higher proliferation rates ($P < 0.01$), while the group with A3 receptor blockade (+PSB10+TEX) showed a decrease in proliferation. Conversely, PCI52 and FaDu demonstrated reduced proliferation with TEX treatment compared to controls ($P < 0.0001$ and $P < 0.001$, respectively). Caspase 3/7 assays were utilized to determine the rate of cell death in each cell line, which endorsed the proliferation findings (**Fig. 7B**).

To understand the direct effects of pro-tumor NØ on tumor cells, we performed a cell spreading and wound healing (scratch) assay. Area quantification between 2 hours (2h) and 48 hours (48h) shows a similar pattern as mentioned before for HNC cell line SCC47. An increase in cell spreading when incubated with TEX-modulated NØ ($P < 0.01$), a tumor regression in the spheroids incubated with NØ+AMPCP+TEX ($P < 0.001$) and +PSB10+TEX ($P < 0.0001$) groups, and a slightly reduction in boosting tumor spreading when NØ were treated with $A2_BR$ blocking before TEX interaction ($P < 0.05$; **Fig. 7C**) could be observed. HNC cell line SCC9 and FaDu did not

presented significant differences between healthy NØ (+NØ) and pro-tumor NØ (+TEX). Besides, FaDu seems to not be affected by the TEX-NØ modulation. Representative figures from the SCC47 cell spreading are shown in **Fig. 7D**.

Next, the scratch assay was performed with HNC cell line SCC47 (**Fig. 7E**) and SCC9. Data further confirmed that TEX-modulated NØ accelerate wound healing in SCC47, with significant differences from the CTRL within 5 hours ($P < 0.01$) and 10 hours ($P < 0.05$). With regards to ADO antagonists, blocking A3R on NØ alters their effects as shown before and slows down the healing rates ($P < 0.05$). The same late healing pattern with +PSB+TEX group could be observed in cell line SCC9 within 10 hours ($P < 0.0001$; Supplementary **Figure 7D**. Lastly, these results corroborate with the proliferation assay in all four cell lines (**Supplementary Figure 7**). To comprehend the diverse responses of cell lines to TEX-mediated NØ interaction, we conducted a cell line characterization. SCC47 and SCC9 exhibit comparable marker expression, except for CD73, which is more elevated in SCC9. In contrast, PCI52 demonstrates a distinct mesenchymal phenotype, while FaDu falls between these observations (**Supplementary Figure 8**).

Taken together, the presented data suggest that pro-tumor NØ can enhance tumor progression, with variable effects across different cell lines. The interaction between tumor cells and pro-tumor NØ also appears to boost PD-L1 expression, highlighting the influence of NØ phenotype on tumor PD-L1 levels.

Discussion

NLR and PD-L1 dynamics in carcinogenesis

The neutrophil-to-lymphocyte ratio (NLR) serves as a recognized inflammatory biomarker, reflecting the balance between neutrophil and lymphocyte counts [30]. Elevated NLR is linked to poor prognosis in various cancers. In HNSCC, NLR is under investigation for its diagnostic, prognostic, and therapeutic response-predicting potential [31,32]. Our study extends this by exploring correlations between NLR and key tumorigenic processes across five primary tumors from distinct head and neck locations, also representing different stages of tumor development. This comprehensive assessment emphasizes the nuanced associations of the identified biomarker with HNSCC progression.

We focused on investigating PD-L1 expression and its cellular localization, recognizing its role in both immunosuppression and cell-intrinsic functions in tumor cells [5,9,10,33]. Our previous studies highlighted PD-L1's influence on cell cycle progression, proliferation, motility, invasion, and survival after irradiation [8,11,34]. PD-L1 expression varies with cell differentiation status, with mesenchymal cells showing higher levels than epithelial cells. Clinically used treatments alter PD-L1 localization, observed differently in highly malignant tumors. In the five tumors under investigation, we observed variations in the subcellular localization of PD-L1, specifically between the cell membrane and cytoplasm. Currently, only membrane expression of PD-L1 is relevant for clinical PD-L1 scoring by IHC. The presence of intracellular PD-L1 is entirely neglected and in most cases is not even detectable with the diagnostic anti-PD-L1 antibodies used. This might explain for the low predictive value of PD-L1 positivity for immune checkpoint inhibition. **Supplementary Figure 9** provides a comparison of three human anti-PD-L1 antibody clones available for diagnostics: 22C3, E1L3N and 28-8. On serial HNSCC tissue sections they differ significantly in PD-L1 detection potential. While 22C3 has the lowest detection capacity, E1L3N and 28-8 detect both, membrane-bound and intracellular PD-L1. Since the highly specific clone 28-8 yielded the strongest mPD-L1 and cPD-L1 detection in this comparison, we decided to perform IHC staining in **Fig. 2E** with clone 28-8. Notably, the localization tends to differ in relation to the tumor's aggressiveness, with a more internal localization observed in highly malignant tumors [35]. This intriguing finding prompted an investigation into the potential correlation between the subcellular localization of PD-L1 and the NLR. Notably, there is a robust positive correlation between NLR values and the expression of PD-L1 in the cytoplasm of tumors. This is supported by IHC data where it shows a positive

correlation between CD66b and PD-L1 markers. This observation suggests a heightened level of crosstalk and interdependence between tumor cells and NØ within the TME.

Pro-tumor neutrophil phenotype is induced by HNSCC-derived TEX

The orchestrated immunosuppression resulting from the concurrent upregulation of CD73 and PD-L1 in the TME has encouraged discussions regarding the mechanisms underlying tumor-immune cross-modulation. In our investigation, subcellular protein fractionation of SCC47 unveiled the presence of PD-L1 in diverse cellular compartments, including the nucleus. Notably, PD-L1 was identified not only in its well-documented glycosylated/deglycosylated states (40–55 kDa) but also in a novel nuclear PD-L1 variant, exhibiting a higher molecular weight of approximately 70 kDa and >150 kDa, as recently reported by Schulz et al. [35]. These findings were similarly observed in six thoroughly characterized HNC cell lines, including SCC9, FaDu, and PCI52. Furthermore, CD73 demonstrated a ubiquitous presence across all subcellular fractions, with particularly pronounced expression in the cytoskeleton, with pro-tumor activity associated with its nucleotidase function. This substantiates the notion that the dynamic trafficking of both proteins may be linked to their release with sEVs, since their high protein expression in the cytoplasm and cytoskeleton may be linked to TEX packing in MVBs and further release [36]. It has been noted in the literature that sEVs are proficient in generating ADO and may indeed encapsulate ADO within their luminal space. The ADO content within TEX has been specifically associated with their immunosuppressive effects [37]. TEX have been shown to carry various bioactive molecules which can be transferred to recipient cells and modulate their behavior and functions [38]. We found that SCC47-derived TEX carry CD73 and PD-L1, immunosuppressive markers that have prognostic value, especially exosomal PD-L1 [39,40]. Exosomes originating from various cancer types exhibit significant expression of CD73, showcasing a robust ability to generate ADO [41]. With this regard, sEVs from HNSCC cell lines were reported to carry the enzyme CD73 [42]. Besides, TEX derived from SCC47 cells were already reported to not only produce ADO through CD73 enzymatic breakdown, but also carries ADO internally [43]. In addition, quantities of PD-L1 found on TEX are associated with the advancement of HNSCC. Recent findings also indicated that PD-L1 is not only present on the surface of vesicles but also within vesicle-like structures. PD-L1-positive TEX, isolated from the supernatants of murine and human HNSCC cell lines, can impede the infiltration of $CD4^+$ and $CD8^+$ T cells into the tumor microenvironment, consequently expediting tumor progression [44–46]. Moreover, to our knowledge this is the first time that the role of ADO release/produced by TEX is investigated specifically in NØ response. CD73 produces extracellular adenosine (ADO) promoting tumor growth by limiting anti-tumor T cell immunity via adenosine receptor (P1R) signaling. On the

same hand, PD-L1, that acts as an immune checkpoint inhibitor for cytotoxic T lymphocytes (CTLs).

Hereby, the exchange of tumor-derived extracellular vesicles (TEX) between tumor and immune cells is crucial for cancer progression and immunomodulation. TEX have been shown to contribute to immune evasion by affecting immune functions, impairing their ability to prime effective anti-tumor responses [22,47]. The key findings of our work demonstrate that TEX have the potential to attract NØ, interact with them, and shift the NØ phenotype from anti-tumor to a pro-tumor phenotype. Numerous studies have focused on investigating the inflammatory profile within the TME, which of particular interest is the excessive activation of NØ, whereby these cells undergo a phenotypic transformation from their canonical function to a pathogenic state [22]. The combination of $CD11b^{+}/CD66^{+}/CD170^{+}$ markers is suggested as a mean to distinguish between NØ subpopulations [27]. The interaction involves CD73 and PD-L1, known immunosuppressive markers, influencing NØ behavior and function. Notably, TEX induce an increase in $CD170^{high}$ expression and PD-L1 expression in NØ, contributing to the modulation of the immunosuppressive TME. Studies have provided evidence highlighting the significance of CD73 as a crucial regulatory molecule involved in cancer cell proliferation, migration, and invasion [42,48]. Previous studies have examined and confirmed the concept that PD-L1 expression on NØ promotes pro-tumor characteristics [49]. It has been observed that PD-1 on breast cancer cells inhibits NØ cytotoxicity, whereas $PD\text{-}L1^{neg}$ NØ possess heightened cytotoxic potential [50]. Moreover, $PD\text{-}L1^{pos}$ NØ have been implicated in promoting tumor growth and progression in tumors, and their presence is considered a negative prognostic factor associated with reduced patient survival [51]. Moreover, NØ have been involved in modulating the TME. In the context of HNSCC, $PD\text{-}L1^{pos}$ NØ cells have been shown to suppress T cell proliferation and activation within the inflammatory TME, consequently predicting an unfavorable prognosis. These TANs severely impair anti-tumor T cell immunity and actively contribute to tumor progression [52].

Interestingly, the PD-L1 bands detected in NØ shown in **Fig. 5D** were with approximately 70 kDa, which is in size 20 kDa heavier than observed to date in most cell types, were PD-L1 is ranging from 45-55 kDa [53]. This specific form of PD-L1 is not well understood yet, but it is known that post-translational modifications (PTMs), such as glycosylation, phosphorylation, or ubiquitination (Ub), can increase the molecular weight of the PD-L1 protein and modulate its stability, functionality and localization [54]. There is compelling evidence suggesting that the regulation of PD-L1-mediated immunosuppression is significantly influenced by these PTMs, which directly influence PD-L1-mediated immune resistance [54]. Ubiquitination and

deubiquitylation play a crucial role in the dynamics of PD-L1 protein expression, aiding tumor cells in evading immunosuppression [55,56]. Besides, a second band with 45 kDa was shown in NØ with MRS1754 in the presence of TEX, which demonstrates that blocking $A2_BR$ the glycosylated canonical isoform is also present. It was reported that glycosylation of PD-L1 is important for binding to the receptor PD-1 [57].

The elevated levels of ADO in the TME are a result of increased ADO production. The deregulated ADO signaling in HNSCC creates an immunosuppressive and pro-tumor milieu [58]. Conversely, the alternative pathway involves the conversion of NAD^+ to ADPR facilitated by CD38. ADPR is subsequently converted to AMP by CD203a/PC-1. Both paths merge at CD73, where AMP is completely broken down into ADO [59]. Moreover, it is imperative to acknowledge the importance of other members of ADO uptake and degradation, such as the isoenzyme adenosine deaminase (ADA) in the final amount of extracellular ADO [60]. ADO, which is highly abundant in TME, exerts its immunosuppressive effects through binding to specific P1R expressed on various immune cells, including NØ. Activation of these receptors leads to the inhibition of immune cell functions, such as T cell proliferation, cytokine secretion, and cytotoxic activity [61]. Therefore, our study aimed to understand the role of ADO signaling in NØ activation spectrum. Our data show that blocking A3R led to a significant decrease in CD73 expression in the pro-tumor subpopulation and inhibited TEX modulation of PD-L1 expression. Targeting ADO signaling in immunotherapy represents a promising avenue to overcome the immunosuppressive TME and improve the effectiveness of cancer with combined treatments [62].

TEX selectively modulate the cytokine profile of NØ, increasing CCL1/I-309 and Serpin E1/PAI-1 secretion. Blocking P1R reverses this effect, suggesting P1R signaling involvement. These cytokines attract immunosuppressive cells to the TME, particularly regulatory T cells (Tregs), tumor-associated macrophages (TAMs) and myeloid-derived suppressor cells (MDSCs), promoting tumor growth and immune evasion [63]. To same extent, PAI-1 can modulate immune response by suppressing cytotoxic T cells, impairing their anti-tumor functions [64]. Moreover, the IHC evaluation from tumor samples corroborates with *in vitro* findings. The NØ infiltration depicts great influence in modulating lymphocyte profile. The positive correlation between NØ and Tregs both in the tumor periphery and the tumor center clearly shows the important role of NØ in the TME immune infiltration. Indeed, a high level of NØ infiltration in solid tumors is associated with poor clinical outcomes in patients, this topic was extensively reviewed showing that not only the presence of NØ but also their specific location within the tumor is prognostically relevant [65]. Recently, it was confirmed that high intratumoral or

peritumoral ratios of $CD66b^+$ to $CD3^+$ immune cells in liver sections from patients with hepatocellular carcinoma (HCC) are predictive of inferior overall survival [66]. With this regard, *in vivo* experiments suggested that TANs support these processes by promoting the infiltration of macrophages ($F4/80^+$) and Tregs ($FoxP3^+$) within the TME [67].

Transition to translational research and clinical combination therapy

Immunotherapy has transformed cancer treatment tremendously. Nevertheless, it faces limitations, as only 20-40% of patients respond, which is often due to tumor adaptability and resistance mechanisms [68,69]. CD73 plays a significant role in this context, and its upregulation in the TME is linked to immunotherapy resistance [70–72]. Our data supports this observation, showing increased CD73 and PD-L1 expression in pro-tumor NØ and tumor co-culture, contributing to an immunosuppressive TME. CDK6 activation correlates with PD-L1 expression, influenced by CD73 activity. Inhibiting CD73 in pro-tumor NØ negatively affects the CD73-CyclinD-CDK4/6-PD-L1 pathway in tumor cells, suggesting a potential therapeutic strategy. The role of CDK6 in regulating PD-L1 was already described by Zhang et al [73]. Inhibition of CDK4/6 increases PD-L1 protein levels by interfering with cyclin D-CDK4-mediated phosphorylation of the speckle-type POZ protein (SPOP), thereby promoting SPOP degradation. CDK4/6 activity on the other hand leads to SPOP phosphorylation, which marks PD-L1 with ubiquitin for proteasomal degradation. Interestingly, the correlation between CD73 activity and PD-L1 in tumor cells has been described as dependent of CDK6, in which extracellular ADO was found to be critical for the regulation of immune checkpoint molecules and PD-L1 levels in human macrophages, suggesting that the PTM of PD-L1 is affected by ADO. A potent selective CD73 inhibitor reversed the effects of ADO on PD-L1 [74]. Our data endorse that by inhibiting CD73 with AMPCP in pro-tumor NØ, has a negative influence the CD73-Cyclin D-CDK4/6-PD-L1 pathway in tumor cells. Moreover, the *in vivo* data depicts the dynamic modulation of CD73/PD-L1 axis by NØ secretome. The differences between a healthy and pro-tumor response in immune cells, has a direct effect in tumor aggressiveness and immunosuppression, especially in the TME. The degradation of PD-L1 by the activation of Cyclin D-CDK4/6 signaling after inflecting NØ secretion and the reduction of CD73 expression, expresses the potential of NØ as adjuvant therapy.

Despite the similar pattern in regulating CD73-Cyclin D-CDK4/6-PD-L1 signaling in tumor cells, the modulation of the NØ pro-tumor phenotype by SCC47-derived TEX does not yield a consistent functional response in all four cell lines. Notably, SCC47 exhibited robust positive feedback when interacting with TEX primed NØ, manifesting increased migration, spreading,

and reduced cell death. Conversely, SCC9 displayed a partially analogous pattern of response, while PCI52 and FaDu exhibited conflicting effects or remained unaffected. Important to point out that the *in vitro* condition is a less complex environment and the interaction with NØ varies between the non-modulated (+NØ) and TEX-modulated NØ (+TEX). The co-incubation culture provides information about the response to the stimuli, and, in this experimental design, we focused our evaluation in comparing the tumor response to healthy non-stimulated NØ and pro-tumor TEX-induced NØ. With this regard, TEX exhibit cell line-specific effects on NØ, highlighting the unique responsiveness of each cell line to external stimuli. This variability emphasizes the need for personalized therapeutic approaches in cancer treatment. To that extent, the very heterogeneity that facilitates TEX utility also presents a challenge in the development of drug delivery systems reliant on exosomes [75]. Furthermore, this variability may elucidate why conventional treatments involving immune cell modulation or exosome-targeted therapies exhibit efficacy in a limited subset of patients, emphasizing the necessity for personalized therapeutic approaches. With this regard, further studies need to be conducted in order to understand the full impact of the target mechanism associated with NØ polarization.

Targeted therapies involving CD39 or CD73 alongside anti-PD-1 or PD-L1 show promise in pre-clinical and clinical studies [76]. A recent report on a phase I clinical trial involving anti-CD73 and anti-PD-L1 revealed tolerable safety profiles and moderate efficacy [77]. Phase II trials targeting CD73, especially in combination with anti-PD-L1, demonstrate enhanced response rates [78,79]. In our study, we propose the use of NØ as therapeutic target, with special regard to A3R as a key player in the activation spectrum. NØ have been proposed as cancer targets due to the easiness in infiltrating TME and cell communication [80–82]. Amidst ongoing investigations into combinations of diverse treatments and additional checkpoint targets, a profound understanding of the TME remains imperative for the advancement of novel therapeutic strategies.

Conclusion

Our study reveals significant insights into the crosstalk between HNSCC-derived extracellular vesicles (TEX) and neutrophils (NØ) within the tumor microenvironment (TME), which is summarized in **Figure 8**. In conclusion, the comprehensive analysis of NLR and PD-L1 dynamics in tumorigenesis has provided valuable insights into the intricate interplay between immune markers and TME. Elevated NLR, indicative of systemic inflammation, has been consistently linked to poor prognosis in various cancers, emphasizing its potential as a diagnostic and predictive tool. The investigation into PD-L1 expression, particularly its subcellular

localization, has revealed a nuanced relationship with tumor aggressiveness, with variations in membrane and cytoplasmic localization linked to differing NLR values.

The study delves into the role of TEX in orchestrating immunosuppression within the TME, highlighting their ability to induce a pro-tumor NØ phenotype. The presence of immunosuppressive factors, including CD73 and PD-L1, in TEX underscores their role in shaping the immune landscape. Moreover, the study elucidates the potential of TEX to modulate cytokine profiles and influence the behavior of immune cells, particularly NØ. We demonstrated that TEX promote NØ chemotaxis and attachment, leading to a shift in NØ phenotype characterized by increased $CD170^{high}$, $CD73^{pos}$, and cPD-L1 expressions, indicative of a pro-tumor transformation. This TEX-induced phenotype modulates the NØ cytokine release profile, enhancing the secretion of immunosuppressive factors like CCL1/I-309 and Serpin E1/PAI-1. Our data underscore the pivotal role of adenosine (ADO) signaling in these processes, suggesting that targeting ADO signaling, especially A3R, could be a promising approach to counteract the immunosuppressive TANs and boost the effectiveness of cancer treatments.

The transition to translational research and clinical combination therapy was discussed, emphasizing the significance of targeting CD73 and PD-L1 concurrently, especially in the context of immunotherapy resistance. The findings support the notion that understanding the dynamic modulation of CD73/PD-L1 axis by NØ could serve as a potential adjuvant therapy, offering insights into the complex regulatory mechanisms underlying immunosuppression. However, the variability in responses to TEX among different cell lines underscores the challenges in developing universally effective therapeutic approaches.

This study contributes significantly to our understanding of the complex interactions within the TME, featuring the potential therapeutic avenues for cancer treatment. The emphasis on personalized approaches and the exploration of novel targets underscores the importance of continued research in unraveling the intricacies of tumor-immune cross-modulation for the development of more effective and tailored cancer therapies.

Consent for publication

All authors agreement with the content of the manuscript and with the submission.

Acknowledgement

This work was supported by Deutsche Forschungsgemeinschaft (DFG, GZ: 3696/7-1), Conselho Nacional de Desenvolvimento Científico e Tecnológico (CNPq – 142520/2020-9), CAPES & Deutscher Akademischer Austauschdienst (CAPES: 88881.895087/2023-01, DAAD: 57705675)

and University Hospital Regensburg (UKR). We thank Maxi Bleicher, Gabriele Schönhammer, Gerlinde Ferstl, Niklas Wenzl and Rudolf Jung for their excellent technical assistance as well as Sophia Rohrmüller, Dr. Nicole Schäfer and Dr. Petra Hoffmann for their valuable support.

Declaration of Interest Statement

The authors declare no conflict of interest.

Author contributions

Dominique S. Rubenich: conceptualization, data curation, formal analysis, investigation, methodology, project administration, supervision, visualization, writing – original draft, writing – review & editing. **Jordana L. Domagalski**: formal analysis, writing – review & editing. **Gabriela F.S. Gentil**: formal analysis, writing – review & editing. **Jonas Eichberger**: data curation, writing – review & editing. **Mathias Fiedler**: data curation, writing – review & editing. **Florian Weber:** data curation**,** formal analysis**. Marianne Federlin**: data curation, resources. **Hendrik Poeck**: data curation, resources. **Torsten E. Reichert**: funding acquisition, resources. **Tobias Ettl**: data curation, funding acquisition, resources. **Richard J. Bauer**: funding acquisition, resources, supervision, writing – review & editing. **Elizandra Braganhol**: conceptualization, supervision, writing – review & editing. **Daniela Schulz**: data curation, formal analysis, investigation, methodology, project administration, supervision, validation, visualization, writing – review & editing.

List of references

[1] H. Sung, J. Ferlay, R.L. Siegel, M. Laversanne, I. Soerjomataram, A. Jemal, F. Bray, Global Cancer Statistics 2020 : GLOBOCAN Estimates of Incidence and Mortality Worldwide for 36 Cancers in 185 Countries, 71 (2021) 209–249. https://doi.org/10.3322/caac.21660.

[2] C.R. Leemans, P.J.F. Snijders, R.H. Brakenhoff, The molecular landscape of head and neck cancer, Nat. Rev. Cancer. 18 (2018) 269–282.

[3] A.L. Giuliani, A.C. Sarti, F. Di Virgilio, Ectonucleotidases in Acute and Chronic Inflammation., Front. Pharmacol. 11 (2020) 619458. https://doi.org/10.3389/fphar.2020.619458.

[4] A. Elmusrati, J. Wang, C. Wang, Tumor microenvironment and immune evasion in head and neck squamous cell carcinoma, Int. J. Oral Sci. 13 (2021) 1–11. https://doi.org/10.1038/s41368-021-00131-7.

[5] K. Mortezaee, Immune escape: A critical hallmark in solid tumors, Life Sci. 258 (2020) 118110. https://doi.org/10.1016/j.lfs.2020.118110.

[6] T. Ettl, M. Grube, D. Schulz, R.J. Bauer, Checkpoint Inhibitors in Cancer Therapy : Clinical Benefits for Head and Neck Cancers, (2022) 1–28.

[7] K.I. Zhou, B. Peterson, A. Serritella, J. Thomas, S. Moya, C. Tan, Y. Wang, D.V.T. Catenacci, Spatial and temporal heterogeneity of PD-L1 expression and tumor mutational burden (TMB) in gastroesophageal adenocarcinoma (GEA) at baseline diagnosis and after chemotherapy, Clin. Cancer Res. 26 (2020) 6453–6463. https://doi.org/10.1158/1078-0432.CCR-20-2085.

[8] D. Schulz, M. Wetzel, J. Eichberger, G. Piendl, G. Brockhoff, A.K. Wege, T.E. Reichert, T. Ettl, R.J. Bauer, Differential expression of pd-l1 during cell cycle progression of head and neck squamous cell carcinoma, Int. J. Mol. Sci. 22 (2021). https://doi.org/10.3390/ijms222313087.

[9] M. Gato-Cañas, M. Zuazo, H. Arasanz, M. Ibañez-Vea, L. Lorenzo, G. Fernandez-Hinojal, R. Vera, C. Smerdou, E. Martisova, I. Arozarena, C. Wellbrock, D. Llopiz, M. Ruiz, P. Sarobe, K. Breckpot, G. Kochan, D. Escors, PDL1 Signals through Conserved Sequence Motifs to Overcome Interferon-Mediated Cytotoxicity, Cell Rep. 20 (2017) 1818–1829. https://doi.org/10.1016/j.celrep.2017.07.075.

[10] L. Chen, Y. Xiong, J. Li, X. Zheng, Q. Zhou, A. Turner, C. Wu, B. Lu, J. Jiang, PD-L1

Expression Promotes Epithelial to Mesenchymal Transition in Human Esophageal Cancer, Cell. Physiol. Biochem. 42 (2017) 2267–2280. https://doi.org/10.1159/000480000.

[11] J. Eichberger, D. Schulz, K. Pscheidl, M. Fiedler, T.E. Reichert, R.J. Bauer, T. Ettl, PD-L1 influences cell spreading, migration and invasion in head and neck cancer cells, Int. J. Mol. Sci. 21 (2020) 1–17. https://doi.org/10.3390/ijms21218089.

[12] D. Allard, P. Chrobak, B. Allard, N. Messaoudi, J. Stagg, Targeting the CD73-adenosine axis in immuno-oncology, Immunol. Lett. 205 (2019) 31–39. https://doi.org/10.1016/j.imlet.2018.05.001.

[13] M. Demeules, A. Scarpitta, R. Hardet, H. Gondé, C. Abad, M. Blandin, S. Menzel, Y. Duan, B. Rissiek, T. Magnus, A.M. Mann, F. Koch-Nolte, S. Adriouch, Evaluation of nanobody-based biologics targeting purinergic checkpoints in tumor models in vivo, Front. Immunol. 13 (2022) 1–14. https://doi.org/10.3389/fimmu.2022.1012534.

[14] J. Ye, N.W. Gavras, D.C. Keeley, A.L. Hughson, G. Hannon, T.G. Vrooman, M.L. Lesch, C.J. Johnston, E.M. Lord, B.A. Belt, D.C. Linehan, J. Eyles, S.A. Gerber, CD73 and PD-L1 dual blockade amplifies antitumor efficacy of SBRT in murine PDAC models, J. Immunother. Cancer. 11 (2023) 1–14. https://doi.org/10.1136/jitc-2023-006842.

[15] W.W. Deng, Y.C. Li, S.R. Ma, L. Mao, G.T. Yu, L.L. Bu, A.B. Kulkarni, W.F. Zhang, Z.J. Sun, Specific blockade CD73 alters the “exhausted” phenotype of T cells in head and neck squamous cell carcinoma, Int. J. Cancer. 143 (2018) 1494–1504.

[16] B. Allard, M.S. Longhi, S.C. Robson, J. Stagg, The ectonucleotidases CD39 and CD73: Novel checkpoint inhibitor targets, Immunol. Rev. 276 (2017) 121–144. https://doi.org/10.1111/imr.12528.

[17] S. Zhang, X. Yang, L. Wang, C. Zhang, Interplay between inflammatory tumor microenvir onment and cancer stem cells (Review), Oncol. Lett. (2018). https://doi.org/10.3892/ol.2018.8716.

[18] A. Carus, M. Ladekarl, H. Hager, H. Pilegaard, P.S. Nielsen, F. Donskov, Tumor-associated neutrophils and macrophages in non-small cell lung cancer: No immediate impact on patient outcome, Lung Cancer. 81 (2013) 130–137. https://doi.org/10.1016/j.lungcan.2013.03.003.

[19] D.S. Rubenich, P.O. de Souza, N. Omizzollo, M.R. Aubin, P.J. Basso, L.M. Silva, E.M. da

Silva, F.C. Teixeira, G.F.S. Gentil, J.L. Domagalski, M.T. Cunha, K.A. Gadelha, L.F. Diel, N.E. Gelsleichter, A.S. Rubenich, G.S. Lenz, A.M. de Abreu, G.M. Kroeff, A.H. Paz, F. Visioli, M.L. Lamers, M.R. Wink, P. V. Worm, A.B. Araújo, J. Sévigny, N.O.S. Câmara, N. Ludwig, E. Braganhol, Tumor-neutrophil crosstalk promotes in vitro and in vivo glioblastoma progression, Front. Immunol. 14 (2023) 1–17. https://doi.org/10.3389/fimmu.2023.1183465.

[20] L. Haas, A.C. Obenauf, Allies or Enemies—The Multifaceted Role of Myeloid Cells in the Tumor Microenvironment, Front. Immunol. 10 (2019) 1–11. https://doi.org/10.3389/fimmu.2019.02746.

[21] S. Gurunathan, M.-H. Kang, M. Jeyaraj, M. Qasim, J.-H. Kim, Review of the Isolation, Characterization, Biological Function, and Multifarious Therapeutic Approaches of Exosomes, Cells. 8 (2019) 307. https://doi.org/10.3390/cells8040307.

[22] D.S. Rubenich, N. Omizzollo, M.J. Szczepański, T.E. Reichert, T.L. Whiteside, N. Ludwig, E. Braganhol, Small extracellular vesicle-mediated bidirectional crosstalk between neutrophils and tumor cells, Cytokine Growth Factor Rev. 61 (2021) 16–26. https://doi.org/10.1016/j.cytogfr.2021.08.002.

[23] H. Oh, B. Siano, S. Diamond, Neutrophil isolation protocol, J. Vis. Exp. (2008) 1–2. https://doi.org/10.3791/745.

[24] C.J. Lin, J.R. Grandis, T.E. Carey, S.M. Gollin, T.L. Whiteside, W.M. Koch, R.L. Ferris, S.Y. Lai, Head and neck squamous cell carcinoma cell lines: Established models and rationale for selection, Head Neck. 29 (2007) 89–201. https://doi.org/https://doi.org/10.1002/hed.20478.

[25] N. Ludwig, B.M. Razzo, S.S. Yerneni, T.L. Whiteside, Optimization of cell culture conditions for exosome isolation using mini-size exclusion chromatography (mini-SEC), Exp. Cell Res. 378 (2019) 149–157.

[26] Y. Chen, R. Corriden, Y. Inoue, L. Yip, N. Hashiguchi, A. Zinkernagel, V. Nizet, P.A. Insel, W.G. Junger, ATP release guides neutrophil chemotaxis via P2Y2 and A3 receptors, Science (80-.). 314 (2006) 1792–1795. https://doi.org/10.1126/science.1132559.

[27] S. Jaillon, A. Ponzetta, D. Di Mitri, A. Santoni, R. Bonecchi, A. Mantovani, Neutrophil diversity and plasticity in tumour progression and therapy, Nat. Rev. Cancer. 20 (2020) 485–503. https://doi.org/10.1038/s41568-020-0281-y.

[28] C. Théry, K.W. Witwer, E. Aikawa, [...] Davide Alcaraz, E.K. Zuba-Surma, Minimal information for studies of extracellular vesicles 2018 (MISEV2018): a position statement of the International Society for Extracellular Vesicles and update of the MISEV2014 guidelines, J. Extracell. Vesicles. 8 (2019) 1535750.

[29] C. Hsu, W. Chou, Y. Hung, S. Lin, C. Hung, K. Yeh, H. Wang, C. Lu, Predictive Value of Albumin and Neutrophil-to-Lymphocyte Ratio Score for Treatment Completeness and Safety Profiles in Patients With Head and Neck Cancer Receiving Definitive Concurrent Chemoradiotherapy, 2883 (2022) 2875–2883. https://doi.org/10.21873/invivo.13028.

[30] M.T. Masucci, M. Minopoli, M.V. Carriero, Tumor Associated Neutrophils. Their Role in Tumorigenesis, Metastasis, Prognosis and Therapy, Front. Oncol. 9 (2019). https://doi.org/10.3389/fonc.2019.01146.

[31] H.I. Yukinori Takenaka, Ryohei Oya, Norihiko Takemoto, Neutrophil-to-lymphocyte ratio as a prognostic marker for head and neck squamous cell carcinoma treated with immune checkpoint inhibitors : Meta-analysis, Head Neck. 44 (2022) 1043–1271. https://doi.org/https://doi.org/10.1002/hed.26997.

[32] A.Z. Marco A. Mascarella, Erin Mannard, Sabrina Daniela Silva, Neutrophil-to-lymphocyte ratio in head and neck cancer prognosis : A systematic review and meta-analysis, Head Neck. 40 (2018) 869–1100. https://doi.org/https://doi.org/10.1002/hed.25075.

[33] V.A. Boussiotis, Molecular and Biochemical Aspects of the PD-1 Checkpoint Pathway Immune Checkpoint Blockase as Cancer Therapy, N Engl J Med. 375 (2017) 1767–1778. https://doi.org/10.1056/NEJMra1514296.Molecular.

[34] D. Schulz, I. Stancev, A. Sorrentino, A.N. Menevse, P. Beckhove, G. Brockhoff, M.G. Hautmann, T.E. Reichert, R.J. Bauer, T. Ettl, Increased PD-L1 expression in radioresistant HNSCC cell lines after irradiation affects cell proliferation due to inactivation of GSK-3beta, Oncotarget. 10 (2019) 573–583. https://doi.org/10.18632/oncotarget.26542.

[35] D. Schulz, L. Feulner, D. Santos Rubenich, S. Heimer, S. Rohrmüller, Y. Reinders, M. Falchetti, M. Wetzel, E. Braganhol, E. Lummertz da Rocha, N. Schäfer, S. Stöckl, G. Brockhoff, A.K. Wege, J. Fritsch, F. Pohl, T.E. Reichert, T. Ettl, R.J. Bauer, Subcellular localization of PD-L1 and cell-cycle-dependent expression of nuclear PD-L1 variants: implications for head and neck cancer cell functions and therapeutic efficacy, Mol. Oncol. (2023) 1–22. https://doi.org/10.1002/1878-0261.13567.

[36] Y. Tang, P. Zhang, Y. Wang, J. Wang, M. Su, Y. Wang, L. Zhou, J. Zhou, W. Xiong, Z. Zeng, Y. Zhou, S. Nie, Q. Liao, The Biogenesis, Biology, and Clinical Significance of Exosomal PD-L1 in Cancer, Front. Immunol. 11 (2020) 1–14. https://doi.org/10.3389/fimmu.2020.00604.

[37] N. Ludwig, D.S. Rubenich, Ł. Zaręba, J. Siewiera, J. Pieper, E. Braganhol, T.E. Reichert, M.J. Szczepański, Potential roles of tumor cell-and stroma cell-derived small extracellular vesicles in promoting a pro-angiogenic tumor microenvironment, Cancers (Basel). 12 (2020) 1–15. https://doi.org/10.3390/cancers12123599.

[38] V.R. Minciacchi, M.R. Freeman, D. Di Vizio, Extracellular Vesicles in Cancer: Exosomes, Microvesicles and the Emerging Role of Large Oncosomes, Semin. Cell Dev. Biol. 40 (2015) 41–51.

[39] D. Daassi, K.M. Mahoney, G.J. Freeman, The importance of exosomal PDL1 in tumour immune evasion, Nat. Rev. Immunol. 20 (2020) 209–215. https://doi.org/10.1038/s41577-019-0264-y.

[40] M. Niu, Y. Liu, M. Yi, D. Jiao, K. Wu, Biological Characteristics and Clinical Significance of Soluble PD-1/PD-L1 and Exosomal PD-L1 in Cancer, Front. Immunol. 13 (2022) 1–14. https://doi.org/10.3389/fimmu.2022.827921.

[41] A. Clayton, S. Al-taei, J. Webber, M.D. Mason, Z. Tabi, Cancer Exosomes Express CD39 and CD73, Which Suppress T Cells through Adenosine Production , (2022). https://doi.org/10.4049/jimmunol.1003884.

[42] Y.M. Lu T, Zhang Z, Zhang J, Pan X, Zhu X, Wang X, Li Z, Ruan M, Li H, Chen W, CD73 in small extracellular vesicles derived from HNSCC defines tumour-associated immunosuppression mediated by macrophages in the microenvironment, J. Extracell. Vesicles. 11 (2022) e12218. https://doi.org/10.1002/jev2.12218.

[43] W.T. Ludwig N, Yerneni SS, Azambuja JH, Gillespie DG, Menshikova EV, Jackson EK, Tumor-derived exosomes promote angiogenesis via adenosine A2B receptor signaling, Angiogenesis. 23 (2020) 599–610. https://doi.org/10.1007/s10456-020-09728-8.

[44] B.M. Razzo, N. Ludwig, C. Hong, P. Sharma, K.P. Fabian, R.J. Fecek, W.J. Storkus, T.L. Whiteside, Tumor-derived exosomes promote carcinogenesis of murine oral squamous cell carcinoma, Carcinogenesis. (2019) 1–9.

[45] N. Seo, K. Akiyoshi, H. Shiku, Exosome - mediated regulation of tumor immunology,

(2018) 2998–3004. https://doi.org/10.1111/cas.13735.

[46] W.T. Theodoraki MN, Yerneni SS, Hoffmann TK, Gooding WE, Clinical Significance of PD-L1+ Exosomes in Plasma of Head and Neck Cancer Patients, Clin. Cancer Res. 24 (2018) 896–905. https://doi.org/10.1158/1078-0432.CCR-17-2664.

[47] T.L. Whiteside, Tumor-Derived Exosomes and Their Role in Cancer Progression, Adv. Clin. Chem. 74 (2016) 103–141.

[48] A.R. Cappellari, M.M. Pillat, H.D.N. Souza, F. Dietrich, F.H. Oliveira, F. Figueiró, A.L. Abujamra, R. Roesler, J. Lecka, J. Sévigny, A.M.O. Battastini, H. Ulrich, Ecto-5'-nucleotidase overexpression reduces tumor growth in a xenograph medulloblastoma model, PLoS One. 10 (2015) 1–18. https://doi.org/10.1371/journal.pone.0140996.

[49] X. Zhang, W. Xu, Neutrophils diminish T-cell immunity to foster gastric cancer progression : the role of GM-CSF / PD-L1 / PD-1 signalling pathway, (2017) 10–13. https://doi.org/10.1136/gutjnl-2017-313923.

[50] O. Yajuk, M. Baron, S. Toker, T. Zelter, T. Fainsod-levi, Z. Granot, The PD-L1 / PD-1 Axis Blocks Neutrophil Cytotoxicity in Cancer, Cells. 10 (2021) 1–13. https://doi.org/10.3390/cells10061510.

[51] T.T. Wang, Y.L. Zhao, L.S. Peng, N. Chen, W. Chen, Y.P. Lv, F.Y. Mao, J.Y. Zhang, P. Cheng, Y.S. Teng, X.L. Fu, P.W. Yu, G. Guo, P. Luo, Y. Zhuang, Q.M. Zou, Tumour-activated neutrophils in gastric cancer foster immune suppression and disease progression through GM-CSF-PD-L1 pathway, Gut. 66 (2017) 1900–1911. https://doi.org/10.1136/gutjnl-2016-313075.

[52] D. Tang, D. Zhang, Y. Heng, X.K. Zhu, H.Q. Lin, J. Zhou, L. Tao, L.M. Lu, Tumor-Infiltrating PD-L1+ Neutrophils Induced by GM-CSF Suppress T Cell Function in Laryngeal Squamous Cell Carcinoma and Predict Unfavorable Prognosis, J. Inflamm. Res. 15 (2022) 1079–1097. https://doi.org/10.2147/JIR.S347777.

[53] C. Li, S. Lim, W. Xia, H. Lee, L. Chan, C. Kuo, K. Khoo, S. Chang, J. Cha, T. Kim, J.L. Hsu, Y. Wu, J. Hsu, H. Yamaguchi, Q. Ding, Y. Wang, J. Yao, C. Lee, H. Wu, A.A. Sahin, J.P. Allison, D. Yu, G.N. Hortobagyi, M. Hung, Glycosylation and stabilization of programmed death ligand-1 suppresses T-cell activity, Nat. Commun. (2016). https://doi.org/10.1038/ncomms12632.

[54] H.M. Hsu JM, Li CW, Lai YJ, Posttranslational Modifications of PD-L1 and Their

Applications in Cancer Therapy, Cancer Res. 78 (2018) 6349–6353. https://doi.org/10.1158/0008-5472.CAN-18-1892.

[55] S. Zhou, J. Zhu, J. Xu, B. Gu, Q. Zhao, C. Luo, Z. Gao, Y.E. Chin, X. Cheng, Anti-tumour potential of PD-L1/PD-1 post-translational modifications, Immunology. 167 (2022) 471–481. https://doi.org/10.1111/imm.13573.

[56] X. Hu, J. Wang, M. Chu, Y. Liu, Z. Wang, X. Zhu, Emerging Role of Ubiquitination in the Regulation of PD-1 / PD-L1 in Cancer Immunotherapy, Mol. Ther. 29 (2021) 908–919. https://doi.org/10.1016/j.ymthe.2020.12.032.

[57] B. Shao, C.-W. Li, S.-O. Lim, L. Sun, Y.-J. Lai, J. Hou, C. Liu, C.-W. Chang, Y. Qiu, J.-M. Hsu, L.-C. Chan, Z. Zha, H. Li, M.-C. Hung, Deglycosylation of PD-L1 by 2-deoxyglucose reverses PARP inhibitor-induced immunosuppression in triple-negative breast cancer., Am. J. Cancer Res. 8 (2018) 1837–1846. http://www.ncbi.nlm.nih.gov/pubmed/30323975%0Ahttp://www.pubmedcentral.nih.gov/articlerender.fcgi?artid=PMC6176188.

[58] Z.H. Ren, C.Z. Lin, W. Cao, R. Yang, W. Lu, Z.Q. Liu, Y.M. Chen, X. Yang, Z. Tian, L.Z. Wang, J. Li, X. Wang, W.T. Chen, T. Ji, C.P. Zhang, CD73 is associated with poor prognosis in HNSCC, Oncotarget. 7 (2016) 61690–61702. https://doi.org/10.18632/oncotarget.11435.

[59] E. Ferretti, A.L. Horenstein, C. Canzonetta, F. Costa, F. Morandi, Canonical and non-canonical adenosinergic pathways, Immunol. Lett. 205 (2019) 25–30. https://doi.org/10.1016/j.imlet.2018.03.007.

[60] Z.W. Gao, L. Yang, C. Liu, X. Wang, W.T. Guo, H.Z. Zhang, K. Dong, Distinct Roles of Adenosine Deaminase Isoenzymes ADA1 and ADA2: A Pan-Cancer Analysis, Front. Immunol. 13 (2022) 1–12. https://doi.org/10.3389/fimmu.2022.903461.

[61] D.S. Rubenich, P.O. De Souza, N. Omizzollo, G.S. Lenz, J. Sevigny, E. Braganhol, Neutrophils : fast and furious — the nucleotide pathway, (2021) 371–383.

[62] N.E. Gelsleichter, J.H. Azambuja, D.S. Rubenich, E. Braganhol, CD73 in glioblastoma: Where are we now and what are the future directions?, Immunol. Lett. 256–257 (2023) 20–27. https://doi.org/10.1016/j.imlet.2023.03.005.

[63] B.-B.I. Korbecki J, Grochans S, Gutowska I, Barczak K, CC Chemokines in a Tumor : A Review of Pro-Cancer and Anti-Cancer Properties of Receptors CCR5 , CCR6 , Int J Mol

Sci. 21 (2020). https://doi.org/10.3390/ijms21207619.

[64] K. Ohuchi, Y. Kambayashi, T. Hidaka, T. Fujimura, Plasminogen Activating Inhibitor-1 Might Predict the Ef fi cacy of Anti- PD1 Antibody in Advanced Melanoma Patients, Front. Oncol. 11 (2021) 1–8. https://doi.org/10.3389/fonc.2021.798385.

[65] M.E. Shaul, Z.G. Fridlender, Tumour-associated neutrophils in patients with cancer, Nat. Rev. Clin. Oncol. 16 (2019) 601–620. https://doi.org/10.1038/s41571-019-0222-4.

[66] M. He, A. Peng, X. Huang, D. Shi, J. Wang, Q. Zhao, H. Lin, Peritumoral stromal neutrophils are essential for c-Met-elicited metastasis in human hepatocellular carcinoma, Oncoimmunology. 5 (2016) 1–11. https://doi.org/10.1080/2162402X.2016.1219828.

[67] S.L. Zhou, Z.J. Zhou, Z.Q. Hu, X.W. Huang, Z. Wang, E.B. Chen, J. Fan, Y. Cao, Z. Dai, J. Zhou, Tumor-Associated Neutrophils Recruit Macrophages and T-Regulatory Cells to Promote Progression of Hepatocellular Carcinoma and Resistance to Sorafenib, Gastroenterology. 150 (2016) 1646-1658.e17. https://doi.org/10.1053/j.gastro.2016.02.040.

[68] Y. Wang, H. Zhang, C. Liu, Z. Wang, W. Wu, N. Zhang, Immune checkpoint modulators in cancer immunotherapy : recent advances and emerging concepts, BioMed Central, 2022. https://doi.org/10.1186/s13045-022-01325-0.

[69] P.A. Ott, F.S. Hodi, C. Robert, CTLA-4 and PD-1 / PD-L1 Blockade : New Immunotherapeutic Modalities with Durable Clinical Benefit in Melanoma Patients CTLA-4 and PD-1 / PD-L1 Blockade : New Immunotherapeutic, (2013) 5300–5309. https://doi.org/10.1158/1078-0432.CCR-13-0143.

[70] N. Bach, R. Winzer, E. Tolosa, W. Fiedler, The Clinical Significance of CD73 in Cancer, (2023) 1–21.

[71] H. Yang, F. Yao, P.F. Davis, S.T. Tan, S.R.R. Hall, CD73 , Tumor Plasticity and Immune Evasion in Solid Cancers, (2021) 1–27.

[72] E.A. Thompson, J.D. Powell, Inhibition of the Adenosine Pathway to Potentiate Cancer Immunotherapy: Potential for Combinatorial Approaches, Annu Rev Med. (2021) 331–348. https://doi.org/10.1146/annurev-med-060619-023155.

[73] C.D. Cdk, J. Zhang, X. Bu, H. Wang, Y. Zhu, Y. Geng, N.T. Nihira, Y. Tan, Y. Ci, F. Wu, X. Dai, J. Guo, Y. Huang, C. Fan, S. Ren, Y. Sun, G.J. Freeman, P. Sicinski, W. Wei, Cyclin D–

CDK4 kinase destabilizes PD-L1 via cullin 3–SPOP to control cancer immune surveillance, Nat. Publ. Gr. (2018). https://doi.org/10.1038/nature25015.

[74] J. Noh, I.P. Lee, N.R. Han, M. Kim, Y.K. Min, S. Lee, S.H. Yun, S. Il Kim, T. Park, H. Chung, D. Park, C.H. Lee, Additive Effect of CD73 Inhibitor in Colorectal Cancer Treatment, Cell. Mol. Gastroenterol. Hepatol. 14 (n.d.) 769–788. https://doi.org/10.1016/j.jcmgh.2022.07.005.

[75] L. Chen, L. Wang, L. Zhu, Z. Xu, Y. Liu, Z. Li, J. Zhou, F. Luo, Exosomes as Drug Carriers in Anti-Cancer Therapy, Front. Cell Dev. Biol. 10 (2022) 1–12. https://doi.org/10.3389/fcell.2022.728616.

[76] K. Laubach, T. Turan, R. Mathew, J. Wilsbacher, J. Engelhardt, J. Samayoa, Tumor-intrinsic metabolic reprogramming and how it drives resistance to anti-PD-1/PD-L1 treatment, Cancer Drug Resist. 6 (2023) 611–641. https://doi.org/10.20517/cdr.2023.60.

[77] J. Bendell, P. LoRusso, M. Overman, A.M. Noonan, D.W. Kim, J.H. Strickler, S.W. Kim, S. Clarke, T.J. George, P.S. Grimison, M. Barve, M. Amin, J. Desai, T. Wise-Draper, S. Eck, Y. Jiang, A.A. Khan, Y. Wu, P. Martin, Z.A. Cooper, N. Elgeioushi, N. Mueller, R. Kumar, S.P. Patel, First-in-human study of oleclumab, a potent, selective anti-CD73 monoclonal antibody, alone or in combination with durvalumab in patients with advanced solid tumors, Cancer Immunol. Immunother. 72 (2023) 2443–2458. https://doi.org/10.1007/s00262-023-03430-6.

[78] R.S. Herbst, M. Majem, F. Barlesi, E. Carcereny, Q. Chu, I. Monnet, A. Sanchez-Hernandez, S. Dakhil, D.R. Camidge, L. Winzer, Y. Soo-Hoo, Z.A. Cooper, R. Kumar, J. Bothos, C. Aggarwal, A. Martinez-Marti, COAST: An Open-Label, Phase II, Multidrug Platform Study of Durvalumab Alone or in Combination with Oleclumab or Monalizumab in Patients with Unresectable, Stage III Non-Small-Cell Lung Cancer, J. Clin. Oncol. 3 (2022). https://doi.org/10.1200/JCO.22.00227.

[79] A. Chang, J. Hao, A tumor intrinsic role of CD73 in pancreatic adenocarcinoma, Ann. Pancreat. Cancer. 5 (2022). https://doi.org/10.21037/APC-2022-2.

[80] I.L. Linde, T.R. Prestwood, J. Qiu, G. Pilarowski, M.H. Linde, X. Zhang, L. Shen, N.E. Reticker-Flynn, D.K.C. Chiu, L.Y. Sheu, S. Van Deursen, L.L. Tolentino, W.C. Song, E.G. Engleman, Neutrophil-activating therapy for the treatment of cancer, Cancer Cell. 41 (2023) 356-372.e10. https://doi.org/10.1016/j.ccell.2023.01.002.

[81] Z. Granot, Neutrophils as a Therapeutic Target in Cancer, Front. Immunol. 10 (2019) 1710. https://doi.org/10.3389/fimmu.2019.01710.

[82] H. Raskov, A. Orhan, S. Gaggar, I. Gögenur, Neutrophils and polymorphonuclear myeloid-derived suppressor cells: an emerging battleground in cancer therapy, Oncogenesis. 11 (2022) 1–16. https://doi.org/10.1038/s41389-022-00398-3.

Figure legend

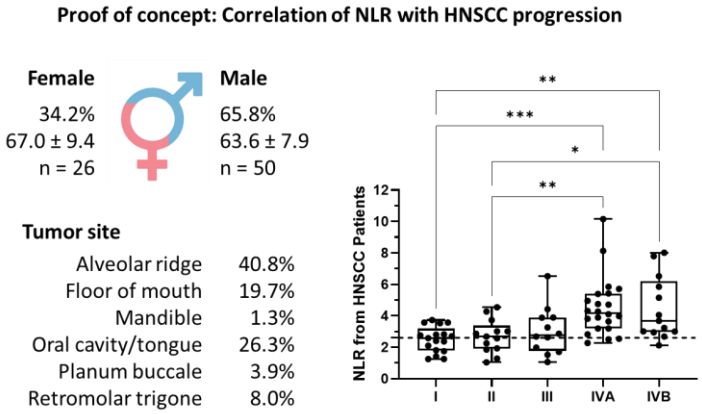

Figure 1: Proof of concept: Correlation of NLR with HNSCC progression. This analysis was performed with clinical data from 76 patients with mixed gender. Hemogram was generated pre-operative. Clinical description illustrated as gender percentage, mean of age in years and tumor site. Bar graph depicts the neutrophil-to-lymphocyte ratio (NLR) divided by the Union for International Cancer Control (UICC) staging system I, II, III, IVA and IVB. The threshold (>2.6) is represented as dot line. The data are presented as mean ± SD, one-way ANOVA with multiple comparison, * $p < 0.05$, ** $p < 0.01$, *** $P < 0.001$. For a more detailed clinical description of the five evaluated HNSCC primary tumors, see **Supplementary Table 1**.

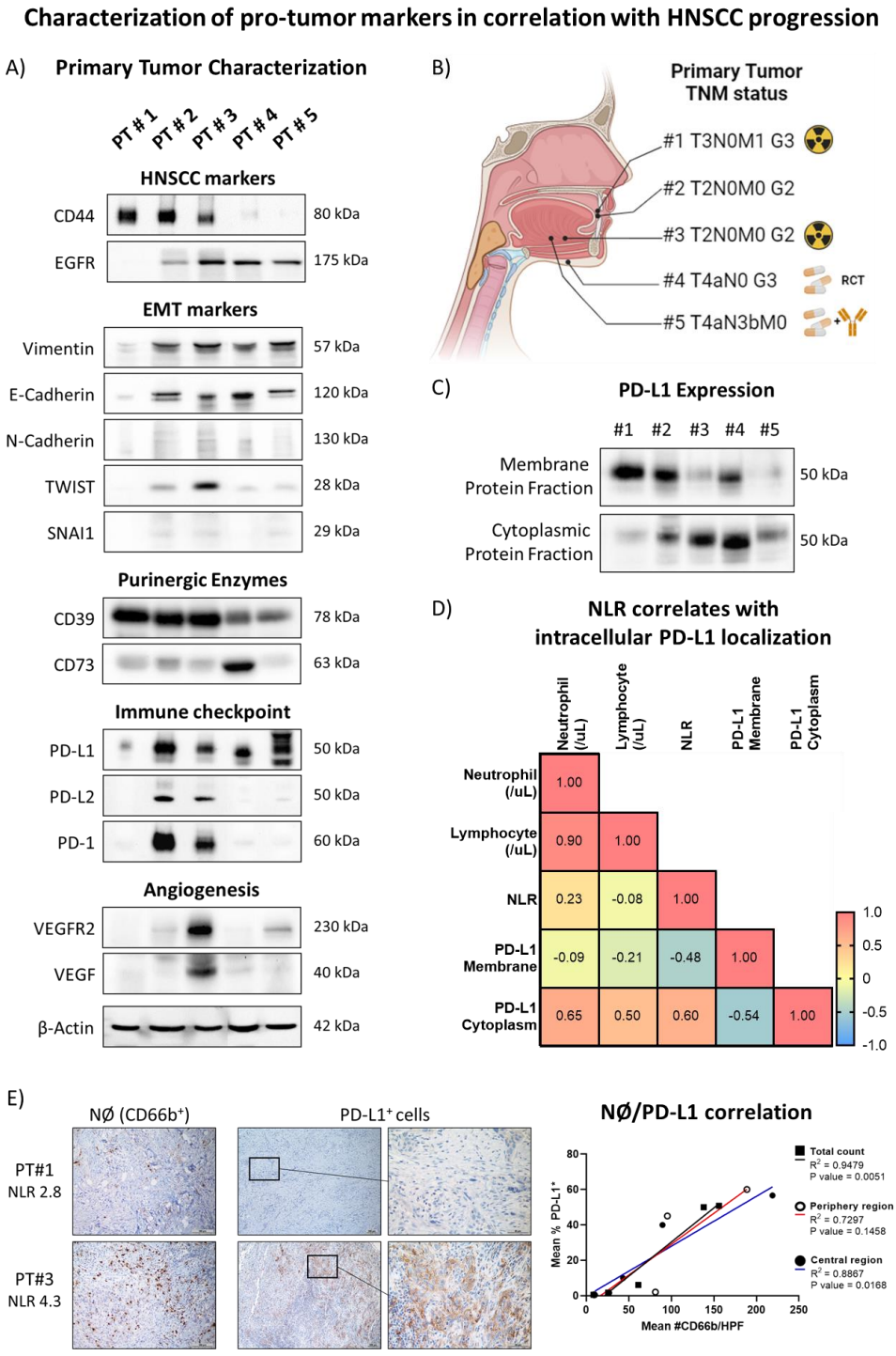

Figure 2: NLR correlates with HNSCC progression and intracellular PD-L1 localization. (**A**) HNSCC primary tumor characterization for PT#1 – PT#5 was achieved by western blotting (WB) analysis. Marker expression was divided by HNSCC markers (CD44, EGFR), EMT markers (vimentin, E-cadherin, N-cadherin, TWIST, Snai1), purinergic enzymes (CD39, CD73), immune checkpoints (PD-L1, PD-L2, PD-1) and angiogenesis markers (VEGFR2, VEGF). Per sample, 25 µg of protein was loaded. B-actin was used as loading control. N = 2. (**B**) HNSCC primary tumor TNM status for PT#1 – PT#5. The figure indicates the location, staging, and follow up treatment

(radiotherapy, illustrated as trefoil; chemotherapy, illustrated as pill; immunotherapy, illustrated as antibody, RCT = radio-/chemotherapy). (**C**) WB analysis of PD-L1 expression after subcellular fractionation into membrane and cytoplasmic proteins for PT#1 – PT#5. N = 2. (**D**) Heat map of Pearson correlation between NLR and PD-L1 localization for PT#1 – PT#5. (**E**) Immunohistochemical (IHC) stainings of HNSCC primary tumor sections from representative PT#3 for neutrophils (NØ, CD66b$^+$) and PD-L1-positive tumors cells (clone 28-8). Correlation of NØ presence and PD-L1$^+$ tumor cells was assessed by simple linear regression analysis. R squared and P values were shown for each evaluation: Mean of total PD-L1 percentage, PD-L1 expressed at the periphery and PD-L1 expressed in the central region. PD-L1 staining was magnified for optimized visualization of subcellular PD-L1 localization. Scale bar NØ (CD66b$^+$) 100 µm (20x magnification), PD-L1$^+$ 100 µm (10x magnification) and 50µm (40x magnification). Original blots and additional IHC stainings for characterization of pro-tumor markers in HNSCC primary tumors are shown in **Supplementary Figure 2**. For positive cell counts see **Supplementary Table 2**.

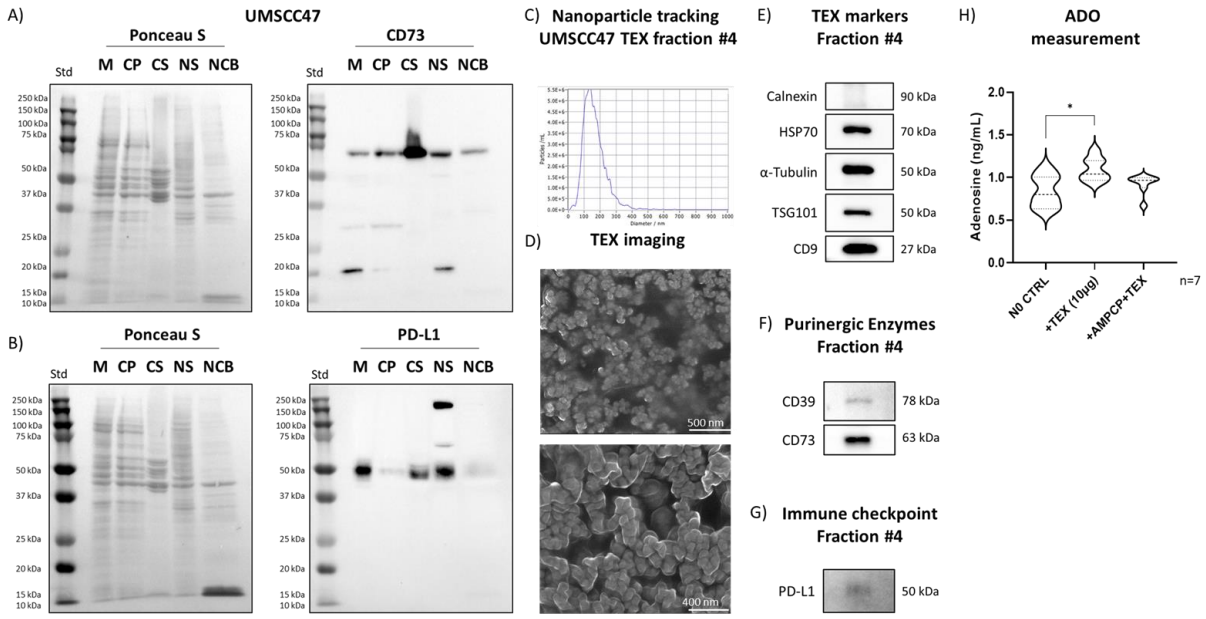

Figure 3: Immunosuppressive TEX carry PD-L1 and adenosine producing enzymes. Immunodetection of CD73 (**A**) and PD-L1 (**B**) by western blotting (WB) after subcellular fractionation. Subcellular fractions were divided into membrane (M), cytoplasmic (CP), cytoskeletal (CS), nuclear soluble (NS) and nuclear chromatin-bound (NCB) protein fraction. Molecular marker is indicated as Std, ranging from 10 to 250 kilodalton (kDa). Per sample, 20 µg of protein was loaded. Equal loading is verified by Ponceau S staining. N = 2. (**C**) Results of nanoparticle tracking analysis of fraction #4 from HNSCC cell line SCC47. Scale bars, 400/500 nm. (**D**) Scanning electron microscopic (SEM) image of fraction #4. N = 2. (**E**) Representative WB of fraction #4 using the TEX markers Calnexin, HSP70, α-Tubulin, TSG101 and CD9. (**F**)

Immunodetection of purinergic enzymes CD39 and CD73. N = 2. (**G**) Immunodetection of immune checkpoint PD-L1. N = 2. For WB analysis, 10 µg of protein lysate was used. (**H**) ELISA analysis of extracellular adenosine in the supernatant of experimental groups. Cells incubated with the respective cell culture medium served as experimental control. Non-conditioned media was used for background signal subtraction. The data are presented as mean ± SD (n = 7). * $p < 0.05$ versus control group. Original blots for SCC47-TEX characterization are shown in **Supplementary Figure 3**.

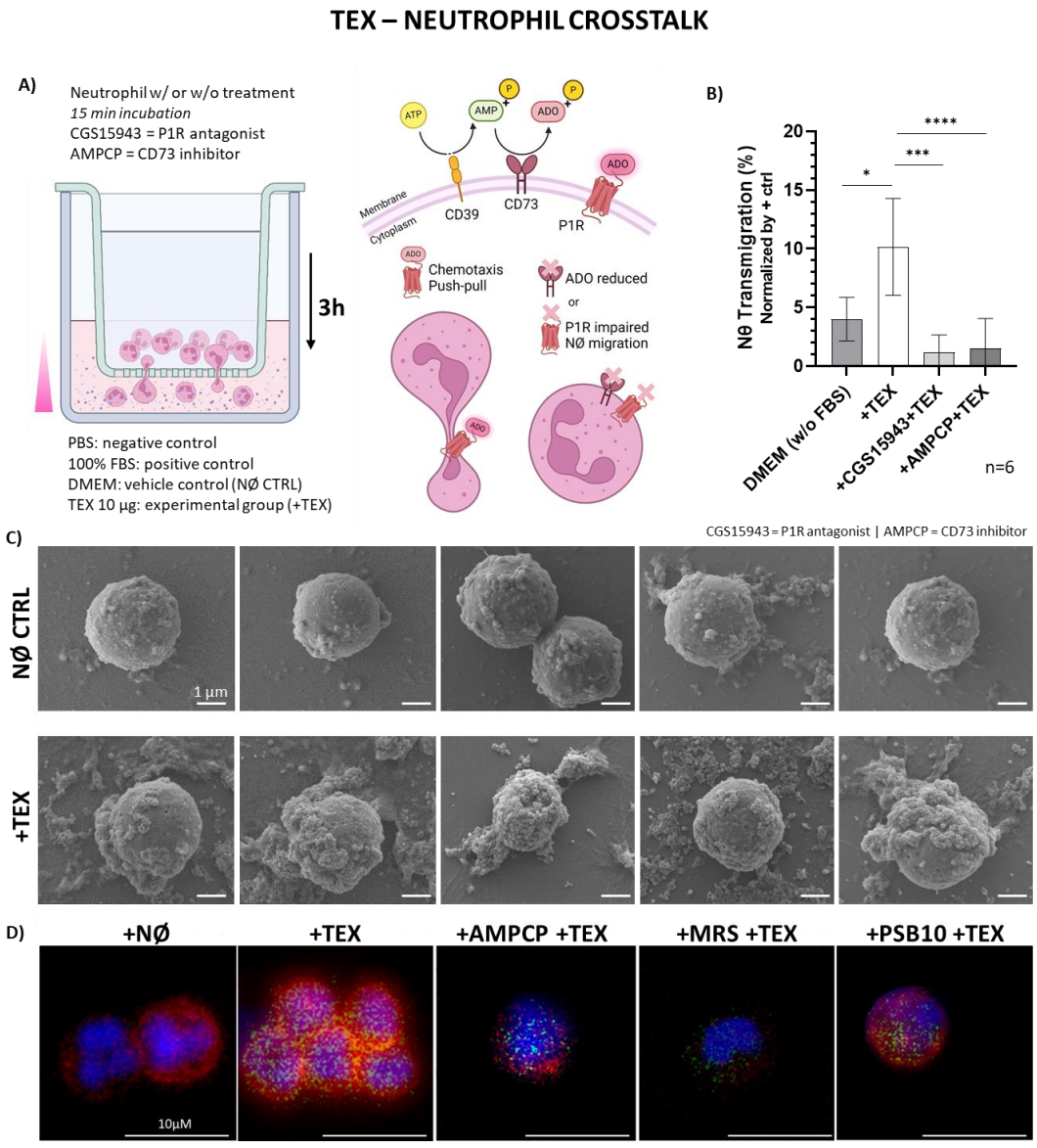

Figure 4: TEX–neutrophil crosstalk. (**A**) Representation of the transmigration assay experimental design and a schematic overview of the neutrophil (NØ) response to ADO signaling inhibition. The upper chamber contains NØ with (w/) or without (w/o) pre-incubation with the P1R antagonist CGS15493 or the CD73 inhibitor AMPCP. The lower chamber contains the following chemoattractants: PBS for negative chemotaxis control; 100% FBS as positive

chemotaxis control; DMEM w/ 10% EDHI FBS, as vehicle/NØ control; and DMEM w/ 10% EDHI FBS +TEX as experimental group. Cells are defined as migrated due to their presence in the bottom chamber after 3 hours of incubation in the experimental transwell setup. (**B**) Normalized percentage of NØ migration through the permeable membrane pores into the bottom chamber (n = 6 per group). Control group was composed by NØ exposed to non-conditioned medium, which was prepared as described in the material and methods section. Graph show mean ± SD and significance values were calculated using multiple one-way ANOVA * $p < 0.05$, **** $p < 0.0001$. (**C**) Selection of 5 representative SEM images from NØ control group (NØ CTRL) vs. NØ interacting with TEX (+TEX). Scale bar = 1 µm (n = 15). (**D**) One representative immunofluorescence image with DAPI = blue, phalloidin = red, TEX = green per group. Scale bar = 10 µm (n = 15 per group).

Characterization of TEX-modulated Neutrophil phenotype

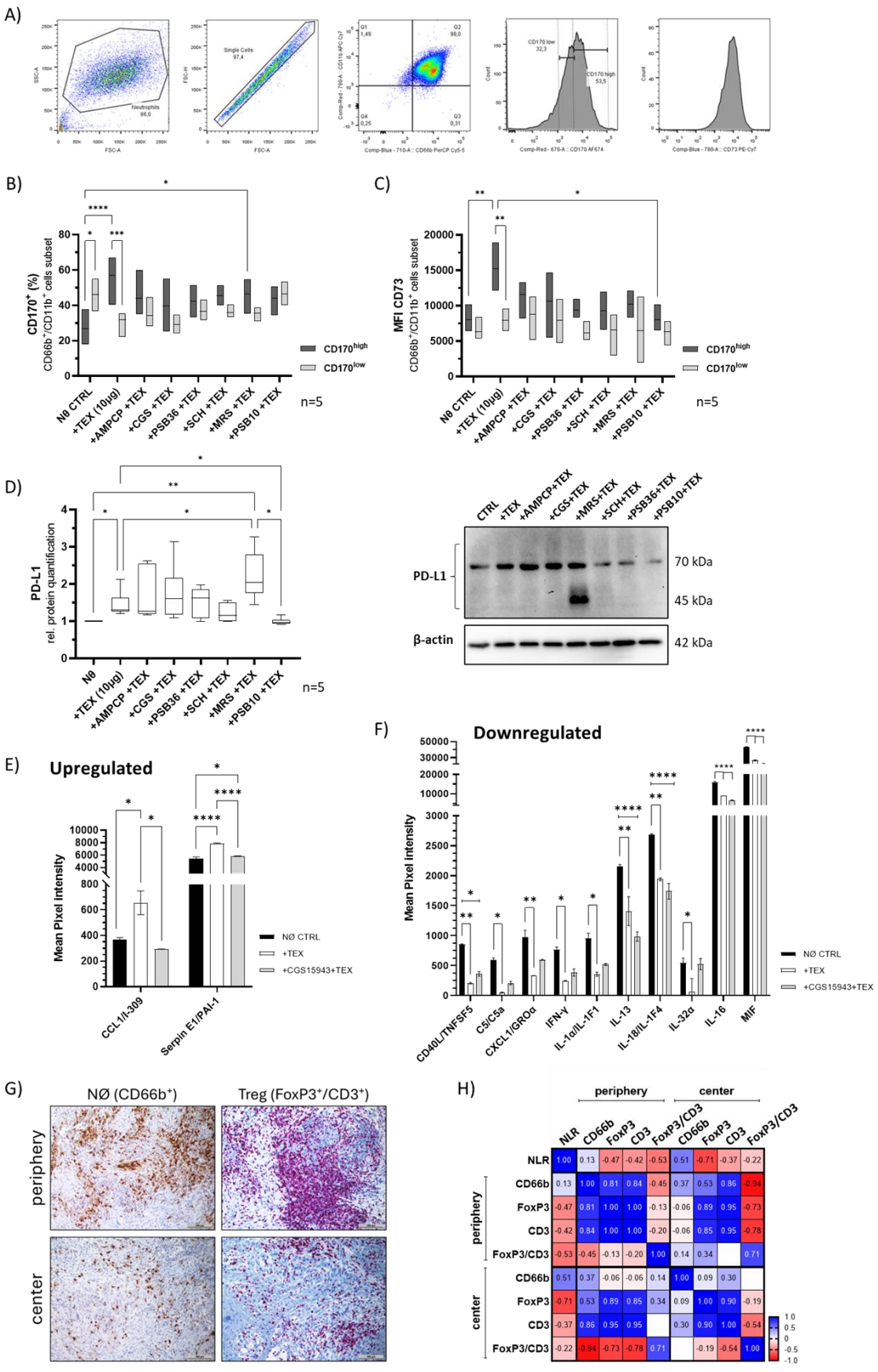

AMPCP (CD73 inhibitor) | CGS15943 (P1 antagonist) | PSB36 (A1R antagonist) | SCH442416 (A_2AR antagonist) | MRS1754 (A_2BR antagonist) | PSB10 hydrochloride (A3R antagonist)

Figure 5: Characterization of TEX-modulated Neutrophils phenotype. (**A**) Representative gating strategy for the detection of $CD170^{high}$ or $CD170^{low}$ subpopulations among NØ. Selection of SSC vs. FSC NØ population follows exclusion of doublets, using FSC-H vs. FSC-A, followed by the selection of $CD66b^{+}/CD11b^{+}$ population. Histograms represent the final strategy to select $CD170^{low}$ and $CD170^{high}$ populations and the MFI for CD73. (**B**) Identification of the anti/pro-tumor phenotype, based on the $CD170^{low}$ and $CD170^{high}$, respectively. Plots are shown for gated live $CD66b^{+}$ $CD11b^{+}$ cells w/ or w/o ADO signaling blockade. (**C**) MFI detection of CD73 cells from gated $CD170^{high}$ or $CD170^{low}$. (**D**) Immunodetection of PD-L1 in NØ. In this representative blot, 25 µg of protein lysate was loaded onto a 10% acrylamide gel. β-actin was used as loading control. Results are shown as fold change relative to control group (NØ) (n = 5 per group). **(E,F)** Human Cytokine Array was used on pool supernatant from five pooled donors per group: non-treated NØ as control (CTRL), NØ cultured with TEX (+TEX) and NØ pre-treated with P1R antagonist CGS15943 and subsequently cultured with TEX (+CGS +TEX) for 48 hours. Pixel intensity analysis of the dots from the membranes was performed to determine the relative expression levels of inflammatory cytokines. Results are representative of a pool of 5 donors in each group. Bars represent pixel intensity analysis of the dots. **(E)** Upregulated cytokine secretion and **(F)** downregulated cytokine secretion. Graphs show mean ± SD and significance values were calculated using multiple 2-way ANOVA. * $p < 0.05$, ** $p < 0.01$, **** $p < 0.0001$. Control group was composed by NØ exposed to non-conditioned medium, which was prepared as described in the material and methods section. **(G)** Representative IHC images from PT#3 for CD66b, CD3 and FoxP3. Scale bar 100 µm (20x magnification). **(H)** Pearson Correlation matrix of IHC analysis for the presented markers CD66b, CD3 and FoxP3 at the periphery and central regions. Positive correlation is highlighted in blue, negative correlation in red. Original dot blots of Human Cytokine Array and additional IHC stainings for correlation of NØ presence with Treg infiltration in HNSCC primary tumors are shown in **Supplementary Figure 4**. For positive cell counts see **Supplementary Table 2**.

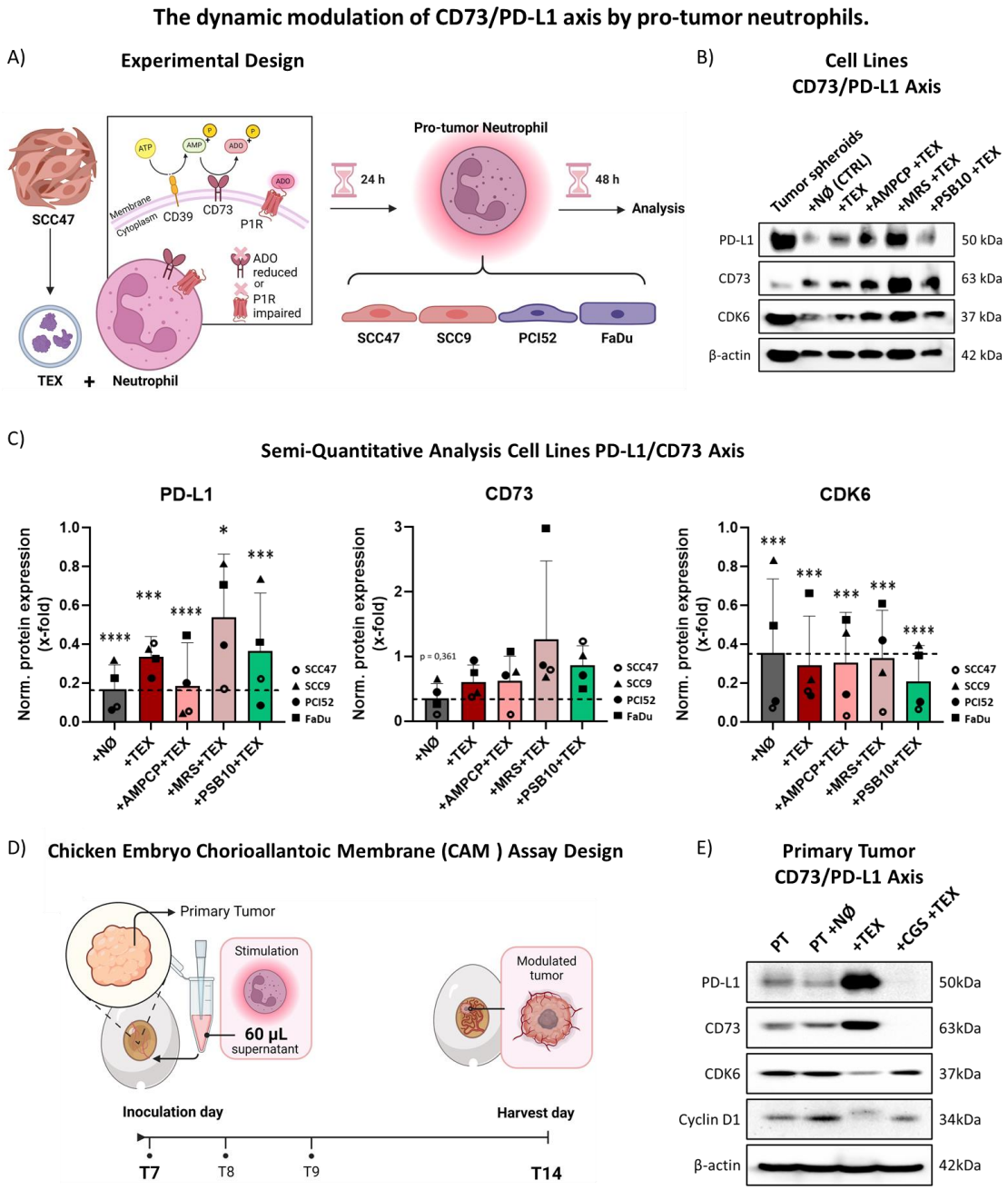

Figure 6: The dynamic modulation of CD73/PD-L1 axis by pro-tumor neutrophils. (**A**) Experimental design of the *in vitro* modulation in HNC cell lines SCC47, SCC9, PCI52 and FaDu. (**B**) Immunodetection of PD-L1, CD73 and CDK6 after treatment with Neutrophils (+NØ), NØ with 10 µg of TEX (+TEX), NØ pre-treated with CD73 inhibitor followed by TEX incubation (+AMPCP +TEX), NØ pre-treated with $A2_BR$ antagonist MRS1754 followed by TEX incubation (+MRS +TEX), NØ pre-treated with A3R antagonist followed by TEX incubation (+PSB10 +TEX) compared to control (HNC cell line = CTRL). Prior to lysis, NØ were washed out to reduce NØ interference in the measurement. Per sample, 10 µg of protein was loaded. β-actin was used as loading control. HNC cell line PCI52 was used as a representative. Additional cell lines FaDu, SCC9 and SCC47 are

shown in **Supplementary Figure 5**. N = 3. (**C**) Semi-quantitative analysis of western blots. Protein expression was normalized to the loading control β-actin. Graphs show mean ± SD and significance values were calculated using multiple two-way ANOVA. * $p < 0.05$, *** $p < 0.001$, **** $p < 0.0001$. (**D**) Illustration of the chicken embryo chorioallantoic membrane (CAM) assay design. (**E**) Immunodetection of PD-L1, CD73, CDK6 and cyclin D1 after 7-day CAM protocol. Groups divided as treatment of HNSCC primary tumor with healthy neutrophil supernatant (PT +NØ), NØ with TEX (+TEX), or NØ pre-treated with P1R antagonist followed by TEX incubation (+CGS +TEX) compared to control (HNSCC primary tumor = PT). Per sample, 25 µg of protein was loaded. β-actin was used as loading control. N = 3. Original blots are shown in **Supplementary Figure 6.**

Endorsement of pro-tumor potential of TEX-modulated Neutrophils

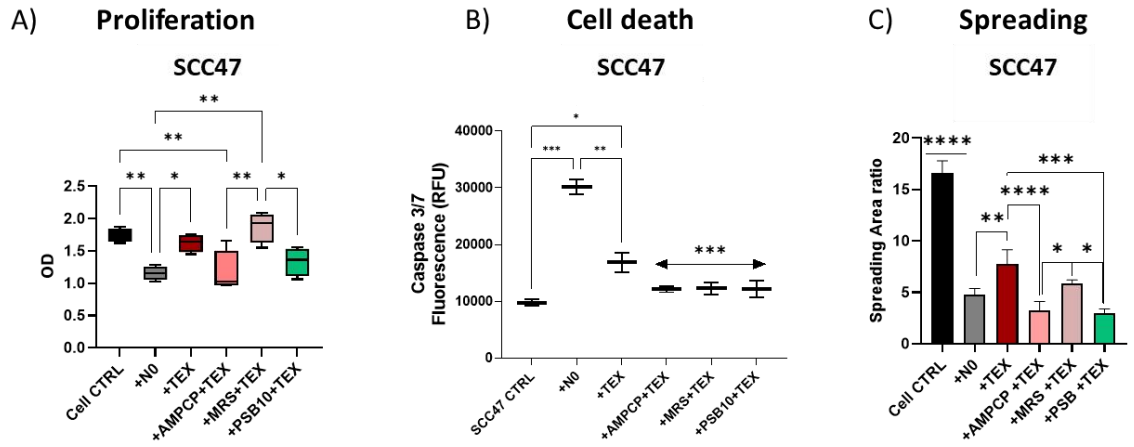

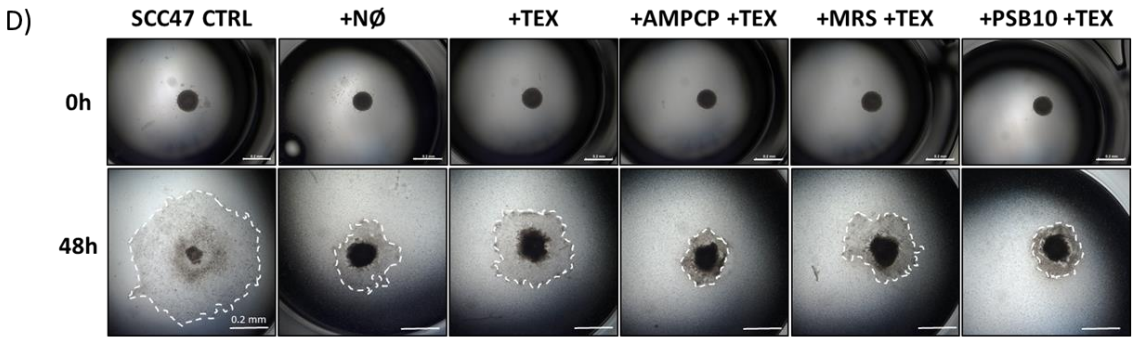

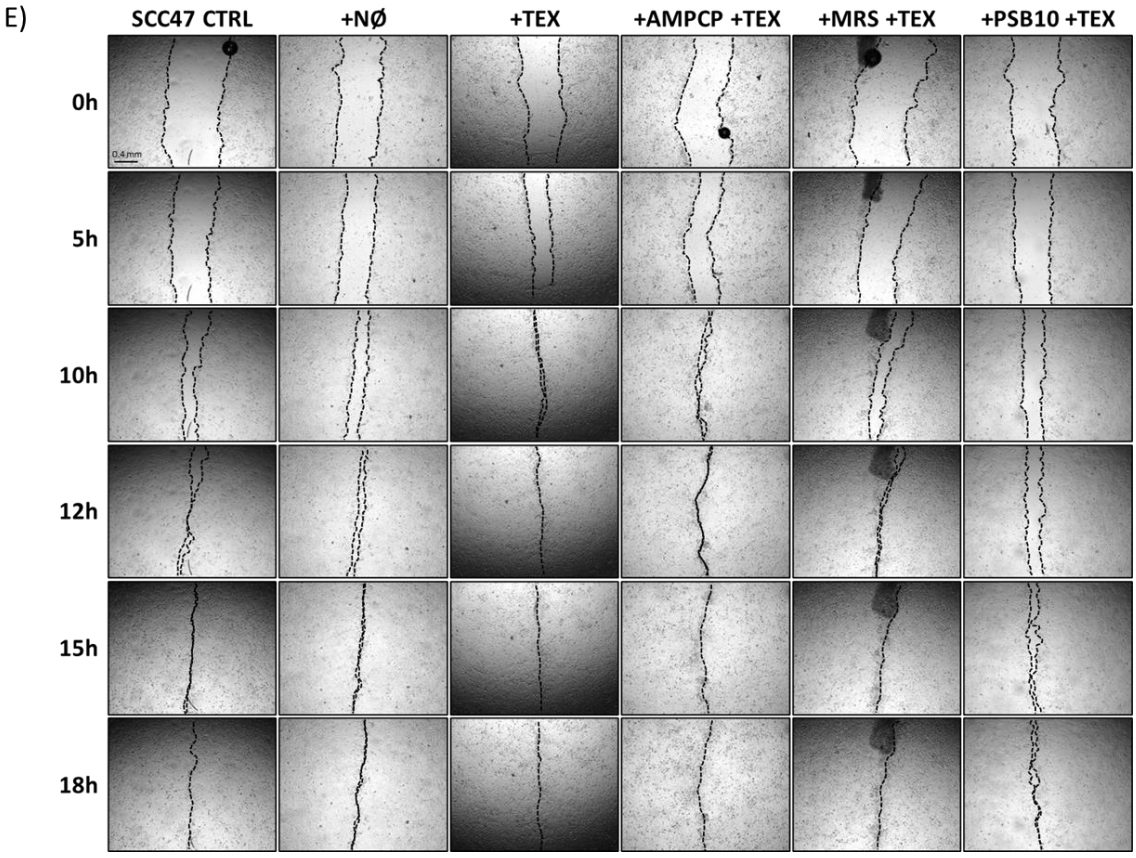

Figure 7: Endorsement of pro-tumor potential of TEX-modulated Neutrophils. Functional assays were performed with HNC cell lines SCC47, SCC9, PCI52 and FaDu with the following treatment groups: control (HNC cell line = CTRL), tumor cells with Neutrophils (+NØ), tumor cells with NØ with 10 µg TEX (+TEX), tumor cells with NØ pre-treated with CD73 inhibitor followed by TEX incubation (+AMPCP +TEX), tumor cells with NØ pre-treated with $A2_BR$ antagonist MRS1754 followed by TEX incubation (+MRS +TEX) and tumor cells with NØ pre-treated with A3R antagonist followed by TEX incubation (+PSB10 +TEX) indicated by distinct symbols and colors. (**A**) Quantitative analysis of cell proliferation assay by MTS absorbance (OD) with the representative HNSCC cell line SCC47. N = 5. Cell lines SCC9, PCI52 and FaDu are shown in **Supplementary Figure 7**. (**B**) Quantitative analysis of cell death assay by caspase 3/7 fluorescence as relative fluorescence units (RFU) with the representative HNSCC cell line SCC47. N = 3. (**C**) Quantitative analysis of spreading assay by area ratio (area 48 hours after incubation divided by area right before treatment) with the representative HNSCC cell line SCC47. N = 3. (**D**) One representative image of spreading assay per group at the beginning of the experiment (0h) and after 48 hours of incubation (48h), performed with representative HNSCC cell line SCC47. Spreading area is highlighted with a dot line. Scale bar = 0.2 mm. N = 3. (**E**) Representative images of wound healing assay 0, 5, 10, 12, 15 and 18 hours after treatment, performed with SCC47. Scratch is highlighted with a dot line. Scale bar = 0.4 mm. N = 3. Graphs express mean ± SD and significance values were calculated using multiple 2-way ANOVA. * $p < 0.05$, ** $p < 0.01$, *** $p < 0.001$. For proper comparison, cells from all groups were incubated in the same cell culture media condition.

The role of tumor-derived extracellular vesicles and neutrophils in orchestrating the dynamic CD73/PD-L1 axis in HNC.

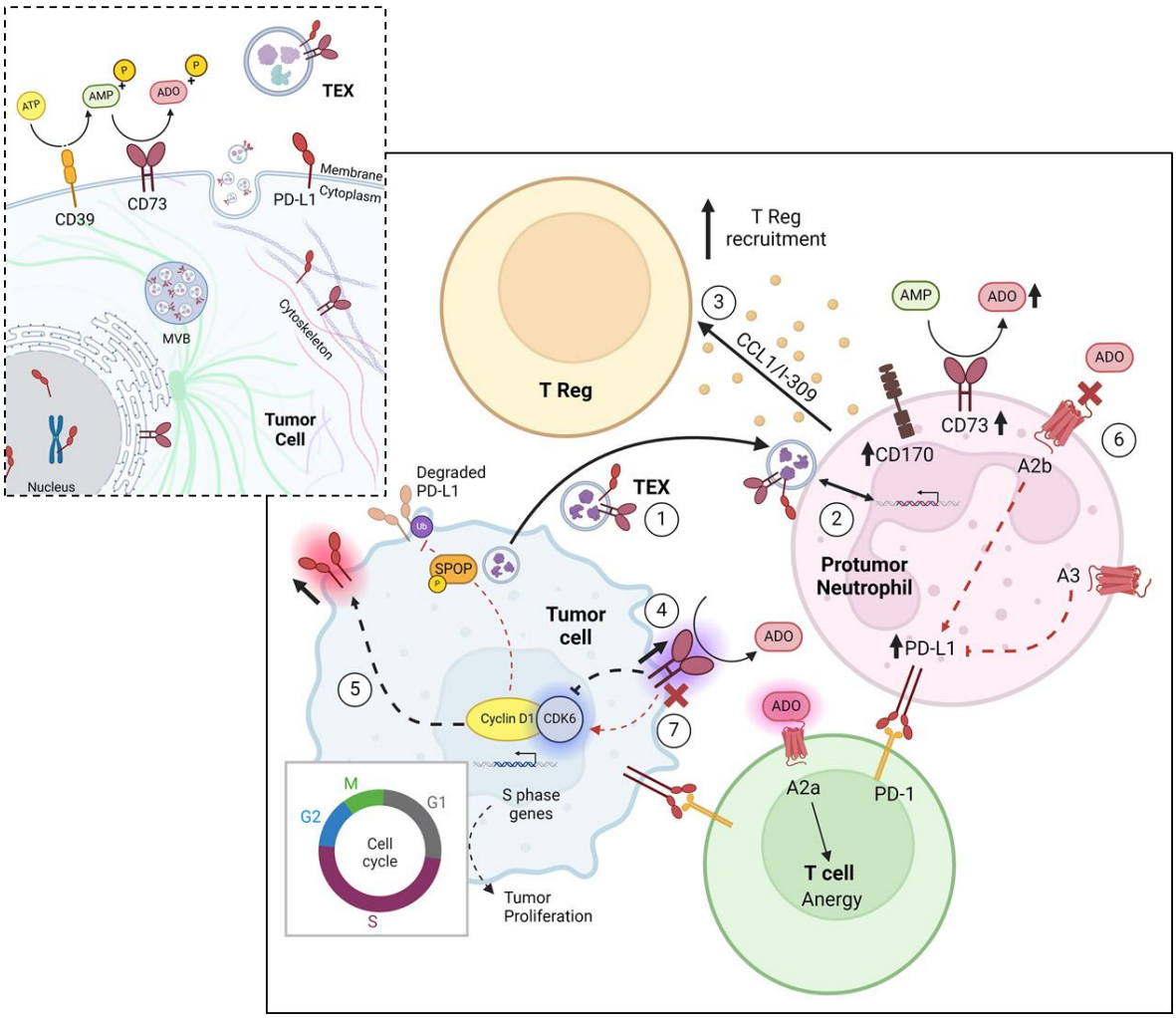

Figure 8: The role of tumor-derived extracellular vesicles and neutrophils in orchestrating the dynamic CD73/PD-L1 axis in HNC. (**1**) Tumor cells secrete TEX carrying immunosuppressive factors, such as PD-L1 and active ADO producing enzyme, CD73. (**2**) TEX interact with NØ inducing a pro-tumor phenotype by increasing expression of CD170, CD73 and PD-L1. (**3**) Pro-tumor NØ secrete immunosuppressive cytokines, recruiting Tregs. (**4**) Extracellular ADO is increased and upregulates CD73 activity on tumor cells. (**5**) CD73 expression inhibits Cyclin D1-CDK4/6, and therefore, increases PD-L1 expression in tumor cells. (**6**) By blocking P1R on NØ, the phenotype is modulated: $A2_BR$ acts synergistic to exosome influence and potentiates the pro-tumor phenotype. A3R inhibits the pro-tumor phenotype by reducing CD73 and PD-L1 expression. (**7**) The reduced ADO and immunosuppressive TME downregulate CD73, which activates Cyclin D1-CDK4/6 signaling, phosphorylating SPOP, resulting in the degradation of PD-L1.

Abbreviations

µg: microgramm
µm: micrometer
µM: micromolar
A3R: adenosine A3 receptor
ADA: adenosine deaminase
ADO: adenosine
APC: antigen-presenting cell
BCA: bicinchoninic acid
CAM: chorioallantoic membrane
CCL1: CC-chemokine ligand 1
CD: cluster of differentiation
CDK6: cyclin-dependent kinase 6
CST: Cell Signaling Technology
CTRL: control
EGF: epidermal growth factor
ELISA: enzyme-linked immunosorbent assay
EMT: epithelial-to-mesenchymal transition
FBS: fetal bovine serum
FSC: forward scatter
FSC-A: forward scatter - area
FSC-H: forward scatter - height
h: hours
HNC: head and neck cancer
HNSCC: head and neck squamous cell carcinoma
HPF: high-power field
HPV: human papilloma virus
I-309: CC-chemokine ligand 1
IFN-γ: Interferon gamma
IHC: immunohistochemistry
kDa: kilodalton
kV: kilovolt
LV: low vacuum
mbar: millibar
MDSC: myeloid-derived suppressor cell
MFI: mean fluorescent intensity
mini-SEC: mini-size exclusion chromatography
ml: milliliter
mm: millimeter
MVB: multivesicular bodies
NLR: neutrophil-to-lymphocyte ratio
nm: nanometer
NØ: neutrophils
NT5E: 5'-nucleotidase ecto
NTPD1: ectonucleoside 5'-triphosphate diphosphohydrolase
OD: optical density
P1R: Adenosine P1 receptor
PAI-1: plasminogen activator inhibitor-1
PBS: phosphate buffered saline
PCR: polymerase chain reaction
PD-L1: programmed death-ligand 1
PT: primary tumor
PVDF: polyvinylidene fluoride
rcf: relative centrifugal force
RT: room temperature
SD: standard deviation
SDS-PAGE: sodium dodecyl sulfate – polyacrylamide gel electrophoresis
SEM: scanning electron microscopy
Serpin E1: plasminogen activator inhibitor gene
sEV: small extracellular vesicle
SPOP: speckle type BTB/POZ protein
SSC: side scatter
TAN: tumor-associated neutrophil
TEX: tumor-derived extracellular vesicles
TME: tumor microenvironment
TNM: tumor, node, metastasis
Treg: regulatory T cell
TRPS: tunable resistive pulse sensing
U/L: units per liter
UICC: Union for International Cancer Control
V: Volt
WB: western blotting

Supporting information

Supplementary Table 1: Clinical description of the five evaluated HNSCC primary tumors

Supplementary Table 2: IHC quantification of primary HNSCC tissue sections

Supplementary Figure 1: Primary healthy neutrophils information. (**A**) Characterization of volunteers. B) Representative image of neutrophils after isolation stained with panoptic. The multilobular shape of nuclei is visible and characteristic of neutrophil morphology. (**C**) MTS assay for neutrophils with tested compounds after 24h incubation.

Supplementary Figure 2: Original blots and additional IHC stainings for characterization of pro-tumor markers in HNSCC primary tumors. (**A**) Characterization of pro-tumor marker protein expression. (**B**) PD-L1 expression in membrane and cytoplasmic protein fractions. (**C**) IHC stainings for correlation of neutrophils with PD-L1-positive tumor cells.

Supplementary Figure 3: Original blots for SCC47-TEX characterization.

Supplementary Figure 4: Original dot blots of Human Cytokine Array and additional IHC staining for correlation of neutrophils with Tregs infiltration. (**A**) Original dot blots of Human Cytokine Array. (**B**) IHC stainings for correlation of neutrophils with Tregs infiltration.

Supplementary Figure 5: Additional blots for immunodetection of PD-L1, CD73 and CDK6 after co-cultivation of HNC cell lines FaDu, PCI52, SCC9 and SCC47 with TEX-modulated neutrophils.

Supplementary Figure 6: Original blots for immunodetection of PD-L1, CD73, CDK6 and cyclin D1 after 7-day CAM protocol.

Supplementary Figure 7: Additional graphs for the endorsement of pro-tumor potential of TEX-modulated Neutrophils with the HNC cell lines FaDu, PCI52, SCC9 and SCC47.

Supplementary Figure 8: HNC cell line characterization.

Supplementary Figure 9: PD-L1 antibody screening for IHC optimization.

Supplementary Table 1: Clinical description of the five evaluated HNSCC primary tumors.

Tumor	Anatomic Site	TNM-Status	Neutrophil (/µL)	Lymphocyte (/µL)	NLR	mPD-L1 (Adj.Vol.)*	cPD-L1 (Adj.Vol.)*
PT # 1	Oral cavity	pT3, pNØ, cM1, pT3, pNØ, cM1, L0, V0, R0, Pn1, G3	4,92	1,72	2,86	2,043E+07	6,033E+05
PT # 2	Oral cavity	pT2, pNØ, cM0, L0, V0, R0, PNØ, G2	80,2	12,4	6,47	1,551E+07	1,331E+06
PT # 3	Oral cavity/ tongue	pT2, pNØ, cM0, L0, V0, R0, Pn1, G2	72,6	17,00	4,27	4,636E+06	2,090E+06
PT # 4	Mandible	yrpT4a, ypNØ, L0, V0, R0, PNØ, G3	78,9	9,70	8,13	1,083E+07	2,907E+06
PT # 5	Tongue	ypT4a, ypn3b, cM0, L0, V0, R1, Pn1	3,93	0,49	8,02	3,631E+06	1,525E+06

*Adjusted volume: total amount of signal for all the pixels within that band (WB) after background subtraction (Image Lab software 6.0.1, Bio-Rad).

Supplementary Table 2: IHC quantification of primary HNSCC tissue sections.

Patient	TMA-Nr.	#CD66b/HPF	Mean (center/periphery)	Mean (total)	#FoxP3/HPF	#CD3/HPF	Ratio FoxP3/CD3	Mean FoxP3/CD3 (center/periphery)	Mean FoxP3/CD3 (total)	PD-L1 (28-8) % pos. TZ*	Mean PD-L1 (center/periphery)	Mean PD-L1 (total)
	M	15	Liver (control)		0	3	0,00	Liver (control)				
PT # 1	1	24	10,33	9,83	57	127	0,45	0,62	0,60	<1	<1	<1
	2	3			46	54	0,85			<1		
	3	4			44	77	0,57			<1		
	4	23			46	112	0,41			<1		
	5	4	9,33		51	93	0,55	0,57		<1	<1	
	6	1			48	63	0,76			<1		
PT # 2	7	47	27,00	27,00	29	85	0,34	0,31	0,31	1	1,67	1,67
	8	28			29	81	0,36			2		
	9	6			16	72	0,22			2		
	10	-			-	-	-			-		
	11	-	-		-	-	-	-		-	-	
	12	-			-	-	-			-		
PT # 3	13	54	89,67	139,33	21	240	0,09	0,22	0,31	20	40,00	50,00
	14	97			128	532	0,24			60		
	15	118			79	248	0,32			40		
	16	29			248	830	0,30			70		
	17	274	189,00		198	488	0,41	0,40		60	60,00	
	18	264			390	768	0,51			50		
PT # 4	19	326	219,00	157,25	22	218	0,10	0,48	0,49	40	56,67	50,83
	20	112			48	56	0,86			60		
	21	-			-	-				70		
	22	140			43	94	0,46			25		
	23	51	95,50		24	48	0,50	0,50		40	45,00	
	24	-			5	9	0,56			70		
PT # 5	25	33	43,33	62,42	20	46	0,43	0,37	0,32	15	10,00	6,00
	26	29			11	32	0,34			5		
	27	68			20	63	0,32			<1		
	28	91			26	97	0,27			<1		
	29	-	81,50		-	-		0,28		<1	2,00	
	30	72			19	64	0,30			2		

*PD-L1: tumor cells with PD-L1 membrane and cytoplasmic expression

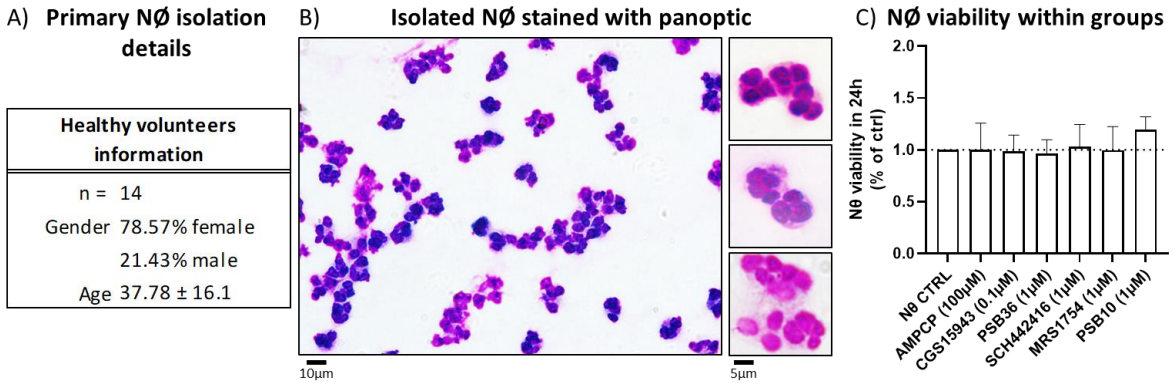

Supplementary Figure 1: Primary healthy neutrophils information. (**A**) Characterization of volunteers for neutrophil (NØ) donation in gender percentage and mean ± SD of age in years. N=14. (**B**) Representative image of NØ after isolation stained with panoptic. Scale bar 10 µm. The multilobular shape of nuclei is visible and characteristic of NØ morphology. Scale bar 5 µm. (**C**) MTS assay for NØ with tested compounds after 24 hours incubation in percentage in relation to control (% of ctrl). The data is presented as mean ± SD, one-way ANOVA with multiple comparison. N = 5

A) Characterization of pro-tumor marker protein expression

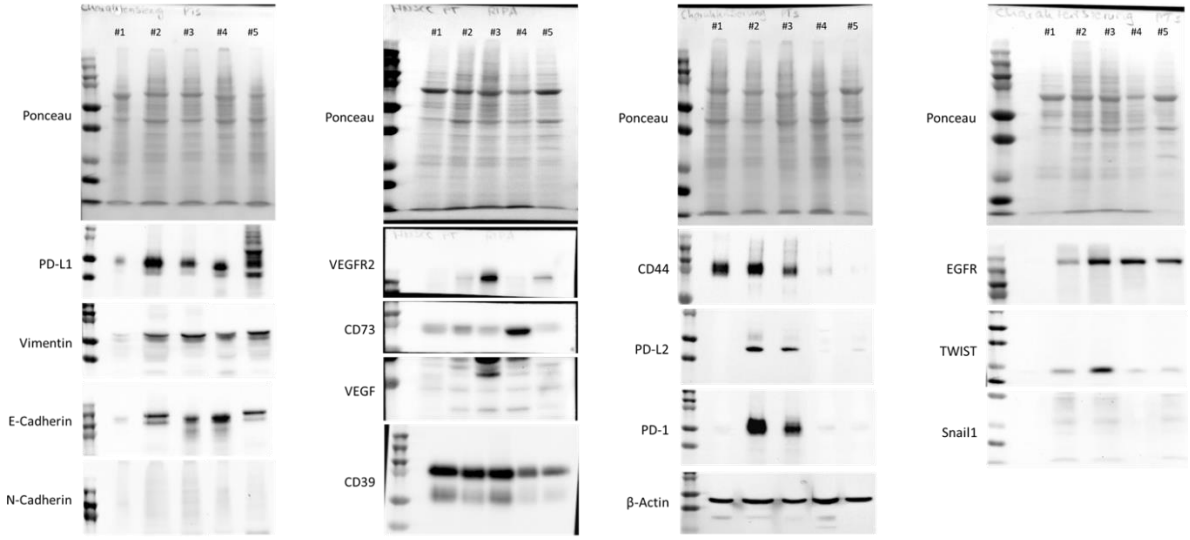

B) PD-L1 expression in membrane and cytoplasmic protein fractions

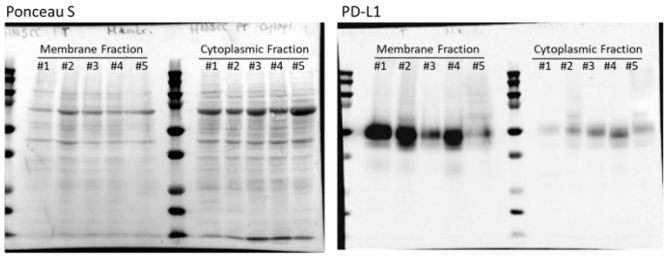

C) IHC staining for correlation of neutrophils with PD-L1-positive tumor cells

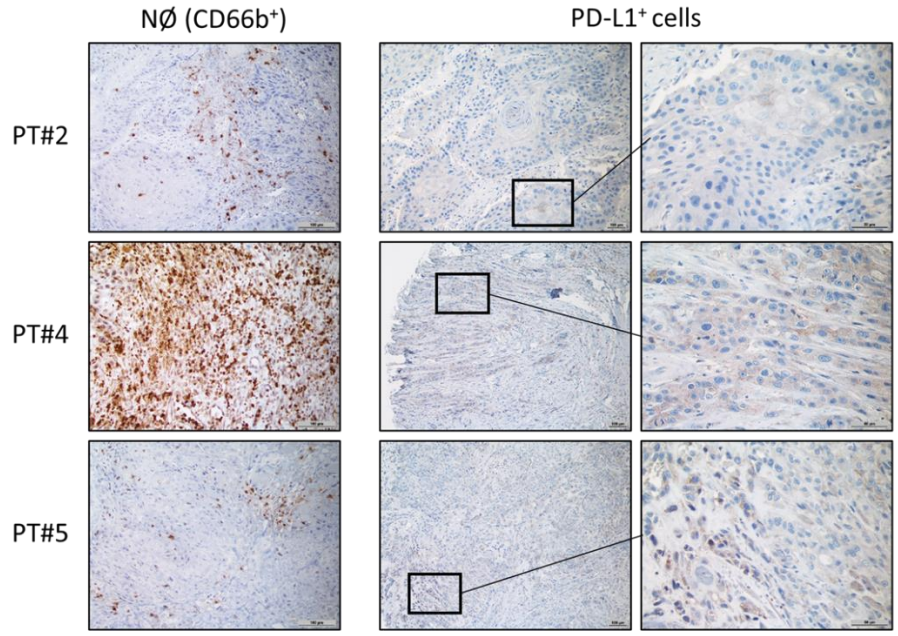

Supplementary Figure 2: Original blots and additional IHC stainings for characterization of pro-tumor markers in HNSCC primary tumors. (**A**) Original blots for characterization of pro-tumor markers in HNSCC primary tumors PT#1 – PT#5. Characterization was achieved by western blotting analysis. Marker expression was divided by HNSCC markers (CD44, EGFR), EMT markers (vimentin, E-cadherin, N-cadherin, TWIST, Snai1), purinergic enzymes (CD39, CD73), immune checkpoints (PD-L1, PD-L2, PD-1) and angiogenesis markers (VEGFR2, VEGF). Per sample, 25 µg of protein was loaded. Ponceau S staining verifies equal loading. N = 2. (**B**) Original blots for determination of PD-L1 expression in membrane and cytoplasmic protein fraction in HNSCC primary tumors PT#1 – PT#5. Western blotting analysis of PD-L1 expression was performed after subcellular fractionation into membrane and cytoplasmic proteins. Per sample, 25 µg of protein was loaded. Ponceau S staining verifies equal loading. N = 2. (**C**) Additional immunohistochemical (IHC) stainings of HNSCC primary tumor sections from PT#2, PT#4 and PT#5 for neutrophils (NØ, $CD66b^{+}$) and PD-L1-positive tumors cells. PD-L1 staining was magnified for optimized visualization of subcellular PD-L1 localization. Scale bar CD66b 100 µm (20x), PD-L1 100 µm (10x) and 50µm (40x). For quantification see **Supplementary Table 2**.

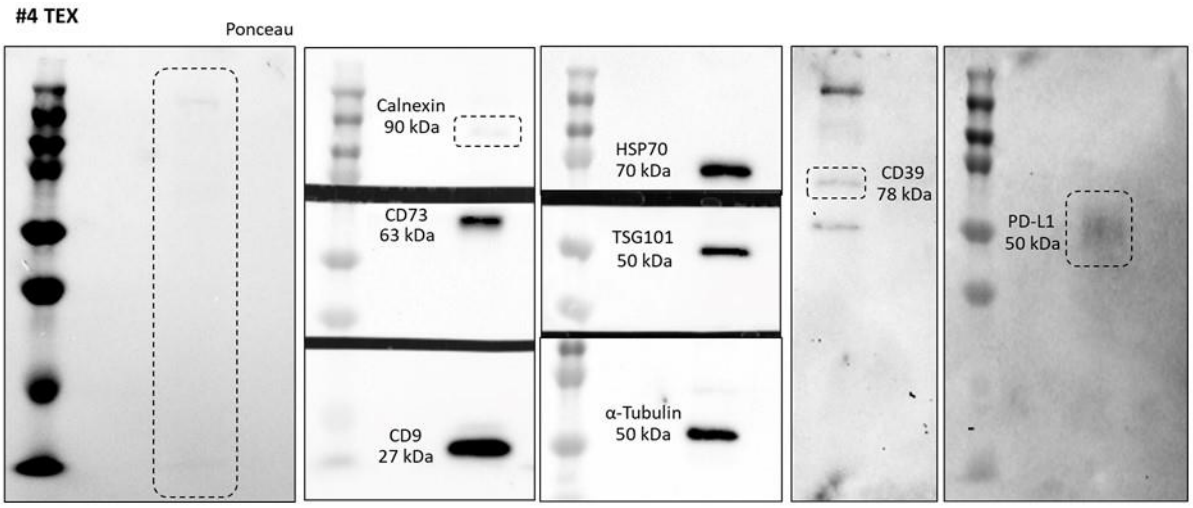

Supplementary Figure 3: Original blots for SCC47-TEX characterization. Characterization was achieved by western blotting analysis using the TEX markers Calnexin, HSP70, α-Tubulin, TSG101 and CD9, the purinergic enzymes CD39, and CD73 and immune checkpoint PD-L1. Per sample, 10 µg of protein lysate was used. Ponceau S staining was used as loading control. Faint bands are highlighted with a dot line. N = 2.

A) Original dot blots of Human Cytokine Array

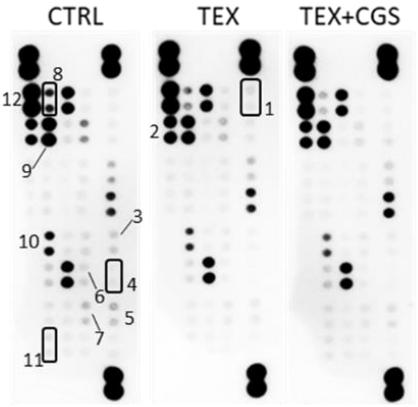

1. CCL1/I-309
2. Serpin E1/PAI-1
3. CD40L/TNFSF5
4. C5/C5a
5. CXCL1/GROα
6. IFN-γ
7. IL-1α/IL-1F1
8. IL-13
9. IL-18/IL-1F4
10. IL-32α
11. IL-16
12. MIF

*CGS15943 (P1 antagonist)

B) IHC staining for correlation of neutrophil presence with Treg infiltration

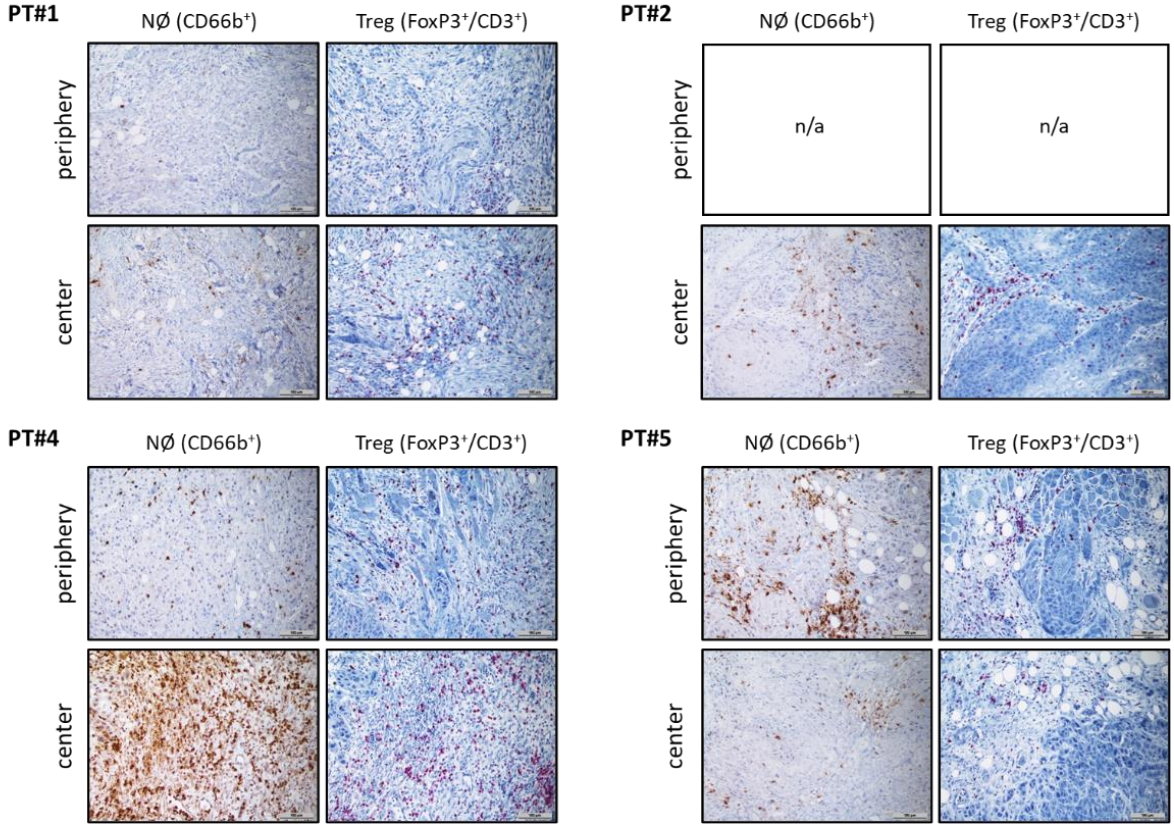

Supplementary Figure 4: **Original dot blots of Human Cytokine Array and additional IHC staining for correlation of neutrophil presence with Tregs infiltration** (**A**) Original dot blots of Human Cytokine Array. Analysis was performed with pooled supernatant from 5 per group: non-treated NØ as control (CTRL), NØ cultured with TEX (+TEX) and NØ pre-treated with P1R antagonist CGS15943 and subsequently cultured with TEX (+CGS+TEX) for 48 hours. Per array 40 µg of protein was used. Positive controls are located in upper left and right corners and lower right corner. Dots with a significant protein expression are highlighted. (**B**) Additional immunohistochemical (IHC) stainings of HNSCC primary tumor sections from PT#1, PT#2, PT#4 and PT#5 at tumor periphery and tumor center for correlation of

neutrophils with Tregs infiltration. For PT#2 only healthy tissue was detectable in the periphery section. Therefore, it was excluded from analysis (n/a = not available). Single staining for neutrophils (NØ, $CD66b^+$, brown), double staining for $FoxP3^+$ (brown) and $CD3^+$ (pink) cells. Scale bar $CD66b^+$ and $FoxP3^+/CD3^+$ staining 100 µm (20x). For quantification see **Supplementary Table 2**.

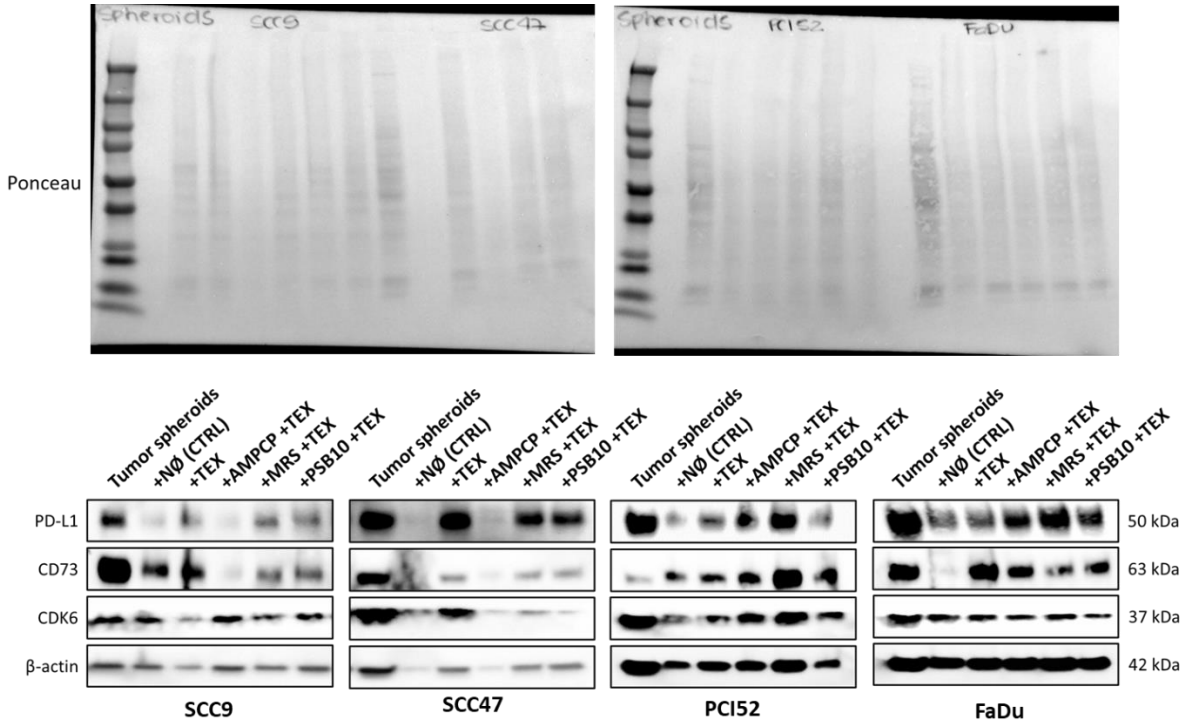

Supplementary Figure 5: Additional blots and for immunodetection of PD-L1, CD73 and CDK6 after co-cultivation of HNC cell lines FaDu, PCI52, SCC9 and SCC47 with TEX-modulated Neutrophils. HNC cell lines were treated with Neutrophils (+NØ), NØ with TEX (+TEX), NØ pre-treated with CD73 inhibitor followed by TEX incubation (+AMPCP+TEX), NØ pre-treated with A2bR antagonist followed by TEX incubation (+MRS+TEX), NØ pre-treated with A3R antagonist followed by TEX incubation (+PSB10+TEX) compared to control (HNC cell line = CTRL). Per sample, 10 µg of protein was loaded. Ponceau S staining was used as loading control. N = 3.

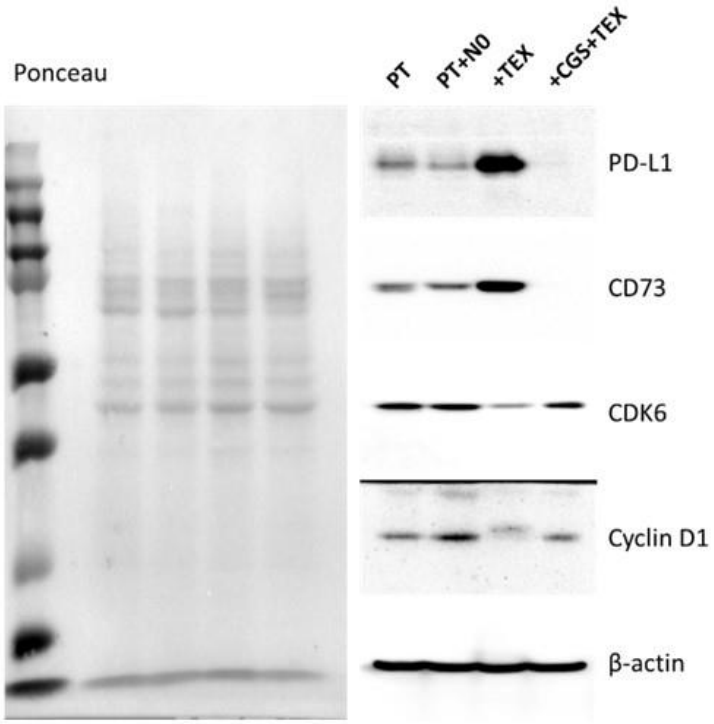

Supplementary Figure 6: Original blots for immunodetection of PD-L1, CD73, CDK6 and cyclin D1 after 7-day CAM protocol. Groups divided as treatment of HNSCC primary tumor with: healthy neutrophil supernatant (PT+NØ), NØ with TEX (+TEX), NØ pre-treated with P1R antagonist followed by TEX incubation (+CGS+TEX) compared to control (HNSCC primary tumor = PT). Per sample, 25 µg of protein was loaded. Ponceau S staining was used as loading control. N = 3.

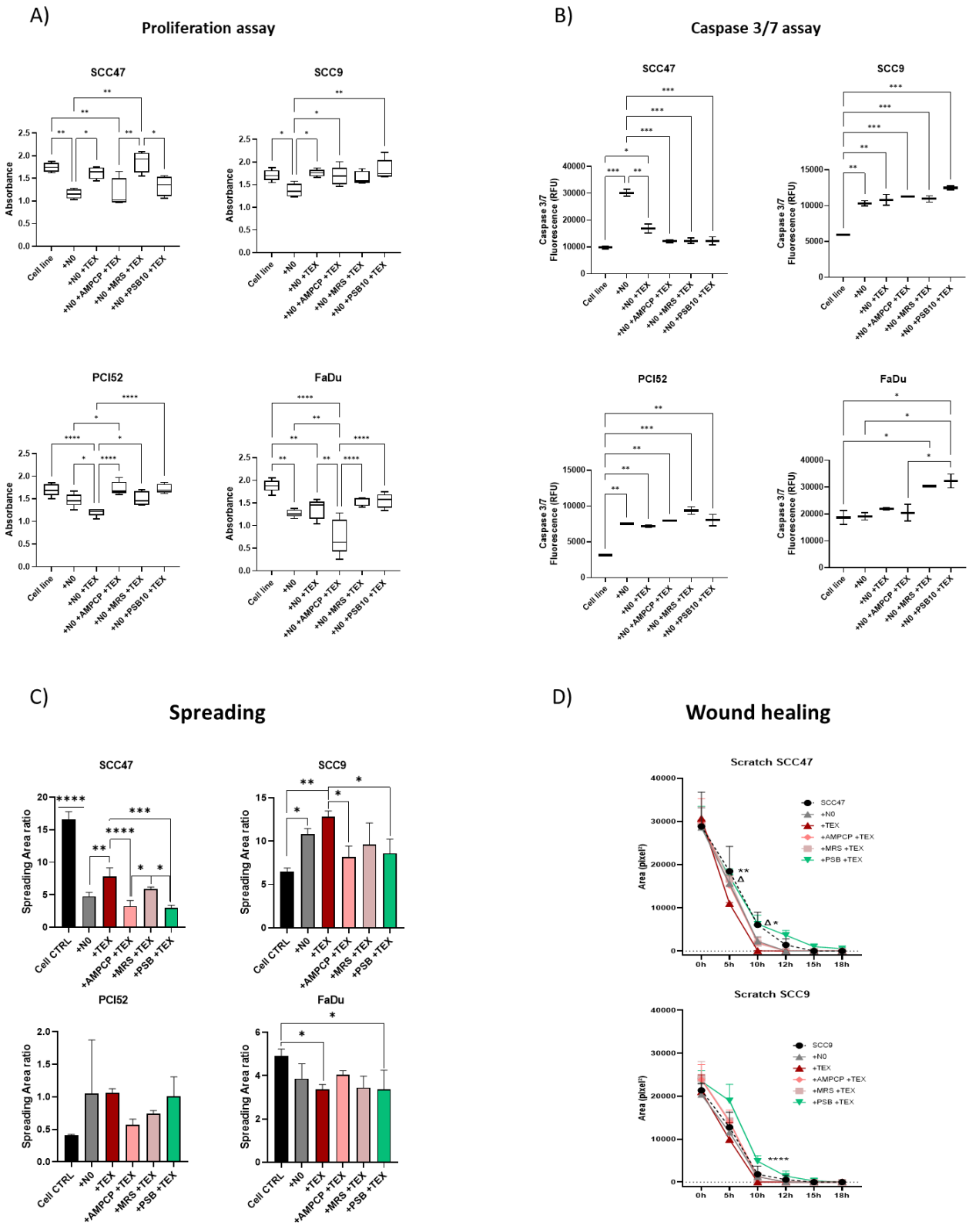
A)
Proliferation assay
SCC47
SCC9
PCI52
FaDu
Absorbance
Cell line
+N0
+N0 +TEX
+N0 +AMPCP +TEX
+N0 +MRS +TEX
+N0 +PSB10 +TEX
B)
Caspase 3/7 assay
Caspase 3/7 Fluorescence (RFU)
C)
Spreading
Spreading Area ratio
Cell CTRL
+N0
+TEX
+AMPCP +TEX
+MRS +TEX
+PSB +TEX
D)
Wound healing
Scratch SCC47
Scratch SCC9
Area (pixel²)
SCC47
+N0
+TEX
+AMPCP +TEX
+MRS +TEX
+PSB +TEX
SCC9
0h
5h
10h
12h
15h
18h

Supplementary Figure 7: Additional graphs for the endorsement of pro-tumor potential of TEX-modulated Neutrophils with the HNC cell lines FaDu, PCI52, SCC9 and SCC47. Cell proliferation and cell death were quantified via MTS and caspase 3/7 assay, cell motility was quantified via spreading and wound healing assay. HNC cell lines were treated with the following groups: the respective cell line (Cell line = control) with Neutrophils (+NØ), NØ with TEX (+TEX), NØ pre-treated with CD73 inhibitor followed by TEX incubation (+AMPCP+TEX), NØ pre-treated with A2bR antagonist MRS1754 followed by TEX incubation (+MRS+TEX) and NØ pre-treated with A3R antagonist followed by TEX incubation (+PSB10+TEX) indicated by distinct symbols and colors. (**A**) Quantitative analysis of cell proliferation assay by MTS absorbance (OD). N = 3. (**B**) Quantitative analysis of cell death assay by Caspase 3/7 fluorescence as relative fluorescence units (RFU). (**C**) Spreading area ratio. (**D**) Kinetics of wound healing assay by pixel per area, performed with SCC47 and SCC9, analyzed with ImageJ. N = 3. Graphs express mean ± SD and significance values were calculated using multiple 1-way ANOVA. *$p < 0.05$, **$p < 0.01$, ***$p < 0.001$, **** $p < 0.0001$.

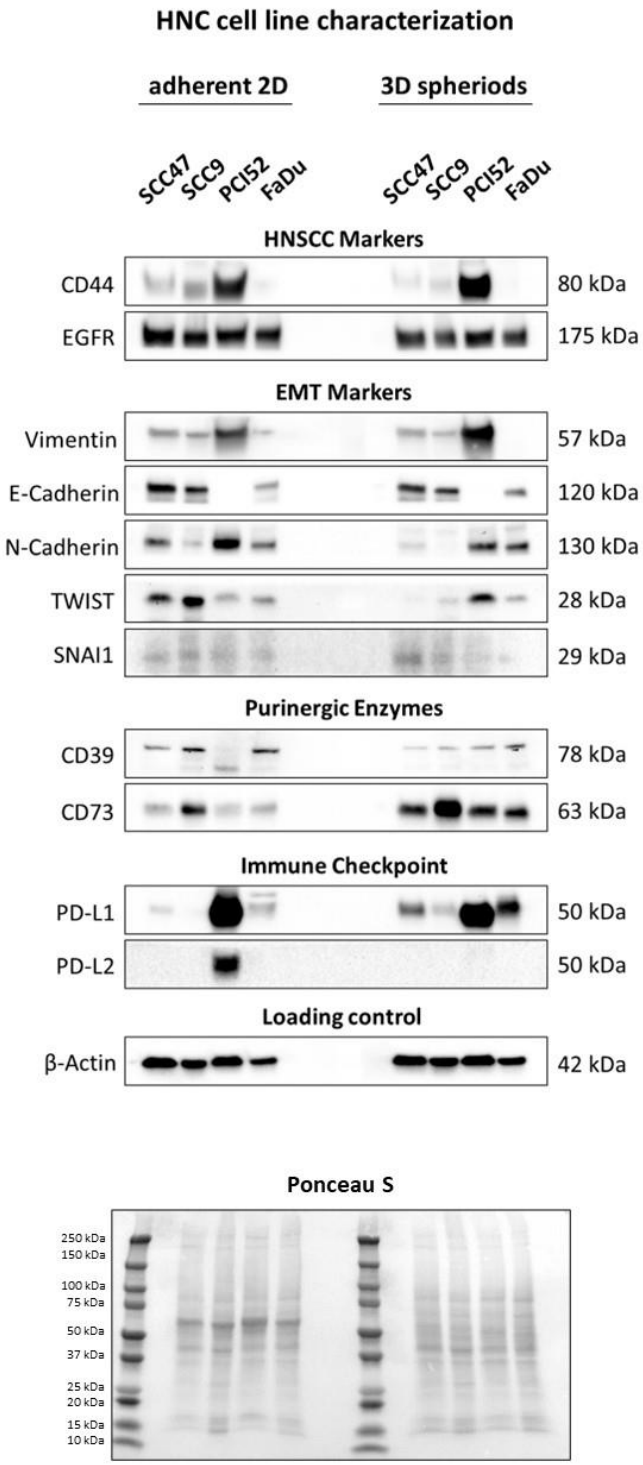

Supplementary Figure 8: HNC cell line characterization. The HNC cell lines SCC47, SCC9, PCI52 and FaDu were characterized in detail to obtain information about their cellular characteristics and differentiation status. Protein expression of adherent cultured cells (2D) and tumor cell spheroids (3D) was analyzed by western blotting. Marker expression was categorized by HNSCC markers (CD44, EGFR), EMT markers (Vimentin, E-cadherin, N-cadherin, TWIST, Snai1), purinergic enzymes (CD39, CD73) and immune checkpoints (PD-L1, PD-L2). 25 µg protein was loaded per sample. The housekeeping protein β-actin was used as a loading control. Ponceau S staining also verified equal loading. N = 2.

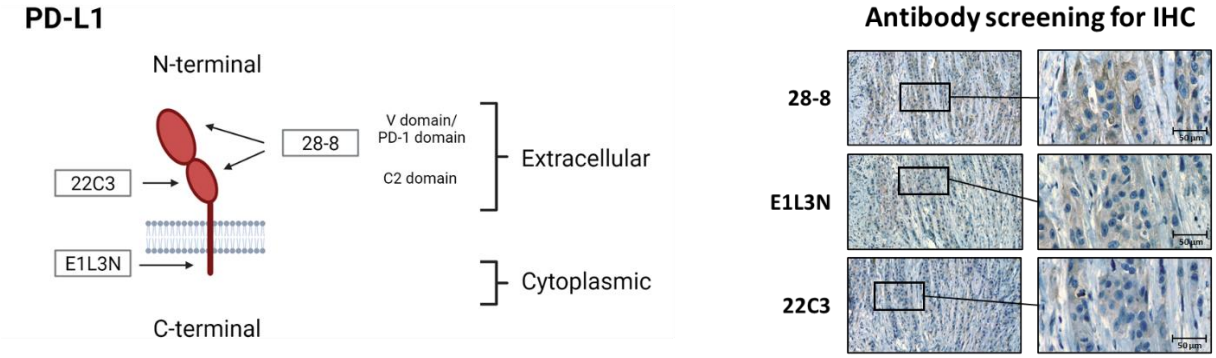

Supplementary Figure 9: PD-L1 antibody screening for IHC optimization. In this study, we evaluated the performance of three distinct human anti-PD-L1 clones on, each targeting different binding sites of the PD-L1 protein: 22C3, E1L3N and 28-8. Clone 28-8 targets the extracellular V/PD-L1 domain and C2 domain of PD-L1. Clone 22C3 targets the extracellular C2 domain of PD-L1. Clone E1L3N targets the cytoplasmic domain of PD-L1. Through serial sections of HNSCC tissues, we observed notable discrepancies in PD-L1 detection among the clones. Notably, clone 22C3 exhibited the lowest detection capacity. Conversely, clones E1L3N and 28-8 demonstrated proficiency in detecting both membrane-bound and intracellular PD-L1. Given its high specificity and performance in detecting both membrane-bound and intracellular PD-L1, clone 28-8 emerged as the optimal choice for PD-L1 IHC in this context. Pictures of PD-L1 staining were magnified for optimized visualization of subcellular PD-L1 localization. Scale bar 50 µm.

Chapter 7: Tumor-neutrophil crosstalk promotes in vitro and in vivo glioblastoma progression

Frontiers in Immunology

(https://www.frontiersin.org/journals/immunology)

Impact Factor: 7.3

DOI: 10.3389/fimmu.2023.1183465

PMID: 37292196

PMCID: PMC10244780

Accepted 04 May 2023

frontiers | Frontiers in Immunology

TYPE Original Research
PUBLISHED 24 May 2023
DOI 10.3389/fimmu.2023.1183465

OPEN ACCESS

EDITED BY
Yuanbo Pan,
Zhejiang University, China

REVIEWED BY
Anm Nazmul Hasan Khan,
University at Buffalo, United States
Xue-Yan He,
Cold Spring Harbor Laboratory,
United States

*CORRESPONDENCE
Elizandra Braganhol
ebraganhol@ufcspa.edu.br

SPECIALTY SECTION
RECEIVED 10 March 2023
ACCEPTED 04 May 2023
PUBLISHED 24 May 2023

CITATION
Rubenich DS, de Souza PO, Omizzollo N, Aubin MR, Basso PJ, Silva LM, da Silva EM, Teixeira FC, Gentil GFS, Domagalski JL, Cunha MT, Gadelha KA, Diel LF, Gelsleichter NE, Rubenich AS, Lenz GS, de Abreu AM, Kroeff GM, Paz AH, Visioli F, Lamers ML, Wink MR, Worm PV, Araújo AB, Sévigny J, Câmara NOS, Ludwig N and Braganhol E (2023) Tumor-neutrophil crosstalk promotes *in vitro* and *in vivo* glioblastoma progression. *Front. Immunol.* 14:1183465. doi: 10.3389/fimmu.2023.1183465

Tumor-neutrophil crosstalk promotes *in vitro* and *in vivo* glioblastoma progression

Dominique S. Rubenich[1], Priscila O. de Souza[1], Natalia Omizzollo[1], Mariana R. Aubin[2], Paulo J. Basso[3], Luisa M. Silva[3], Eloisa M. da Silva[3], Fernanda C. Teixeira[1], Gabriela F.S. Gentil[1], Jordana L. Domagalski[1], Maico T. Cunha[1], Kerolainy A. Gadelha[1], Leonardo F. Diel[4], Nicolly E. Gelsleichter[1], Aline S. Rubenich[1], Gabriela S. Lenz[1], Aline M. de Abreu[1], Giselle M. Kroeff[1], Ana H. Paz[2], Fernanda Visioli[2], Marcelo L. Lamers[5], Marcia R. Wink[1], Paulo V. Worm[6], Anelise B. Araújo[2], Jean Sévigny[7,8], Niels O. S. Câmara[3], Nils Ludwig[9] and Elizandra Braganhol[1]*

[1]Programa de Pós-Graduação em Biociências, Universidade Federal de Ciências da Saúde de Porto Alegre (UFCSPA), Porto Alegre, RS, Brazil, [2]Laboratório de Células, Tecidos e Genes, Hospital de Clínicas de Porto Alegre (HCPA), Porto Alegre, RS, Brazil, [3]Departamento de Imunologia, Universidade de São Paulo (USP), São Paulo, Brazil, [4]Faculdade de Odontologia, Universidade Federal do Rio Grande do Sul (UFRGS), Porto Alegre, RS, Brazil, [5]Departamento de Ciências Morfológicas (ICBS), Universidade Federal do Rio Grande do Sul (UFRGS), Porto Alegre, RS, Brazil, [6]Serviço de Neurocirurgia, Hospital São José, Irmandade Santa Casa de Misericórdia de Porto Alegre (ISCMPA), Departamento de Cirurgia-Universidade Federal de Ciências da Saúde de Porto Alegre (UFCSPA), Porto Alegre, RS, Brazil, [7]Centre de Recherche du Centre Hospitalier Universitaire (CHU) de Québec, Université Laval, Québec City, QC, Canada, [8]Département de Microbiologie-Infectiologie et d'Immunologie, Faculté de Médecine, Université Laval, Québec City, QC, Canada, [9]Department of Oral and Maxillofacial Surgery, University Hospital Regensburg, Regensburg, Germany

Introduction: The tumor microenvironment (TME) of glioblastoma (GB) is characterized by an increased infiltration of immunosuppressive cells that attenuate the antitumor immune response. The participation of neutrophils in tumor progression is still controversial and a dual role in the TME has been proposed. In this study, we show that neutrophils are reprogrammed by the tumor to ultimately promote GB progression.

Methods: Using *in vitro* and *in vivo* assays, we demonstrate the existence of bidirectional GB and neutrophil communication, directly promoting an immunosuppressive TME.

Results and discussion: Neutrophils have shown to play an important role in tumor malignancy especially in advanced 3D tumor model and Balb/c nude mice experiments, implying a time- and neutrophil concentration-dependent modulation. Studying the tumor energetic metabolism indicated a mitochondria mismatch shaping the TME secretome. The given data suggests a cytokine milieu in patients with GB that favors the recruitment of neutrophils, sustaining an anti-inflammatory profile which is associated with poor prognosis. Besides, glioma-neutrophil crosstalk has sustained a tumor prolonged activation via NETs formation, indicating the role of NFκB signaling in tumor progression. Moreover,

clinical samples have indicated that neutrophil-lymphocyte ratio (NLR), IL-1β, and IL-10 are associated with poor outcomes in patients with GB.

Conclusion: These results are relevant for understanding how tumor progression occurs and how immune cells can help in this process.

KEYWORDS

tumor associated neutrophils, glioblastoma, tumor microenvironment, cancer, neutrophil extracellular traps

Highlights

1) Glioma progression and malignancy is positively modulated by neutrophils.
2) Neutrophils induce glioma mitochondrial recovery.
3) Glioma-neutrophil crosstalk supports an immunosuppressive microenvironment.
4) Gliomas modulate neutrophil activation and increase lifespan.
5) Neutrophils affect cytokine profile production, correlating with poor prognosis.

Introduction

Glioblastoma (GB) represents over 80% of the total cases of malignant gliomas and is confined to the central nervous system, rarely metastasizing to distant sites (1, 2). However, its histology shows that it is highly invasive and infiltrative with an acceleration of cellular and mitotic activity, angiogenesis, and necrosis (1). The tumor microenvironment (TME) of GB is characterized by an increased infiltration abundant in immunosuppressive cell populations attenuating the antitumor immune response (3). Interestingly, the infiltration rates of these immune cells are closely related to clinical outcomes (4). The permanence of immune cells, especially in the TME, supports an abnormal microenvironment of chronic inflammation – considered a hallmark of cancer (5, 6). In spite of leucocyte invasion, GB is considered a "cold tumor" due to its tall sums of regulatory B and T cells, as well as immunosuppressive myeloid cells (7).

Regarding the complexity of immune cell subpopulations, it was suggested in recent studies that neutrophils might play a significant role in stimulating disease progression in GB. Patients with increased levels of circulating neutrophils have increased neutrophils infiltration in the tumor tissue, which was linked to poor prognosis (8, 9). Neutrophils are myeloid components of the innate immune system, representing 50 to 70% of circulating leukocytes (10). They effectively participate in immune responses, using various mechanisms, such as phagocytosis, degranulation, and/or formation of neutrophil extracellular trap (NET) (11). Overall, neutrophils can be characterized by their phenotypic and functional plasticity as pro-tumor or anti-tumor cells (12). The controversy of the contribution of neutrophils to tumor progression has been used to explain their dual role in the TME (13).

The contribution of nonmalignant cells to tumor development and progression is now indisputable (14). The diffuse nature of the tumor, which infiltrates adjacent tissues and varies in character and location within the brain, result in the inability to resect the tumor completely. Despite the many studies, it is difficult to establish efficient immunotherapies against GB due to tumor evasion mechanisms (15). Therefore, effective therapies have yet to be discovered, which makes this tumor an important target for studies with different approaches. Neutrophils might be a potential target for better patient outcome (16). Thus, this study proposes that neutrophils promote GB progression after being reprogrammed by the tumor. We report the existence of GB-neutrophil bidirectional communication with direct impact on promoting an immunosuppressive TME.

Materials and methods

Material

The chemicals employed in this study are listed in Supplementary Table 1. All other chemicals and solvents were obtained from standard commercial suppliers with analytical grade standard and were used as received.

Human cell culture

Human U87MG glioma cell line obtained from ATCC (American Type Cell Collection; Rockville, Maryland, USA) was grown in Dulbecco's modified Eagle's medium (DMEM – Sigma-Aldrich, USA) prepared with 8.4 mM HEPES, 23.8 mM sodium bicarbonate ($NaHCO_3$), 0.1% fungizone, 100 U/L penicillin/streptomycin 0.5 U/L and 10% of heat-inactivated Fetal Bovine Serum (FBS – Gibco, USA), at final pH of 7.4. Cells were incubated at 37°C with 95% minimum relative humidity and 5% CO_2.

Primary neutrophil cultures

Peripheral blood was collected from healthy volunteers into EDTA blood collection tubes. Within less than 15 min after the donation, the blood was processed following the described protocol elsewhere (17). Briefly, the blood was entirely diluted with an equal volume of 2% Dextran (Sigma-Aldrich, USA) in saline solution and incubated for 20 min at room temperature (RT). Afterwards, leucocytes were collected and gently loaded on top of Histopaque-1077® (Sigma-Aldrich, USA) with 1:2 volume proportion. Continuous centrifugation, at 428 × g, for 30 min, at RT, was used for separation of low-density leucocytes from high-density ones. The high-density fraction with polymorphonuclear cells (PMN) was further subjected to red blood cell lysis with Milli-Q water for 25 seconds and neutralization with HBSS 10x concentration. To remove the lysis product, the sample was centrifuged for 10 min, at 400 × g, and at RT. Isolated neutrophils (Nθ) were cultured in DMEM supplemented with 10% FBS. The institutional ethics review board of Hospital de Clínicas de Porto Alegre (n° 2.969.418) approved this study.

2D Glioblastoma-neutrophil co-culture

U87MG cells were seeded in 48-well plates (15×10^3 cells/well) and cultured for 1.5 h before neutrophils were added in the ratios 1:30, or 1:60, (GB to Nθ, respectively). Co-cultures were incubated for 24, 72, and 120 h. Monocultures of GB and Nθ cells were applied as controls. The following assays were performed:

MTT assay

Soluble MTT [3-(4,5-dimethylthiazol-2-yl)-2,5-diphenyltetrazolium bromide] reduction assay to formazan crystals was performed as previously described (18). The absorbance was determined at 560 and 630 nm on a microplate reader (SpectraMax® M3-Molecular Devices). Data were expressed as absorbance and estimated by the difference between 560 and 630 nm, and the MTT absorbance of U87MG cells were considered as the control (CRTL) group by 100%.

SRB assay

The sulforhodamine B (SRB) assay was used for cell density determination and it is based on the measurement of cellular protein content. U87MG monolayers were fixed with 10% trichloroacetic acid for 1 h, stained with SRB solution for 15 min, and the excess dye was completely removed by washing repeatedly with 1% acetic acid. The protein-bound dye was dissolved in 10 mM Tris base solution for optical density (OD) determination at 515 nm using a microplate reader (19). Data were expressed as percentage of CTRL.

Trypan blue assay

Viable and dead neutrophils were counted in a Neubauer chamber after trypan-blue staining (2%) as previously described (20).

Flow cytometry

To test cell viability, cells were stained with Live/Dead fluorescent dye – AmCyam 1:400 (Thermo Fisher, EUA). Cells were clustered by FSC x SSC, followed by doublets removal and selection of live cells only (Supplementary Figure 1). For mitochondria assay, cells were washed in PBS and stained with 200 nM MitoTracker Green (Invitrogen, Carlsbad, CA), 50 nM MitoTracker Deep Red (Invitrogen), and MitoSOX (5 μM). For glucose-uptake assay, after washing with PBS, cells were resuspended in 100 μL of RPMI1640 without bicarbonate, containing 5 mM glucose and 5 mM glucose fluorescent analogue, 2-(N-(7-Nitrobenz-2-oxa-1,3-diazol-4- yl)amino)-2-Deoxyglucose (2-NBDG), for 20 min at 37°C. After the incubation period, cells were washed and resuspended in PBS containing 2% FBS and immediately acquired in a flow cytometer. Samples were analyzed using a FACSCanto flow cytometer driven by BD FACS Diva software (BD Biosciences, San Diego, USA) and were processed using Flow-Jo software (FlowJo LLC, Ashland OR).

Glucose and lactate determination

Quantification of glucose and lactate in supernatants was performed using enzymatic systems (ref n° 133 and ref n° 138, Labtest), according to manufacturer's recommendations. Absorbance was determined at 505 nm (glucose) and 550 nm (lactate) wavelengths in a spectrophotometer (Synergy™ Mx Microplate Reader; BioTek) coupled to Gen5™ software (BioTek). Results were expressed as mg/dL of culture supernatant normalized per mg of protein.

Cytokine cytometric bead array

The Human-Inflammatory Cytokine Based Assay (CBA) kit for IL-8, IL-1β, IL-6, IL-10, TNFα, and IL-12p70 (BD Biosciences, San Diego, CA, USA) was performed according to manufacturer's recommendations.

GB-neutrophil 3D co-culture

Three-dimensional spheroids were generated using the hanging drop technique (21). After the enzymatic dissociation of the U87MG culture, the cell suspension was diluted to a final concentration of 25×10^3 cells per 30 μL. Each drop containing 30 μL was placed inside the cap of a 48-well plate previously treated with agarose 1.5% and filled with 300 μL of PBS 1× in order to prevent dryness of the drop (22). Rolling and falling off from drops were considered as failed procedure. Plates were kept immobile in incubators at 37°C and 5% CO_2, during 4 days for the establishment of cell aggregates. After that, each well was filled to their maximum volume with DMEM supplemented with 10% FBS for the purpose of causing the sphere to fall gently into the well. Only one spheroid per well was cultured for more than 2 days. The co-culture procedure started with 7.5×10^3/500 μL neutrophils for each spheroid to mimic initial tumor communication and the 3D media was totally removed and replaced with the one containing

recently isolated PMNs. GB and Nθ cultured alone were considered the control of experiment. The following assays were performed:

Advanced tumor model

The neutrophil infiltrate assay aimed to mimic neutrophil communication with advanced tumors. During the assay, a "pool" of neutrophils was applied to the environment of an U87MG sphere. Thus, after removing the cell aggregate from the culture medium, 7.5×10^5/500 µL of neutrophils were added to each tumor spheroid. The spheroids were incubated for 24 h and 72 h, at 37°C, and at 5% CO_2.

Histopathologic evaluation of 3D cultures

The spheroids were fixed with 4% paraformaldehyde for 18 h and left immersed in PBS until histological processing. The protocol adapted from the agarose block was used as a 2% agarose template containing microwells for each bead (23). The mold was inserted into the histological cassette for processing in the OMA pv.85 histotechnical equipment (Instrumental OMA Ltda, São Paulo, Brazil). The material was dehydrated with a series of alcoholic solutions with increasing concentrations (50%, 70%, 90% methanol bath and four baths in 100% methanol, 1 h each), followed by the clarification process of 3 baths of xylene (1 h each) and impregnation with liquid paraffin (2 baths of 2 h each). Sections of 4 µm slides were performed on a Leica RM2255 microtome (Leica Microsystems, Inc., Wetzlar, Germany). The material obtained was collected with positively charged microscopy glass slides.

For hematoxylin and eosin (HE), staining slides were dewaxed with 3 baths of xylene (5 min each) and rehydrated in descending scale ethanol baths (1 min each). Staining was performed with hematoxylin monohydrate (Merck KGaA, Darmstadt, Germany) and yellowish eosin (Synth, Diadema, Brazil).

For immunohistochemistry, slides were submitted to the antigen recovery process, using a solution composed of 10 mM sodium citrate (pH 6.0) for Ki67. The samples were incubated with the respective recovery solutions at 98°C, for 30 min. The blockage of endogenous peroxidase activity was performed with 5% hydrogen peroxide solution (Merck KGaA), and nonspecific binding was blocked with 1% BSA (Sigma-Aldrich, St. Louis, Missouri, USA). Anti-Ki67 (1:100, Dako, Santa Clara, USA) antibody was incubated for 12 h, at 4°C. The detection kit (Dako, Santa Clara, USA) was used according to the manufacturer's recommendations. The percentage of positively labeled cells for each sample was counted from the average of the total positives and negatives of five images per sample using ImageJ Software. The slides were analyzed in a blinded manner by a pathologist.

Time-lapse microscopy

The spheroids were submerged into an environment containing 10^6 neutrophil, and time-lapse images were captured for a period of 20 h, at 10-min intervals, with camera (Axiocam mrn, Zeiss, Göttingen, Germany) attached to an inverted microscope (Axio Observer Z1, Zeiss, Göttingen, Germany). The sphere area from each time point was plotted and analyzed using ImageJ software. The growth of spheres was determined by comparing the initial and the final size of each spheroid and expressed as area (pixel^2).

Annexin V/propidium iodide assay

Apoptosis/necrosis was evaluated using annexin V/propidium iodide (PI) staining followed by flow cytometry. Glioma spheroids produced and treated with neutrophils for 72 h and 120 h were collected from the four groups and dissociated. Cells were centrifuged at 300 × *g* for 5 min and washed twice with cold PBS. Afterwards, the cells were resuspended in binding buffer and incubated with PI and Annexin V-FITC (BD Biosciences Pharmingen, San Diego, CA) for 15 min, at RT. A total of 10,000 events were collected and analyzed by flow cytometry (FACSCanto, BD). As tumor and Nθ cells exhibit highly distinct size and complexity patterns, the neutrophil and tumor cell population gate were based on scatter plot. Initial apoptotic cells were taken as Annexin V-positive/PI-negative, while late apoptotic cells were taken as Annexin V-positive/PI-positive and necrotic cells were taken as Annexin V-negative/PI-positive cells. Live cells were taken as Annexin V-negative/PI-negative.

In vivo tumorigenicity experiment

The animal ethics committee of Hospital de Clínicas de Porto Alegre approved our studies with animals (n° 2020-0708). Male and female BALB/c-nude mice (n=40; specific-pathogen free; 8-12 weeks old; 22-26 g) were housed at 20-24°C with a relative humidity of 40-60%, consuming an average of 3-5 g of food and 5-10 mL of water per day, with a light/dark cycle of 12 h/12 h. The mice were divided into four groups with ten nude mice in each group (5 male, 5 female). The tumorigenicity experiments were performed within a laminar flow cabinet. The following analysis consisted of a subcutaneous heterotopic model with the implantation of 10^6 U87MG with increasing concentrations of neutrophils (3%, 10%, and 20%) injected into the right flank of mice. Cell suspension (100 µL) and Matrigel (Sigma-Aldrich, E1270) (100 µL; 5-6 mg/mL) were applied to the animals subcutaneously (final volume applied 200 µL). The control group received only tumor cells. The two distances (diameters) at right angles were measured every two days, i.e., the width (w) – which is the greatest transverse diameter, and the length (l) – the greatest longitudinal diameter) until tumors reached the endpoint of 2000 mm^3. At the end of the experiments, tumors were fixed with 4% paraformaldehyde and processed for HE histological staining and immunohistochemical for Ki67 as described above. The slices were analyzed by a pathologist in a blinded manner.

$$Volume\ \ (mm^3) = \left(\frac{w^2 * l}{2}\right) \times 1000$$

In vivo neutrophil maturation status

Neutrophils extracted from the bone marrow of C57/BL6 mice according to the protocol described by Liu and colleagues (24).

Therefore, murine Nθ were challenged with GL261 cells (mouse glioma cell line obtained from ATCC) following the same conditions as U87MG + Nθ described earlier for 24h. $CD11b^{+}$ cells (1:400) were further divided into the following groups: mature: $Ly6G^{high}$ (1:400), $CXCR4^{-}$ (1:100), $CXCR2^{+}$ (1:100); immature: $Ly6G^{low/mid}$, $CXCR4^{+}$, $CXCR2^{low}$; aged: $Ly6G^{high}$, $CXCR4^{+}$, $CXCR2^{-}$ (25). Animal studies were approved by the ethics committee of UFCSPA and USP (n° 278/20 and n° 6769171122, respectively).

Sytox green: NETs assay

Aliquots of 10^{6} neutrophils/mL in HBSS/Ca^{+2} (1 mL) was prepared in microtubes following the planned groups. The sytox green reagent (Invitrogen) was added to each tube at a final concentration of 0.2 μM. Cells exposed to HBSS 1× or Triton 100× were applied as negative and positive controls, respectively. U87MG conditioned media was produced according to the following parameters: after reaching 85% confluency in T75-flask, 10 mL of DMEM with 0.5% or 10% FBS were kept for 72 h, at 37°C, 5% CO_2. PMA (100 nM) and LPS (1 μg/mL) groups were performed as control. PMNs were incubated for 3 h and 200 μL of each condition was transferred to a separate well of a 96-well black plate. Fluorescence was quantified at excitation/emission wavelengths of 488/520 nm with a microplate reader (26). The results were expressed as relative fold change by dividing the average of the experimental condition by the average of the untreated condition (negative control).

In silico TCGA analysis

Data from GBM dataset (n = 172) was downloaded from the Cancer Genome Atlas (TCGA; https://gdc.nci.nih.gov). Gene expression profiles were analyzed for glioma poor prognosis markers (IDH and MGMT), cell signaling pathways (TGFβ1 and NFκB1), epithelial-mesenchymal transition (CDH1 and CDH2), mitochondria activation (FOXO3 and ATF5) and neutrophil markers (MPO and ELANE) using the XENA browser (UC Santa Cruz) (27). Pearson test correlation matrix was performed to analyze the strength of association. Correlation was indicated as follow: small is 0.1-0.3 (positive) and −0.1 to −0.3 (negative); medium is 0.3 to 0.5 (positive) and −0.3 to −0.5 (negative); and large is 0.5 to 1.0 (positive) and −0.5 to −1.0 (negative) for the same gene set.

Glioma patients

Medical records of 43 patients who underwent surgery for glioma resection at Irmandade Santa Casa de Misericórdia de Porto Alegre (ISCMPA) from 2019 to 2022 were prospectively reviewed. Blood was collected at time of surgery. Patients were divided into two groups based on histopathological classification (glioblastoma vs. non-glioblastoma). The following variables for each patient were studied: sex, age, and the number of leucocytes, neutrophils, lymphocytes, and monocytes in the circulation. The neutrophil to lymphocyte ratio (NLR) was estimated. The institutional ethics review board of ISCMPA (n° 3.204.937) approved this study. Voluntary donors signed the informed consent form.

Statistical analysis

Data are expressed as mean and standard deviation (SD) or as standard error of the mean (SEM) when appropriate of at least three independent experiments and were subjected to two-way analysis of variance (ANOVA) followed by Tukey–Kramer *post-hoc* test (for multiple comparisons) or One-way ANOVA, Bonferroni's test or Student's *t*-test, when appropriate. Differences between mean values were considered significant when $P < 0.05$.

Results

Glioma-neutrophil crosstalk induces tumor cell proliferation

To assess the bidirectional communication between cultured glioma cells (U87MG) and human neutrophils, we performed co-culture studies. Firstly, the viability of U87MG cultures was measured by flow cytometry in the presence and absence of neutrophils (Figure 1). U87MG viability was sustained regardless of neutrophil interaction (Figures 1A, B). However, U87MG protein synthesis (Figure 1C) and MTT absorbance (Figure 1D) suggests that, in the first 24 h and 72 h of culture, neutrophils negatively affect the viability of U87MG cells. After 120 h of neutrophil-glioma co-culture, tumor growth seemed to extrapolate the previous pattern. Moreover, protein synthesis was proportional to MTT absorbance, indicating a metabolic recovery. We also observed the cellular interactions of U87MG (red arrow) and neutrophils (black arrow) by light microscopy (Figure 1E), and neutrophil distribution changed over time, clustering around tumor cells. Furthermore, 3D culture was used to test neutrophil infiltration capability and tumor proliferation. Figure 1F shows the experimental groups of the 3D culture experiment, with U87MG spheres as CTRL, U87MG with neutrophils sphere formation representing initial tumor, and U87MG spheres immersed on neutrophil pool representing advanced tumor. Therefore, to investigate the effect of neutrophils on apoptosis of U87MG 3D culture, the cells were double-stained with Annexin V and PI, prior to detection using flow cytometry (Figures 1G, H). Quantitative analysis demonstrated a slight reduction in cell viability, followed by an increase in U87MG cells undergoing late apoptosis in the presence of neutrophils in advanced tumor 3D model (Figure 1I), in addition to augmentation of necrotic death (Figure 1J). Given data suggests interaction with neutrophils stimulates glioma proliferation over time in the 2D culture model, while late apoptosis was detected in the advanced tumor spheroids.

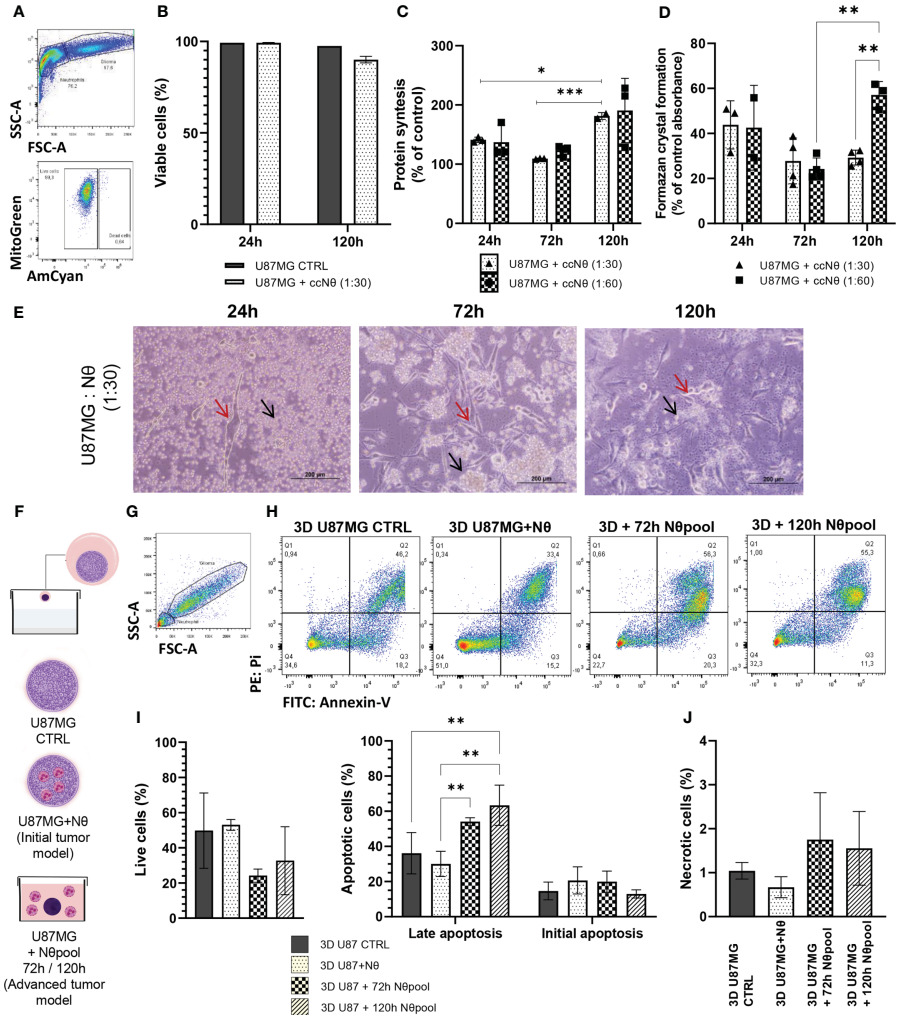

FIGURE 1
(A) Gating strategy to select living glioma cells (U87MG), by FSC x SSC, followed by selection of live cells only. **(B)** Quantification of U87MG live cells percentage. **(C)** SRB assay performed on a monolayer of U87MG with or without neutrophil coculture (ccNq) after 24 h, 72 h, and 120 h. The data is expressed by cell growth considering U87MG control result as 100% in each time. **(D)** MTT assay performed on a monolayer of U87MG with or without neutrophil co-culture after 24 h, 72 h, and 120 h. The data is expressed by MTT percentage considering U87MG control result as 100% in each time. **(E)** Representative images of glioma and neutrophil culture. Red arrow glioma and black arrow neutrophil. **(F)** Hang drop technique protocol. **(G)** Gating strategy to select glioma cells (U87MG) from 3D culture. **(H)** Gating strategy for initial apoptotic cells were taken as Annexin Vpositive/PI-negative, while late apoptotic cells were taken as Annexin V-positive/PI-positive and necrotic cells were taken as Annexin V-negative/ PIpositive cells. Live cells were taken as Annexin V-negative/PI-negative. Apoptosis measurement using Annexin V/PI double staining of 3D U87MG culture. Bar graphs representing the percentage of live cells and apoptotic cells **(I)** and necrotic **(J)** with or without neutrophil. Two-way ANOVA, multiple comparisons, Tukey test, in which a = 0.05 and *P < 0.05, **P < 0.005, ***P < 0.001. Error bars are mean ± SD.

3D culture model indicates that neutrophils alter glioma cell organization

Given the results regarding tumor cell proliferation, we hypothesized that neutrophils have further tumor-promoting effects. Therefore, we evaluated the growth of 3D spheres for 20 h using time-lapse technology. Glioma spheres with neutrophil pool expanded significantly faster ($P < 0.05$; Figures 2A, B) and showed a distinct growth pattern over time (Figure 2C). While glioma spheres seemed to grow linearly in the presence of neutrophils, the U87MG control showed a peak between 800 and 1000 min and stabilizes itself. Thus, we conducted a histopathological analysis, including HE staining of spheres (Figure 2D) and Ki67 staining to assess cell proliferation (Figure 2E). These experiments revealed a shift of glioma cell morphology. While CTRL cells were characterized by a fusiform cell shape, groups with neutrophils appeared as small and homogeneous cells (Supplementary Table 2). The quantification of Ki67 staining revealed a significant increase of cell proliferation in neutrophil-treated groups ($P < 0.01$; Figure 2G), especially in the border zones of the spheres (Figure 2E), along with slightly extension of the necrotic area (Figure 2F). The neutrophil infiltration in the spheroids was accessed by CD45 immunostaining and a small percentage of positive cells was detected (Figure S1). Taken together, these data are in line with the results obtained using 2D culture model and reinforce the role of neutrophils as promoters of GB cell proliferation.

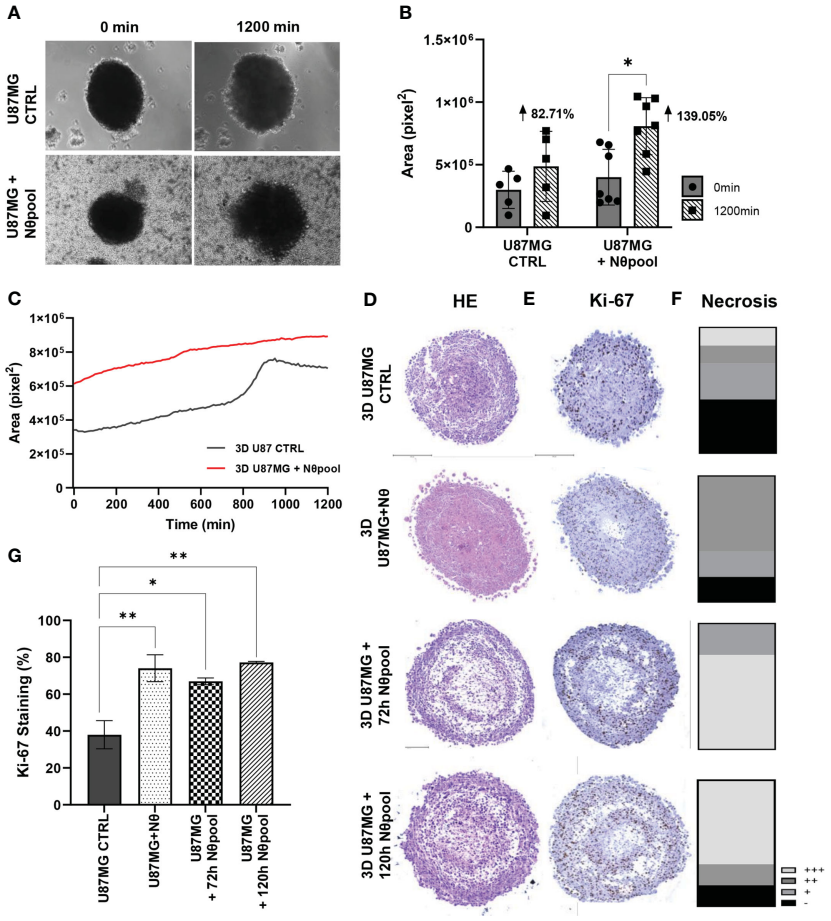

FIGURE 2
(A) Neutrophil interaction with 3D U87MG promotes sphere growth. 3D U87MG culture were placed with 10^6 neutrophils and performed time-lapse analysis during 20 h. **(B)** Initial (0 h) and final (20 h) areas were compared between groups **(C)**, and the mean tumor growth pattern was also observed. **(D)** Representative image from HE, **(E)** Ki-67 staining and **(F)** necrosis extent analysis. **(G)** Ki-67 quantification representing the percentage of positive cells. Two-way ANOVA, multiple comparisons. Tukey test, in which a = 0.05, *P < 0.05 and **P < 0.005. Error bars are mean ± SD.

Glioma-neutrophil crosstalk attenuates initial tumor growth, but stimulates growth pattern in advanced tumors

To confirm our results *in vivo*, we injected, subcutaneously, 10^6 U87MG cells along with increased proportions of neutrophils (3%, 10%, and 20%) into the right flank of athymic BALB/c nude mice (Figure 3A). Figure 3B shows the tumor volume of each group. Notably, CTRL tumors (only U87MG cells) have a slightly bigger initial growth than other groups (with neutrophils), however, the tumorigenesis pattern shifts after day 18, in which 10% of the neutrophil groups emerged above control ($P < 0.05$). Despite the use of both male and female BALB/c nude mice, the histopathology showed no differences between sex regarding intratumor hemorrhage and edema (Figure 3C), necrosis extent (Figure 3D), and Ki67 staining (Figure 3E). In addition, no neutrophil infiltration was detected in all experimental groups analyzed following 20 days of tumor implant (Supplementary Table 3). Although tumor proliferation did not present statistically significant difference, the 10% neutrophil group seemed to be concentrated in around 50% of Ki67 staining while the other groups have a broader distribution. Representative images of tumor size (Figure 3F), HE staining (Figure 3G), and Ki67 staining (Figure 3H) are displayed according to each group. Overall, the given data suggest that tumor-associated neutrophils induce a significative, but modest, *in vivo* tumor progression using the preclinical model of glioblastoma in nude mice. It is probably that an integral immune system interaction is required to neutrophils drive effective *in vivo* tumor growth.

Energy metabolism of glioma cells shifts due to glioma-neutrophil interactions

Another set of experiment addressed the energy metabolism of glioma cells in the presence and absence of neutrophils and, thus, we evaluated tumor mitochondria functionality using mitochondrial probes. The results indicate that glioma cells sustain the number of mtROS (mitochondrial reactive oxygen species) production in the first 24 h, followed by a decrease after 120 h of co-culture with neutrophils ($P < 0.005$; Figures 4A, B). Meanwhile the opposite effect was observed for mtROS negative clustering as it increases after 120 h

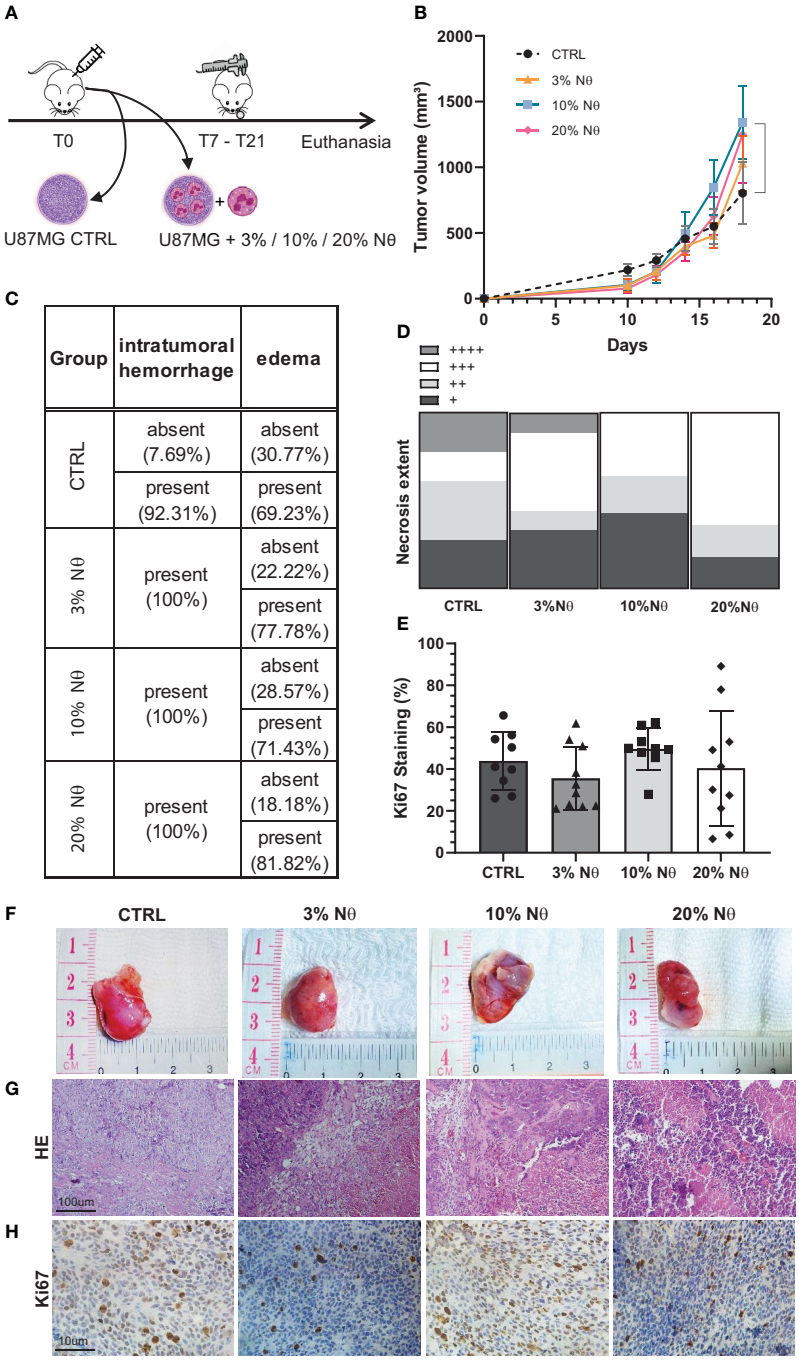

FIGURE 3
(A) *In vivo* glioblastoma protocol. **(B)** Tumor growth measured by day. **(C)** Histopathological quantitative analysis. **(D)** Necrosis extent quantification. **(E)** Ki67 staining percentage. **(F)** Representative images from tumor at euthanasia, **(G)** from HE staining, and **(H)** Ki-67. Two-way ANOVA, multiple comparisons. Tukey test, in which a = 0.05, *P < 0.05. Error bars are mean ± SD.

of co-culture with neutrophils ($P < 0.005$). MitoTracker DeepRed indicated a sharp disruption of the mitochondrial membrane potential after 120 h of co-culture with neutrophils ($P < 0.005$; Figures 4C, D). Altogether, this data implies glioma mitochondrial recovery after culture with neutrophils for 120 h, along with a reduction of membrane potential in the presence of neutrophils, indicating dysfunctional organelles.

Glioma-neutrophil crosstalk results in the release of an immunosuppressive secretome

To explore factors modulating the cell-to-cell communication in the glioma-neutrophil crosstalk soluble factors, we assessed the release by either the glioma cells or by the neutrophils. First,

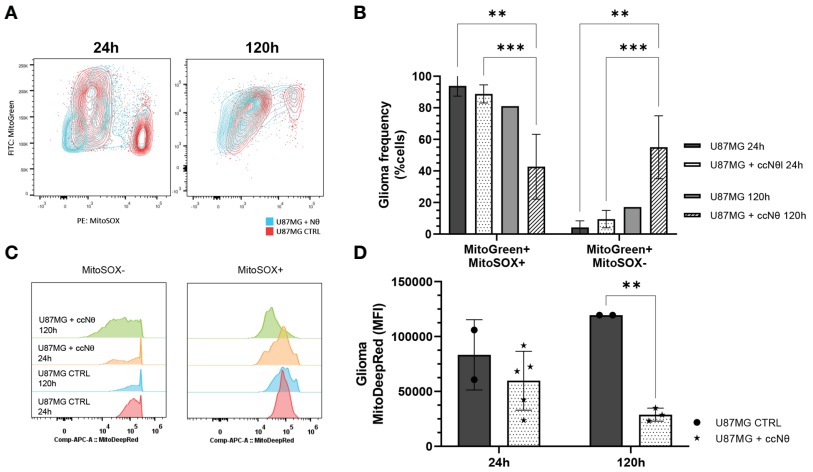

FIGURE 4
Evaluation of mitochondrial function by flow cytometry mitochondrial probes MitoTracker Green, MitoTracker Red and MitoSOX Red. **(A)** Gating strategy overlaps between groups. **(B)** Quantification of mtROS production from selected MitoTracker Green+ cells. **(C)** MitoTracker DeepRed MFI between groups. **(D)** Quantification of MFI in U87MG cell line with or without neutrophils for 24 h and 120 h. Two-way ANOVA, multiple comparisons. Tukey test, in which a = 0.05, **P < 0.005 and ***P < 0.001. Error bars are mean ± SEM.

glucose and lactate production were evaluated in culture media after 24 h and 120 h of culture (Figure 5A). The bar graph shows great use of glucose and, consequently, higher production of lactate over time, especially regarding glioma-neutrophil culture. We then analyzed glucose-uptake, which revealed that glioma cells have a slight glucose uptake increase after 24 h of co-culture with neutrophils, followed by a complete cell recovery after 120 h (Figures 5B, C). Similarly, neutrophils appeared to increase their glucose-uptake after 120 h of co-culture with glioma cells as well (Figures 5D, E), indicating that glucose consumption by both cells contributes to lactate production. Additionally, a Human Inflammatory Cytometric Bead Array (CBA) was conducted to determine the *in vitro* cytokine production of glioma-neutrophil culture over time and with different proportions of neutrophils (1:30 or 1:60). *In vitro* cytokine production showed three different states that can be clustered by culture duration (Figure 5F). In the first 24 h, glioma-neutrophil cultures produced high amounts of IL-8 and TNFα, slightly increased amounts of IL-12p70, and low to zero levels of IL-1β, IL-6, and IL-10. After 72 h, we identified a proportional increase of tested cytokines, especially with regards to IL-8, IL-10, and IL-12p70, while the production of TNFα was reduced. However, after 120 h, this pattern shifted and there was a rise in IL-1β and IL-6 release, while IL-8 declined and there was almost no IL-10, TNFα, and IL-12p70 production. All control neutrophils, regardless of culture duration, showed very low or no cytokine production. A detailed quantification and analysis demonstrated a significant IL-8 production of glioma-neutrophil co-cultures after 24 and 72 h, with a sharp downturn after 120 h (Figure 5G). The opposite was observed for IL-6 in glioma-neutrophil (1:30) experimental group, in which IL-6 production was 10 times higher (Figure 5H). Despite only detecting low levels of IL-12p70, its expression pattern is comparable with IL-8, showing increased levels in the first hours, followed by basically absent production after 120 h (Figure 5I). Differently from IL-6, the antithesis of the production of TNFα had a high initial expression, proportionally decreasing over the hours (Figure 5J). Finally, there were no significant alterations in IL-10 and IL-1β production (Figures 5K, L). Overall, the data suggest that the neutrophil-glioblastoma crosstalk potentiates the differential release of immune cell recruiting and suppression molecules described as drivers of tumor progression.

Glioma cells reprogram cellular functions of neutrophils

In addition to the analysis of effects of the neutrophil-glioma crosstalk on the tumor cells, we also evaluated alterations in the neutrophil population. Staining with trypan-blue, along with an analysis by flow cytometry, revealed that the co-culture of neutrophils and U87MG increased the neutrophil life span when compared with neutrophils cultured in absence of tumor cells (Figure 6A-C). The amount of live neutrophils in the presence of glioma significantly increased, considering the period of 120 h (Figure 6D). In addition to experiments with human cells, we extracted neutrophils from murine bone marrow and cultured them with murine GL-261 cells for 24 h (Figure 6E). This co-culture resulted in a reduction of neutrophil ($CD11b^{+}$) viability ($P < 0.05$; Figure 6F). However, different maturation states can be observed when murine neutrophils were challenged with GL-261. With this regard, we detected an increase of over 10% of mature neutrophils, after co-culture with GL-261 ($P < .05$), and significant decreases of the immature ($P < 0.001$) and of aged population ($P < 0.0001$; Figures 6G–I). Furthermore, we evaluated neutrophil mitochondria functionality with mitochondrial probes. Gating strategy for MitoTracker $Green^{high}$ MitoSOX red $^{-/+}$ (Figure 6J)

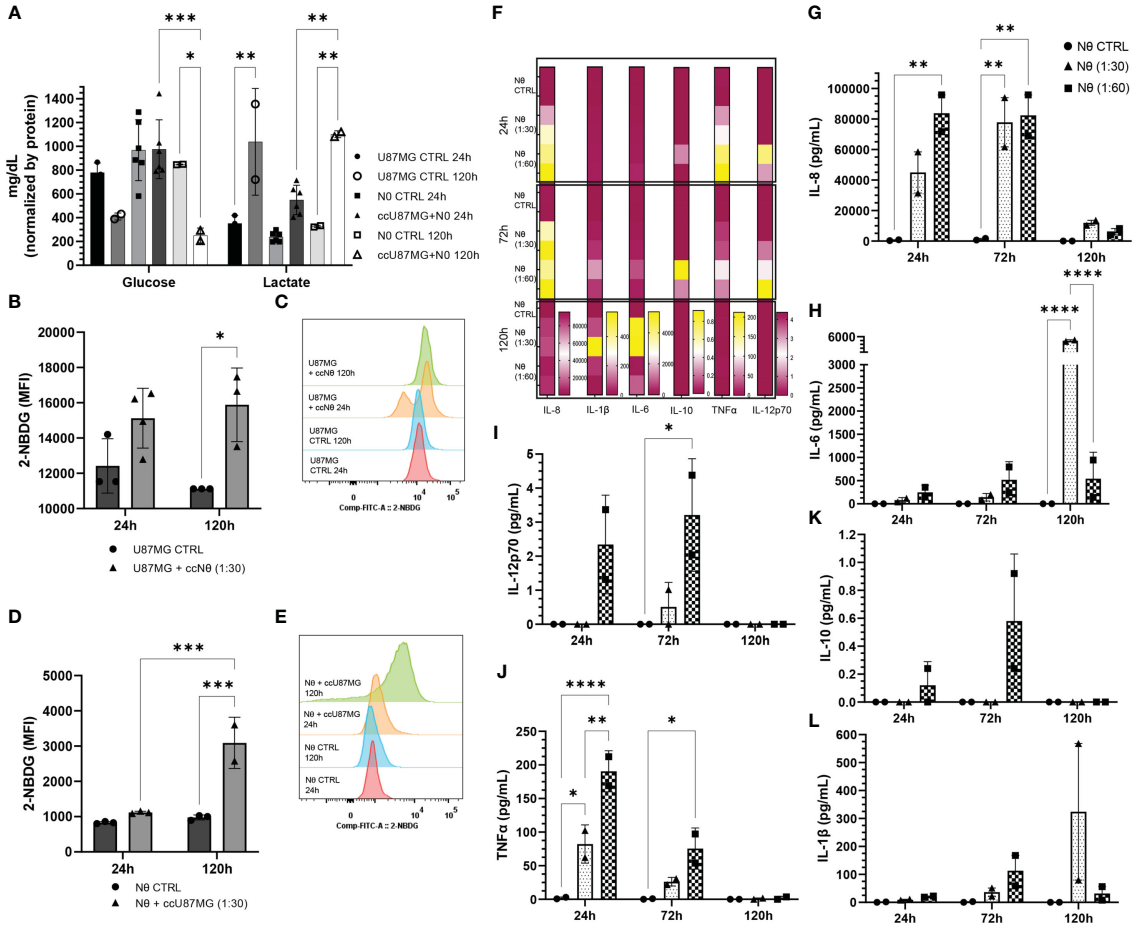

FIGURE 5
(A) Quantification of glucose consumption and lactate production from co-culture (cc) supernatant compared to control in 24 h and 120 h. Data normalized by protein. **(B)** 2-NBDG uptake assay: U87MG quantification **(B)** and MFI **(C)**; and neutrophil quantification **(D)** and MFI **(E)**. Cytokines pattern release in co-culture supernatant express in heat map **(F)** and quantification of IL-8 **(G)**, IL-6 **(H)**, IL-12p70 **(I)**, TNFα **(J)**, IL-10 **(K)**, and IL-1β **(L)**. Two-way ANOVA followed by Bonferroni & Šidák corrections for multiple comparisons, in which $\alpha = 0.05$, $^{*}P < 0.05$, $^{**}P < 0.005$, $^{***}P < 0.001$, and $^{****}P < 0.0001$. Data shown as mean ± SEM.

demonstrated different neutrophil populations after 24 h (Figure 6K) and 120 h (Figure 6L), which indicates a substantial amount of MitoSOX^{-} neutrophils when cultured with glioma cells (Figure 6M). Moreover, the data illustrates no significant alterations in mitochondrial membrane potential (Figure 6N, O). Concerning NETs release, neutrophils were treated with conditioned medium harvested from cultured U87MG cells and compared with commonly used chemicals (PMA 100 nM and LPS 1 µg/mL) for 3 h. Data revealed that glioma soluble factors were able to induce neutrophil DNA extravasation ($P < 0.005$; $P < 0.001$; Figure 6P). Altogether, the data have demonstrated the great ability of tumors to modulate the life span and response of neutrophils.

Cytokines play an important role in recruiting neutrophils and sustaining anti-inflammatory state

To validate a potential role of neutrophils in clinical samples, a principal component analysis was performed (Loadings plot, Figure 7A). The results showed that the variables CDH1 and FOXO3 are clustered closely together, indicating that these two variables are positively correlated, similar to MGMT and MPO and to IDH1, TGFβ1, and NFκB1. In comparison, the vectors for FOXO3 and MGMT form a nearly 180° angle, indicating that these variables are negatively correlated; the same was observed with CDH1 and ELANE. Finally, the vectors for variables FOXO3 and CDH1 form a nearly right angle with IDH1, TGFβ1, and NFκB1, suggesting that these variables are likely uncorrelated. Overall, the data suggests that neutrophils act in accordance with immunosuppressive signaling pathways, especially with MGMT (Figure 7B). In our patient cohort, we performed a correlation analysis between neutrophils, lymphocytes, leucocytes, and neutrophil-lymphocyte ratio (NLR) in healthy volunteers (Figure 7C) and glioma patients (Figure 7D). This analysis illustrated a considerable shift in blood count in glioma patients. The results imply an important neutrophil-monocyte correlation improvement in glioma patients (Figures 7E, F), which can explain the role of innate cells in sustaining immunosuppressive TME in glioma. To sum up, a descriptive analysis of glioma patient dataset shows a considerable amount of glioblastoma grade IV (n =

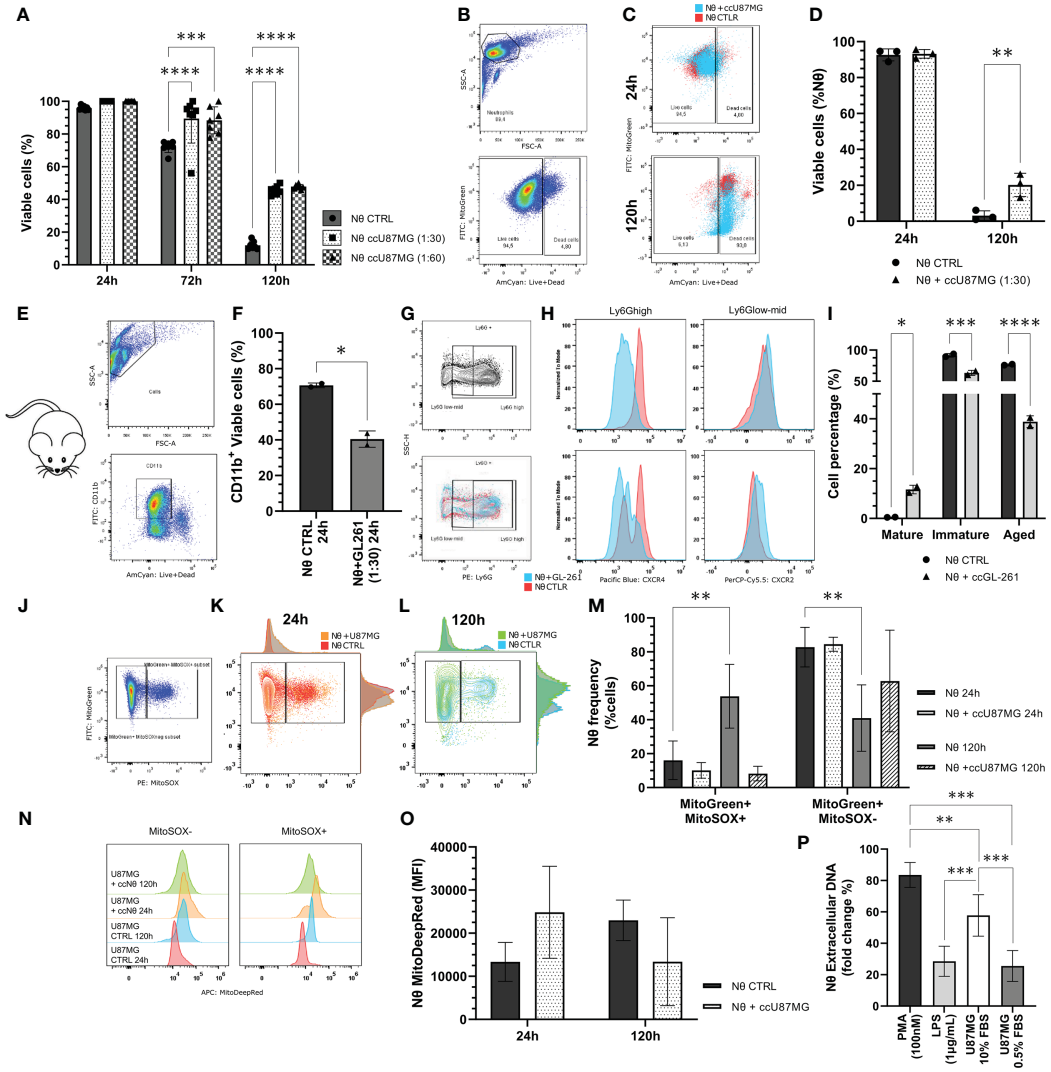

FIGURE 6
(A) Neutrophil viability tests performed using the trypan blue dye exclusion test throughout 24 h, 72 h and 120 h of co-culture along with U87MG (ccU87MG) in different proportions (1 U87MG: 30/60 Nq). **(B)** Gating strategy to analyze neutrophil viability. **(C)** Live/Dead overlap between experimental groups. **(D)** Percentage of live neutrophils. **(E)** Gate strategy to select CD11b+ cells **(F)** Cell viability quantification from neutrophil derived from mice C5/BL6 bone marrow isolation. **(G)** Gating strategy to select Ly6G populations. **(H)** MFI for CXCL4 and CXCL8. **(I)** Quantification of neutrophil maturation state according to mature: Ly6Ghigh, CXCR4-, CXCR2+; immature: Ly6Glow/mid, CXCR4+, CXCR2low; and aged: Ly6Ghigh, CXCR4+, CXCR2-. **(J)** Gating strategy to cluster MitoGreen/MitoSOX **(K)** in 24 h and **(L)** 120 h. Evaluation of neutrophil mitochondrial function by flow cytometry mitochondrial probes MitoTracker Green, MitoTracker Red, and MitoSOX Red. **(M)** Quantification of the percentage of mitochondrial ROS production in neutrophils with or without U87MG, for 24 h and 120 h. **(N)** MitoTracker DeepRed MFI distribution and **(O)** quantification. **(P)** NETs formation observed after 3h incubation with SytoxGreen reagent. Two-way ANOVA, multiple comparisons, Tukey test, in which a = 0.05, *P < 0.05, **P < 0.005, ***P < 0.001, and ****P < 0.0001.

27), notably with IDH wild-type (n = 19) (Supplementary Table 4). Patients IDH status was stratified according to grading system to visualize the existence of any condition related to IDH (Figure 7G). Furthermore, the amount of circulating neutrophil significantly increased in glioblastoma patients, when compared with non-glioblastoma (Supplementary Table 4 - P < 0.0001). The correlation analysis between NLR, Ki-67 staining, and grade from glioma patients was performed to test the connection between those parameters. This graph shows no correlation between NLR and Ki-67 staining, the dashed line represents the limit between the ratio considered normal (NLR = 3.0; Figure 7H). Afterwards, the Human Inflammatory CBA was conducted in blood serum from glioma patients and the Kaplan-Meyer survival graph was used to analyze the data (Figure 7I). The data indicates poor prognostic value of NLR >3, IL-1β, and IL-10, which validates our *in vitro* results described above. Cytokines from each patient was stratified to understand the big picture, the last one (n° 48) represents the healthy subject (Figure 7J). Quantified data shows high amount of serum IL-8, which is consistent with neutrophil mobilization, recruitment, and tumor infiltration. IL-6 and IL-10 also showed considerable amounts, which converses with the immunosuppressive state (Figure 7K). Pearson's test demonstrated correlation between serum IL-1β, IL-10, TNFα, and IL-12p70; while IL-10 is also closely related to IL-8 (Figure 7L). Overall, the given data suggests a cytokine milieu in

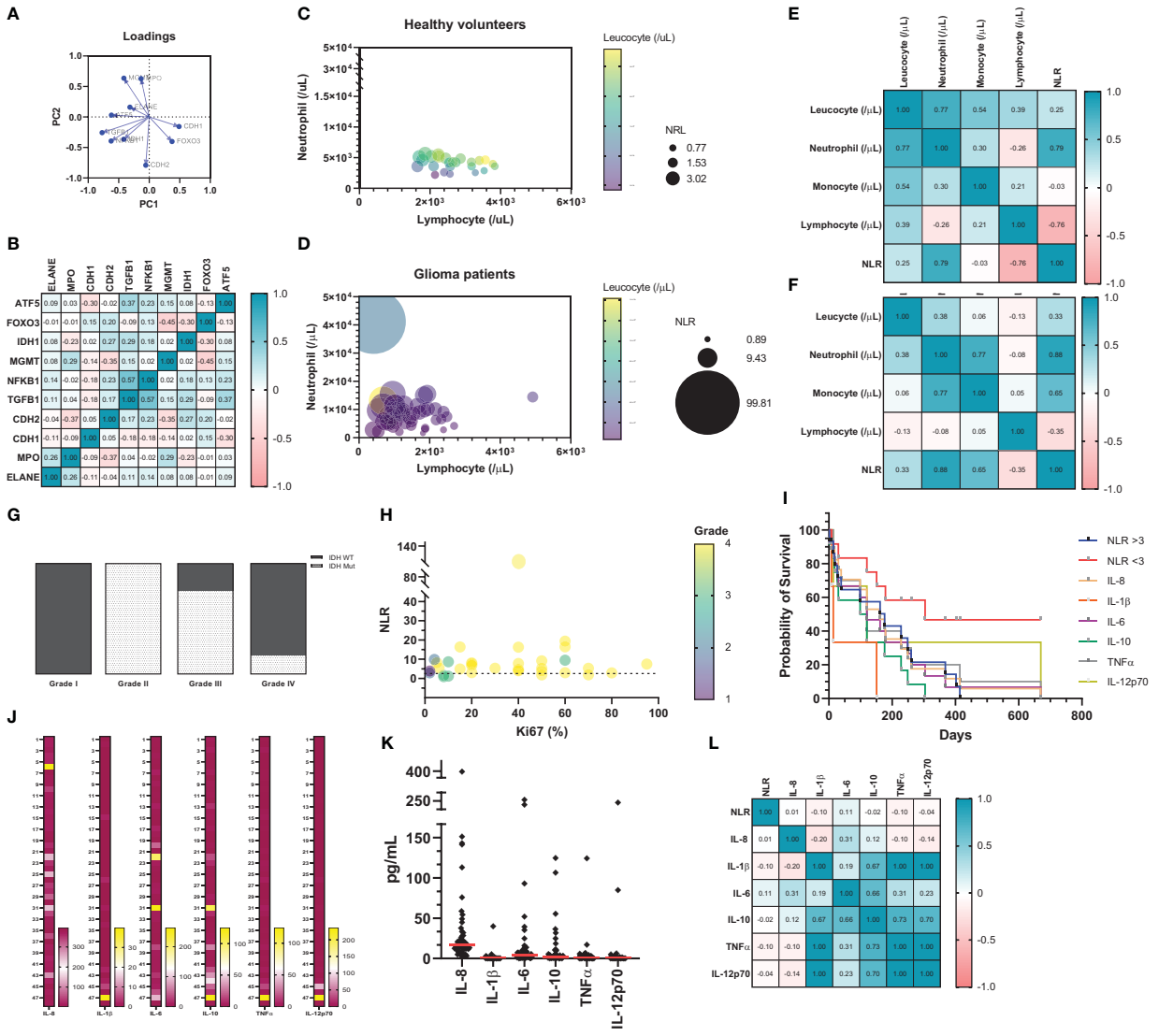

FIGURE 7
(A) Data download from TCGA GBM and analyzed by XENA browser (n = 172). The principal component analysis (Loadings plot) **(B)** Pearson's correlation matrix test, in which the strength of association is indicated. Correlation analysis between Neutrophil, Lymphocyte, Leucocyte, and NLR from healthy volunteers **(C)** and glioma patients **(D)**. On this graph, about 20 healthy volunteers and 50 glioma patients are shown as individual circles. The X-coordinate of each circle represents circulating neutrophils/μL, whereas the Y-coordinate represents the circulating lymphocyte/μL. The size of each symbol is proportionate to the NLR. Finally, the color of each symbol represents the total circulating leucocyte/μL. Correlation matrix (Pearson's coefficient) indicates strength of association from patients database (n = 20 healthy **(E)**; n = 50 GB patients **(F)**. **(G)** IDH status stratify according to grading system. **(H)** Correlation analysis between NLR, Ki67 staining and grade from glioma patients. On this graph, about 50 glioma patients are shown as individual circles. The X-coordinate of each circle represents circulating Ki67 staining in percentage (%), whereas the Y coordinate represents the NLR, in which the dashed line represents the limit between the ratio considered normal and high (NLR = 3.0). The size of each symbol is proportionate to tumor grade (I – IV). **(I)** Kaplan-Meier survival analysis. Cytokine quantification in heat map **(J)** and dot plot **(K)**. **(L)** Heat map with correlation analysis between NLR and cytokine from blood serum of glioma patients.

glioma patients that favors recruitment of neutrophils, sustaining an immunosuppressive profile, that which is associated with poor prognosis.

Discussion

The intercellular interaction and communication within the tumor is crucial for understanding the TME (28, 29). The tumor niche includes, in addition to tumor and stromal cells, fibroblasts, immune, and endothelial cells (5, 30). The immune infiltrate, including neutrophils, is a feature of chronic inflammation, contributing to tissue damage and ultimately to tumor progression (13). In this context, we were able to demonstrate that neutrophils act as expected in the first 24h after being in contact with glioma cells: they attack tumor cells and compromise their viability. This action persists until the next hours, and after 72 h it is possible to observe a slight change in this behavior,

suggesting that from that point on, tumor cells are successful in reprogramming the functions of neutrophils. The data suggest an important role of neutrophils in tumor progression, both *in vitro* and *in vivo*. The neutrophil plasticity happens according to the stimuli received, and time seems to be a major factor for their reprogramming. Other authors as well have presented evidence supporting this theory (13, 31–33). After 120 h, we observed that the tumor reacts to the presence of the neutrophils and its viability increases. This behavior shows that the "contact time" factor is a variable that must be considered when studying a neutrophil response in tumor progression. It also indicates that tumor-infiltrating neutrophils may have heterogenous functions depending on their actual time in the TME.

The results of Ki-67 labeling demonstrated that the neutrophil sphere groups proliferated almost exclusively in the periphery – consistent with the literature and with clinical findings in glioma patients (34) – since this region has greater access to nutrients and oxygen, while the central area shows necrosis. Additionally, while the control sphere, U87MG, revealed Ki-67 positivity of about 40%, the neutrophil groups, in both initial and advanced tumor 3D models, reached a plateau of about 80%, demonstrating that growth was significantly higher when there is crosstalk between these cells. Necrosis is a relevant finding in clinical tumor samples, being an indication of malignancy (35). Thus, since our experiments revealed increased levels of necrosis in the presence of neutrophils, it is suggested that neutrophils could help in inducing necrosis within the tumor niche, favoring the poor prognosis in glioma patients. Moreover, tumor infiltration of neutrophils has been described as an indicator of poor prognosis (36) and the location within the tumor mass has prognostic relevance, since they are usually found in the peritumoral area (23, 37, 38). Our *in vitro* data suggests that neutrophils can attach to glioma sphere at the periphery (data not shown), similar to studies which have described mostly peritumoral neutrophil infiltration in tumor patients (4, 39). These results suggest that the location of the immune infiltration in the tumor is of high prognostic importance and impacts on its malignancy, and that the presence of neutrophils in the intratumoral region is highly associated with cancer progression and growth.

Furthermore, glioma mitochondria metabolism indicates a possible mitochondria distress, which can result in mtDNA release. The tumor depends on mitochondrial mismatch in its tumor escape process (40, 41). According to cell energy necessity, the ATP production is increased in stress conditions, such as immune interaction, high oxidative phosphorylation (OXPHOS) activity, necrosis, and hypoxia (42). High ATP production need leads to mitochondria fusion (43), which can explain the low MFI in MitoTracker DeepRed after 120 h with neutrophils culture. However, in tumor cells, such as glioma, the ATP produced is mostly used as a signal, being extravasated *via* pannexin channels, activating purinergic receptors, such as $P2Y_2$ in immune cells, and leading to the activation and chemotaxis of neutrophils (44). The Warburg effect can be observed by the high lactate production in the mixed culture. This effect describes the use of glucose preferentially in the glycolytic pathway, even in the presence of oxygen, which accelerates tumor metabolism and, consequently, lactate production (45, 46). Cell stress can initiate various signaling pathways (47). Our data implies the possibility of glioma mtDNA release into cytosol. Tumor cells can initiate NFκB signaling, increasing IL-8 and reducing IL-6 secretion, mtDNA can activate cyclic GMP-AMP synthase and inflammasome pathways. Mobilizing cGAS-STING1 and canonical NFκB signaling stimulates TNFα and IL-6 cytokine secretion, while inflammasome mechanism cleavage IL-1β and, together, activate immune responses (48–50). With this regard, our *in vitro* results suggest that in 24 h and 72 h there is an increase in IL-8 production in glioma cells challenged with neutrophils, which might be explained by the NFκB signaling. This converses with glioma viability, protein synthesis, and MTT absorbance. Neutrophils first interaction cause glioma distress, which has a turnover over the hours. The remaining living glioma cells might be able to activate cGAS-STING1 pathway and release TNFα. On the other hand, after 120 h, glioma mitochondria data indicates mitochondria recovery and fusion, which can be due to the increase in energy metabolism and ATP production necessity (43). Authors have evaluated ATP increase in distress glioma cells (46). Moreover, cell resurgence is in accordance with the increase in IL-6 and IL-1β *in vitro* production, after 120 h.

Neutrophils are formed from the common myeloid precursor in the bone marrow and circulate for a limited time, capable of being active for approximately 3 days after stimulation (13, 31, 51). The aging process of the cell is marked by the phenotypic activation triggered by some disturbance (52). Nonetheless, there is evidence that survival rate changes when there is cellular hyperresponsiveness; the mechanisms by which the life span is increased are still under investigation for different chronic inflammatory diseases (53–57). Notably, neutrophil modulation indicates onset by the third day, while the viability of U87MG in that same period suggests a break in the immune cell attack process against the tumor. In other words, a period of prolonged contact is necessary for neutrophils to effectively assist in tumor growth. Indeed, glioma mtDNA can activate neutrophil response *via* TLR9 (58, 59) leading to the increased release of inflammatory cytokines, including TNFα, IL-6 and IL-1β (58). Moreover, mtDNA can trigger NETs release (60).

Neutrophils are well-known for modulating their own metabolism under environmental circumstances (61). Neutrophils have few mitochondria; during maturation process, however, they have an increase in OXPHOS (62–64), describing a metabolic shift towards free fatty acids (FFAs)-dependent OXPHOS (65). Our data suggests that neutrophil mtROS production is decreased and probably not the major ROS source production in these cells. Oxidative neutrophils have an essential role in inhibiting T cell activation, especially in environments with limited glucose (61, 63, 66). Similar observations were made in our study. Both, tumor cells and neutrophils, increased glucose-uptake, with subsequent increase of lactate production. Moreover, high lactate production has been described to contribute to immunosuppression in the TME (67, 68).

Neutrophil azurophilic granules are rich in myeloperoxidase (MPO) and in proteolytic and bactericidal proteins, being directly involved with phagocytosis (69, 70). During neutrophil oxidative burst, MPO granules inside the cell generate HOCl. Those oxidants are essential to NETosis (71). NETs are a nuclear network composed of granular proteins such as elastase (NE) and MPO (72). This process is considered a mechanism of cell death different from apoptosis and necrosis since it consists of disintegrating the nuclear envelope, exposing the content in the cytosol. The detriment of the intercellular membrane leads to the loss of organelles, and, consequently, the integrity of the plasma membrane is impaired (73). DNA-binding proteins, such as High Mobility Group Box 1 (HMGB1), are increased in NETs-mediated activation of TLR4 and TLR9 (74). One study revealed that HMGB1 interaction with RAGE/NFκB receptors from glioma cells induces IL-8 expression in tumor cells (75). The data suggest a higher NETs release in the presence of glioma soluble factors. Under tumor conditions, NETs have been linked to the formation of metastases, because, theoretically, these bonds capture the circulating tumor cells and facilitate the disposition in other tissues (76, 77). Moreover, NETosis pathway requires ROS generation and increase in intracellular Ca^{2+} (78). This is mediated by mitochondria ATP production which sustain a positive feedback loop specially by activating purinergic receptors, such as $P2Y_2$ (44). Although the NETs release is a cell death mechanism, studies have demonstrated that some neutrophils remain alive after NETosis due to the chromatin source, which is mitochondrial (79). Therefore, it is suggested that GB-neutrophil crosstalk have a prolonged tumor activation that could involve NETs formation and the release of HMGB1, MPO and NE proteins by neutrophils, which activates glioma cells by NFκB signaling, inducing oxidative mutations, impairing mitochondrial function and secreting immunosuppressive cytokines.

One study observed in a zebrafish glioblastoma model that neutrophils are recruited very early during oncogenesis and their presence increases tumor cell proliferation. The study suggests that this is due to the release of ROS, capable of causing DNA damage and inducing oncogenesis in cells around the tumor (80). We observed in our *in vivo* experiments that neutrophils can shift tumor growth pattern and increase its size along time. However, the animal model revealed that neutrophil alone have low effect in the overall outcome, BALB/c nude mice have no adaptive immune system, and the implantation of human neutrophils might not have the strength to recruit mice innate cells, such as monocytes. A recent study demonstrated the ability of neutrophils to recruit macrophages and regulatory T cells in hepatocellular carcinoma *via* cytokine release (81). Moreover, our clinical dataset demonstrated a strong positive correlation between circulating neutrophils and monocytes in GB patients. Our patients dataset revealed that high-grade glioblastoma had Ki-67 positivity increased by almost two times when compared with non-glioblastoma, in accordance with higher NLR (>3). Studies have demonstrated that higher percentage of Ki-67-positive cells in gliomas is related to the higher concentration of neutrophils in relation to lymphocytes in peripheral blood. Furthermore, this proportion is considerably higher in grade IV tumors (82). Overall, the data suggest a relevant crosstalk between inflammation and Ki-67 in glioma, corroborating our findings in the U87MG spheres, in *in vivo* BALB-c nude mice and clinical samples, in which there is a propensity between cell proliferation in control group and in groups with neutrophils.

It is not unusual to find pro-inflammatory cytokines in the TME, acting as stimulators of tumor progress and metastasis (83). Cytokines such as TNFα and IL-1β – known for their generally pro-inflammatory functions – and IL-10, a cytokine with immunosuppressive capacity are often found in the TME (84). Within the TME, some of the main cytokine-producing cells are B and T lymphocytes, dendritic cells, tumor-associated macrophages, TANs, MDSCs, and NK cells (85–87). Furthermore, IL-6, IL-8, and IL-10 production by cells from the TME mediate pro-tumor functions of immune cells, such as neutrophils and macrophages (88, 89). Our data demonstrates that glioma patients present an important cytokine-related worse outcome, especially regarding IL-1β and IL-10. Notably, the information provided by the release of cytokines in patients with glioma corroborates those found *in vitro*. In general, there is a high amount of circulating IL-8, in the same way that there is an increase in gliomas challenged with neutrophils. We found this pattern of late release of IL-1β and IL-6, which shows to be related to a worse prognosis in our patients. Moreover, the importance of IL-10, being preferentially released by immune cells, in this case, neutrophils, as indicated in the literature (84, 90–92). These data together with the NLR indicate great relevance of the role of neutrophils in both local and systemic immunosuppression.

Overall, our study answers an important question about the ability of dual communication followed by cell modulation between glioma and neutrophils (Figure 8). Bringing out the important role of neutrophil immunosuppression activation. Briefly, we have shown that, when cells are in contact, there is a constant and time dependent modulation. With tumor activation by mitochondrial disruption and mtROS release. The set of cytokines released is consistent with the maintenance of an immunosuppressed environment, which would explain the important role of this communication for the perpetuation of a TME favorable to the tumor. Due to cellular activation, both cells consume glucose, which leads to an increase in lactate in the environment and potentiates the effects of immune inhibition. On the other hand, pathways yet to be discussed activate neutrophils, promoting the release of NETs and ROS, which in turn contribute to the maintenance of the chronic inflammatory state found in the TME. It is important to emphasize that the activation pathways that lead to these signals need to be better elucidated. New experiments should be carried out to try to enlighten the open questions raised in our study about the signaling pathways between glioma-neutrophil crosstalk.

Concluding remarks

Thus, the data demonstrates a bidirectional crosstalk between glioma cells and neutrophils in modulating not only each other but also the local microenvironment. This study allowed insights into the complex interaction between tumor cells and the

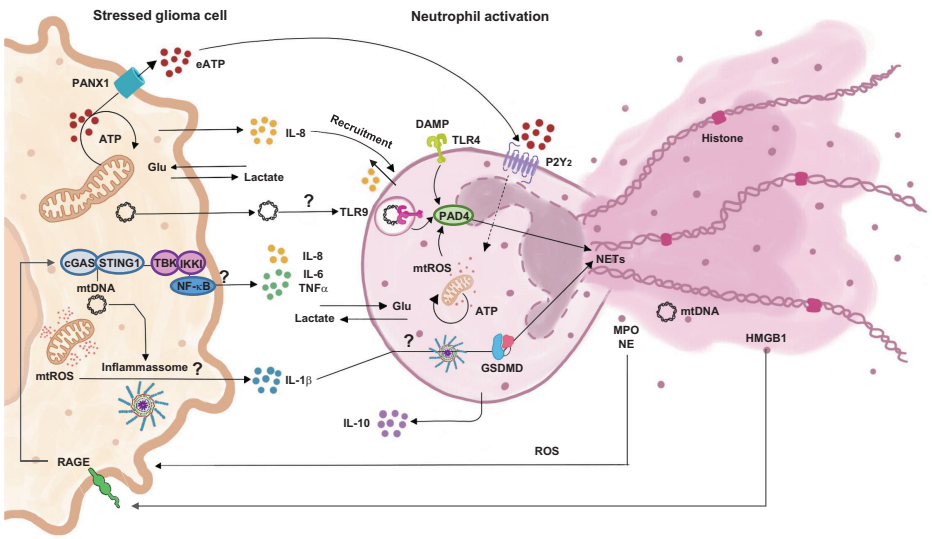

FIGURE 8
Proposition of cell signaling pathways involved in dual communication between glioblastoma and neutrophils.

microenvironment that surrounds them. Briefly, we observed that the presence of neutrophils closely located to the tumor is capable of inducing tumor-promoting effects. We have verified that there is a glioma-neutrophil crosstalk, resulting in further increase of neutrophil recruitment as well as elongation of neutrophil lifespan. These results are relevant to understand how tumor progression occurs and how immune cells contribute to that process. However, further studies are needed to confirm the magnitude of this interaction.

Data availability statement

The original contributions presented in the study are included in the article/Supplementary Material. Further inquiries can be directed to the corresponding author.

Ethics statement

The studies involving human participants were reviewed and approved by Irmandade Santa Casa de Misericórdia de Porto Alegre. The patients/participants provided their written informed consent to participate in this study. The animal studies were reviewed and approved by Hospital de Clınicas de Porto Alegre, UFCSPA, and USP.

Author contributions

DR and EB contributed to the study conception and design. DR, NO, PS, MA, PB, LS, LD, NG, AR, GL, AMA, GK, AP, FV, ML, MW, PW, ABA, JS, NC, NL performed material preparation, data collection and/or analysis. DR wrote the first draft of the manuscript. EB supervised the study and granted financial support. All authors commented on previous versions of the manuscript. All authors have read and approved the final manuscript.

Funding

The authors would like to thank the Research Support Foundation of the state of Rio Grande do Sul (FAPERGS -19/2551-0000663-2; 21/2551-0000078-3; 22/2551-0000388-5; 22/2551-0000388-5), Coordination for the Improvement of Higher Education Personnel (CAPES; code 001), National Council for Scientific and Technological Development (CNPq - 312187/2018-1; 400882/2019-1; 400882/2019-1; 315522/2021-6), Research Incentive Fund of the Hospital de Clínicas de Porto Alegre (FIPE 2019–0446; 2020-0708), Santa Casa de Misericórdia de Porto Alegre and Universidade Federal de Ciências da Saúde de Porto Alegre. DR, NO, MC, GG, NG, KG, JD, VT, PS, FT, GK, MW and EB were recipients of CNPq, CAPES, FAPERGS and UFCSPA fellowships. ABA and AP were supported by FIPE. PB, LS, ES and NC were also supported by FAPESP. NL was supported by the Walter Schulz Foundation. JS received support from the Natural Sciences and Engineering Research Council of Canada (NSERC; RGPIN-2023-05498). DR, NO, MRA, MC, GG, NG, KG, JD, VT, PS, FT, GK, MW and EB were recipients of CNPq, CAPES, FAPERGS or UFCSPA fellowships.

Conflict of interest

The authors declare that the research was conducted in the absence of any commercial or financial relationships that could be construed as a potential conflict of interest.

Publisher's note

Supplementary material

The Supplementary Material for this article can be found online at: https://www.frontiersin.org/articles/10.3389/fimmu.2023.1183465/full#supplementary-material

SUPPLEMENTARY FIGURE 1
Analysis of neutrophil infiltration in U87MG spheroids by CD45 immunohistochemistry. Representative images from **(A)** U87MG sphere; **(B)** U87MG + N0 sphere; **(C)** U87MG + pool N0 sphere for 72h; **(D)** U87MG + pool N0 sphere for 120 h (magnification 40x).

SUPPLEMENTARY TABLE 1
List of materials.

SUPPLEMENTARY TABLE 2
3D histopathological analysis.

SUPPLEMENTARY TABLE 3
Histopathological analysis of HE stained slices of glioblastomas implanted in Balb/c male and female nude mice.

SUPPLEMENTARY TABLE 4
Glioma patients group description. *anaplastic astrocytoma, metastatic adenocarcinoma, transitional meningioma, "no evidence of neoplasia in histological findings," pilocytic astrocytoma, oligodendroglioma, diffuse Large B Cell Lymphoma, and "astrocytoma" – all described as per medical report.

References

1. Omuro A, DeAngelis LM. Glioblastoma and other malignant gliomas: a clinical review. *JAMA - J Am Med Assoc* (2013) 310:1842–50. doi: 10.1001/jama.2013.280319

2. Tiziano D, Carlo D, Cagnazzo F, Benedetto N, Morganti R, Perrini P, et al. Multiple high-grade gliomas : epidemiology , management , and outcome. *A systematic Rev meta-analysis* (2017) 42:263–275. doi: 10.1007/s10143-017-0928-7

3. Nørøxe DS, Poulsen HS, Lassen U. Hallmarks of glioblastoma: a systematic review. *ESMO Open* (2016) 1:1–9. doi: 10.1136/esmoopen-2016-000144

4. Shaul ME, Fridlender ZG. Tumour-associated neutrophils in patients with cancer. *Nat Rev Clin Oncol* (2019) 16:601–20. doi: 10.1038/s41571-019-0222-4

5. Hanahan D, Weinberg RA. Hallmarks of cancer: the next generation. *Cell* (2011) 144:646–74. doi: 10.1016/j.cell.2011.02.013

6. Smolen JS, Aletaha D, McInnes IB. Rheumatoid arthritis. *Lancet* (2016) 388:2023–38. doi: 10.1016/S0140-6736(16)30173-8

7. Dapash M, Hou D, Castro B, Lee-Chang C, Lesniak MS. The interplay between glioblastoma and its microenvironment. *Cells* (2021) 10:1–14. doi: 10.3390/cells10092257

8. Takakura K, Ito Z, Suka M, Kanai T, Matsumoto Y, Odahara S, et al. Comprehensive assessment of the prognosis of pancreatic cancer: peripheral blood neutrophil-lymphocyte ratio and immunohistochemical analyses of the tumour site. *Scand J Gastroenterol* (2016) 51:610–7. doi: 10.3109/00365521.2015.1121515

9. Massara M, Persico P, Bonavita O, Poeta VM, Locati M, Simonelli M, et al. Neutrophils in gliomas. *Front Immunol* (2017) 8:1349. doi: 10.3389/fimmu.2017.01349

10. Lawrence SM, Corriden R, Nizet V. The ontogeny of a neutrophil: mechanisms of granulopoiesis and homeostasis. *Microbiol Mol Biol Rev* (2018) 82:1–22. doi: 10.1128/mmbr.00057-17

11. Silvestre-Roig C, Fridlender ZG, Glogauer M, Scapini P. Neutrophil diversity in health and disease. *Trends Immunol* (2019) 40:565–83. doi: 10.1016/j.it.2019.04.012

12. Hellebrekers P, Vrisekoop N, Koenderman L. Neutrophil phenotypes in health and disease. *Eur J Clin Invest* (2018) 48:e12943. doi: 10.1111/eci.12943

13. Giese MA, Hind LE, Huttenlocher A. Neutrophil plasticity in the tumor microenvironment. *Blood* (2019) 133:2159–67. doi: 10.1182/blood-2018-11-844548

14. Binnewies M, Roberts EW, Kersten K, Chan V, Fearon DF, Merad M, et al. Understanding the tumor immune microenvironment (TIME) for effective therapy. *Nat Med* (2018) 24:541–50. doi: 10.1038/s41591-018-0014-x

15. Yu MW, Quail DF. Immunotherapy for glioblastoma: current progress and challenge. *Front Immunol* (2021) 12:676301. doi: 10.3389/fimmu.2021.676301

16. Granot Z. Neutrophils as a therapeutic target in cancer. *Front Immunol* (2019) 10:1710. doi: 10.3389/fimmu.2019.01710

17. Oh H, Siano B, Diamond S. Neutrophil isolation protocol. *J Vis Exp* (2008) 17:1–2. doi: 10.3791/745

18. Azambuja JH, Ludwig N, Braganhol E, Whiteside TL. Inhibition of the adenosinergic pathway in cancer rejuvenates innate and adaptive immunity. *Int J Mol Sci* (2019) 20(22):5698. doi: 10.3390/ijms20225698

19. Vichai V, Kirtikara K. Sulforhodamine b colorimetric assay for cytotoxicity screening. *Nat Protoc* (2006) 1:1112–6. doi: 10.1038/nprot.2006.179

20. Crowley LC, Marfell BJ, Christensen ME, Waterhouse NJ. Measuring cell death by trypan blue uptake and light microscopy. *Cold Spring Harb. Protoc* (2016) 2016:643–6. doi: 10.1101/pdb.prot087155

21. Gao B, Jing C, Ng K, Pingguan-Murphy B, Yang Q. Fabrication of three-dimensional islet models by the geometry-controlled hanging-drop method. *Acta Mech Sin* (2019) 35:329–37. doi: 10.1007/s10409-019-00856-z

22. Friedrich J, Seidel C, Ebner R, Kunz-Schughart LA. Spheroid-based drug screen: considerations and practical approach. *Nat Protoc* (2009) 4:309–24. doi: 10.1038/nprot.2008.226

23. Umansky V, Blattner C, Gebhardt C, Utikal J. The role of myeloid-derived suppressor cells (MDSC) in cancer progression. *Vaccines* (2016) 4(50):e2597. doi: 10.3390/vaccines4040036

24. Liu X, Quan N. Immune cell isolation from mouse femur bone marrow. *Bio Protoc* (2015) 5(20):e1631. doi: 10.21769/bioprotoc.1631

25. Jaillon S, Ponzetta A, Di Mitri D, Santoni A, Bonecchi R, Mantovani A. Neutrophil diversity and plasticity in tumour progression and therapy. *Nat Rev Cancer* (2020) 20:485–503. doi: 10.1038/s41568-020-0281-y

26. Carmona-Rivera C, Kaplan MJ. Induction and quantification of NETosis. *Curr Protoc Immunol* (2016) 2016:14.41.1–14.41.14. doi: 10.1002/cpim.16

27. Goldman MJ, Craft B, Hastie M, Repečka K, McDade F, Kamath A, et al. Visualizing and interpreting cancer genomics data *via* the xena platform. *Nat Biotechnol* (2020) 38:675–8. doi: 10.1038/s41587-020-0546-8

28. Domingues P, González-Tablas M, Otero Á., Pascual D, Miranda D, Ruiz L, et al. Tumor infiltrating immune cells in gliomas and meningiomas. *Brain Behav Immun* (2016) 53:1–15. doi: 10.1016/j.bbi.2015.07.019

29. Wu S, Yang W, Zhang H, Ren Y, Fang Z, Yuan C, et al. The prognostic landscape of tumor-infiltrating immune cells and immune checkpoints in glioblastoma. *Technol Cancer Res Treat* (2019) 18:1–10. doi: 10.1177/1533033819869949

30. Uribe-Querol E, Rosales C. Neutrophils in cancer: two sides of the same coin. *J Immunol Res* (2015) 9:113. doi: 10.1155/2015/983698

31. Rosales C. Neutrophil: a cell with many roles in inflammation or several cell types? *Front Physiol* (2018) 9:113. doi: 10.3389/fphys.2018.00113

32. Buckley CD, Ross EA, McGettrick HM, Osborne CE, Haworth O, Schmutz C, et al. Identification of a phenotypically and functionally distinct population of long-lived neutrophils in a model of reverse endothelial migration. *J Leukoc. Biol* (2006) 79:303–11. doi: 10.1189/jlb.0905496

33. Patel S, Fu S, Mastio J, Dominguez G, Abhilasha P, Kossenkov A, et al. Unique pattern of neutrophil migration and function during tumor progression. *Nat Immunol* (2018) 19:1236–47. doi: 10.1038/s41590-018-0229-5

34. Hanif F, Muzaffar K, Perveen K, Malhi SM, Simjee SU. Glioblastoma multiforme: a review of its epidemiology and pathogenesis through clinical presentation and treatment. *Asian Pacific J Cancer Prev* (2017) 18:3–9. doi: 10.22034/APJCP.2017.18.1.3

35. Bi Y, Wu ZH, Cao F. Prognostic value and immune relevancy of a combined autophagy-, apoptosis- and necrosis-related gene signature in glioblastoma. *BMC Cancer* (2022) 22:1–21. doi: 10.1186/s12885-022-09328-3

36. Wang J, Jia Y, Wang N, Zhang X, Tan B, Zhang G. The clinical significance of tumor-infiltrating neutrophils and neutrophil-to-CD8+ lymphocyte ratio in patients with resectable esophageal squamous cell carcinoma. *J Transl Med* (2014) 220(2):236–42. doi: 10.1016/j.imbio.2014.07.017

37. Keskinov AA, Shurin MR. Myeloid regulatory cells in tumor spreading and metastasis. *Immunobiology* (2015) 220:236–42. doi: 10.1016/j.imbio.2014.07.017

38. Solito S, Falisi E, Diaz-Montero CM, Doni A, Pinton L, Rosato A, et al. A human promyelocytic-like population is responsible for the immune suppression mediated by myeloid-derived suppressor cells. *Blood* (2011) 118:2254–65. doi: 10.1182/blood-2010-12-325753

39. Lin YJ, Wei KC, Chen PY, Lim M, Hwang TL. Roles of neutrophils in glioma and brain metastases. *Front Immunol* (2021) 12:701383. doi: 10.3389/fimmu.2021.701383

40. Guerra F, Arbini AA, Moro L. Mitochondria and cancer chemoresistance. *Biochim Biophys Acta - Bioenerg* (2017) 1858:686–99. doi: 10.1016/j.bbabio.2017.01.012

41. Di Gregorio J, Petricca S, Iorio R, Toniato E, Flati V. Mitochondrial and metabolic alterations in cancer cells. *Eur J Cell Biol* (2022) 101:151225. doi: 10.1016/j.ejcb.2022.151225

42. Breda CNdeS, Davanzo GG, Basso PJ, Saraiva Câmara NO, Moraes-Vieira PMM. Mitochondria as central hub of the immune system. *Redox Biol* (2019) 26:101255. doi: 10.1016/j.redox.2019.101255

43. Gao Z, Li Y, Wang F, Huang T, Fan K, Zhang Y, et al. Mitochondrial dynamics controls anti-tumour innate immunity by regulating CHIP-IRF1 axis stability. *Nat Commun* (2017) 8(1):1805. doi: 10.1038/s41467-017-01919-0

44. Rubenich DS, De Souza PO, Omizzollo N, Lenz GS, Sevigny J, Braganhol E. Neutrophils : fast and furious — the nucleotide pathway. *Purinergic Signal* (2021) 17 (3):371–83. doi: 10.1007/s11302-021-09786-7

45. Marie SKN, Shinjo SMO. Metabolism and brain cancer. *Clinics* (2011) 66:33–43. doi: 10.1590/S1807-59322011001300005

46. Strickland M, Stoll EA. Metabolic reprogramming in glioma. *Front Cell Dev Biol* (2017) 5:43. doi: 10.3389/fcell.2017.00043

47. Sever R, Brugge JS. Signal transduction in cancer. *Cold Spring Harb Perspect Med* (2015) 3(30):eaat4579. doi: 10.1101/cshperspect.a006098

48. Muruve DA, Pétrilli V, Zaiss AK, White LR, Clark SA, Ross PJ, et al. The inflammasome recognizes cytosolic microbial and host DNA and triggers an innate immune response. *Nature* (2008) 452:103–7. doi: 10.1038/nature06664

49. Zhou R, Yazdi AS, Menu P, Tschopp J. A role for mitochondria in NLRP3 inflammasome activation. *Nature* (2011) 469:221–6. doi: 10.1038/nature09663

50. Marchi S, Guilbaud E, Tait SWG, Yamazaki T, Galluzzi L. Mitochondrial control of inflammation. *Nat Rev Immunol* (2022) 23(3):159–173. doi: 10.1038/s41577-022-00760-x

51. Görgens A, Radtke S, Möllmann M, Cross M, Dürig J, Horn PA, et al. Revision of the human hematopoietic tree: granulocyte subtypes derive from distinct hematopoietic lineages. *Cell Rep* (2013) 3:1539–52. doi: 10.1016/j.celrep.2013.04.025

52. Liu K, Huang HH, Yang T, Jiao YM, Zhang C, Song JW, et al. Increased neutrophil aging contributes to T cell immune suppression by PD-L1 and arginase-1 in HIV-1 treatment naïve patients. *Front Immunol* (2021) 12:670616. doi: 10.3389/fimmu.2021.670616

53. Li K, Zheng L, Guo H, Hong F, Yang S, Zheng L, et al. LTB4-induced anti-apoptosis and infiltration of neutrophils in rheumatoid arthritis. *Clin Exp Rheumatol* (2020) 38:543–51.

54. Ibrahim SA, Kulshrestha A, Katara GK, Riehl V, Sahoo M, Beaman KD. Cancer-associated V-ATPase induces delayed apoptosis of protumorigenic neutrophils. *Mol Oncol* (2020) 14:590–610. doi: 10.1002/1878-0261.12630

55. Aga E, Mukherjee A, Rane D, More V, Patil T, van Zandbergen G, et al. Type-1 interferons prolong the lifespan of neutrophils by interfering with members of the apoptotic cascade. *Cytokine* (2018) 112:21–6. doi: 10.1016/j.cyto.2018.06.027

56. Ley K, Hoffman HM, Kubes P, Cassatella MA, Zychlinsky A, Hedrick CC, et al. Neutrophils: new insights and open questions. *Sci Immunol* (2018) 3. doi: 10.1126/sciimmunol.aat4579

57. Isao N, Suzuki K, Murakami T, Niyonsaba F, Tamura H, Hirata M. Evaluation of the effect of α-defensin human neutrophil peptides on neutrophil apoptosis. *Int J Mol Med* (2010) 26:925–34. doi: 10.3892/ijmm_00000544

58. Fang C, Wei X, Wei Y. Mitochondrial DNA in the regulation of innate immune responses. *Protein Cell* (2016) 7:11–6. doi: 10.1007/s13238-015-0222-9

59. Tian J, Avalos AM, Mao SY, Chen B, Senthil K, Wu H, et al. Toll-like receptor 9-dependent activation by DNA-containing immune complexes is mediated by HMGB1 and RAGE. *Nat Immunol* (2007) 8:487–96. doi: 10.1038/ni1457

60. Tall AR, Westerterp M. Inflammasomes, neutrophil extracellular traps, and cholesterol. *J Lipid Res* (2019) 60:721–7. doi: 10.1194/jlr.S091280

61. Injarabian L, Devin A, Ransac S, Marteyn BS. Neutrophil metabolic shift during their lifecycle: impact on their survival and activation. *Int J Mol Sci* (2020) 21:1–23. doi: 10.3390/ijms21010287

62. Borregaard N, Herlin T. Energy metabolism of human neutrophils during phagocytosis. *J Clin Invest* (1982) 70:550–7. doi: 10.1172/JCI110647

63. Kumar S, Dikshit M. Metabolic insight of neutrophils in health and disease. *Front Immunol* (2019) 10:2099. doi: 10.3389/fimmu.2019.02099

64. Rice CM, Davies LC, Subleski JJ, Maio N, Gonzalez-Cotto M, Andrews C, et al. Tumour-elicited neutrophils engage mitochondrial metabolism to circumvent nutrient limitations and maintain immune suppression. *Nat Commun* (2018) 9(1):5099. doi: 10.1038/s41467-018-07505-2

65. Jeon JH, Hong CW, Kim EY, Lee JM. Current understanding on the metabolism of neutrophils. *Immune Netw* (2020) 20:1–13. doi: 10.4110/in.2020.20.e46

66. Stojkov D, Gigon L, Peng S, Lukowski R, Ruth P, Karaulov A, et al. Physiological and pathophysiological roles of metabolic pathways for NET formation and other neutrophil functions. *Front Immunol* (2022) 13:826515. doi: 10.3389/fimmu.2022.826515

67. Wang ZH, Peng WB, Zhang P, Yang XP, Zhou Q. Lactate in the tumour microenvironment: from immune modulation to therapy. *EBioMedicine* (2021) 73:103627. doi: 10.1016/j.ebiom.2021.103627

68. Wang JX, Choi SYC, Niu X, Kang N, Xue H, Killam J, et al. Lactic acid and an acidic tumor microenvironment suppress anticancer immunity. *Int J Mol Sci* (2020) 21:1–14. doi: 10.3390/ijms21218363

69. Mollinedo F. Neutrophil degranulation, plasticity, and cancer metastasis. *Trends Immunol* (2019) 40:228–42. doi: 10.1016/j.it.2019.01.006

70. Cassatella MA, Östberg NK, Tamassia N, Soehnlein O. Biological roles of neutrophil-derived granule proteins and cytokines. *Trends Immunol* (2019) 40:648–64. doi: 10.1016/j.it.2019.05.003

71. Parker H, Winterbourn CC. Reactive oxidants and myeloperoxidase and their involvement in neutrophil extracellular traps. *Front Immunol* (2013) 3:424. doi: 10.3389/fimmu.2012.00424

72. Brinkmann V, Reichard U, Goosmann C, Fauler B, Uhlemann Y, Weiss DS, et al. Neutrophil extracellular traps kill bacteria. *Science* (2004) 303:1532–5. doi: 10.1126/science.1092385

73. Fuchs TA, Abed U, Goosmann C, Hurwitz R, Schulze I, Wahn V, et al. Novel cell death program leads to neutrophil extracellular traps. *J Cell Biol* (2007) 176:231–41. doi: 10.1083/jcb.200606027

74. Huang H TA, Tohme S, Al-Khafaji AB, Tai S, Loughran P, Chen L, et al. Damage-associated molecular pattern-activated neutrophil extracellular trap exacerbates sterile inflammatory liver injury. *Hepatology* (2015) 62:600–14. doi: 10.1002/hep.27841

75. Zha C, Meng X, Li L, Mi S, Qian D, Li Z, et al. Neutrophil extracellular traps mediate the crosstalk between glioma progression and the tumor microenvironment *via* the HMGB1/RAGE/IL-8 axis. *Cancer Biol Med* (2020) 17:154–68. doi: 10.20892/j.issn.2095-3941.2019.0353

76. Cools-Lartigue J, Spicer J, McDonald B, Gowing S, Chow S, Giannias B, et al. Neutrophil extracellular traps sequester circulating tumor cells and promote metastasis. *J Clin Invest* (2013) 123:3446–58. doi: 10.1172/JCI67484

77. Park J, Wysocki RW, Amoozgar Z, Maiorino L, Fein MR, Jorns J, et al. Cancer cells induce metastasis-supporting neutrophil extracellular DNA traps. *Sci Transl Med* (2016) 8(361):361ra138–361ra138. doi: 10.1126/scitranslmed.aag1711

78. Douda DN, Khan MA, Grasemann H, Palaniyar N. SK3 channel and mitochondrial ROS mediate NADPH oxidase-independent NETosis induced by calcium influx. *Proc Natl Acad Sci U. S. A.* (2015) 112:2817–22. doi: 10.1073/pnas.1414055112

79. Yousefi S, Mihalache C, Kozlowski E, Schmid I, Simon HU. Viable neutrophils release mitochondrial DNA to form neutrophil extracellular traps. *Cell Death Differ* (2009) 16:1438–44. doi: 10.1038/cdd.2009.96

80. Powell D, Lou M, Barros Becker F, Huttenlocher A. Cxcr1 mediates recruitment of neutrophils and supports proliferation of tumor-initiating astrocytes *in vivo*. *Sci Rep* (2018) 8:2–13. doi: 10.1038/s41598-018-31675-0

81. Zhou SL, Zhou ZJ, Hu ZQ, Huang XW, Wang Z, Chen EB, et al. Tumor-associated neutrophils recruit macrophages and T-regulatory cells to promote progression of hepatocellular carcinoma and resistance to sorafenib. *Gastroenterology* (2016) 150:1646–1658.e17. doi: 10.1053/j.gastro.2016.02.040

82. Xu G, Li C, Wang Y, Ma J, Zhang J. Correlation between preoperative inflammatory markers, ki-67 and the pathological grade of glioma. *Med (Baltimore)* (2021) 100:e26750. doi: 10.1097/MD.0000000000026750

83. Lippitz BE. Cytokine patterns in patients with cancer: a systematic review. *Lancet Oncol* (2013) 14:e218–28. doi: 10.1016/S1470-2045(12)70582-X

84. Moore KW, Malefyt RDW, Robert L, Garra AO. I Nterleukin -10 and the I nterleukin -10. *Mol Cell Biol* (2001) 1:683–765.

85. Wu T, Dai Y. Tumor microenvironment and therapeutic response. *Cancer Lett* (2017) 387:61–8. doi: 10.1016/j.canlet.2016.01.043

86. Wei R, Liu S, Zhang S, Min L, Zhu S. Cellular and extracellular components in tumor microenvironment and their application in early diagnosis of cancers. *Anal Cell Pathol 2020* (2020) 2020:6283796. doi: 10.1155/2020/6283796

87. Li L, Yu R, Cai T, Chen Z, Lan M, Zou T, et al. Effects of immune cells and cytokines on inflammation and immunosuppression in the tumor microenvironment. *Int Immunopharmacol* (2020) 88:106939. doi: 10.1016/j.intimp.2020.106939

88. Zhang X, Zhang W, Yuan X, Fu M, Qian H, Xu W. Neutrophils in cancer development and progression: roles, mechanisms, and implications (Review). *Int J Oncol* (2016) 49:857–67. doi: 10.3892/ijo.2016.3616

89. Codony VL, Tavassoli M. Hypoxia-induced therapy resistance: available hypoxia-targeting strategies and current advances in head and neck cancer. *Transl Oncol* (2021) 14:101017. doi: 10.1016/j.tranon.2021.101017

90. Shrihari TG. Dual role of inflammatory mediators in cancer. *Ecancermedicalscience* (2017) 11:1–9. doi: 10.3332/ecancer.2017.721

91. De Santo C, Arscott R, Booth S, Karydis I, Jones M, Asher R, et al. Invariant NKT cells modulate the suppressive activity of IL-10-secreting neutrophils differentiated with serum amyloid a. *Nat Immunol* (2010) 11:1039–46. doi: 10.1038/ni.1942

92. Wilke CM, Wei S, Wang L, Kryczek I, Kao J, Zou W. Dual biological effects of the cytokines interleukin-10 and interferon-γ. *Cancer Immunol Immunother* (2011) 60:1529–41. doi: 10.1007/s00262-011-1104-5

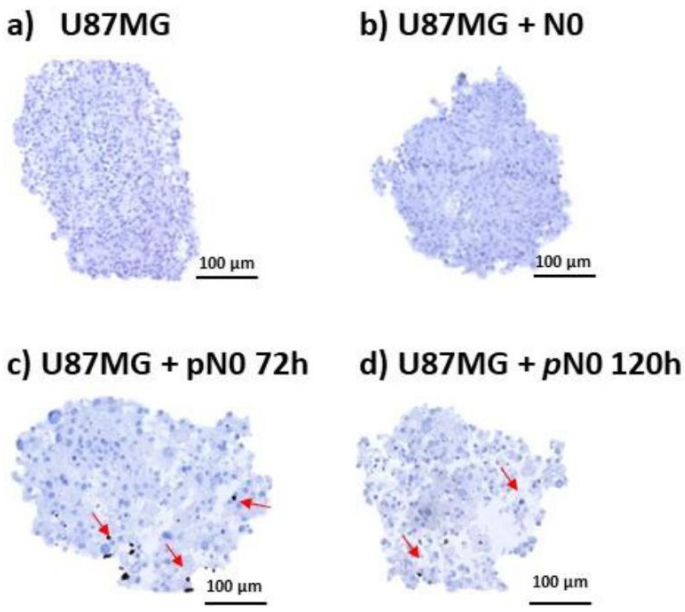

Supplementary Figure 1 | Analysis of neutrophil infiltration in U87MG spheroids by CD45 immunohistochemistry. Representative images from (A) U87MG sphere; (B) U87MG + N0 sphere; (C) U87MG + pool N0 sphere for 72h; (D) U87MG + pool N0 sphere for 120 h (magnification 40x).

Supplementary tables:

Table S1: List of materials

Reagent or Resource	**Source**	**Identifier**
Chemicals		
DMEM-Dulbecco's modified Eagle's medium	Gibco™ (Gibco BRL, Gaithersburg, USA)	31600-34
HEPES - 4-(2-Hydroxyethyl)piperazine-1-ethanesulfonic acid, N-(2-Hydroxyethyl)piperazine-N'-(2-ethanesulfonic acid)	Sigma-Aldrich (Sigma Chemical C0., ST. Louis, USA)	7365-45-9
Sodium bicarbonate (NaHCO3)	Neon Comercial Ltda, BRL	1715
Fetal bovine serum (FBS)	Gibco™ (Gibco BRL, Gaithersburg, USA)	12657-029
Fungizone	Gibco™ (Gibco BRL, Gaithersburg, USA)	15290-018
Penicillin/streptomycin	Gibco™ (Gibco BRL, Gaithersburg, USA)	15140-122

Dextran from Leuconostoc spp.	Sigma-Aldrich (Sigma Chemical C0., ST. Louis, USA)	31389
Histopaque®-1077	Sigma-Aldrich (Sigma Chemical C0., ST. Louis, USA)	10771
MTT - (3-(4,5-Dimethylthiazol-2-yl)-2,5-Diphenyltetrazolium Bromide)	Sigma-Aldrich (Sigma Chemical C0., ST. Louis, USA)	M2128
SRB | Sulforhodamine B	Merck KGaA, Darmstadt, Germany	S1402
Acetic Acid, Glacial	Merck KGaA, Darmstadt, Germany	A6283
Tris base | Tris(hydroxymethyl)aminomethane (10mmol/L pH 10,5)	Merck KGaA, Darmstadt, Germany	252859
Trypan Blue Solution, 0.4%	Gibco™ (Gibco BRL, Gaithersburg, USA)	15250061
Agarose	Merck KGaA, Darmstadt, Germany	A9539
Paraformaldehyde	Merck KGaA, Darmstadt, Germany	P6148
Hematoxylin monohydrate	Merck KGaA, Darmstadt, Germany	3971
Yellowish eosin	Synth, Diadema, Brazil	45380
Hydrogen peroxide solution	Merck KGaA, Darmstadt, Germany	107298
BSA | Albumin bovine serum	Sigma-Aldrich (Sigma Chemical C0., ST. Louis, USA)	A7906
Matrigel	Sigma-Aldrich (Sigma Chemical C0., ST. Louis, USA)	E1270
SYTOX™ Green Ready Flow™	Invitrogen | Thermo Fisher Scientific Inc. (Waltham, USA)	R37168
PMA | Phorbol 12-myristate 13-acetate	Merck KGaA, Darmstadt, Germany	P1585
LPS | Lipopolysaccharides	Sigma-Aldrich (Sigma Chemical C0., ST. Louis, USA)	L3024
Antibodies		
LIVE/DEAD™ Fixable Dead Cell Stain Sampler Kit (1:400)	Thermo Fisher Scientific Inc. (Waltham, USA)	L34960
Anti-Ki67 (1:100)	Dako | Agilent (Santa Clara, USA)	M7240
FITC Annexin V-PE Propidium iodide Apoptosis Detection Kit	BD Biosciences Pharmingen (San Diego, USA)	555670
Anti-CD11b |M1/70 (1:400)	BioLegend (San Diego, USA)	101206

Anti-Ly6G | 1A8 (1:400)	BioLegend (San Diego, USA)	127608
Anti-CD184 (CXCR4) | L276F12 (1:100)	BioLegend (San Diego, USA)	146511
Anti-CD182 (CXCR2) | TG11/CXCR2 (1:100)	BioLegend (San Diego, USA)	129103
Probes		
MitoTracker Green	Invitrogen | Thermo Fisher Scientific Inc. (Waltham, USA)	M7514
MitoTracker Deep red	Invitrogen | Thermo Fisher Scientific Inc. (Waltham, USA)	M46753
MitoSOX	Invitrogen | Thermo Fisher Scientific Inc. (Waltham, USA)	M36008
2-NBDG (2-(N-(7-Nitrobenz-2-oxa-1,3-diazol-4- yl)amino)-2-Deoxyglucose)	Invitrogen | Thermo Fisher Scientific Inc. (Waltham, USA)	N13195
Critical Commercial Assays		
GLICOSE Liquiform	Labtest Diagnóstica S/A (BRL)	133
Enzymatic system for lactate	Labtest Diagnóstica S/A (BRL)	138
CBA - Cytokine cytometric bead array	BD Biosciences (San Diego, USA)	552364
EnVision™+ Dual Link System-HRP	Dako | Agilent (Santa Clara, USA)	K4061
Liquid DAB+ Substrate Chromogen System	Dako | Agilent (Santa Clara, USA)	K3468
Solutions		
PBS 1x	100mL | Milli-Q water / 0,8g NaCl, 0,02g KCl, 0.115g Na_2HPO_4 e 0.02g KH_2PO_4 pH 7.4	x
HBSS 10x	1000mL | Milli-Q water / 80g NaCl, 4g KCl, 0.6g Na_2HPO_4, 0.6g KH_2PO_4, 10g glucose	x

Table S2: 3D histopathological analysis

Group	Mitosis (n°)	Necrosis	Descriptive analysis
U87MG CTRL	0	-	fusiform cell shape
	4	-	
	0	++	
	4	-	
U87MG+Nθ	1	++	cavitaded
	1	+	

	0	++	
	0	++	
U87MG + 72h Nθ pool	1	+	small and homogeneous tumor cells / cavitaded
	0	++	
	1	++	
	1	+++	
U87MG + 120h Nθpool	0	++	small and homogeneous tumor cells / cavitaded
	0	++	
	8	-	
	0	++	
	1	++	

Table S3: Histopathological analysis of HE stained slices of glioblastomas implanted in Balb/c male and female nude mice.

Group	intratumoral hemorrhage	coagulative necrosis	necrosis extent	immune cell infiltration	edema	vascular proliferation
Male CTRL	no	present	++	no	no	no
	present	present	+	no	no	no
	present	present	+	no	present	no
	present	present	+++	no	present	no
	present	present	++	no	present	no
	present	present	++	no	present	no
	present	present	++++	no	present	No
	present	present	+	no	no	No
Male 3% Nθ	present	present	+++	no	no	No
	present	present	+++	no	present	No
	present	present	+	no	no	No
	present	present	++++	no	present	No
	present	present	+++	no	present	No
Male 10% Nθ	present (+++)	present	++	no	present	No
	present	present	+++	no	present	No
	present	present	+	no	no	No
	present	present	+++	no	present	No
	present	present	+	no	no	No
	present	present	+	no	present	No
Male 20% Nθ	present	present	+++	no	no	No
	present	present	+++	no	present	No
	present	present	+++	no	present	No
	present	present	++	no	present	No
	present	present	++	no	present	No

Group	intratumoral hemorrhage	coagulative necrosis	necrosis extent	immune cell infiltration	edema	vascular proliferation
Female CTRL	present (+++)	present	++	no	present	no
	present	present	+++	no	present	no
	present	present	+++	no	present	no
	present	present	+	no	no	no
	present	present	++	no	present	no
	present	present	++	no	present	no
	present	present	+	no	present	no
Female 3% Nθ	present	present	+	no	present	
	present	present	+++	no	present	no
	present	present	+	no	present	no
	present	present	++	no	present	no
Female 10% Nθ	present	present	++	no	present	no
	present	present	+	no	no	no
	present	present	+	no	no	no
	present	present	++	no	present	no
	present	present	+	no	present	no
	present	present	+++	no	present	no
	present	present	+++	no	present	no
	present	present	+++	no	present	no
Female 20% Nθ	present	present	+++	no	present	no
	no	present	+	no	no	no
	present	present	+++	no	present	no
	present	present	+	no	present	no
	present	present	+++	no	present	no
	present	present	+++	no	present	no

Table S4: Glioma patients group description

*anaplastic astrocytoma, metastatic adenocarcinoma, transitional meningioma, "no evidence of neoplasia in histological findings," pilocytic astrocytoma, oligodendroglioma, diffuse Large B Cell Lymphoma, and "astrocytoma" – all described as per medical report.

Histopathological classification	Total number (n)	Sex (mean age ±SD)	IDH (n)**			Ki-67 (%)	Neutrophil (/µL)	Lymphocyte (/µL)	NLR
			WT	Mut	Inconclusive				

Glioblastoma	27	Women (57.9±21.1) / Men (57.6±17.3)	19	3	5	45.4±24.2	9048.0±4428.3	1550.1±777.3	8.4±7.1
Non-Glioblastoma*	16	Women (60.3±14.2) / Men (60.2±11.5)	6	3	1	25.6±28.8	5090.3±2707.0	1554.9±911.8	4.7±3.8

*anaplastic astrocytoma, metastatic adenocarcinoma, transitional meningioma, "no evidence of neoplasia in histological findings," pilocytic astrocytoma, oligodendroglioma, diffuse Large B Cell Lymphoma, and "astrocytoma" – all described as per medical report.

DISCUSSION

Effective crosstalk between tumor cells and surrounding cells is crucial for maintaining tissue function and promoting tumor growth. This significantly influence disease initiation, progression, and patient prognosis. Rudolf Virchow initially proposed the link between chronic inflammation and tumorigenesis in 1863, stating that infiltrating leukocytes were a common feature of tumors (BALKWILL; MANTOVANI, 2001). Subsequent studies have extensively characterized the TME, adding complexity to the challenge of comprehending and treating cancer. Tumors exhibit diverse microenvironmental compositions, including varying proportions and activation states of stromal cells. Indeed, in the 1950s, Burnet and Thomas proposed that the immune system could recognize and eliminate tumor cells, a notion initially met with controversy due to early experimental setbacks (SCHREIBER; OLD; SMYTH, 331AD). With this regard, immunosurveillance shapes tumors by eliminating vulnerable cells, allowing those that evade detection to thrive and propagate, leading to immune-resistant tumors (SHANKARAN *et al.*, 2001). The TME evolves in response to changing environmental conditions and oncogenic signals, highlighting the dynamic nature of TME influences on metastasis during cancer progression (HANAHAN; WEINBERG, 2011). Therefore, the diverse role of NØ in cancer is a current focus for potential therapeutic targets, with the transition from surveillance to tumor-promoting activity upon tumor presence. While the exact mechanisms are not fully understood, studies highlight the underestimated significance of NØ in cancer, linking them to metastasis, cancer-associated thrombosis, and immunosuppression (GIESE; HIND; HUTTENLOCHER, 2019; MANTOVANI *et al.*, 2011). A crucial aspect of tumor progression involves evading and suppressing the host immune system (MOTZ; COUKOS, 2013). Tumor-NØ communication can occur through various mechanisms, including cell-cell direct contact, traditional paracrine signaling involving cytokines or growth factors and their receptors and, recently, exosome release has emerged as another mode of cell-to-cell signaling.

The impact of TEX on the TME necessitates further investigations., however it is known that depleting cancer cells or sEV effectors inconsistently hindered

cancer progression (BOOMGARDEN; SHEEHAN; D'SOUZA-SCHOREY, 2020; FIANI *et al.*, 2020; MATARREDONA; PASTOR, 2019). Moreover, exosomes released by the primary tumor educate the surrounding environment to create a supportive niche for tumor growth and guide bone marrow-derived progenitor cells to enhance and facilitate metastatic spread (BARCELLOS-HOFF; LYDEN; WANG, 2013). The **chapter 01** highlights the reprogramming potential of EVs from different sources and diseases. It is clear that NØ can exert their inflammatory or regenerative functions when in need. This information corroborates with the currently discussion about NØ phenotype in cancer (GRANOT, 2019). Literature suggests that TEX mediate neutrophil recruitment, activation, and reprogramming into pro-tumor phenotype. The present study has demonstrated that communication between tumor cells and neutrophils occurs through sEVs released either by TEX or by neutrophils (NEX). Neutrophils exhibit diverse phenotypes and functions of inducing pro-inflammation or regulation of immune response, likely reflected in the heterogeneity of NEX. The molecular content of NEX varies based on the microenvironmental conditions of the parent cells, potentially resulting in distinct N1- and N2-NEX. N1-NEX may exert anti-tumor effects and enhance the anti-tumor immune response, particularly involving lymphocytes. In contrast, N2-NEX carry cargo components that promote tumor growth, survival, angiogenesis, and immune evasion.

With this regards, TEX emerged as strong contributor to sustaining a permissive TME. It is imperative to mention that exosomes carry diverse cargo from the parent cell, reflecting its physiological and functional state. This cargo includes proteins (enzymes, receptors, signaling molecules), nucleic acids (mRNA, miRNA, DNA fragments), lipids, and metabolites (WORTZEL *et al.*, 2019). Upon uptake by recipient cells via endocytosis or membrane fusion, exosomal cargo can activate or inhibit specific cellular pathways, influencing behavior and responses. Notably, TEX may contain oncogenic cargo that promotes tumorigenesis in neighboring or distant cells (GUO *et al.*, 2020; YANG *et al.*, 2017). Therefore, in **chapter 02** we conducted a bioinformatics study with two TEX gene signatures in HNSCC. The cancer progression relies on an immunosuppressive niche supporting tumor growth and metastasis (RAD *et al.*, 2022). TEX play a role in intercellular communication, and

our analysis reveal their association with immunosuppressive pathways, such as PD-L1, CD73 and TGFβ upregulation. Moreover, it correlates to immune infiltration and HNSCC tumor malignancy. These data support the notion of TEX as important mediators in reprogramming non-tumor cells. Recently, TEX have been associated with promoting angiogenesis, immune escape and metastasis (FIANI *et al.*, 2020; LUDWIG, Nils *et al.*, 2020; YANG *et al.*, 2017). In accordance to our findings, it was shown that TEX promote the differentiation of immune cells into immunosuppressive subtypes, reshaping the tumor microenvironment to favor tumor growth (LIANG *et al.*, 2019; QIAN, Mingyu *et al.*, 2019). For instance, exosomes from bladder cancer trigger the transformation of normal fibroblasts into cancer-associated fibroblasts (CAFs) by TGFβ activation, supporting tumor progression (BERNARD *et al.*, 2018). TEX also induce a suppressive phenotype in CD8+ T cells, impairing their anti-tumor functions (MAYBRUCK *et al.*, 2017). In addition, a pan-cancer analysis confirms elevated levels of CAFs, M2-like macrophages, and MDSCs in the high-TEXscore subgroup, demonstrating a strong association between TEXscore and immune inhibitory factors (WU, Jiani *et al.*, 2021). Within this context, TEX not only contributes to tumor growth but induce NØ reprogramming, which can in turn facilitate the immunosuppression. Therefore, the following steps was to investigate how the TEX-NØ reprogramming influence in the tumor-NØ crosstalk.

By unraveling this communication, we gain insights into cancer's adaptive strategies and vulnerabilities. This understanding can guide the development of novel interventions aimed at disrupting detrimental tumor-neutrophil interactions while harnessing beneficial aspects for therapeutic benefit. With this regard, NLR is a powerful biomarker that has emerged as a crucial indicator of the inflammatory milieu within the TME (WENG *et al.*, 2018). This ratio is calculated from routine blood tests, serves as a surrogate marker for systemic inflammation and immune response. Elevated NLR (>3) levels have been associated with poorer prognosis across a spectrum of cancers (GOMES DOS SANTOS *et al.*, 2021; MASCARELLA *et al.*, 2018; WANG, Jianbo *et al.*, 2014).

Our study in **chapter 03** correlates NLR with tumorigenic processes, emphasizing tumor PD-L1 cytoplasmic expression in clinical samples of HNSCC.

Variations in PD-L1 subcellular localization are observed, with heightened crosstalk between tumor cells and NØ in highly malignant tumors. The PD-L1 sublocalization have been associated with high tumor staging and low therapy rate response (SCHULZ, Daniela *et al.*, 2023). Besides, the expression of PD-L1 is directly affected by chemotherapy and radiotherapy in HNSCC, which contribute to the poor prognosis (FIEDLER *et al.*, 2020; SCHULZ, Daniela *et al.*, 2019). The positive correlation of NLR and cytoplasmic PD-L1 strengthen the hypothesis that NØ are crucial in the disease progression. The NØ phenotype modulation is a recent topic that discloses the ability to respond according to signal form the environment (GRANOT; JABLONSKA, 2015). Our *in vitro* data illustrates the upregulation of pro-tumor and immunosuppressive markers on NØ after TEX interaction shows the deep and strong effect of tumor cells on NØ. Both flow cytometer (FACS) and Western blot (WB) analysis showed the increase in CD73, $CD170^{high}$ and PD-L1 in NØ, corroborating to pro-tumor TAN phenotype described (JAILLON *et al.*, 2020). Our study also explores the relevant action of NØ in promoting and sustaining the *cold*-tumor TME, releasing immunosuppressive cytokines that recruit and increase the amount Tregs, as demonstrate by both *in vitro* protein array and patient sample immunohistochemistry (IHC). These findings suggest that pro-tumor NØ affects the CD73-Cyclin D-CDK4/6-PD-L1 pathway on tumor cells, visualized either *in vitro* with four cell lines, and with primary tumor inoculated in chicken embryo chorioallantoic membrane (CAM) assay. Therefore, the increase in CD73/PD-L1 expression contributes to tumor immune escape and to suppress immune response by the elevate production of ADO by the CD73 enzyme activity. Studies have been discussing the role of purinergic signaling, especially the upregulation of CD73 in tumor cells as key players in tumor progression in HNSCC (CAPPELLARI *et al.*, 2015; REN *et al.*, 2016).

CD73 plays a crucial role in the TME, with its upregulation linked to resistance against immunotherapy in a variety of cancer cells, including the ones in this thesis (HNSCC and GB) (THOMPSON; POWELL, 2021). Our data supports this by revealing concomitant increased CD73 and PD-L1 expression in NØ and tumor, contributing to an immunosuppressive TME. Moreover, inhibiting CD73 in NØ negatively affects the CD73-CyclinD-CDK4/6-PD-L1 pathway in tumor cells,

suggesting a potential therapeutic strategy. The differences in NØ response between healthy and pro-tumor states shown in this chapter directly affect tumor aggressiveness and immunosuppression in the TME. Briefly, we could observe in our data that these two phenotypes promote opposite reaction in tumor cells. Besides, despite a similar pattern in regulating the CD73-Cyclin D-CDK4/6-PD-L1 signaling in all four tumor cells, the modulation of the pro-tumor phenotype in NØ by SCC47-TEX does not consistently elicit a functional response related to cell proliferation, invasion and spreading in all these tested cell lines. This heterogeneity poses a challenge in developing drug delivery systems reliant on exosomes. However, targeted therapies involving CD73 alongside anti-PD-1 or PD-L1 show promise in both pre-clinical and clinical studies (BENDELL *et al.*, 2023; HERBST *et al.*, 2022; LAUBACH *et al.*, 2023).

NØ play a pivotal role in immunosuppression within the TME, and their lifespan is linked to this function. In cancer, NØ can exhibit prolonged survival, contributing to a state of chronic inflammation and immune evasion that supports tumor progression (GIESE; HIND; HUTTENLOCHER, 2019). The extended lifespan of TANs is often associated with deregulated signaling pathways, such as those involving cytokines like granulocyte colony-stimulating factor (G-CSF) and tumor-derived factors. These alterations not only promote NØ recruitment to tumors but also enhance their immunosuppressive properties (LE'NEGRATE *et al.*, 2003). Studying the mechanisms that support tumor progression, such as the extended lifespan of TANs, is crucial for advancing our understanding of cancer biology and developing effective therapeutic strategies.

Investigating how TANs acquire an extended lifespan within tumors can provide critical insights into immune evasion, tumor growth, and metastasis. With this regard, the following step was to assess cell death and survival pathways in TANs. Therefore, **chapter 04** explores the impact of HNSCC-TEX on NØ lifespan. TEX treatment prolongs NØ survival, highlighting the role of tumors in promoting NØ pro-tumor functions, such as sustaining immunosuppression and tumor malignancy.

The disruption of NØ apoptosis plays a significant role in the pathogenesis of chronic diseases. It is understood that molecular mechanisms that suppress

apoptosis are activated when they infiltrate damaged areas (NOSEYKINA; SCHEPETKIN; ATOCHIN, 2021). NØ typically have a short lifespan of around 24 hours in the bloodstream, thanks to tightly controlled programmed cell death processes involving both intrinsic and extrinsic apoptotic pathways (GIESE; HIND; HUTTENLOCHER, 2019; MCCRACKEN; ALLEN, 2014). Transcriptomic analysis shows that NØ generally follow a consistent path of development and maturation. However, their gene expression profiles differ depending on their maturity, the initial stimuli they receive, and the particular tissue where they are recruited (MCLAREN *et al.*, 2023). Single-cell RNA sequencing (scRNA-seq) studies conducted under both normal and inflammatory conditions, such as bacterial infection and cancer, have identified different subsets of NØ. These subsets exhibit specific functions such as promoting angiogenesis, proliferation, and invasion. Notably, these subsets exhibit common structural characteristics across different types of tumors (GUNGABEESOON *et al.*, 2023; XIE *et al.*, 2020). Therefore, we re-analyzed a previously published scRNA-seq dataset focused on HNSCC (KÜRTEN *et al.*, 2021) with a specific emphasis on identifying and characterizing NØ subpopulations and their lifespan-related pathways. Our analysis revealed eight distinct subpopulations exhibiting diverse gene expression profiles and associated functions. Clusters 0-5 displayed characteristics of canonical NØ activation with pro-inflammatory roles, whereas clusters 6 and 7 exhibited unique transcriptomic profiles potentially contributing to a pro-tumor phenotype. Notably, cluster 7 stood out for its activation of NF-κB signaling and presentation of a deregulated intrinsic apoptosis pathway, implicating it in cell survival mechanisms within the TME.

Our experimental *in vitro* findings demonstrate that TEX can extend the lifespan of NØ. Notably, we identified two ADO receptors, A2a and A3, as critical regulators of NØ survival. ADO within the TME serves as a crucial signaling molecule implicated in a range of physiological and pathological functions (AZAMBUJA *et al.*, 2019; CAMPOS-CONTRERAS; DÍAZ-MUÑOZ; VÁZQUEZ-CUEVAS, 2020). While ADO typically supports cell survival and tissue preservation, excessive extracellular ADO can activate the A3 and initiate apoptosis pathways. Activation of A3 stimulates downstream signaling cascades that can enhance the activation of caspases (AZAMBUJA *et al.*, 2019). Blocking specific ADO signaling

pathways affects NØ survival, revealing the intricate role of ADO receptors in shaping the TME. Here we describe that by blocking A2a decreased NØ lifespan, whereas blocking A3 increased it. Additionally, TEX treatment led to a significant reduction in levels of various proteins involved in the intrinsic apoptosis pathway within NØ, including the proteins caspase-3, Bcl-2, cytochrome C. This disruption of NØ apoptosis is particularly relevant in chronic diseases, as molecular mechanisms suppressing apoptosis are activated when neutrophils migrate to sites of tissue damage (NOSEYKINA; SCHEPETKIN; ATOCHIN, 2021). Moreover, our findings suggest an upregulation of NF-κB pathway in TEX-modulated NØ. This pathway is closely related to cell survival (RUBEL *et al.*, 2003). Besides, this chapter demonstrates that ADO receptors play a significant role in modulating NF-κB signaling in NØ through WB techniques, either activating or inhibiting it depending on the specific ADO receptor involved.

To that extent, Annexin-V/Pi assay data reveals that the majority of neutrophils exhibit prolonged lifespan, while those initiating cell death pathways prominently follow a necrotic trajectory. This observation prompts us to question whether this pattern could signify the release of NETs. These are web-like structures composed of chromatin (DNA) fibers, histones, and antimicrobial proteins. These structures are released in response to various stimuli, such as infections or inflammatory signals. The process of NETs formation, also known as NETosis, involves the activation of NØ leading to the expulsion of their DNA and associated proteins into the extracellular space (ERPENBECK; SCHÖN, 2017; HANN *et al.*, 2020).

Recent studies have emphasized the important role of EVs in inducing NET formation (SU *et al.*, 2023). The role of NETosis in cancer have been extensively described as tumor promoting function in TME in solid tumors and at the periphery in HNSCC (ARPINATI *et al.*, 2020; CHEN, Naifei; HE; CUI, 2022; DECKER *et al.*, 2019). With this regard, the **chapter 05** discourses that TEX effectively induce *in vitro* NETs release, contributing to inflammation and tissue damage. During our analysis of NETs markers like extracellular DNA, histone H3, elastase, and MMP-9, we identified three distinct bands in the MMP-9 protein profile representing different

isoforms: the precursor form (92 kDa), the active form (84 kDa), and a unique MMP-9 isoform (65 kDa). Notably, the 65 kDa MMP-9 isoform emerged as a valuable biomarker for tracking tumor progression, particularly from early neoplastic stages to metastasis (ROSSANO *et al.*, 2022). The dysregulation of MMP-9 and its isoforms suggests a potential biomarker for tumor progression in HNSCC. In addition, primary tumor inoculated in CAM reveals that TEX influence NETs to create an immune-evading environment characterized by increased expression of tumor PD-L1, and decrease of PD-1, tumor proliferation by increasing EGFR, and induction of EMT by raising the Vimentin and CD44 markers, for instance. Blocking ADO signaling directly impacts NETs markers associated with TEX, prompting discussion on ADO's role in modulating NØ phenotypes and activation. NØ metabolomics data suggests ADO signaling sustains NØ activation towards TEX. However, blocking the ADO receptors (P1) in NØ not only counteracts TEX-induced cell activation but also reduces NETs release markers, ultimately reversing tumor marker expression.

Besides, it is important to mention that NETs have been closely related to promoting angiogenesis (ALDABBOUS *et al.*, 2016). With this regard, our results demonstrate that the NETs enriched secretome promotes a shunting of blood vessels towards tumor, however, the intratumoral markers showed a reduction of new vessels formation, which can be explained by the presence of tumor necrosis, which was not evaluated in this thesis. The initiation and maintenance of angiogenesis are key characteristics of solid tumors. In HNSCC, various pro-angiogenic factors are found to be overexpressed, correlating with the advancement of a more aggressive disease phenotype (IDA MICAILY, 2020). Given the pivotal role of NØ in promoting angiogenesis and the previous findings indicating vessel dislocation towards, but not within, the tumor, **chapter 06** was conducted to assess the ability of TANs to induce tumorigenic angiogenesis.

In 1971, Folkman published a groundbreaking article suggesting that all tumors rely on angiogenesis for survival (SHERWOOD, L. M., PARRIS, E. E., & FOLKMAN, 1971). Angiogenesis, essential for supplying oxygen and nutrients from the bloodstream, is now recognized as a hallmark of cancer, preventing tumor

dormancy (HANAHAN; WEINBERG, 2011). The establishment of a functional vascular network is crucial for supporting the rapid proliferation of HNSCC cells (GONG *et al.*, 2023). However, tumor blood vessels often exhibit immaturity, impairing their proper function (VIALLARD; LARRIVÉE, 2017). Tumor microvasculature displays abnormal features, including high turnover of vessels, poor perfusion and increased leakage. A structurally and functionally defective tumor vasculature creates a permissive environment for cancer cells (HENDRY *et al.*, 2016). The improper angiogenesis can be partially attributed to abnormal secretion levels of growth factors, particularly VEGF and angiopoietins (Ang) (CARMELIET; JAIN, 2011).

In our study, the NØ protein secretome reveals the release of angiogenic proteins; however, the combination of the expression of these proteins contributes to deficient angiogenesis. The upregulation of Coagulation Factor III, Serpin E1 and TIMP-1 subsidize means to build a scaffold of new vessel by influencing extracellular matrix remodeling. Along with the downregulation of PTX3, FGF2, TSP-1, for example, are proteins that inhibit the angiogenesis process. These findings strongly indicate that TEX can induce a pro-tumor angiogenic phenotype in NØ, potentially promoting tumor progression. Our investigations demonstrated that TEX-mediated modulation of NØ secretome that in contact with CAM model resulted in a narrower main vessel and an increased number of microvessels, indicative of compromised pro-angiogenic potential. Furthermore, analysis of protein levels showed elevated concentrations of VEGF-A and Ang-2, suggesting a possible connection between TEX-modulated NØ and abnormal vasculature. This destabilization contributes to the formation of immature and leaky blood vessels in solid tumors (AUGUSTIN *et al.*, 2009; THOMAS; AUGUSTIN, 2009). Therefore, the dysregulation of VEGF-A and Ang-2 signaling in solid tumors leads to the development of abnormal vasculature, which not only impairs immunotherapy efficiency but also promotes tumor growth (LEONG; KIM, 2020). Moreover, these observations regarding protein deregulation in blood vessels were validated through *in vivo* experimentation using primary tumor inoculation in a CAM model. With this experiment, we aimed to increase the complexity of the environment and observe the synergistic effects of the tumor and the NØ secretome.

Normalizing tumor vasculature is a therapeutic strategy focused on restoring the integrity of blood vessels in the TME. In solid tumors like GB and HNSCC, abnormal vasculature results from rapid and chaotic angiogenesis driven by tumor-derived pro-angiogenic factors (GOEL; WONG; JAIN, 2012). This strategy aims to improve vessel quality to enhance oxygen, nutrient, and drug delivery while reducing hypoxia and acidosis. By targeting angiogenic pathways, the goal is to rebalance pro-angiogenic and anti-angiogenic factors to promote a more "normal" vascular phenotype resembling healthy tissue vasculature (AL-HUSEIN B, ABDALLA M, TREPTE M, DEREMER DL, 2013; QIAN, Chao Nan *et al.*, 2016). Antiangiogenic therapy relies on inhibiting VEGF signaling, crucial for tumor angiogenesis and metastasis (HENDRY *et al.*, 2016; STACKER; ACHEN, 2013). Solid tumors often exhibit overexpression of factors involved in the VEGF signaling pathway (CHOI; JUNG, 2023). Thus, in an effort to restore normal tumor vasculature, we investigated the inhibition of P1R in NØ angiogenic features. We found that, blocking P1R resulted in the normalization of angiogenesis-related proteins, specifically VEGF-A and Ang-2. This suggests that the formation of blood vessels becomes more regulated and balanced.

The first section clearly demonstrated diverse mechanisms through which TAN promote tumor progression and malignancy in HNSCC. A potential therapeutic target was identified in the impairment of ADO signaling in NØ to enhance tumor response to combined therapy. This section focused on elucidating interactions within the TME, highlighting the impact of TEX on various cellular processes. Effective crosstalk between tumor and surrounding cells shapes tissue function, supports tumor growth, and influences disease progression and patient prognosis. Our studies demonstrate the critical roles of TEX and NØ in driving the TME towards a pro-tumor state, emphasizing the therapeutic implications of targeting these interactions to disrupt tumor-supportive pathways involving NØ lifespan, apoptotic pathways, and angiogenic potential.

The second section of this thesis aimed to explore if NØ reproduce similar outcomes in glioblastoma. In GB, there is a high infiltration of NØ associated with a significant increase in circulating NØ (WENG *et al.*, 2018). The damage to the blood-

brain barrier caused by chronic inflammation promotes the infiltration of non-routine inflammatory cells into the brain, constituting the previous described *cold tumor* TME. It has been observed that tumor cells influence the release of G-CSF and the maturation of NØ in the bone marrow, inducing their migration into the peripheral blood (PEREZ-DE-PUIG *et al.*, 2015; RODRIGUES; GRANGER, 2015). GB exists within a complex and heterogeneous TME where immune cells play a significant role. The importance of the interaction between NØ and GB is increasingly recognized, where crosstalk may efficiently contribute to tumor progression, highlighting a potential therapeutic target (CHEN, Zhihong; HAMBARDZUMYAN, 2018).

Therefore, the **chapter 07** aimed to investigate the dynamics of interaction between NØ and glioma cells within the TME, focusing on understanding how these interactions contribute to tumor progression and modulation of immune responses. The findings suggest that the long exposure of NØ to glioma cells is critical in determining their role in tumor progression. Initially, NØ exhibit anti-tumor effects, but over time, they are reprogrammed by glioma cells, ultimately promoting tumor growth. Moreover, the time-dependent modulation indicated an increase in challenged NØ. Our data determined that in vitro NØ increase their life-spam when interacting with glioma cell line. Indeed, NØ have a longer life-spam than previously thought, and increasing evidence indicates their plasticity and capacity to alter their phenotype based on the tissue environment (DUMITRU; LANG; BRANDAU, 2013; GIESE; HIND; HUTTENLOCHER, 2019; LIEW; KUBES, 2019).

The study also revealed increased necrosis in a 3D model in the presence of NØ, potentially indicating a poor prognosis for glioma patients. Furthermore, the study highlighted the importance of cytokine release, such as IL-8, IL-1 β and IL-10, and metabolic changes, as an example the increase in lactate production, in the TME induced by NØ-glioma cell interactions, contributing to immune suppression and chronic inflammation conducive to tumor progression. The TME is characterized by the presence of various cytokines and chemokines produced by tumor cells, immune cells, and stromal cells (NØRØXE; POULSEN; LASSEN, 2016). Cytokines like TNF-α and IL-1β, known for their pro-inflammatory effects, along with IL-10,

which has immunosuppressive properties, are frequently detected in the TME (RAHBAR *et al.*, 2016). Our findings indicate that glioma patients experience a significant negative impact related to cytokine high levels, particularly IL-1β and IL-10, which are associated with poorer outcomes.

In addition, this chapter shows that the energy metabolism of glioma cells shifts due to glioma-neutrophil interactions. This can be observed by mitochondrial recovery after culture with neutrophils for 120 h, along with a reduction of membrane potential, indicating dysfunctional organelles. Besides, the increase in lactate production corroborates with this metabolic turnover and strengthen immunosuppression. With this regard, it was already described that tumor cells adapt their metabolism to rapidly generate energy and produce biosynthetic materials essential for growth. This reprogramming enables cancer cells to meet their energy demands and generate biomolecular precursors essential for rapid proliferation (BERNHARD *et al.*, 2023; LANDIS *et al.*, 2018). GB cells, similar to other cancer cells, heavily rely on glycolysis for energy even in the presence of functional mitochondria, a phenomenon known as the Warburg effect (LAUBACH *et al.*, 2023; STRICKLAND; STOLL, 2017). This metabolic shift involves increased glucose uptake and lactate production. Aerobic glycolysis generates less energy than oxidative metabolism but enables cancer cells to quickly convert resources into biomass (lipids, nucleotides, amino acids). This adaptation is crucial for cancer cell survival and proliferation, especially under hypoxic conditions (HEIDEN *et al.*, 2009). Moreover, enhanced acidification of TME promotes tumor invasion while inhibiting immune cell function, contributing to immune evasion (QUIROGA *et al.*, 2022).

To this end, we chose to focus on the ADO signaling pathway in NØ as it plays a key role in the phenotypic modulation of TANs. Our attention to this pathway is driven by its significant physiological role in our cells and its influence on the expression and activity of enzymes related to ADO production in the TME. Therefore, **chapter 8** focuses on the interplay between CD73 and PD-L1 within the TME, highlighting a coordinated effort to suppress immune responses, wherein pro-tumor NØ may significantly contribute to promoting immunosuppression. As for this, both *in vitro* studies and clinical samples from patients with grade IV glioma show a

coordinated upregulation of *ADORA1*, *NT5E*, and *ADORA2A* genes. In contrast, grade II and III gliomas exhibit high expression of *ADORA2B* and *ADORA3*. This differential expression suggests distinct adenosine receptor profiles and signaling pathways between high-grade and lower-grade gliomas.

High-grade tumors exhibit elevated expression of PD-L1, CD73, E-cadherin, and Rel-A, with CD73 and PD-L1 playing immunomodulatory roles. Moreover, elevated *NT5E* expression in NØ correlates with higher tumor PD-L1 expression, contributing to T cell exhaustion. High concentrations of ADO, together with ROS production by NØ modulation and alterations in tumor metabolism and biology, by decrease of PTEN expression for example, the immunosuppressive system is well-organized, allowing the tumor to use proteins typically associated with immune evasion, such as PD-L1, in a manner more focused on promoting tumor proliferation. Recent studies reveal various subcellular localizations of PD-L1, including nuclear, cytoplasmic, and soluble forms (NIU *et al.*, 2022). This subcellular localization has been observed to influence increased in HNSCC tumor malignancy by inducing radioresistance, invasiveness, migration, and cell survival (EICHBERGER *et al.*, 2020; SCHULZ, D. *et al.*, 2021; SCHULZ, Daniela *et al.*, 2023). Indeed, our findings show predominant cytoskeletal and nuclear PD-L1 in glioma patients, with higher nuclear PD-L1 in grade IV tumors correlating with increased proliferation and a high NLR. Nuclear PD-L1 (<150kDa) contribute to tumor cell survival and resistance (SCHULZ, D. *et al.*, 2021). Elevated nuclear PD-L1 is linked to increased neoantigen presentation, possibly explaining the responsiveness of high PD-L1 patients to PD-1/PD-L1 therapies.

Further analysis is required to thoroughly investigate the elevated high molecular weight PD-L1 band (~150kDa) and elucidate the factors contributing to this observation. The PD-L1 protein is encoded by the *CD274* gene (HGNC: 17635; ENSG00000120217) located on chromosome 9p24.1. This gene produces two main alternative transcripts. The longest transcript (3.6 kbp; NCBI: NM_014143.3; ENST00000381577.3) encodes a 290-amino acid protein (NCBI: NP_054862), while the shorter transcript (3.3 kbp; NM_001267706.1) encodes a 176-amino acid isoform (NP_001254635). The longest transcript has seven exons, with a coding

sequence around 800 bp long, and encodes a 33kDa PD-L1 protein. This protein includes two immunoglobulin domains: V-like and C-like while the shorter transcript lacks exon 3, resulting in a PD-L1 isoform without the IgV-like domain (FABRIZIO FP, TROMBETTA D, ROSSI A, SPARANEO A, CASTELLANA S, 2018). To understand why the protein found in the nuclear fraction is larger than what is usually observed (> 150kDa). RNA sequencing could provide some explanations if deletions, insertions, or duplications are found along the nucleotide chain. If such variations are present, they could explain the elongation of the peptide chain, which could lead to a range of functional abnormalities or overexpression. However, if no such variations are found, the hypothesis of a genetic alteration might be ruled out, and the observed length could possibly be explained by the post-translational modifications or multimers.

In its typical form, PD-L1 weighs around 40-50kDa, however, this weight can increase significantly due to glycosylation. It can substantially augment the molecular weight of PD-L1, leading to sizes reaching 60-70kDa or more (PARRA; VILLALOBOS; RODRIGUEZ-CANALES, 2019; ZHOU *et al.*, 2022). Notably, Yu et al. proposed an intriguing hypothesis suggesting that nuclear PD-L1 (> 150kDa on immunoblots) undergoes more complex glycosylation than plasma membrane PD-L1 (~50kDa). It is suggest that nuclear PD-L1 may undergo extensive glycosylation after translation in the endoplasmic reticulum and Golgi apparatus, followed by direct transport into the nucleus via binding to glycosylation binding proteins (YU *et al.*, 2020). However, Schulz et al. have contested this hypothesis. Through an alternative approach involving heat disruption at 95°C for varying durations, they observed that over time, immunodetection of PD-L1 bands exceeding 150kDa decreased, while detection of the approximately 70kDa band intensified. This specific response to heat disruption suggests that PD-L1 multimerization, rather than glycosylation alone, is likely responsible for the observed high molecular weight. Moreover, this study assessed the nuclear PD-L1 binding partners attesting interactions with proteins primarily associated with DNA remodeling and mRNA splicing (SCHULZ, Daniela *et al.*, 2023).

The link between ADO-related gene expression in NØ and tumor markers such as nuclear PD-L1 and CD73 emphasizes the complex interactions within TME. ADO signaling and immune evasion mechanisms are also influenced by NØ, which play a role in maintaining immunosuppression and promoting tumor growth.

To that extent, NØ impact extends beyond secreting chemokines and cytokines to recruit regulatory cells, as they also play a critical role in shaping the TME by promoting angiogenesis, degrading the extracellular matrix, and facilitating metastasis (HURT *et al.*, 2017; MASUCCI; MINOPOLI; CARRIERO, 2019a). Several studies have discussed the phenotypic changes in NØ (GRANOT, 2019; GRANOT; JABLONSKA, 2015; LECOT *et al.*, 2019a; RAPOPORT *et al.*, 2020). While most studies focus on protein markers, secretome, or underlying mechanisms, pro-tumor NØ have been visually depicted with altered nuclei shapes compared to pro-inflammatory NØ (GRANOT; JABLONSKA, 2015; MASUCCI; MINOPOLI; CARRIERO, 2019b). This graphical representation suggests that not only does the phenotype change, but the nuclei are also affected by this specific activation. The **chapter 09** aimed to investigate the morphological changes in NØ nuclei and their correlation with clinical outcomes, particularly in glioblastoma patients. The classical morphology of NØ nuclei typically consists of multilobulated structures with 3 to 4 lobules separated by constrictions, which can increase to more than 5 lobules during inflammatory conditions like bacterial infections (SKINNER; JOHNSON, 2017). The hypothesis was that pro-tumor NØ undergo nuclear reshaping characterized by a unique morphology associated with poor prognosis. *In vitro* experiments revealed that chemical induction of NØ polarization led to significant nuclei enlargement, although visual observations did not show prominent changes upon direct contact with the U87MG tumor cell line. Notably, the most significant nuclei reshaping was observed in glioblastoma patients, showing a loss of constrictions and the presence of amorphous nuclei resembling immature NØ associated with bacterial infection. The study conducted a correlation analysis between nuclei enlargement and NLR, recurrence status and overall survival for each patient, revealing a significant positive correlation for increasing NLR and recurrence rate, while reducing drastically probability of survival. This indicates that amorphous nuclei shape and enlargement could serve as biomarkers for tumor

strength in modulating immune cells, with potential implications for guiding medical decisions and predicting prognosis in GB patients.

It would be advantageous to track tumor development and treatment outcomes using a non-invasive test that can be conducted regularly at a reasonable cost, such as a blood test. New technologies that leverage improved knowledge of immune responses to tumors and AI are emerging to discover diagnostic and prognostic markers integrated into contemporary medical practices (RAMÓN *et al.*, 2020). Considering the morphological adaptability exhibited by NØ in reaction to stimuli released by tumors, we suggest that these traits could be utilized to identify the anti- or pro-tumor tendencies of these immune cells in the bloodstream of cancer patients through AI methods. Therefore, **chapter 10** focuses on identifying changes in cellular structure using computerized medical image analysis aided by machine learning (ML) techniques to classify and detect the polarization of peripheral NØ in GB patients. Despite the software still being in the refinement phase, and the prototype not delivering results at the expected rate, this approach offers an improved method for analyzing outcomes and devising patient care strategies, facilitating simplified progress monitoring.

In this second section, the chapters highlight the dynamic nature of these interactions, where NØ initially exhibit anti-tumor effects but become reprogrammed over time, ultimately promoting tumor growth and contributing to poor clinical outcomes. Besides, the integration of advanced technologies, such as AI-driven image analysis, holds promise for leveraging TAN phenotypic changes as diagnostic and prognostic biomarkers, ultimately advancing personalized cancer care.

CONCLUSION

In conclusion, this thesis provides substantial evidence supporting the intricate cross-communication between tumor cells and NØ, facilitated through direct contact, exosomal interactions, and/or secreted factors. Notably, within the contexts of both HNSCC and GB, observations reveal a pivotal role for NØ modulation towards a pro-tumor phenotype, significantly driving tumor progression. This phenomenon manifests through enhanced tumorigenic angiogenesis, metastasis, tumor evasion, growth promotion, and immunosuppression. Moreover, the correlation between NØ morphology and clinical outcomes highlights the potential novel prognostic biomarker. Altogether, this thesis advances our understanding of the crucial role played by TAN in facilitating and accelerating tumor progression, thereby contributing significantly to the field of cancer biology and clinical management strategies.

The bidirectional modulation of TANs not only reinforces the complexity of tumor biology but also opens new avenues for therapeutic intervention. By elucidating the mechanisms through which NØ support tumor growth and identifying their potential as prognostic markers, this research lays the groundwork for future studies aimed at targeting NØ-tumor interactions. Lastly, these findings indicates the importance of developing strategies to modulate NØ activity within the TME.

PERSPECTIVES

1. One promising avenue for future research involves developing a project aimed at utilizing the phenotypic modulation of NØ through the blockade of CD73. This can be achieved by employing siRNA to inhibit CD73 expression in NØ . The primary objective of this research will be to assess the impact of NØ CD73 removal to tumor progression. By understanding the role of NØ in the tumor microenvironment, we can explore their potential as an adjuvant immunotherapy. This approach could open new pathways for cancer treatment by leveraging the body's immune system to combat tumor growth more effectively.

2. Building on the findings observed in glioblastoma (GB) patients, future research should focus on investigating the nuclear band of PD-L1, which appears at a molecular weight greater than 150kDa. The aim is to elucidate the reasons behind its elevated molecular weight and to determine whether it interacts with partner proteins. Additionally, understanding the integrated function of this form of PD-L1 in modulating tumor biology will provide deeper insights into its role in glioblastoma. This knowledge could contribute to the development of more targeted and effective therapies for GB patients.

3. To further improve the prognostic capabilities of the software developed during this study, future efforts should focus on incorporating a comprehensive database of images of healthy NØ . These images can then be compared with those of NØ from patients, allowing for a more robust analysis and validation of the software's accuracy. Moreover, conducting a clinical study to evaluate the software's feasibility and effectiveness as a prognostic tool is essential. This clinical validation will not only strengthen the software's reliability but also pave the way for its potential adoption in clinical settings, ultimately improving patient outcomes through better diagnostic precision.

REFERÊNCIAS

AL-HUSEIN B, ABDALLA M, TREPTE M, DEREMER DL, Somanath PR. Anti-angiogenic therapy for cancer : An update. **Pharmacotherapy**, vol. 32, no. 12, p. 1095–1111, 2013. https://doi.org/10.1002/phar.1147.

ALDABBOUS, Lulwah; ABDUL-SALAM, Vahitha; MCKINNON, Tom; DULUC, Lucie; PEPKE-ZABA, Joanna; SOUTHWOOD, Mark; AINSCOUGH, Alexander J.; HADINNAPOLA, Charaka; WILKINS, Martin R.; TOSHNER, Mark; WOJCIAK-STOTHARD, Beata. Neutrophil extracellular traps promote angiogenesis. **Arteriosclerosis, Thrombosis, and Vascular Biology**, vol. 36, no. 10, p. 2078–2087, 2016. https://doi.org/10.1161/ATVBAHA.116.307634.

ALLARD, Bertrand; LONGHI, Maria Serena; ROBSON, Simon C.; STAGG, John. The ectonucleotidases CD39 and CD73: Novel checkpoint inhibitor targets. **Immunological Reviews**, vol. 276, no. 1, p. 121–144, 2017. https://doi.org/10.1111/imr.12528.

ALLARD, David; CHROBAK, Pavel; ALLARD, Bertrand; MESSAOUDI, Nouredin; STAGG, John. Targeting the CD73-adenosine axis in immuno-oncology. **Immunology Letters**, vol. 205, no. May 2018, p. 31–39, 2019. DOI 10.1016/j.imlet.2018.05.001. Available at: https://doi.org/10.1016/j.imlet.2018.05.001.

ALMEIDA, Vitor H.; RONDON, Araci M. R.; GOMES, Tainá; MONTEIRO, Robson Q. Novel Aspects of Extracellular Vesicles as Mediators of Cancer-Associated Thrombosis. **Cells**, vol. 8, no. 7, p. 716, 2019. https://doi.org/10.3390/cells8070716.

AMULIC;, B.; SOLLBERGER, Gabriel. Why Immune Cells Extrude Webs of DNA and Protein. NETS: two faced players in Immunity. **The Scientist**, vol. 33, p. 44–51, 2018. .

ARAB, Samaneh; HADJATI, Jamshid. Adenosine blockage in tumor microenvironment and improvement of cancer immunotherapy. **Immune Network**,

vol. 19, no. 4, p. 1–19, 2019. https://doi.org/10.4110/in.2019.19.e23.

ARPINATI, Ludovica; SHAUL, Merav E.; KAISAR-ILUZ, Naomi; MALI, Shira; MAHROUM, Sojod; FRIDLENDER, Zvi G. NETosis in cancer: a critical analysis of the impact of cancer on neutrophil extracellular trap (NET) release in lung cancer patients vs. mice. **Cancer Immunology, Immunotherapy**, vol. 69, no. 2, p. 199–213, 2020. DOI 10.1007/s00262-019-02474-x. Available at: https://doi.org/10.1007/s00262-019-02474-x.

AUGUSTIN, Hellmut G.; YOUNG KOH, Gou; THURSTON, Gavin; ALITALO, Kari. Control of vascular morphogenesis and homeostasis through the angiopoietin - Tie system. **Nature Reviews Molecular Cell Biology**, vol. 10, no. 3, p. 165–177, 2009. https://doi.org/10.1038/nrm2639.

AZAMBUJA, Juliana Hofstätter; LUDWIG, Nils; BRAGANHOL, Elizandra; WHITESIDE, Theresa L. Inhibition of the adenosinergic pathway in cancer rejuvenates innate and adaptive immunity. **International Journal of Molecular Sciences**, vol. 20, no. 22, 2019. https://doi.org/10.3390/ijms20225698.

BAKEMA, Jantine E.; GANZEVLES, Sonja H.; FLUITSMA, Donna M.; SCHILHAM, Marco W.; BEELEN, Robert H. J.; VALERIUS, Thomas; LOHSE, Stefan; GLENNIE, Martin J.; MEDEMA, Jan Paul; VAN EGMOND, Marjolein. Targeting FcαRI on Polymorphonuclear Cells Induces Tumor Cell Killing through Autophagy. **The Journal of Immunology**, vol. 187, no. 2, p. 726–732, 2011. https://doi.org/10.4049/jimmunol.1002581.

BALKWILL, Fran; MANTOVANI, Alberto. Inflammation and cancer: back to Virchow? **Lancet**, vol. 357, no. 9255, p. 539–545, 2001. https://doi.org/10.1016/S0140-6736(00)04046-0.

BALLESTEROS, Iván; RUBIO-PONCE, Andrea; GENUA, Marco; LUSITO, Eleonora; KWOK, Immanuel; FERNÁNDEZ-CALVO, Gabriel; KHOYRATTY, Tariq E.; VAN GRINSVEN, Erinke; GONZÁLEZ-HERNÁNDEZ, Sara; NICOLÁS-ÁVILA, José Ángel; VICANOLO, Tommaso; MACCATAIO, Antonio; BENGURÍA, Alberto; LI, Jackson Liang Yao; ADROVER, José M.; AROCA-CREVILLEN, Alejandra;

QUINTANA, Juan A.; MARTÍN-SALAMANCA, Sandra; MAYO, Francisco; … HIDALGO, Andrés. Co-option of Neutrophil Fates by Tissue Environments. **Cell**, vol. 183, no. 5, p. 1282-1297.e18, 2020. https://doi.org/10.1016/j.cell.2020.10.003.

BARCELLOS-HOFF, Mary Helen; LYDEN, David; WANG, Timothy C. The evolution of the cancer niche during multistage carcinogenesis. **Nature Publishing Group**, vol. 13, no. July, p. 511–518, 2013. https://doi.org/10.1038/nrc3536.

BASANTA, David; ANDERSON, Alexander R.A. Homeostasis back and forth: An ecoevolutionary perspective of cancer. **Cold Spring Harbor Perspectives in Medicine**, vol. 7, no. 9, p. 1–19, 2017. https://doi.org/10.1101/cshperspect.a028332.

BEBELMAN, Maarten P.; SMIT, Martine J.; PEGTEL, D. Michiel; BAGLIO, S. Rubina. Biogenesis and function of extracellular vesicles in cancer. **Pharmacology and Therapeutics**, vol. 188, p. 1–11, 2018. DOI 10.1016/j.pharmthera.2018.02.013. Available at: https://doi.org/10.1016/j.pharmthera.2018.02.013.

BEHRENS, Leonie M.; VAN EGMOND, Marjolein; VAN DEN BERG, Timo K. Neutrophils as immune effector cells in antibody therapy in cancer. **Immunological Reviews**, vol. 314, no. 1, p. 280–301, 2023. https://doi.org/10.1111/imr.13159.

BENDELL, Johanna; LORUSSO, Patricia; OVERMAN, Michael; NOONAN, Anne M.; KIM, Dong Wan; STRICKLER, John H.; KIM, Sang We; CLARKE, Stephen; GEORGE, Thomas J.; GRIMISON, Peter S.; BARVE, Minal; AMIN, Manik; DESAI, Jayesh; WISE-DRAPER, Trisha; ECK, Steven; JIANG, Yu; KHAN, Anis A.; WU, Yuling; MARTIN, Philip; … PATEL, Sandip Pravin. First-in-human study of oleclumab, a potent, selective anti-CD73 monoclonal antibody, alone or in combination with durvalumab in patients with advanced solid tumors. **Cancer Immunology, Immunotherapy**, vol. 72, no. 7, p. 2443–2458, 2023. DOI 10.1007/s00262-023-03430-6. Available at: https://doi.org/10.1007/s00262-023-

03430-6.

BERNARD, Cassandra Ringuette Goulet Genevieve; TREMBLAY, Sarah; CHABAUD, Stephane; BOLDUC, Stephane; POULIOT, Frederic. Exosomes Induce Fibroblast Differentiation into Cancer-Associated Fibroblasts through TGF b Signaling d e. **Molecular Cancer Research**, vol. 16, no. 7, p. 1196–1204, 2018. https://doi.org/10.1158/1541-7786.MCR-17-0784.

BERNHARD, Chlo; REITA, Damien; MARTIN, Sophie; ENTZ-WERLE, Natacha. Glioblastoma Metabolism: Insights and Therapeutic Strategies. **International Journal of Molecular Sciences**, vol. 24, no. 11, 2023. https://doi.org/10.3390/ijms24119137.

BONECCHI, Raffaella; MANTOVANI, Alberto; JAILLON, Sebastien. Chemokines as Regulators of Neutrophils: Focus on Tumors, Therapeutic Targeting, and Immunotherapy. **Cancers**, vol. 14, no. 3, p. 1–19, 2022. https://doi.org/10.3390/cancers14030680.

BOOMGARDEN, Alex C.; SHEEHAN, Colin; D'SOUZA-SCHOREY, Crislyn. Extracellular Vesicles in the Tumor Microenvironment: Various Implications in Tumor Progression. **Advances in Experimental Medicine and Biology**, vol. 1259, p. 155–170, 2020. https://doi.org/10.1007/978-3-030-43093-1_9.

BUI, Triet M.; MASCARENHAS, Lorraine A.; SUMAGIN, Ronen. Extracellular vesicles regulate immune responses and cellular function in intestinal inflammation and repair. **Tissue Barriers**, vol. 6, no. 2, p. 1–14, 2018. DOI 10.1080/21688370.2018.1431038. Available at: https://doi.org/10.1080/21688370.2018.1431038.

CAMPOS-CONTRERAS, Anaí Del Rocío; DÍAZ-MUÑOZ, Mauricio; VÁZQUEZ-CUEVAS, Francisco G. Purinergic Signaling in the Hallmarks of Cancer. **Cells**, vol. 9, no. 7, p. 1–24, 2020. https://doi.org/10.3390/cells9071612.

CAPPELLARI, Angélica R.; PILLAT, Micheli M.; SOUZA, Hellio D.N.; DIETRICH, Fabrícia; OLIVEIRA, Francine H.; FIGUEIRÓ, Fabrício; ABUJAMRA, Ana L.;

ROESLER, Rafael; LECKA, Joanna; SÉVIGNY, Jean; BATTASTINI, Ana Maria O.; ULRICH, Henning. Ecto-5′-nucleotidase overexpression reduces tumor growth in a xenograph medulloblastoma model. **PLoS ONE**, vol. 10, no. 10, p. 1–18, 2015. https://doi.org/10.1371/journal.pone.0140996.

CARMELIET, Peter; JAIN, Rakesh K. Molecular mechanisms and clinical applications of angiogenesis. **Nature**, vol. 473, no. 7347, p. 298–307, 2011. https://doi.org/10.1038/nature10144.

CARNEVALE, Silvia; GHASEMI, Somayehsadat; RIGATELLI, Anna; JAILLON, Sebastien. The complexity of neutrophils in health and disease : Focus on cancer. **Seminars in Immunology**, 2020. https://doi.org/https://doi.org/10.1016/j.smim.2020.101409 Get rights and content.

CERVANTES-VILLAGRANA, Rodolfo Daniel; ALBORES-GARCÍA, Damaris; CERVANTES-VILLAGRANA, Alberto Rafael; GARCÍA-ACEVEZ, Sara Judit. Tumor-induced neurogenesis and immune evasion as targets of innovative anti-cancer therapies. **Signal Transduction and Targeted Therapy**, vol. 5, no. 1, 2020. DOI 10.1038/s41392-020-0205-z. Available at: http://dx.doi.org/10.1038/s41392-020-0205-z.

CHEN, Daniel S; MELLMAN, Ira. Elements of cancer immunity and the cancer – immune set point. **Nature**, vol. 541, no. 7637, p. 321–330, 2017. https://doi.org/10.1038/nature21349.

CHEN, Naifei; HE, Dongsheng; CUI, Jiuwei. A Neutrophil Extracellular Traps Signature Predicts the Clinical Outcomes and Immunotherapy Response in Head and Neck Squamous Cell Carcinoma. **Frontiers in Molecular Biosciences**, vol. 9, no. February, p. 1–18, 2022. https://doi.org/10.3389/fmolb.2022.833771.

CHEN, Yu; YAO, Yongli; SUMI, Yuka; LI, Andrew; KIM TO, Uyen; ELKHAL, Abdallah; INOUE, Yoshiaki; WOEHRLE, Tobias; ZHANG, Qin; HAUSER, Carl; JUNGER, Wolfgang G. Purinergic signaling: A fundamental mechanism in neutrophil activation. **Science Signaling**, vol. 3, no. 125, 2010. https://doi.org/10.1126/scisignal.2000549.

CHEN, Zhihong; HAMBARDZUMYAN, Dolores. Immune microenvironment in glioblastoma subtypes. **Frontiers in Immunology**, vol. 9, no. MAY, p. 1–8, 2018. https://doi.org/10.3389/fimmu.2018.01004.

CHOI, Yechan; JUNG, Keehoon. Normalization of the tumor microenvironment by harnessing vascular and immune modulation to achieve enhanced cancer therapy. **Experimental & Molecular Medicine**, vol. 55, no. July, p. 2308–2319, 2023. https://doi.org/https://doi.org/10.1038/s12276-023-01114-w.

COOLS-LARTIGUE, Jonathan; SPICER, Jonathan; NAJMEH, Sara; FERRI, Lorenzo. Neutrophil extracellular traps in cancer progression. **Cellular and Molecular Life Sciences**, vol. 71, no. 21, p. 4179–4194, 2014. https://doi.org/10.1007/s00018-014-1683-3.

CORRIDEN, Ross; CHEN, Yu; INOUE, Yoshiaki; BELDI, Guido; ROBSON, Simon C.; INSEL, Paul A.; JUNGER, Wolfgang G. Ecto-nucleoside triphosphate diphosphohydrolase 1 (E-NTPDase1/CD39) regulates neutrophil chemotaxis by hydrolyzing released ATP to adenosine. **Journal of Biological Chemistry**, vol. 283, no. 42, p. 28480–28486, 2008. https://doi.org/10.1074/jbc.M800039200.

DE LEVE, Simone; WIRSDÖRFER, Florian; JENDROSSEK, Verena. Targeting the immunomodulatory CD73/adenosine system to improve the therapeutic gain of radiotherapy. **Frontiers in Immunology**, vol. 10, no. APR, 2019. https://doi.org/10.3389/fimmu.2019.00698.

DECKER, Anna Sophie; PYLAEVA, Ekaterina; BRENZEL, Alexandra; SPYRA, Ilona; DROEGE, Freya; HUSSAIN, Timon; LANG, Stephan; JABLONSKA, Jadwiga. Prognostic role of blood NETosis in the progression of head and neck cancer. **Cells**, vol. 8, no. 9, p. 1–15, 2019. https://doi.org/10.3390/cells8090946.

DEMERS, Melanie; WAGNER, Denisa D. NETosis: A new factor in tumor progression and cancer-associated thrombosis. **Seminars in Thrombosis and Hemostasis**, vol. 40, no. 3, p. 277–283, 2014. https://doi.org/10.1055/s-0034-1370765.

DI VIRGILIO, Francesco; VUERICH, Marta. Purinergic signaling in the immune system. **Autonomic Neuroscience: Basic and Clinical**, vol. 191, p. 117–123, 2015. DOI 10.1016/j.autneu.2015.04.011. Available at: http://dx.doi.org/10.1016/j.autneu.2015.04.011.

DOSCH, Michel; GERBER, Joël; JEBBAWI, Fadi; BELDI, Guido. Mechanisms of ATP release by inflammatory cells. **International Journal of Molecular Sciences**, vol. 19, no. 4, p. 1–16, 2018. https://doi.org/10.3390/ijms19041222.

DUMITRU, Claudia A.; LANG, Stephan; BRANDAU, Sven. Modulation of neutrophil granulocytes in the tumor microenvironment: Mechanisms and consequences for tumor progression. **Seminars in Cancer Biology**, vol. 23, no. 3, p. 141–148, 2013. DOI 10.1016/j.semcancer.2013.02.005. Available at: http://dx.doi.org/10.1016/j.semcancer.2013.02.005.

EICHBERGER, Jonas; SCHULZ, Daniela; PSCHEIDL, Kristian; FIEDLER, Mathias; REICHERT, Torsten Eugen; BAUER, Richard Josef; ETTL, Tobias. PD-L1 influences cell spreading, migration and invasion in head and neck cancer cells. **International Journal of Molecular Sciences**, vol. 21, no. 21, p. 1–17, 2020. https://doi.org/10.3390/ijms21218089.

EL-BENNA, Jamel; HURTADO-NEDELEC, Margarita; MARZAIOLI, Viviana; MARIE, Jean Claude; GOUGEROT-POCIDALO, Marie Anne; DANG, Pham My Chan. Priming of the neutrophil respiratory burst: role in host defense and inflammation. **Immunological Reviews**, vol. 273, no. 1, p. 180–193, 2016. https://doi.org/10.1111/imr.12447.

ERPENBECK, L.; SCHÖN, M. P. Neutrophil extracellular traps: Protagonists of cancer progression? **Oncogene**, vol. 36, no. 18, p. 2483–2490, 2017. DOI 10.1038/onc.2016.406. Available at: http://dx.doi.org/10.1038/onc.2016.406.

ERUSLANOV, Evgeniy B.; BHOJNAGARWALA, Pratik S.; QUATROMONI, Jon G.; STEPHEN, Tom Li; RANGANATHAN, Anjana; DESHPANDE, Charuhas; AKIMOVA, Tatiana; VACHANI, Anil; LITZKY, Leslie; HANCOCK, Wayne W.; CONEJO-GARCIA, José R.; FELDMAN, Michael; ALBELDA, Steven M.;

SINGHAL, Sunil. Tumor-associated neutrophils stimulate T cell responses in early-stage human lung cancer. **Journal of Clinical Investigation**, vol. 124, no. 12, p. 5466–5480, 2014. https://doi.org/10.1172/JCI77053.

FABRIZIO FP, TROMBETTA D, ROSSI A, SPARANEO A, CASTELLANA S, Muscarella LA. Gene code CD274/PD-L1: from molecular basis toward cancer immunotherapy. **Therapeutic Advances in Medical Oncology**, vol. Dec, 2018. https://doi.org/10.1177/1758835918815598.

FENG, Wenlong; DEAN, Dylan C.; HORNICEK, Francis J.; SHI, Huirong; DUAN, Zhenfeng. Exosomes promote pre-metastatic niche formation in ovarian cancer. **Molecular Cancer**, vol. 18, no. 1, p. 1–11, 2019. https://doi.org/10.1186/s12943-019-1049-4.

FIANI, Maria Luisa; BARRECA, Valeria; SARGIACOMO, Massimo; FERRANTELLI, Flavia; MANFREDI, Francesco; FEDERICO, Maurizio. Exploiting manipulated small extracellular vesicles to subvert immunosuppression at the tumor microenvironment through mannose receptor/CD206 targeting. **International Journal of Molecular Sciences**, vol. 21, no. 17, p. 1–20, 2020. https://doi.org/10.3390/ijms21176318.

FIEDLER, Mathias; SCHULZ, Daniela; PIENDL, Gerhard; BROCKHOFF, Gero; EICHBERGER, Jonas; MENEVSE, Ayse Nur; BECKHOVE, Philipp; HAUTMANN, Matthias; REICHERT, Torsten E.; ETTL, Tobias; BAUER, Richard J. Buparlisib modulates PD-L1 expression in head and neck squamous cell carcinoma cell lines. **Experimental Cell Research**, vol. 396, no. 1, p. 112259, 2020. DOI 10.1016/j.yexcr.2020.112259. Available at: https://doi.org/10.1016/j.yexcr.2020.112259.

FRANCIS, Nikita; BORNIGER, Jeremy C. Cancer as a homeostatic challenge: the role of the hypothalamus. **Trends in Neurosciences**, vol. 44, no. 11, p. 903–914, 2021. https://doi.org/10.1016/j.tins.2021.08.008.

GALDIERO, Maria Rosaria; VARRICCHI, Gilda; LOFFREDO, Stefania; MANTOVANI, Alberto; MARONE, Gianni. Roles of neutrophils in cancer growth

and progression. **Journal of Leukocyte Biology**, vol. 103, no. 3, p. 457–464, 2018. https://doi.org/10.1002/JLB.3MR0717-292R.

GELSLEICHTER, Nicolly Espindola; AZAMBUJA, Juliana Hofstätter; RUBENICH, Dominique Santos; BRAGANHOL, Elizandra. CD73 in glioblastoma: Where are we now and what are the future directions? **Immunology Letters**, vol. 256–257, no. January, p. 20–27, 2023. https://doi.org/10.1016/j.imlet.2023.03.005.

GIESE, Morgan A.; HIND, Laurel E.; HUTTENLOCHER, Anna. Neutrophil plasticity in the tumor microenvironment. **Blood**, vol. 133, no. 20, p. 2159–2167, 2019. https://doi.org/10.1182/blood-2018-11-844548.

GIULIANI, Anna Lisa; SARTI, Alba Clara; DI VIRGILIO, Francesco. Ectonucleotidases in Acute and Chronic Inflammation. **Frontiers in pharmacology**, vol. 11, p. 619458, 2020. https://doi.org/10.3389/fphar.2020.619458.

GOEL, Shom; WONG, Andus Hon Kit; JAIN, Rakesh K. Vascular normalization as a therapeutic strategy for malignant and nonmalignant disease. **Cold Spring Harbor Perspectives in Medicine**, vol. 2, no. 3, p. 1–24, 2012. https://doi.org/10.1101/cshperspect.a006486.

GOMES DOS SANTOS, Alexandra; DE CARVALHO, Rodolfo Figueiredo; DE MORAIS, Artur Nobrega Lima Rodrigues; SILVA, Tamires Martins; BAYLÃO, Victor Matheus Ribeiro; AZEVEDO, Mayara; DE OLIVEIRA, Adilson J.M. Role of neutrophil-lymphocyte ratio as a predictive factor of glioma tumor grade: A systematic review. **Critical Reviews in Oncology/Hematology**, vol. 163, no. July 2020, 2021. https://doi.org/10.1016/j.critrevonc.2021.103372.

GONÇALVES, Bryan Ôrtero Perez; FIALHO, Sílvia Ligório; SILVESTRINI, Bárbara Reis; SENA, Isadora Fernandes Gilson; DOS SANTOS, Gabryella Soares Pinheiro; ASSIS GOMES, Dawidson; SILVA, Luciana Maria. Central nervous system (CNS) tumor cell heterogeneity contributes to differential platinum-based response in an in vitro 2D and 3D cell culture approach. **Experimental and Molecular Pathology**, vol. 116, no. August, p. 104520, 2020.

https://doi.org/10.1016/j.yexmp.2020.104520.

GONG, Yingying; BAO, Lisha; XU, Tong; YI, Xiaofen; CHEN, Jinming; WANG, Shanshan; PAN, Zongfu; HUANG, Ping; GE, Minghua. The tumor ecosystem in head and neck squamous cell carcinoma and advances in ecotherapy. **Molecular Cancer**, vol. 22, no. 1, p. 1–17, 2023. https://doi.org/10.1186/s12943-023-01769-z.

GOVERNA, Valeria; TRELLA, Emanuele; MELE, Valentina; TORNILLO, Luigi; AMICARELLA, Francesca; CREMONESI, Eleonora; MURARO, Manuele Giuseppe; XU, Hui; DROESER, Raoul; DÄSTER, Silvio R.; BOLLI, Martin; ROSSO, Raffaele; OERTLI, Daniel; EPPENBERGER-CASTORI, Serenella; TERRACCIANO, Luigi M.; IEZZI, Giandomenica; SPAGNOLI, Giulio C. The interplay between neutrophils and CD8+ T cells improves survival in human colorectal cancer. **Clinical Cancer Research**, vol. 23, no. 14, p. 3847–3858, 2017. https://doi.org/10.1158/1078-0432.CCR-16-2047.

GRANOT, Zvi. Neutrophils as a Therapeutic Target in Cancer. **Frontiers in immunology**, vol. 10, no. July, p. 1710, 2019. https://doi.org/10.3389/fimmu.2019.01710.

GRANOT, Zvi; JABLONSKA, Jadwiga. Distinct Functions of Neutrophil in Cancer and Its Regulation. **Mediators of Inflammation**, vol. 2015, 2015. https://doi.org/10.1155/2015/701067.

GRASSI, Fabio. Purinergic control of neutrophil activation. **Journal of Molecular Cell Biology**, vol. 2, no. 4, p. 176–177, 2010. https://doi.org/10.1093/jmcb/mjq014.

GUNGABEESOON, Jeremy; GORT-FREITAS, Nicolas A.; KISS, Máté; BOLLI, Evangelia; MESSEMAKER, Marius; SIWICKI, Marie; HICHAM, Mehdi; BILL, Ruben; KOCH, Peter; CIANCIARUSO, Chiara; DUVAL, Florent; PFIRSCHKE, Christina; MAZZOLA, Michael; PETERS, Solange; HOMICSKO, Krisztian; GARRIS, Christopher; WEISSLEDER, Ralph; KLEIN, Allon M.; PITTET, Mikael J. A neutrophil response linked to tumor control in immunotherapy. **Cell**, vol. 186, no. 7, p. 1448-1464.e20, 2023. https://doi.org/10.1016/j.cell.2023.02.032.

GUO, Weihua; LI, Yashan; PANG, Wei; SHEN, Hong. Exosomes: A Potential Therapeutic Tool Targeting Communications between Tumor Cells and Macrophages. **Molecular Therapy**, vol. 28, no. 9, p. 1953–1964, 2020. DOI 10.1016/j.ymthe.2020.06.003. Available at: https://doi.org/10.1016/j.ymthe.2020.06.003.

HAAS, Lisa; OBENAUF, Anna C. Allies or Enemies—The Multifaceted Role of Myeloid Cells in the Tumor Microenvironment. **Frontiers in Immunology**, vol. 10, no. November, p. 1–11, 2019. https://doi.org/10.3389/fimmu.2019.02746.

HANAHAN, Douglas; WEINBERG, Robert A. Hallmarks of cancer: The next generation. **Cell**, vol. 144, no. 5, p. 646–674, 2011. DOI 10.1016/j.cell.2011.02.013. Available at: http://dx.doi.org/10.1016/j.cell.2011.02.013.

HANN, J.; BUEB, J. L.; TOLLE, F.; BRÉCHARD, S. Calcium signaling and regulation of neutrophil functions: Still a long way to go. **Journal of Leukocyte Biology**, vol. 107, no. 2, p. 285–297, 2020. https://doi.org/10.1002/JLB.3RU0719-241R.

HEIDEN, Matthew G Vander; CANTLEY, Lewis C; THOMPSON, Craig B; MAMMALIAN, Proliferating; EXHIBIT, Cells; METABOLISM, Anabolic. Understanding the Warburg Effect : Cell Proliferation. **Science**, vol. 324, no. May, p. 1029–1033, 2009. https://doi.org/10.1126/science.1160809.

HENDRY, Shona A.; FARNSWORTH, Rae H.; SOLOMON, Benjamin; ACHEN, Marc G.; STACKER, Steven A.; FOX, Stephen B. The role of the tumor vasculature in the host immune response: Implications for therapeutic strategies targeting the tumor microenvironment. **Frontiers in Immunology**, vol. 7, no. DEC, p. 1–21, 2016. https://doi.org/10.3389/fimmu.2016.00621.

HERBST, Roy S.; MAJEM, Margarita; BARLESI, Fabrice; CARCERENY, Enric; CHU, Quincy; MONNET, Isabelle; SANCHEZ-HERNANDEZ, Alfredo; DAKHIL, Shaker; CAMIDGE, D. Ross; WINZER, Leanne; SOO-HOO, Yee; COOPER, Zachary A.; KUMAR, Rakesh; BOTHOS, John; AGGARWAL, Charu; MARTINEZ-

MARTI, Alex. COAST: An Open-Label, Phase II, Multidrug Platform Study of Durvalumab Alone or in Combination with Oleclumab or Monalizumab in Patients with Unresectable, Stage III Non-Small-Cell Lung Cancer. **Journal of Clinical Oncology**, vol. 3, no. 29, 2022. https://doi.org/10.1200/JCO.22.00227.

HURT, Brian; SCHULICK, Richard; EDIL, Barish; EL KASMI, Karim C.; BARNETT, Carlton. Cancer-promoting mechanisms of tumor-associated neutrophils. **American Journal of Surgery**, vol. 214, no. 5, p. 938–944, 2017. DOI 10.1016/j.amjsurg.2017.08.003. Available at: https://doi.org/10.1016/j.amjsurg.2017.08.003.

IDA MICAILY, Jennifer Johnson and Athanassios Argiris. An update on angiogenesis targeting in head and neck squamous cell carcinoma. **Cancers Head Neck**, vol. 5, no. 5, 2020. https://doi.org/10.1186/s41199-020-00051-9.

JAILLON, Sebastien; PONZETTA, Andrea; DI MITRI, Diletta; SANTONI, Angela; BONECCHI, Raffaella; MANTOVANI, Alberto. Neutrophil diversity and plasticity in tumour progression and therapy. **Nature Reviews Cancer**, vol. 20, no. 9, p. 485–503, 2020. DOI 10.1038/s41568-020-0281-y. Available at: http://dx.doi.org/10.1038/s41568-020-0281-y.

JEPPESEN, Dennis K.; FENIX, Aidan M.; FRANKLIN, Jeffrey L.; HIGGINBOTHAM, James N.; ZHANG, Qin; ZIMMERMAN, Lisa J.; LIEBLER, Daniel C.; PING, Jie; LIU, Qi; EVANS, Rachel; FISSELL, William H.; PATTON, James G.; ROME, Leonard H.; BURNETTE, Dylan T.; COFFEY, Robert J. Reassessment of Exosome Composition. **Cell**, vol. 177, no. 2, p. 428-445.e18, 2019. DOI 10.1016/j.cell.2019.02.029. Available at: https://doi.org/10.1016/j.cell.2019.02.029.

KALLINGER, Isabella; RUBENICH, Dominique S; GŁUSZKO, Alicja; KULKARNI, Aditi; SPANIER, Gerrit; SPOERL, Steffen; TAXIS, Juergen; POECK, Hendrik; SZCZEPA, Mirosław J; ETTL, Tobias; REICHERT, Torsten E; MEIER, Johannes K; BRAGANHOL, Elizandra; FERRIS, Robert L; WHITESIDE, Theresa L; LUDWIG, Nils. Tumor gene signatures that correlate with release of extracellular

vesicles shape the immune landscape in head and neck squamous cell carcinoma. **Clinical and Experimental Immunology**, vol. xx, p. 1–12, 2023. https://doi.org/https://doi.org/10.1093/cei/uxad019.

KALLURI, Raghu; LEBLEU, Valerie S. The biology, function, and biomedical applications of exosomes. **Science**, vol. 367, no. 6478, 2020. https://doi.org/10.1126/science.aau6977.

KATHER, Jakob Nikolas; SUAREZ-CARMONA, Meggy; CHAROENTONG, Pornpimol; WEIS, Cleo-aron; HIRSCH, Daniela; BANKHEAD, Peter; HORNING, Marcel; FERBER, Dyke; KEL, Ivan; HERPEL, Esther; SCHOTT, Sarah; JA, Dirk. Topography of cancer-associated immune cells in human solid tumors. **eLife**, vol. 7, no. e36967, p. 1–19, 2018. https://doi.org/https://doi.org/10.7554/eLife.36967.

KOGA, Yuhki; MATSUZAKI, Akinobu; SUMINOE, Aiko; HATTORI, Hiroyoshi; HARA, Toshiro. Neutrophil-Derived TNF-Related Apoptosis-Inducing Ligand (TRAIL): A Novel Mechanism of Antitumor Effect by Neutrophils. **Cancer Research**, vol. 64, no. 3, p. 1037–1043, 2004. https://doi.org/10.1158/0008-5472.CAN-03-1808.

KORSHUNOV, A.; CASALINI, B.; CHAVEZ, L.; HIELSCHER, T.; SILL, M.; RYZHOVA, M.; SHARMA, T.; SCHRIMPF, D.; STICHEL, D.; CAPPER, D.; REUSS, D. E.; STURM, D.; ABSALYAMOVA, O.; GOLANOV, A.; LAMBO, S.; BEWERUNGE-HUDLER, M.; LICHTER, P.; HEROLD-MENDE, C.; WICK, W.; … SAHM, F. Integrated molecular characterization of IDH-mutant glioblastomas. **Neuropathology and Applied Neurobiology**, vol. 45, no. 2, p. 108–118, 2019. https://doi.org/10.1111/nan.12523.

KÜRTEN, Cornelius H.L.; KULKARNI, Aditi; CILLO, Anthony R.; SANTOS, Patricia M.; ROBLE, Anna K.; ONKAR, Sayali; REEDER, Carly; LANG, Stephan; CHEN, Xueer; DUVVURI, Umamaheswar; KIM, Seungwon; LIU, Angen; TABIB, Tracy; LAFYATIS, Robert; FENG, Jian; GAO, Shou Jiang; BRUNO, Tullia C.; VIGNALI, Dario A.A.; LU, Xinghua; … FERRIS, Robert L. Investigating immune and non-immune cell interactions in head and neck tumors by single-cell RNA sequencing.

Nature Communications, vol. 12, no. 1, p. 1–16, 2021. https://doi.org/10.1038/s41467-021-27619-4.

LANDIS, Catherine J; NHAT, Anh; SCOTT, Sarah E; GRIGUER, Corinne; HJELMELAND, Anita B. The pro-tumorigenic effects of metabolic alterations in glioblastoma including brain tumor initiating cells. **BBA - Reviews on Cancer**, vol. 1869, no. June 2017, p. 175–188, 2018. https://doi.org/10.1016/j.bbcan.2018.01.004.

LAUBACH, Kyra; TURAN, Tolga; MATHEW, Rebecca; WILSBACHER, Julie; ENGELHARDT, John; SAMAYOA, Josue. Tumor-intrinsic metabolic reprogramming and how it drives resistance to anti-PD-1/PD-L1 treatment. **Cancer Drug Resistance**, vol. 6, no. 3, p. 611–641, 2023. https://doi.org/10.20517/cdr.2023.60.

LE'NEGRATE, G.; ROSTAGNO, P.; AUBERGER, P.; ROSSI, B.; HOFMAN, P. Downregulation of caspases and Fas ligand expression, and increased lifespan of neutrophils after transmigration across intestinal epithelium. **Cell Death and Differentiation**, vol. 10, no. 2, p. 153–162, 2003. https://doi.org/10.1038/sj.cdd.4401110.

LECOT, Pacôme; SARABI, Matthieu; PEREIRA ABRANTES, Manuela; MUSSARD, Julie; KOENDERMAN, Leo; CAUX, Christophe; BENDRISS-VERMARE, Nathalie; MICHALLET, Marie Cécile. Neutrophil Heterogeneity in Cancer: From Biology to Therapies. **Frontiers in Immunology**, vol. 10, no. September, p. 1–19, 2019a. https://doi.org/10.3389/fimmu.2019.02155.

LECOT, Pacôme; SARABI, Matthieu; PEREIRA ABRANTES, Manuela; MUSSARD, Julie; KOENDERMAN, Leo; CAUX, Christophe; BENDRISS-VERMARE, Nathalie; MICHALLET, Marie Cécile. Neutrophil Heterogeneity in Cancer: From Biology to Therapies. **Frontiers in Immunology**, vol. 10, 2019b. https://doi.org/10.3389/fimmu.2019.02155.

LEEMANS, C. René; SNIJDERS, Peter J. F.; BRAKENHOFF, Ruud H. The molecular landscape of head and neck cancer. **Nature Reviews Cancer**, vol. 18,

no. 5, p. 269–282, 2018. .

LEONG, Alessandra; KIM, Minah. The angiopoietin-2 and tie pathway as a therapeutic target for enhancing antiangiogenic therapy and immunotherapy in patients with advanced cancer. **International Journal of Molecular Sciences**, vol. 21, no. 22, p. 1–20, 2020. https://doi.org/10.3390/ijms21228689.

LI, Yaomin; REN, Zhonglu; PENG, Yuping; LI, Kaishu; WANG, Xiran; HUANG, Guanglong; QI, Songtao; LIU, Yawei. Classification of glioma based on prognostic alternative splicing. **BMC Medical Genomics**, vol. 12, no. 1, p. 1–16, 2019. https://doi.org/10.1186/s12920-019-0603-7.

LIANG, Zhen-xing; LIU, Hua-shan; WANG, Feng-wei; XIONG, Li; ZHOU, Chi; HU, Tuo; HE, Xiao-wen; WU, Xiao-jian; XIE, Dan; WU, Xian-rui; LAN, Ping. LncRNA RPPH1 promotes colorectal cancer metastasis by interacting with TUBB3 and by promoting exosomes-mediated macrophage M2 polarization. **Cell Death and Disease**, vol. 10, no. 829, 2019. DOI 10.1038/s41419-019-2077-0. Available at: http://dx.doi.org/10.1038/s41419-019-2077-0.

LIEW, Pei Xiong; KUBES, Paul. The Neutrophil's role during health and disease. **Physiological Reviews**, vol. 99, no. 2, p. 1223–1248, 2019. https://doi.org/10.1152/physrev.00012.2018.

LINDEN, Joel. Regulation of Leukocyte Function by Adenosine Receptors. **Advances in Pharmacology**, vol. 61, p. 95–114, 2011. https://doi.org/10.1016/B978-0-12-385526-8.00004-7.

LOFFREDO, Stefania; BORRIELLO, Francesco; IANNONE, Raffaella; FERRARA, Anne L.; GALDIERO, Maria R.; GIGANTINO, Vincenzo; ESPOSITO, Pasquale; VARRICCHI, Gilda; LAMBEAU, Gerard; CASSATELLA, Marco A.; GRANATA, Francescopaolo; MARONE, Gianni. Group V secreted phospholipase A2 induces the release of proangiogenic and antiangiogenic factors by human neutrophils. **Frontiers in Immunology**, vol. 8, no. APR, p. 1–10, 2017. https://doi.org/10.3389/fimmu.2017.00443.

LUDWIG, Nils; RUBENICH, Dominique S.; ZARĘBA, Łukasz; SIEWIERA, Jacek; PIEPER, Josquin; BRAGANHOL, Elizandra; REICHERT, Torsten E.; SZCZEPAŃSKI, Mirosław J. Potential roles of tumor cell-and stroma cell-derived small extracellular vesicles in promoting a pro-angiogenic tumor microenvironment. **Cancers**, vol. 12, no. 12, p. 1–15, 2020. https://doi.org/10.3390/cancers12123599.

LUDWIG, Sonja; SHARMA, Priyanka; THEODORAKI, Marie-Nicole; PIETROWSKA, Monika; YERNENI, Saigopalakrishna S.; LANG, Stephan; FERRONE, Soldano; WHITESIDE, Theresa L. Molecular and Functional Profiles of Exosomes From HPV(+) and HPV(−) Head and Neck Cancer Cell Lines. **Frontiers in Oncology**, vol. 12, no. 8, p. 445, 2018. .

MACKEY, John B.G.; COFFELT, Seth B.; CARLIN, Leo M. Neutrophil maturity in cancer. **Frontiers in Immunology**, vol. 10, no. AUG, p. 1–11, 2019. https://doi.org/10.3389/fimmu.2019.01912.

MAJD, Nazanin; DE GROOT, John. Challenges and strategies for successful clinical development of immune checkpoint inhibitors in glioblastoma. **Expert Opinion on Pharmacotherapy**, vol. 20, no. 13, p. 1609–1624, 2019. DOI 10.1080/14656566.2019.1621840. Available at: https://doi.org/10.1080/14656566.2019.1621840.

MANTOVANI, Alberto; CASSATELLA, Marco A.; COSTANTINI, Claudio; JAILLON, Sébastien. Neutrophils in the activation and regulation of innate and adaptive immunity. **Nature Reviews Immunology**, vol. 11, no. 8, p. 519–531, 2011. DOI 10.1038/nri3024. Available at: http://dx.doi.org/10.1038/nri3024.

MASCARELLA, Marco A.; MANNARD, Erin; SILVA, Sabrina Daniela; ZEITOUNI, Anthony. Neutrophil-to-lymphocyte ratio in head and neck cancer prognosis: A systematic review and meta-analysis. **Head and Neck**, vol. 40, no. 5, p. 1091–1100, 2018. https://doi.org/10.1002/hed.25075.

MASUCCI, Maria Teresa; MINOPOLI, Michele; CARRIERO, Maria Vincenza. Tumor Associated Neutrophils: Their Role in Tumorigenesis, Metastasis,

Prognosis and Therapy. **Frontiers in Oncology**, vol. 9, no. November, p. 1–16, 2019a. https://doi.org/10.3389/fonc.2019.01146.

MASUCCI, Maria Teresa; MINOPOLI, Michele; CARRIERO, Maria Vincenza. Tumor Associated Neutrophils. Their Role in Tumorigenesis, Metastasis, Prognosis and Therapy. **Frontiers in Oncology**, vol. 9, 2019b. https://doi.org/10.3389/fonc.2019.01146.

MATARREDONA, ER; PASTOR, AM. Extracellular Vesicle-Mediated Communication between the Glioblastoma and Its Microenvironment. **Cells**, vol. 9, no. 1, p. 96, 2019. https://doi.org/10.3390/cells9010096.

MATHIEU, Mathilde; MARTIN-JAULAR, Lorena; LAVIEU, Grégory; THÉRY, Clotilde. Specificities of secretion and uptake of exosomes and other extracellular vesicles for cell-to-cell communication. **Nature Cell Biology**, vol. 21, no. 1, p. 9–17, 2019. DOI 10.1038/s41556-018-0250-9. Available at: http://dx.doi.org/10.1038/s41556-018-0250-9.

MAYADAS, Tanya N.; CULLERE, Xavier; LOWELL, Clifford A. The multifaceted functions of neutrophils. **Annual Review of Pathology: Mechanisms of Disease**, vol. 9, p. 181–218, 2014. https://doi.org/10.1146/annurev-pathol-020712-164023.

MAYBRUCK, Brian T; PFANNENSTIEL, Lukas W; DIAZ-MONTERO, Marcela; GASTMAN, Brian R. Tumor-derived exosomes induce CD8 + T cell suppressors. **Journal of ImmunoTherapy of Cancer**, vol. 5, no. 65, p. 1–15, 2017. https://doi.org/10.1186/s40425-017-0269-7.

MCCRACKEN, Jenna M.; ALLEN, Lee Ann H. Regulation of human neutrophil apoptosis and lifespan in health and disease. **Journal of Cell Death**, vol. 7, no. 1, p. 15–23, 2014. https://doi.org/10.4137/JCD.S11038.

MCLAREN, Alistair S.; FETIT, Rana; WOOD, Colin S.; FALCONER, John; STEELE, Colin W. Single cell sequencing of neutrophils demonstrates phenotypic heterogeneity and functional plasticity in health, disease, and cancer. **Chinese Clinical Oncology**, vol. 12, no. 2, p. 0–3, 2023. https://doi.org/10.21037/cco-22-

121.

MICHAELI, Janna; SHAUL, Merav E.; MISHALIAN, Inbal; HOVAV, Avi Hai; LEVY, Liran; ZOLOTRIOV, Lidia; GRANOT, Zvi; FRIDLENDER, Zvi G. Tumor-associated neutrophils induce apoptosis of non-activated CD8 T-cells in a TNFα and NO-dependent mechanism, promoting a tumor-supportive environment. **OncoImmunology**, vol. 6, no. 11, 2017. https://doi.org/10.1080/2162402X.2017.1356965.

MINCIACCHI, Valentina R.; FREEMAN, Michael R.; DI VIZIO, Dolores. Extracellular Vesicles in Cancer: Exosomes, Microvesicles and the Emerging Role of Large Oncosomes. **Seminars in Cell and Developmental Biology**, vol. 40, p. 41–51, 2015. .

MÓCSAI, Attila. Diverse novel functions of neutrophils in immunity, infammation, and beyond. **Journal of Experimental Medicine**, vol. 210, no. 7, p. 1289–1299, 2013. https://doi.org/10.1084/jem.20122220.

MONTALDO, Elisa; LUSITO, Eleonora; BIANCHESSI, Valentina; CARONNI, Nicoletta; SCALA, Serena; BASSO-RICCI, Luca; CANTAFFA, Carla; MASSERDOTTI, Alice; BARILARO, Mattia; BARRESI, Simona; GENUA, Marco; VITTORIA, Francesco Maria; BARBIERA, Giulia; LAZAREVIC, Dejan; MESSINA, Carlo; XUE, Elisabetta; MARKTEL, Sarah; TRESOLDI, Cristina; MILANI, Raffaella; … OSTUNI, Renato. Cellular and transcriptional dynamics of human neutrophils at steady state and upon stress. **Nature Immunology**, vol. 23, no. 10, p. 1470–1483, 2022. https://doi.org/10.1038/s41590-022-01311-1.

MORELLO, Silvana; CAPONE, Mariaelena; SORRENTINO, Claudia; GIANNARELLI, Diana; MADONNA, Gabriele; MALLARDO, Domenico; GRIMALDI, Antonio M.; PINTO, Aldo; ASCIERTO, Paolo Antonio. Soluble CD73 as biomarker in patients with metastatic melanoma patients treated with nivolumab. **Journal of Translational Medicine**, vol. 15, no. 1, p. 1–9, 2017. DOI 10.1186/s12967-017-1348-8. Available at: https://doi.org/10.1186/s12967-017-1348-8.

MORTEZAEE, Keywan. Immune escape: A critical hallmark in solid tumors. **Life**

Sciences, vol. 258, no. July, p. 118110, 2020. DOI 10.1016/j.lfs.2020.118110. Available at: https://doi.org/10.1016/j.lfs.2020.118110.

MOTZ, Greg T; COUKOS, George. Deciphering and Reversing Tumor Immune Suppression. **Immunity**, vol. 39, no. 1, p. 61–73, 2013. DOI 10.1016/j.immuni.2013.07.005. Available at: http://dx.doi.org/10.1016/j.immuni.2013.07.005.

NATHAN, Carl. Neutrophils and immunity: Challenges and opportunities. **Nature Reviews Immunology**, vol. 6, no. 3, p. 173–182, 2006. https://doi.org/10.1038/nri1785.

NIU, Mengke; LIU, Yiming; YI, Ming; JIAO, Dechao; WU, Kongming. Biological Characteristics and Clinical Significance of Soluble PD-1/PD-L1 and Exosomal PD-L1 in Cancer. **Frontiers in Immunology**, vol. 13, no. March, p. 1–14, 2022. https://doi.org/10.3389/fimmu.2022.827921.

NØRØXE, Dorte Schou; POULSEN, Hans Skovgaard; LASSEN, Ulrik. Hallmarks of glioblastoma: A systematic review. **ESMO Open**, vol. 1, no. 6, p. 1–9, 2016. https://doi.org/10.1136/esmoopen-2016-000144.

NOSEYKINA, E M; SCHEPETKIN, I A; ATOCHIN, D N. Molecular Mechanisms for Regulation of Neutrophil Apoptosis under Normal and Pathological Conditions. **Journal of Evolutionary Biochemistry and Physiology**, vol. 57, no. 3, p. 429–450, 2021. https://doi.org/10.1134/S0022093021030017.

OMURO, Antonio; DEANGELIS, Lisa M. Glioblastoma and other malignant gliomas: A clinical review. **JAMA - Journal of the American Medical Association**, vol. 310, no. 17, p. 1842–1850, 2013. https://doi.org/10.1001/jama.2013.280319.

PARRA, Edwin R; VILLALOBOS, Pamela; RODRIGUEZ-CANALES, Jaime. The Multiple Faces of Programmed Cell Death Ligand 1 Expression in Malignant and Nonmalignant Cells. **Appl Immunohistochem Mol Morphol**, vol. 27, no. 4, p. 287–294, 2019. https://doi.org/10.1097/PAI.0000000000000602.

PEREZ-DE-PUIG, Isabel; MIRÓ-MUR, Francesc; FERRER-FERRER, Maura; GELPI, Ellen; PEDRAGOSA, Jordi; JUSTICIA, Carles; URRA, Xabier; CHAMORRO, Angel; PLANAS, Anna M. Neutrophil recruitment to the brain in mouse and human ischemic stroke. **Acta Neuropathologica**, vol. 129, no. 2, p. 239–257, 2015. https://doi.org/10.1007/s00401-014-1381-0.

PILLAY, Janesh; TAK, Tamar; KAMP, Vera M.; KOENDERMAN, Leo. Immune suppression by neutrophils and granulocytic myeloid-derived suppressor cells: Similarities and differences. **Cellular and Molecular Life Sciences**, vol. 70, no. 20, p. 3813–3827, 2013. https://doi.org/10.1007/s00018-013-1286-4.

PONZETTA, Andrea; CARRIERO, Roberta; CARNEVALE, Silvia; BARBAGALLO, Marialuisa; MOLGORA, Martina; PERUCCHINI, Chiara; MAGRINI, E.; GIANNI, Francesca; KUNDERFRANCO, P.; POLENTARUTTI, N.; PASQUALINI, F.; DI MARCO, Sabrina; SUPINO, Domenico; PEANO, Clelia; CANANZI, Ferdinando; COLOMBO, Piergiuseppe; PILOTTI, Silvana; ALOMAR, Suliman Yousef; BONAVITA, Eduardo; … JAILLON, Sebastien. Neutrophils Driving Unconventional T Cells Mediate Resistance against Murine Sarcomas and Selected Human Tumors. **Cell**, vol. 178, no. 2, p. 346-360.e24, 2019. DOI 10.1016/j.cell.2019.05.047. Available at: https://doi.org/10.1016/j.cell.2019.05.047.

QIAN, Chao Nan; TAN, Min Han; YANG, Jun Ping; CAO, Yun. Revisiting tumor angiogenesis: vessel co - option , vessel remodeling , and cancer cell - derived vasculature formation. **Chinese Journal of Cancer**, vol. 35, no. 10, p. 2–7, 2016. https://doi.org/https://doi.org/10.1186/s40880-015-0070-2.

QIAN, Mingyu; WANG, Shaobo; GUO, Xiaofan; WANG, Jian; ZHANG, Zongpu; QIU, Wei; GAO, Xiao; CHEN, Zihang; XU, Jianye; ZHAO, Rongrong; XUE, Hao; LI, Gang. Hypoxic glioma-derived exosomes deliver microRNA-1246 to induce M2 macrophage polarization by targeting TERF2IP via the STAT3 and NF- κ B pathways. **Oncogene**, 2019. DOI 10.1038/s41388-019-0996-y. Available at: http://dx.doi.org/10.1038/s41388-019-0996-y.

QUIROGA, John; ALARCÓN, Pablo; MANOSALVA, Carolina; TEUBER, Stefanie;

CARRETTA, María Daniella; BURGOS, Rafael Agustín. D-lactate-triggered extracellular trap formation in cattle polymorphonuclear leucocytes is glucose metabolism dependent. **Developmental and Comparative Immunology**, vol. 135, no. March, 2022. https://doi.org/10.1016/j.dci.2022.104492.

RAD, Habib Sadeghi; SHIRAVAND, Yavar; RADFAR, Payar; LADWA, Rahul; PERRY, Chris; HAN, Xiaoyuan; WARKIANI, Majid Ebrahimi; ADAMS, Mark N.; HUGHES, Brett G.M.; O'BYRNE, Ken; KULASINGHE, Arutha. Understanding the tumor microenvironment in head and neck squamous cell carcinoma. **Clinical and Translational Immunology**, vol. 11, no. 6, p. 1–14, 2022. https://doi.org/10.1002/cti2.1397.

RAEVEN, Pierre; ZIPPERLE, Johannes; DRECHSLER, Susanne. Extracellular vesicles as markers and mediators in sepsis. **Theranostics**, vol. 8, no. 12, p. 3348–3365, 2018. https://doi.org/10.7150/thno.23453.

RAHBAR, Afsar; CEDERARV, Madeleine; WOLMER-SOLBERG, Nina; TAMMIK, Charlotte; STRAGLIOTTO, Giuseppe; PEREDO, Inti; FORNARA, Olesja; XU, Xinling; DZABIC, Mensur; TAHER, Chato; SKARMAN, Petra; SÖDERBERG-NAUCLÉR, Cecilia. Enhanced neutrophil activity is associated with shorter time to tumor progression in glioblastoma patients. **OncoImmunology**, vol. 5, no. 2, 2016. https://doi.org/10.1080/2162402X.2015.1075693.

RAMÓN, Santiago; SESÉ, Marta; CAPDEVILA, Claudia; AASEN, Trond; MATTOS-ARRUDA, Leticia De. Clinical implications of intratumor heterogeneity : challenges and opportunities. **Journal of Molecular Medicine**, no. 98, p. 161–177, 2020. https://doi.org/10.1007/s00109-020-01874-2.

RAPOPORT, Bernardo L.; STEEL, Helen C.; THERON, Annette J.; SMIT, Teresa; ANDERSON, Ronald. Role of the neutrophil in the pathogenesis of advanced cancer and impaired responsiveness to therapy. **Molecules**, vol. 25, no. 7, p. 1–22, 2020. https://doi.org/10.3390/molecules25071618.

REN, Zhen Hu; LIN, Cheng Zhong; CAO, Wei; YANG, Rong; LU, Wei; LIU, Zhe Qi; CHEN, Yi Ming; YANG, Xi; TIAN, Zhen; WANG, Li Zhen; LI, Jiang; WANG, Xu;

CHEN, Wan Tao; JI, Tong; ZHANG, Chen Ping. CD73 is associated with poor prognosis in HNSCC. **Oncotarget**, vol. 7, no. 38, p. 61690–61702, 2016. https://doi.org/10.18632/oncotarget.11435.

RODRIGUES, Stephen F.; GRANGER, D. Neil. Blood cells and endothelial barrier function. **Tissue Barriers**, vol. 3, no. 1, p. 1–2, 2015. https://doi.org/10.4161/21688370.2014.978720.

ROSALES, Carlos. Neutrophil: A cell with many roles in inflammation or several cell types? **Frontiers in Physiology**, vol. 9, no. FEB, p. 1–17, 2018. https://doi.org/10.3389/fphys.2018.00113.

ROSSANO, Rocco; LAROCCA, Marilena; MACELLARO, Margherita; BILANCIA, Domenico; RICCIO, Paolo. Unveiling a hidden biomarker of inflammation and tumor progression: The 65 kDa isoform of MMP-9 new horizons for therapy. **Current Issues in Molecular Biology**, vol. 44, no. 1, p. 105–116, 2022. https://doi.org/10.3390/cimb44010008.

RUBEL, Carolina; GÓMEZ, Sonia; FERNÁNDEZ, Gabriela C.; ISTURIZ, Martín A.; CAAMAÑO, Jorge; PALERMO, Marina S. Fibrinogen-CD11b/CD18 interaction activates the NF-κB pathway and delays apoptosis in human neutrophils. **European Journal of Immunology**, vol. 33, no. 5, p. 1429–1438, 2003. https://doi.org/10.1002/eji.200323512.

RUBENICH, Dominique S.; DE SOUZA, Priscila O.; OMIZZOLLO, Natalia; AUBIN, Mariana R.; BASSO, Paulo J.; SILVA, Luisa M.; DA SILVA, Eloisa M.; TEIXEIRA, Fernanda C.; GENTIL, Gabriela F.S.; DOMAGALSKI, Jordana L.; CUNHA, Maico T.; GADELHA, Kerolainy A.; DIEL, Leonardo F.; GELSLEICHTER, Nicolly E.; RUBENICH, Aline S.; LENZ, Gabriela S.; DE ABREU, Aline M.; KROEFF, Giselle M.; PAZ, Ana H.; … BRAGANHOL, Elizandra. Tumor-neutrophil crosstalk promotes in vitro and in vivo glioblastoma progression. **Frontiers in Immunology**, vol. 14, no. May, p. 1–17, 2023. https://doi.org/10.3389/fimmu.2023.1183465.

RUBENICH, Dominique S.; OMIZZOLLO, Natália; SZCZEPAŃSKI, Mirosław J.; REICHERT, Torsten E.; WHITESIDE, Theresa L.; LUDWIG, Nils; BRAGANHOL,

Elizandra. Small extracellular vesicle-mediated bidirectional crosstalk between neutrophils and tumor cells. **Cytokine and Growth Factor Reviews**, vol. 61, no. August, p. 16–26, 2021. https://doi.org/10.1016/j.cytogfr.2021.08.002.

SADIK, Christian D.; KIM, Nancy D.; LUSTER, Andrew D. Neutrophils cascading their way to inflammation. **Trends in Immunology**, vol. 32, no. 10, p. 452–460, 2011. https://doi.org/10.1016/j.it.2011.06.008.

SCAPINI, Patrizia; CASSATELLA, Marco A. Social networking of human neutrophils within the immune system. **Blood**, vol. 124, no. 5, p. 710–719, 2014. https://doi.org/10.1182/blood-2014-03-453217.

SCHREIBER, Robert D; OLD, Lloyd J; SMYTH, Mark J. Cancer Immunoediting : Integrating Suppression and Promotion. **Science**, vol. 2011, no. 6024, p. 1565–1570, 331AD. https://doi.org/10.1126/science.1203486.

SCHULZ, D.; STRELLER, M.; PIENDL, G.; BROCKHOFF, G.; REICHERT, T. E.; MENEVSE, A. N.; BECKHOVE, P.; HAUTMANN, M. G.; BAUER, R. J.; ETTL, T. Differential localization of PD-L1 and Akt-1 involvement in radioresistant and radiosensitive cell lines of head and neck squamous cell carcinoma. **Carcinogenesis**, vol. 41, no. 7, p. 984–992, 2021. https://doi.org/10.1093/CARCIN/BGZ177.

SCHULZ, Daniela; FEULNER, Laura; SANTOS RUBENICH, Dominique; HEIMER, Sina; ROHRMÜLLER, Sophia; REINDERS, Yvonne; FALCHETTI, Marcelo; WETZEL, Martin; BRAGANHOL, Elizandra; LUMMERTZ DA ROCHA, Edroaldo; SCHÄFER, Nicole; STÖCKL, Sabine; BROCKHOFF, Gero; WEGE, Anja K.; FRITSCH, Jürgen; POHL, Fabian; REICHERT, Torsten E.; ETTL, Tobias; BAUER, Richard J. Subcellular localization of PD-L1 and cell-cycle-dependent expression of nuclear PD-L1 variants: implications for head and neck cancer cell functions and therapeutic efficacy. **Molecular Oncology**, , p. 1–22, 2023. https://doi.org/10.1002/1878-0261.13567.

SCHULZ, Daniela; STANCEV, Irene; SORRENTINO, Antonio; MENEVSE, Ayse Nur; BECKHOVE, Philipp; BROCKHOFF, Gero; HAUTMANN, Matthias Günther;

REICHERT, Torsten Erich; BAUER, Richard Josef; ETTL, Tobias. Increased PD-L1 expression in radioresistant HNSCC cell lines after irradiation affects cell proliferation due to inactivation of GSK-3beta. **Oncotarget**, vol. 10, no. 5, p. 573–583, 2019. https://doi.org/10.18632/oncotarget.26542.

SHANKARAN, Vijay; IKEDA, Hiroaki; BRUCE, Allen T; WHITE, J Michael; SWANSON, Paul E; OLD, Lloyd J; SCHREIBER, Robert D. IFN g and lymphocytes prevent primary tumour development and shape tumour immunogenicity. **Letters to Nature**, vol. 410, no. April, p. 1107–1111, 2001. .

SHARMA, Padmanee; ALLISON, James P. The future of immune checkpoint therapy. **Science**, vol. 348, no. 6230, p. 56–61, 2015. https://doi.org/10.1126/science.aaa8172.

SHERWOOD, L. M., PARRIS, E. E., & FOLKMAN, J. Tumor Angiogenesis: Therapeutic Implications. **New England Journal of Medicine**, vol. 285, no. 21, p. 1182–1186, 1971. https://doi.org/10.1056/nejm197111182852108.

SKINNER, Benjamin M.; JOHNSON, Emma E.P. Nuclear morphologies: their diversity and functional relevance. **Chromosoma**, vol. 126, no. 2, p. 195–212, 2017. https://doi.org/10.1007/s00412-016-0614-5.

STACKER, Steven A; ACHEN, Marc G. The VEGF signaling pathway in cancer: the road ahead. **Chinese Journal of Cancer**, vol. Jun, no. 6, p. 297–302, 2013. https://doi.org/10.5732/cjc.012.10319.

STRICKLAND, Marie; STOLL, Elizabeth A. Metabolic Reprogramming in Glioma. **Front Cell Dev Biol.**, vol. 5, no. April, 2017. https://doi.org/10.3389/fcell.2017.00043.

STUPP, Roger; VAN DEN BENT, Martin J.; HEGI, Monika E. Optimal role of temozolomide in the treatment of malignant gliomas. **Current Neurology and Neuroscience Reports**, vol. 5, no. 3, p. 198–206, 2005. https://doi.org/10.1007/s11910-005-0047-7.

SU, Xin; BRASSARD, Ariane; BARTOLOMUCCI, Alexandra; DHOPAREE-

DOOMAH, Iqraa; QIU, Qian; TSERING, Thupten; ROHANIZADEH, Ramin; KOUFOS, Olivia; GIANNIAS, Betty; BOURDEAU, France; FENG, Lixuan; MESSINA-PACHECO, Julia; LEO, Sabrina; SANGWAN, Veena; QUAIL, Daniela; TANKEL, James; SPICER, Jonathan; BURNIER, Julia Valdemarin; BAILEY, Swneke Donovan; … COOLS-LARTIGUE, Jonathan. Tumour extracellular vesicles induce neutrophil extracellular traps to promote lymph node metastasis. **Journal of Extracellular Vesicles**, vol. 12, no. 8, 2023. https://doi.org/10.1002/jev2.12341.

SUT, Burcu Biterge. A comprehensive analysis of the angiogenesis-related genes in glioblastoma multiforme vs. Brain lower grade glioma. **Arquivos de Neuro-Psiquiatria**, vol. 78, no. 1, p. 34–38, 2020. https://doi.org/10.1590/0004-282X20190131.

TANG, L. M.; ZHU, J. F.; WANG, F.; QIAN, J.; ZHU, J.; MO, Q.; LU, H. H.; LI, G. Q.; WANG, X. H. Activation of Adenosine A2A Receptor Attenuates Inflammatory Response in a Rat Model of Small-for-Size Liver Transplantation. **Transplantation Proceedings**, vol. 42, no. 5, p. 1915–1920, 2010. DOI 10.1016/j.transproceed.2010.02.084. Available at: http://dx.doi.org/10.1016/j.transproceed.2010.02.084.

TAZZYMAN, Simon; LEWIS, Claire E.; MURDOCH, Craig. Neutrophils: Key mediators of tumour angiogenesis. **International Journal of Experimental Pathology**, vol. 90, no. 3, p. 222–231, 2009. https://doi.org/10.1111/j.1365-2613.2009.00641.x.

THOMAS, Markus; AUGUSTIN, Hellmut G. The role of the angiopoietins in vascular morphogenesis. **Angiogenesis**, vol. 12, no. 2, p. 125–137, 2009. https://doi.org/10.1007/s10456-009-9147-3.

THOMPSON, Elizabeth A; POWELL, Jonathan D. Inhibition of the Adenosine Pathway to Potentiate Cancer Immunotherapy: Potential for Combinatorial Approaches. **Annu Rev Med**, no. 72, p. 331–348, 2021. https://doi.org/10.1146/annurev-med-060619-023155.

URIBE-QUEROL, Eileen; ROSALES, Carlos. Neutrophils in cancer: Two sides of the same coin. **Journal of Immunology Research**, vol. 2015, 2015. https://doi.org/10.1155/2015/983698.

VIALLARD, Claire; LARRIVÉE, Bruno. Tumor angiogenesis and vascular normalization: alternative therapeutic targets. **Angiogenesis**, vol. 20, no. 4, p. 409–426, 2017. https://doi.org/10.1007/s10456-017-9562-9.

VLAJKOVIC, Srdjan M.; THORNE, Peter R. Purinergic Signalling in the Cochlea. **International Journal of Molecular Sciences**, vol. 23, no. 23, 2022. https://doi.org/10.3390/ijms232314874.

WANG, Jianbo; JIA, Yibin; WANG, Nana; ZHANG, Xiaomei; TAN, Bingxu; ZHANG, Guangyu; CHENG, Yufeng. The clinical significance of tumor-infiltrating neutrophils and neutrophil-to-CD8+ lymphocyte ratio in patients with resectable esophageal squamous cell carcinoma. **Journal of Translational Medicine**, vol. 12, no. 1, p. 1–10, 2014. https://doi.org/10.1186/1479-5876-12-7.

WANG, Jing. Neutrophils in tissue injury and repair. **Cell and Tissue Research**, vol. 371, no. 3, p. 531–539, 2018. https://doi.org/10.1007/s00441-017-2785-7.

WANG, Sheng; GAO, Songsen; ZHOU, Dexi; QIAN, Xueyi; LUAN, Jiajie; LV, Xiongwen. The role of the CD39–CD73–adenosine pathway in liver disease. **Journal of Cellular Physiology**, vol. 236, no. 2, p. 851–862, 2021. https://doi.org/10.1002/jcp.29932.

WEI, Rui; LIU, Si; ZHANG, Shutian; MIN, Li; ZHU, Shengtao. Cellular and Extracellular Components in Tumor Microenvironment and Their Application in Early Diagnosis of Cancers. **Analytical Cellular Pathology**, vol. 2020, no. Figure 1, 2020. https://doi.org/10.1155/2020/6283796.

WENG, Weiji; CHEN, Xu; GONG, Shaohui; GUO, Liemei; ZHANG, Xiaohua. Preoperative neutrophil–lymphocyte ratio correlated with glioma grading and glioblastoma survival. **Neurological Research**, vol. 40, no. 11, p. 917–922, 2018. https://doi.org/10.1080/01616412.2018.1497271.

WORTZEL, Inbal; DROR, Shani; KENIFIC, Candia M.; LYDEN, David. Exosome-Mediated Metastasis: Communication from a Distance. **Developmental Cell**, vol. 49, no. 3, p. 347–360, 2019. DOI 10.1016/j.devcel.2019.04.011. Available at: https://doi.org/10.1016/j.devcel.2019.04.011.

WU, Jiani; ZENG, Dongqiang; ZHI, Shimeng; YE, Zilan; QIU, Wenjun; HUANG, Na; SUN, Li; WANG, Chunlin; WU, Zhenzhen; BIN, Jianping; LIAO, Yulin; SHI, Min; LIAO, Wangjun. Single - cell analysis of a tumor - derived exosome signature correlates with prognosis and immunotherapy response. **Journal of Translational Medicine**, vol. 19, no. 381, p. 1–18, 2021. DOI 10.1186/s12967-021-03053-4. Available at: https://doi.org/10.1186/s12967-021-03053-4.

WU, Shiman; YANG, Wenli; ZHANG, Hua; REN, Yan; FANG, Ziwei; YUAN, Chengjie; YAO, Zhenwei. The Prognostic Landscape of Tumor-Infiltrating Immune Cells and Immune Checkpoints in Glioblastoma. **Technology in cancer research & treatment**, vol. 18, p. 1–10, 2019. https://doi.org/10.1177/1533033819869949.

XIE, Xuemei; SHI, Qiang; WU, Peng; ZHANG, Xiaoyu; KAMBARA, Hiroto; SU, Jiayu; YU, Hongbo; PARK, Shin Young; GUO, Rongxia; REN, Qian; ZHANG, Sudong; XU, Yuanfu; SILBERSTEIN, Leslie E.; CHENG, Tao; MA, Fengxia; LI, Cheng; LUO, Hongbo R. Single-cell transcriptome profiling reveals neutrophil heterogeneity in homeostasis and infection. **Nature Immunology**, vol. 21, no. 9, p. 1119–1133, 2020. DOI 10.1038/s41590-020-0736-z. Available at: http://dx.doi.org/10.1038/s41590-020-0736-z.

YANG, Naibin; LI, Shanshan; LI, Guoxiang; ZHANG, Shengguo; TANG, Xinyue; NI, Shunlan; JIAN, Xiaomin; XU, Cunlai; ZHU, Jiayin; LU, Mingqin. The role of extracellular vesicles in mediating progression, metastasis and potential treatment of hepatocellular carcinoma. **Oncotarget**, vol. 8, no. 2, p. 3683–3695, 2017. https://doi.org/10.18632/oncotarget.12465.

YU, Jia; QIN, Bo; MOYER, Ann M.; NOWSHEEN, Somaira; TU, Xinyi; DONG, Haidong; BOUGHEY, Judy C.; GOETZ, Matthew P.; WEINSHILBOUM, Richard; LOU, Zhenkun; WANG, Liewei. Regulation of sister chromatid cohesion by nuclear

PD-L1. **Cell Research**, vol. 30, no. 7, p. 590–601, 2020. DOI 10.1038/s41422-020-0315-8. Available at: http://dx.doi.org/10.1038/s41422-020-0315-8.

YUE, Binglin; YANG, Haiyan; WANG, Jian; RU, Wenxiu; WU, Jiyao; HUANG, Yongzheng; LAN, Xianyong; LEI, Chuzhao; CHEN, Hong. Exosome biogenesis, secretion and function of exosomal miRNAs in skeletal muscle myogenesis. **Cell Proliferation**, vol. 53, no. 7, p. 1–10, 2020. https://doi.org/10.1111/cpr.12857.

ZHA, Caijun; MENG, Xiangqi; LI, Lulu; MI, Shan; QIAN, Da; LI, Ziwei; WU, Pengfei; HU, Shaoshan; ZHAO, Shihong; CAI, Jinquan; LIU, Yanhong. Neutrophil extracellular traps mediate the crosstalk between glioma progression and the tumor microenvironment via the HMGB1/RAGE/IL-8 axis. **Cancer Biology and Medicine**, vol. 17, no. 1, p. 154–168, 2020. https://doi.org/10.20892/j.issn.2095-3941.2019.0353.

ZHANG, Yuting; LIU, Guoqiang; SUN, Miaomiao; LU, Xin. Targeting and exploitation of tumor-associated neutrophils to enhance immunotherapy and drug delivery for cancer treatment. **Cancer Biology and Medicine**, vol. 17, no. 1, p. 32–43, 2020. https://doi.org/10.20892/j.issn.2095-3941.2019.0372.

ZHOU, Shimeng; ZHU, Jinfeng; XU, Jingwei; GU, Bingzi; ZHAO, Qiao; LUO, Congzhou; GAO, Zhoufeng; CHIN, Y. Eugene; CHENG, Xiaju. Anti-tumour potential of PD-L1/PD-1 post-translational modifications. **Immunology**, vol. 167, no. 4, p. 471–481, 2022. https://doi.org/10.1111/imm.13573.